26807

National Library of Canada
Bibliothèque nationale du Canada

CANADIAN THESES ON MICROFICHE

THÈSES CANADIENNES SUR MICROFICHE

NAME OF AUTHOR/*NOM DE L'AUTEUR* JUAN FRANCISCO KUON

TITLE OF THESIS/*TITRE DE LA THÈSE* MULTIVARIABLE FREQUENCY-DOMAIN
DESIGN TECHNIQUES

UNIVERSITY/*UNIVERSITÉ* The University of Alberta

DEGREE FOR WHICH THESIS WAS PRESENTED/*GRADE POUR LEQUEL CETTE THÈSE FUT PRÉSENTÉE* Ph. D.

YEAR THIS DEGREE CONFERRED/*ANNÉE D'OBTENTION DE CE GRADE* 1975

NAME OF SUPERVISOR/*NOM DU DIRECTEUR DE THÈSE* D. G. FISHER

Permission is hereby granted to the NATIONAL LIBRARY OF CANADA to microfilm this thesis and to lend or sell copies of the film.

The author reserves other publication rights, and neither the thesis nor extensive extracts from it may be printed or otherwise reproduced without the author's written permission.

L'autorisation est, par la présente, accordée à la BIBLIOTHÈQUE NATIONALE DU CANADA de microfilmer cette thèse et de prêter ou de vendre des exemplaires du film.

L'auteur se réserve les autres droits de publication; ni la thèse ni de longs extraits de celle-ci ne doivent être imprimés ou autrement reproduits sans l'autorisation écrite de l'auteur.

DATED/*DATÉ* Oct. 20, 1975 SIGNED/*SIGNÉ*

PERMANENT ADDRESS/*RÉSIDENCE FIXE* 500 Dawes Road, Apt. 1017, Toronto
Ontario

NL-91 (3-74)

THE UNIVERSITY OF ALBERTA

MULTIVARIABLE FREQUENCY-DOMAIN
DESIGN TECHNIQUES

by

JUAN F. KUON ©

A THESIS
SUBMITTED TO THE FACULTY OF GRADUATE STUDIES AND RESEARCH
IN PARTIAL FULFILMENT OF THE REQUIREMENTS FOR THE DEGREE
OF DOCTOR OF PHILOSOPHY

DEPARTMENT OF CHEMICAL ENGINEERING

EDMONTON, ALBERTA

FALL, 1975

THE UNIVERSITY OF ALBERTA

FACULTY OF GRADUATE STUDIES AND RESEARCH

The undersigned certify that they have read, and recommend to the Faculty of Graduate Studies and Research, for acceptance, a thesis entitled "MULTIVARIABLE FREQUENCY-DOMAIN DESIGN TECHNIQUES" submitted by JUAN F. KUON in partial fulfilment of the requirements for the degree of Doctor of Philosophy.

(Supervisor)

(External Examiner)

Date October 5 1975

To My Parents

ABSTRACT

Several multivariable frequency domain techniques that can be used to assist with the design of linear, feedback control systems are investigated and compared with other methods. The inverse Nyquist array, the characteristic locus, the direct Nyquist array, the optimal quadratic and the multiloop methods are evaluated, by experimental application to a double-effect, pilot plant evaporator.

The direct Nyquist array method was derived by direct, intuitive extension of the conventional single-input, single-output, Nyquist design procedure and also based on the same theory that underlies the inverse Nyquist array and characteristic locus methods. It was concluded that the direct Nyquist array technique is a more practical and convenient design technique than the inverse Nyquist array and the characteristic locus methods and the intuitive development provides greater insight into the physical meaning of each step in the design procedure. The direct Nyquist array method was also applied to to the design of a control system for a binary distillation column model which contained pure time delays.

The characteristic locus method was found to be slightly more general, but less practical, than either the direct or the inverse Nyquist array methods.

The three frequency domain design techniques were also compared with a multiloop control scheme and the optimal regulator control method. All of the multivariable techniques were found to produce better control of the evaporator than the multiloop control scheme. The frequency domain techniques produce controllers that gave closed-loop performance equivalent to other multivariable schemes but

gave the designer better insight and opportunity for incorporating practical factors such as integrity, into the design, than optimal control techniques.

ACKNOWLEDGEMENT

The author wishes to express his deep and sincere gratitude to Dr. D. G. Fisher for his guidance, enthusiasm and understanding throughout the course of the research.

The author is also grateful to Dr. R. K. Wood for providing the distillation column model which was used in this study and to Dr. D. E. Seborg for commenting on the rough draft of this thesis. Special thanks are also due to Dr. J. Belletrutti, the external examiner, for his helpful comments and suggestions on all aspects of frequency domain techniques.

The author's thanks are further extended to the members of the control research group for providing a stimulating and warm atmosphere, and to the DACS center personnel for their technical assistance.

Financial support from the National Research Council of Canada and the University of Alberta is gratefully acknowledged.

TABLE OF CONTENTS

PAGE

LIST OF TABLES xiv

LIST OF FIGURES xvi

CHAPTER ONE : INTRODUCTION 1

1.1 Objectives of This Study 3

1.2 Structure of the Thesis 4

1.3 Comments on the Thesis Format and Use 5

CHAPTER TWO : LITERATURE SURVEY OF MULTIVARIABLE FREQUENCY DOMAIN TECHNIQUES 8

2.1 Introduction 8

2.2 Multiloop Control System Design 9

2.3 Multivariable Control System Design 13

2.3.1 Non-interacting Design Techniques 14

2.3.2 Inverse Nyquist Array Technique 15

2.3.3 Commutative Controller Method 16

2.3.4 Characteristic Locus Method 18

2.3.5 Direct Nyquist Array Method 21

2.3.6 Sequential Return-difference Method 22

2.3.7 Owen's Modification of the Sequential Return-difference Method 24

2.3.8 Another Modification of the Sequential Return-difference Matrix 26

2.4 Conclusions 28

PAGE

CHAPTER THREE : THE INVERSE NYQUIST ARRAY METHOD 29

3.1 Introduction 29
3.2 The Inverse Nyquist Method 30
3.3 The Inverse Nyquist Array Method 33
3.4 Use of a Bilinear Transformation 42
3.5 An Alternative to the Inverse Nyquist Method 43
3.6 Design of a Multivariable Regulator for the Third Order Evaporator Model 43
3.7 Design of a Multivariable Regulator for the Fifth Order Evaporator Model 54
3.8 Conclusions 66

CHAPTER FOUR : THE CHARACTERISTIC LOCUS METHOD 68

4.1 Introduction 68
4.2 The Characteristic Locus Method 69
    4.2.1 Basic Theory 69
    4.2.2 Design Objectives: Stability, Integrity, Non-interaction and Accuracy 72
    4.2.3 Design Procedure 75
    4.2.4 General Comments 76
4.3 Design of a Multivariable Regulator for the Third Order Evaporator Model 80
4.4 Conclusions 88

PAGE

CHAPTER FIVE : THE DIRECT NYQUIST ARRAY METHOD 90

5.1 Introduction 90

5.2 The Direct Nyquist Array Method 91

5.2.1 Stability Criterion 91

5.2.2 Design Procedure 93

5.2.3 Advantages of the Direct Nyquist Array Method 95

5.3 Development of The Direct Nyquist Array Method by Extension of Conventional Design Techniques 96

5.3.1 Formulation of the Design Problem 97

5.3.2 Development of the Transfer Function Relating Each Input-Output Pair 100

5.3.3 Development of the Multivariable Frequency Domain Design Method 104

5.3.3.1 Direct Application of Nyquist Techniques to Each Input-Output . 104

5.3.3.2 Development of a Practical Frequency Domain Design Method . 105

5.3.4 Extensions to the Direct Nyquist Array Method 109

5.3.5 Conclusions 111

5.4 Design of a Multivariable Regulator for the Third Order Evaporator Model 112

5.5 Design of a Multivariable Regulator for the Fifth Order Evaporator Model 119

PAGE

5.6 Conclusions 134

CHAPTER SIX : EXPERIMENTAL RESULTS AND COMPARISON WITH OTHER METHODS 136

6.1 Introduction 136

6.2 Experimental Tuning of the Constant Compensator Obtained for the Third and Fifth Order Models Using the Inverse, Direct Nyquist Array and Characteristic Locus Methods 141

6.2.1 Selection of the Proportional Gains 141

6.2.2 Selection of the Integral Constants 145

6.3 Experimental Tuning of the Dynamic Compensator for the Fifth Order Model Obtained Using the Inverse and Direct Nyquist Array Methods 146

6.4 Experimental Results with the Optimal Regulator Control Method and the Third Order Evaporator Model 149

6.4.1 Proportional Control 151

6.4.2 Proportional-Integral Control 152

6.5 Experimental Results with the Optimal Regulator Control Method and the Fifth Order Evaporator Model 153

6.5.1 Proportional Control 153

6.5.2 Proportional-Integral Control 154

6.6 Experimental Results Using a Multiloop Control Scheme 155

PAGE

6.7 Comparison and Conclusions of the Experimental Results 157

6.7.1 Proportional Versus Proportional-Integral Control 157

6.7.2 About the Control System Design Method ... 158

6.7.3 About the Order of the Model 160

6.7.4 The Effect of Diagonal Dominance 161

CHAPTER SEVEN : CONTROL SYSTEM DESIGN FOR MULTIVARIABLE PROCESSES CONTAINING TIME DELAYS 164

7.1 Introduction 164

7.2 Design of a Control System for a Binary Distillation Column Model with Time Delays 165

7.3 Conclusions 175

CHAPTER EIGHT : CONCLUSIONS AND FURTHER RESEARCH 176

8.1 Contributions 176

8.2 Comparison of Frequency Domain Techniques and State Space Methods 176

8.3 Comparison of Frequency Domain Design Methods 178

8.4 Further Research 183

NOMENCLATURE 323

REFERENCES 328

ADDITIONAL REFERENCES 334

APPENDICES

A - Pilot Plant Evaporator and its models 335

PAGE

B - Controller Matrices 341

C - Limiting Values for the $\phi_{ji}(z)$ Factors 350

D - Stability Theorem 355

E - Diagonalization of the Double-Effect Pilot Plant Evaporator 359

LIST OF TABLES

TABLE	TITLE	PAGE
3.1	z-Transfer Function Matrix Derived from the Third Order Evaporator Model	45
3.2	w-Transfer Function Matrix Derived from the Third Order Evaporator Model	46
3.3	Poles of the Third Order Evaporator Model	46
3.4	Inverse of the w-Transfer Function Matrix Based on the Third Order Evaporator Model	47
3.5	z-Transfer Function Matrix Derived from the Fifth Order Evaporator Model	55
3.6	w-Transfer Function Matrix Derived from the Fifth Order Evaporator Model	56
3.7	Poles of the Fifth Order Evaporator Model	54
3.8	Inverse of w-Transfer Function Matrix Derived from the Fifth Order Evaporator Model	58
6.1	Experimental Runs Performed in this Study	139
6.2	Control Settings for Multiloop Runs	157
7.1	Distillation Column Transfer Function Matrix	167
A.1	Description of the Evaporator Variables	338
A.2	Fifth Order Discrete Evaporator Model	339
A.3	Third Order Discrete Evaporator Model	340
B.1	Proportional Control Matrices Designed for the Third and Fifth Order Evaporator Model Using the Inverse Nyquist Array, the characteristic Locus and the Direct Nyquist Array Method	342
B.2	Proportional-Integral Control Matrices Designed for the Third and Fifth-Order Evaporator Model Using the Inverse Nyquist Array, the Characteristic Locus and the Direct Nyquist Array Method	344

List of Tables (continued)

B.3 Dynamic Compensator Matrices Designed for the Fifth Order Model Using the Inverse and Direct Nyquist Array Methods 345

B.4 Proportional Control Matrices Designed for the Fifth Order Model using the Direct Nyquist Array Method 347

B.5 Explanation of the Code used for Figures 348

LIST OF FIGURES

FIGURE PAGE

2.1 Multivariable Feedback Control System Expressed in a Block Diagram Notation 186

2.2 Schematic Diagram of the Sequential Return-Difference Method 187

2.3 Multivariable Feedback Control System with all the Loops Open. 188

2.4 Schematic Diagram of the Sequential Return-Difference Method Using Full Output Feedback 189

2.5 Schematic Diagram of a Modification of the Sequential Return-Difference Method 190

3.1 Nyquist Contour in the z-Plane 191

3.2 Nyquist Contour in the w-Plane 192

3.3 Inverse Nyquist Array of $G(w)$ /G=3/ 0.1 to 10.0 /$G^{-1}(w)$ / $K = I$/ 193

3.4 Diagonal Elements of $G^{-1}(w)$ with their Gershgorin Bands /G=3/ 0.1 to 10.0/ $G^{-1}(W)$ / $K = I$/ 194

3.5 Inverse Nyquist Array of $Q_1(w)$ /G=3/ 0.1 to 10.0/ $Q_1^{-1}(w)$ /$K^{-1} = (3.25)$/ 195

3.6 Diagonal Elements of $Q_1^{-1}(w)$ with their Gershgorin Bands /G=3/ 0.1 to 10.0/ $Q_1^{-1}(w)$/ $K_1^{-1} = (3.25)$/ 196

3.7 Inverse Nyquist Array of $Q_2(w)$ /G=3/ 0.1 to 10.0/ $Q_2^{-1}(w)$/ $K_2^{-1}K_1^{-1} = (3.28)$/ 197

3.8 Diagonal Elements of $Q_2^{-1}(w)$ with their Gershgorin Bands /G=3/ 0.1 to 10.0/ $Q_2^{-1}(w)$/ $K_2^{-1}K_1^{-1} = (3.28)$/ 198

3.9 Inverse Nyquist Array of $Q_3(w)$ /G=3/ 0.1 to 10.0/ $Q_3^{-1}(w)$/ $K_3^{-1}K_2^{-1}K_1^{-1} = (3.32)$/ 199

3.10 Diagonal Elements of $Q_4^{-1}(w)$ with their Gershgorin Bands /G=3/ 0.1 to 10.0/ $Q_2^{-1}(w)$/ $K_4^{-1}K_3^{-1}K_2^{-1}K_1^{-1} = (3.32)$/ 200

FIGURE PAGE

3.11 Effect of Increasing the Gains in Constant Compensator from Frequency Domain Techniques FD0310: ++++, FD0320: ----, FD0330: — —, FD0350: —— /G=3/ FD0310/ 0320/ 0330/ 0350/ SIM 3/ K= Table B.1/ INA + CL/ P/ ± 20% F/ 201

3.12 Effect of Using the Ultimate Gains in Constant Compensator from Frequency Domain Techniques /G=3/ FD0390/ SIM 3/ K = Table B.1/ INA + DNA + CL/ P/ + 20% F/ 202

3.13 Effect of Increasing the Gains in Constant Compensator from Frequency Domain Technique for a Step Change in Setpoint of C_2 FD0320: ----, FD0350: —— /G=3/ FD0320/ 0350/ SIM 3/ K = Table B.1/ INA + DNA + CL/ P/ + 10% C_2/ 203

3.14 Inverse Nyquist Array of G(w) /G=5/ 0.1 to 1.0/ $G^{-1}(w)$/ K = I/ 204

3.15 Diagonal Elements of $G^{-1}(w)$ with their Gershgorin Bands /G=5/ 0.1 to 1.0/ $G^{-1}(w)$/ K = I/ 205

3.16 Inverse Nyquist Array of $Q_1(w)$ /G=5/ 0.1 to 1.0/ $Q_1^{-1}(w)$/ K_1^{-1} = (3.39)/ 206

3.17 Diagonal Elements of $Q_1^{-1}(w)$ with their Gershgorin Bands /G=5/ 0.1 to 1.0/ $Q_1^{-1}(w)$/ K_1^{-1} = (3.39)/ 207

3.18 Inverse Nyquist Array of $Q_2(w)$ /G=5/ 0.1 to 1.0 $Q_2^{-1}(w)$/ $K_2^{-1}K_1^{-1}$ = (3.40)(3.39)/ 208

3.19 Diagonal Elements of $Q_2^{-1}(w)$ with their Gershgorin Bands /G=5/ 0.1 to 1.0/ $Q_2^{-1}(w)$/ $K_2^{-1}K_1^{-1}$ = (3.40)(3.39)/ 209

3.20 Inverse Nyquist Array of $Q_3(w)$ /G=5/ 0.1 to 1.0/ $Q_3^{-1}(w)$/ $K_3^{-1}K_2^{-1}K_1^{-1}$ = (3.42) (3.40)(3.39)/ 210

3.21 Diagonal Elements of $Q_3^{-1}(w)$ with their Gershgorin Bands /G=5/ 0.1 to 1.0 $Q_3^{-1}(w)$/ $K_3^{-1}K_2^{-1}K_1^{-1}$ = (3.42) (3.40)(3.39)/ 211

FIGURE		PAGE
3.22	Inverse Nyquist Array of $Q_4(w)$ /G=5/ 0.1 to 1.0/ $Q_4^{-1}(w)$/ $K_4^{-1}K_3^{-1}K_2^{-1}K_1^{-1}$ = (3.43)(3.42)(3.40)(3.39)/	212
3.23	Diagonal Elements of $Q_4^{-1}(w)$ with their Gershgorin Bands /G=5/ 0.1 to 1.0/ $Q_4^{-1}(w)$/ $K_4^{-1}K_3^{-1}K_2^{-1}K_1^{-1}$ = (3.43)(3.42)(3.40)(3.39)/	213
3.24	Diagonal Elements of $Q_5^{-1}(w)$ with their Gershgorin Bands /G=5/ 0.01 to 1.0/ $Q_5^{-1}(w)$/ K_5^{-1} ... K_1^{-1} = (3.44) ... (3.39)/	214
3.25	Diagonal Elements of $Q_5^{-1}(w)$ with their Gershgorin Bands /G=5/ 0.01 to 0.5/ $Q_5^{-1}(w)$/ K_5^{-1} ... K_1^{-1} = (3.44) ... (3.39)/	215
3.26	Diagonal Elements of $Q_5(w)$ with their Gershgorin Bands /G=5/ 0.1 to 5.0/ $Q_5^{-1}(w)$/ $K_5^{-1}K_4^{-1}$ ... K_1^{-1} = (3.44)(3.43) ... (3.39)/	216
3.27	Inverse Nyquist Array of $Q_2^{1}(w)$ /G=5/ 0.1 to 1.0/ $(Q_2^{1}(w))^{-1}$/ $(K_2^{1})^{-1}K_1^{-1}$ = (3.45)(3.39)/	217
3.28	Diagonal Elements of $(Q_2^{1}(w))^{-1}$ with their Gershgorin Bands /G=5/ 0.1 to 1.0/ $(Q_2^{1}(w))^{-1}$/ $(K_2^{1})^{-1}K_1^{-1}$ = (3.45)(3.39)/	218
3.29	Inverse Nyquist Array of $Q_3^{1}(w)$ /G=5/ 0.1 to 1.0/ $(Q_3^{1}(w)^{-1}$/ $(K_2^{1})^{-1}K_1^{-1}$ = (3.45)(3.39)/	219
3.30	Diagonal Elements of $(Q_3^{1}(w))^{-1}$ with their Gershgorin Bands /G=5/ 0.1 to 1.0/ $(Q_3^{1}(w))^{-1}$/ $(K_3^{1})^{-1}(K_2^{1})^{-1}$ = (3.47)(3.45)(3.39)/	220
3.31	Inverse Nyquist Array of $Q_4^{1}(w)$ (G=5/ 0.1 to 1.0/ $(Q_4^{1}(w))^{-1}$/ $K_4^{1})^{-1}(K_3^{1})^{-1}$ $(K_2^{1})^{-1}(K_1)^{-1}$ = (3.50)(3.47)(3.45)(3.39)/	221
3.32	Diagonal Elements of $(Q_4^{1}(w))^{-1}$ with their Gershgorin Bands /G=5/ 0.1 to 1.0/ $(Q_4^{1}(w)^{-1}$/ $(K_4^{1})^{-1}(K_3^{1})^{-1}$ $K_2^{1})^{-1}(K_1)^{-1}$ = (3.50) (3.47)(3.45)(3.39)/	222

FIGURE PAGE

3.33 Diagonal Elements of $(Q_5^1(w)^{-1}$ with their Gershgorin Bands
/G=5/ 0.1 to 1.0/ $(Q_5^1(w))^{-1}$/ $(K_5^1)^{-1}(K_4^1)^{-1}$ ... $(K_1^1)^{-1}$ = (3.53)(3.50) ... (3.39)/ 223

3.34 Diagonal Elements of $(Q_6^1(w))^{-1}$ with their Gershgorin Bands
/G=5/ 0.1 to 1.0/ $Q_6^1(w))^{-1}$/ $(K_6^1\ )^{-1}(K_5^1)^{-1}$ ... $(K_1^1)^{-1})^{-1}$ = (3.55)/ 224

3.35 Effect of the Proportional and Dynamic Compensator from Frequency Domain Techniques
FD0310: ----, NADY0510: ——
/G-3,5/ FD0310/ NADY0310/ SIM 5/ K = Tables B.1, B.3/ INA + DNA/ + 20% F/ 225

3.36 Effect of the Proportional and Dynamic Compensator from Frequency Domain Techniques
FD0320: ----, NADY0320: ——
/G=3,5/ FD0320/ NADY0320/ SIM 5/ K = Tables B.1, B.3/ INA + DNA/ + 20% F/ 226

3.37 Effect of the Proportional and Dynamic Compensator from Frequency Domain Techniques
FD0330: ----, NADY0330: ——
/G=3,5/ FD0330/ NADY0330/ SIM 5/ K = Tables B.1, B.3/ INA + DNA/ + 20% F/ 227

3.38 Effect of the Proportional and Dynamic Compensator from Frequency Domain Techniques for a Step Change in Setpoint of C_2
FD0320: ----, NADY0520: ——
/G=3,5/ FD0320/ NADY0320/ SIM 5/ K = Tables B.1, B.3/ INA + DNA/ + 10% C_2/ 228

4.1 Characteristic Locus No. 1 of G(w)
/G=3/ 0.1 to 10.0 /CL/ G(w) /K=1/
a) Characteristic locus
b) Magnitude of characteristic locus
c) Alignment of the corresponding eigenvector 229

4.2 Characteristic Locus No. 2 of G(w)
/G=3/ 0.1 to 10.0 /CL/ G(w) /K=1/
a) Characteristic locus
b) Magnitude of characteristic locus
c) Alignment of the corresponding eigenvector 230

FIGURE PAGE

4.3 Characteristic Locus No. 3 of G(w)
/G=3/ 0.1 to 10.0 /CL/ G(w) /K=1/
a) Characteristic locus
b) Magnitude of characteristic locus
c) Alignment of the corresponding eigenvector 231

4.4 Characteristic Locus No. 1 of $Q_1(w)$
/G=3/ 0.1 to 10.0 /CL/ $Q_1(w)$ /K_1^1 = (4.23)/
a) Characteristic locus
b) Magnitude of the characteristic locus
c) Alignment of the corresponding eigenvector 232

4.5 Characteristic Locus No. 2 of $Q_1(w)$
/G=3/ 0.1 to 10.0 /CL/ $Q_1(w)$ K_1^1 = /(4.23)/
a) Characteristic locus
b) Magnitude of the characteristic locus
c) Alignment of the corresponding eigenvector 233

4.6 Characteristic Locus No. 3 of $Q_1(w)$
/G=3/ 0.1 to 10.0 /CL/ $Q_1(w)$ /K_1^1 = (4.23)/
a) Characteristic locus
b) Magnitude of the characteristic locus
c) Alignment of the corresponding eigenvector 234

4.7 Characteristic Locus No. 1 of $Q_2(w)$
/G=3/ 0.1 to 10.0 /CL/ $Q_2(w)$ /K_1K_2 = (4.25)(423)/
a) Characteristic locus
b) Magnitude of the characteristic locus
c) Alignment of the corresponding eigenvector 235

4.8 Characteristic Locus No. 2 of $Q_2(w)$
/G=3/ 0.1 to 10.0 /CL/ $Q_2(w)$ /K_1K_2 = (4.25)(4.23)/
a) Characteristic locus
b) Magnitude of the characteristic locus
c) Alignment of the corresponding eigenvector 236

4.9 Characteristic Locus No. 3 of $Q_2(w)$
/G=3/ 0.1 to 10.0 /CL/ $Q_2(w)$ /K_1K_2 = (4.25)(4.23)/
a) Characteristic locus
b) Magnitude of the characteristic locus
c) Alignment of the corresponding eigenvector 237

4.10 Characteristic Locus No. 1 of $Q_1^1(w)$
/G=3/ 0.1 to 10.0 /CL/ $Q_1 1(w)$ $K_1 1$ = (4.28)/
a) Characteristic locus
b) Magnitude of the characteristic locus
c) Alignment of the corresponding eigenvector 238

FIGURE PAGE

4.11 Characteristic Locus No. 2 of $Q_1^1(w)$
/G=3/ 0.1 to 10.0 /CL/ $Q_1^1(w)$ /K_1^1 = (4.28) /
a) Characteristic locus
b) Magnitude of the characteristic locus
c) Alignment of the corresponding vector 239

4.12 Characteristic Locus No. 3 of $Q_1^1(w)$
/G=3/ 0.1 to 10.0 /CL/ $Q_1^1(w)$ /K_1^1 = (4.28)/
a) Characteristic locus
b) Magnitude of the characteristic locus
c) Alignment of the corresponding eigenvector 240

4.13 Characteristic Locus No. 1 of $Q_2^1(w)$
/G=3/ 0.1 to 10.0 /CL/ $Q_2^1(w)$ /$K_1K_2^1$ = (4.32)/
a) Characteristic locus
b) Magnitude of the characteristic locus
c) Alignment of the corresponding eigenvector 241

4.14 Characteristic Locus No. 2 of $Q_2^1(w)$
/G=3/ 0.1 to 10.0 /CL/ $Q_2^1(w)$ /$K_1^1K_2^1$ = (4.32)/
a) Characteristic locus
b) Magnitude of the characteristic locus
c) Alignment of the corresponding eigenvector 242

4.15 Characteristic Locus No. 3 of $Q_2^1(w)$
/G=3/ 0.1 to 10.0 /CL/ $Q_2^1(w)$ /$K_1K_2^1$ = (4.32)/
a) Characteristic locus
b) Magnitude of the characteristic locus
c) Alignment of the corresponding eigenvector 243

5.1 Multivariable Feedback Control System Expressed in Block Diagram Notation with an Open-Loop Transfer Function Matrix $Q(z) = G(z)\ K(z)$ 244

5.2 An Expanded Representation of an Augmented Multivariable System

5.3 Two-Input Two-Output System with One Loop Closed 246

5.4 Nyquist Array of $G(w)$
/G=3/ 0.15 to 10.0/ $G(w)$/ $K = I$/ 247

5.5 Diagonal Elements of $G(w)$ with their Gershgorin Bands
/G=3/ 0.15 to 10.0/ $G(w)$/ $K = I$/ 248

5.6 Nyquist Array of $Q_1(w)$
/G=3/ 0.15 to 10.0/ $Q_1(w)$/ K_1 = (5.25)/ 249

5.7 Diagonal Elements of $Q_1(w)$ with their Gershgorin Bands
/G=3/ 0.15 to 10.0/ $Q_1(w)$/ K_1 = (5.25)/ 250

FIGURE PAGE

5.8 Nyquist Array of $Q_2(w)$
/G=3/ 0.15 to 10.0/ $Q_2(w)$/ K_1K_2 = (5.25)(5.26)/ 251

5.9 Diagonal Elements of $Q_2(w)$ with their Gershgorin Bands
/G=3/ 0.15 to 10.0/ $Q_2(w)$/ K_1K_2 = (5.25)(5.26)(5.28)/ 252

5.10 Nyquist Array of $Q_3(w)$
/G=3/ 0.15 to 10.0/ $Q_3(w)$/ $K_1K_2K_3$ = (5.25)(5.26)(5.28)/ 253

5.11 Diagonal Elements of $Q_3(w)$ with their Gershgorin Bands
/G=3/ 0.15 to 10.0/ $Q_3(w)$/ $K_1K_2K_3$ = (5.25)(5.26)(5.28)/ 254

5.12 Diagonal Elements of $Q_4(w)$ with their Gershgorin Bands
/G=3/ 0.15 to 10.0/ $Q_4(w)$/ $K_1K_2K_3K_4$ = (5.25)(5.26)(5.28)(5.29)/ 255

5.13 Diagonal Elements of $Q_5(w)$ with their Gershgorin Bands
/G=3/ 0.15 to 10.0/ $Q_5(w)$/ $K_1K_2K_3K_4K_5$ = (5.32)/ 256

5.14 Nyquist Array of G(w)
/G=5/ 0.1 to 5.0/ G(w)/ K = I/ 257

5.15 Diagonal Elements of G(w) with their Gershgorin Bands
/G=5/ 0.1 to 5.0/ G(w)/ K = I/ 258

5.16 Nyquist Array of $Q_1(w)$
/G=5/ 0.1 to 5.0/ $Q_1(w)$/ K_1 = 5.43)/ 259

5.17 Diagonal Elements of $Q_1(w)$ with their Gershgorin Bands
/G=5/ 0.1 to 5.0/ $Q_1(w)$/ K_1 = (5.43)/ 260

5.18 Nyquist Array of $Q_2(w)$
/G=5/ 0.1 to 5.0/ $Q_2(w)$/ K_1K_2 = (5.43)(5.44)/ 261

5.19 Diagonal Elements of $Q_2(w)$ with their Gershgorin Bands
/G=5/ 0.1 to 5.0/ $Q_2(w)$/ K_1K_2 = (5.43)(5.44)/ 262

5.20 Nyquist Array of $Q_3(w)$
/G=5/ 0.1 to 5.0/ $Q_3(w)$/ $K_1K_2K_3$ = (5.43)(5.44)(5.45)/ 263

FIGURE PAGE

5.21 Diagonal Elements of $Q_3(w)$ with their Gershgorin Bands /G=5/ 0.1 to 5.0/ $Q_3(w)$/ $K_1K_2K_3$ = (5.43)(5.44)(5.45)/ 264

5.22 Nyquist Array of $Q_4(w)$ /G=5/ 0.1 to 5.0/ $Q_4(w)$/ $K_1K_2K_3K_4$ = (5.43)(5.44)(5.45)(5.47)/ 265

5.23 Diagonal Elements of $Q_4(w)$ with their Gershgorin Bands /G=5/ 0.1 to 5.0/ $Q_4(w)$/ $K_1K_2K_3K_4$ = (5.43)(5.44)(5.45)(5.47)/ 266

5.24 Nyquist Array of $Q_5(w)$ /G=5/ 0.1 to 5.0/ $Q_5(w)$/ $K_1K_2K_3K_4K_5$ = (5.51)/ 267

5.25 Diagonal Elements of $Q_5(w)$ with their Gershgorin Bands /G=5/ 0.1 to 5.0/ $Q_5(w)$/ $K_1K_2K_3K_4K_5$ = (5.51)/ 268

5.26 Nyquist Array of $Q_6(w)$ /G=5/ 0.1 to 5.0/ $Q_6(w)$/ $K_1K_2K_3K_4K_5K_6$ = (5.53)/ 269

5.27 Diagonal Elements of $Q_6(w)$ with their Gershgorin Bands /G=5/ 0.1 to 5.0/ $Q_6(w)$/ $K_1K_2K_3K_4K_5K_6$ = (5.53)/ 270

5.28 Nyquist Array of $Q_3^1(w)$/ $K_1K_2K_3^1$ = (5.43)(5.44)(5.55)/

5.29 Diagonal Elements of $Q_3^1(w)$ with their Gershgorin Bands /G=5/ 0.1 to 5.0/ $Q_3^1(w)$/ $K_1K_2K_3^1$ = (5.43)(5.44)(5.55)/ 272

5.30 Nyquist Array of $Q_4^1(w)$ /G=5/ 0.1 to 5.0/ $Q_4^1(w)$/ $K_1K_2K_3^1K_4^1$ = (5.43)(5.44)(5.55)(5.58)/ 273

5.31 Diagonal Elements of $Q_4^1(w)$ with their Gershgorin Bands /G=5/ 0.1 to 5.0/ $Q_4^1(w)$/$K_1K_2K_3^1K_4^1$ = (5.43)(5.44)(5.55)(5.58)/ 273

5.32 Nyquist Array of $Q_5^1(w)$ /G=5/ 0.1 to 5.0/ $Q_5^1(w)$/ $K_1K_2K_3K_4^1K_5^1$ = (5.43)(5.44)(5.55)(5.58)(5.60)/ 275

FIGURE PAGE

5.33 Diagonal Elements of $Q_5^1(w)$ with their Gershgorin Bands /G=5/ 0.1 to 5.0/ $Q_5^1(w)$/ $K_1K_2K_3K_4K_5^1$ = (5.43) (5.44)(5.55)(5.58)(5.60)/ 276

5.34 Diagonal Elements of $Q_6^1(w)$ with their Gershgorin Bands /G=5/ 0.1 to 5.0/ $Q_6^1(w)$/ $K_1K_2K_3^1K_4^1K_5^1K_6^1$ = (5.64)/ 277

5.35 Stable Gain Space for the Fifth Order Evaporator Model when using the compensator given by Equation (5.54).

5.36 Effect of Improving Diagonal Dominance in the Open-Loop Compensated Plant Controller K (Equation 5.51): — —; Controller K_B (Equation 5.53): ----, Controller $K_B^{\dagger}$ (Equation 5.65): —— /G=5/OL005 / SIM 5/ K = (5.51),(5.53),(5.65)/ DNA/ 5% C_2/ 279

5.37 Effect of Improving Diagonal Dominance in the Closed-Loop Evaporator. DNA0520: — —, FD0320: ------, NADY0520: ——— /G=5/ DNA0520/ FD0320/ NADY0520/ SIM 5/ K = Table B.1,B.3,B.4/ DNA/ P/ + 20% F/ 280

5.38 Effect of Improving Diagonal Dominance in the Closed-Loop Evaporator for a Step Change in a Setpoint. Controller K_A (Equation 5.51): — — Controller K_B (Equation 5.53): ----, Controller $K_B^{\dagger}$ (Equation 5.65): —— /G=5/ DNA0520/ FD0320/ NADY0520/ SIM 5/ K = Table B.1, B.3, B.4/ DNA/ P/ + 10% C_2/ 281

6.1 Experimental Proportional Controller FD0310 from Frequency Domain Techniques /G=3,5/ FD0310/ Exp/ K = Table B.1/ INA + DNA + CL/ P/ ± 20% F/ 0/ 282

6.2 Experimental Proportional Controller FD0320 from Frequency Domain Techniques /G=3,5/ FD0320/ Exp/ K = Table B.1/ INA + DNA + CL/ P/ ± 20% F/ 0/ 283

6.3 Experimental Proportional Controller FD0330 from Frequency Domain Techniques /G=3,5/ FD0330/ Exp/ K = Table B.1/ INA + DNA + CL/ P/ ± 20% F/ 0/ 284

FIGURE PAGE

6.4 Experimental Proportional Controller FD0320 from Frequency Domain Techniques /G=3,5/ FD0320/ Exp/ K = Table B.1/ INA + DNA + CL/ P/ ± 20% FC/ 0/ 285

6.5 Experimental Setpoint Change Using Proportional Controller FD0320 from Frequency Domain Techniques /G=3,5/ FD0320/ Exp/ K = Table 3.1/ INA + DNA + CL/ P/ ± 10% C_2/ 0/ 286

6.6 Experimental Setpoint Change Using Proportional Controller FD0320 from Frequency Domain Techniques /G=3,5/ FD0320/ Exp/ K Table 3.1/ INA + DNA + CL/ P/ ± 10% C_2/ 0/ 287

6.7 Experimental Proportional-integral Controller FD1320 from Frequency Domain Techniques /G=3,5/ FD1320/ Exp/ K = Table B.2/ INA + DNA + CL/ P + I/ ± 20% F/ 0/ 288

6.8 Experimental Proportional-integral Controller FD1315 from Frequency Domain Techniques /G=3,5/ FD1315/ Exp/ K = Table B.2/ INA +DNA + CL/ P + I/ ± 20% F/ 0/ 289

6.9 Experimental Proportional-integral Controller FD1315.1 from Frequency Domain Techniques /G=3,5/ FD1315.1/ Exp/ K = Table B.2/ INA + DNA + CL/ P + I/ ± 20% F/ 0/ 290

6.10 Experimental Dynamic Controller NADY0510 from Frequency Domain Techniques /G=5/ NADY0510/ Exp/ K = Table B.3/ INA + DNA/ D + P/ ± 20% F/ 0/ 291

6.11 Experimental Dynamic Controller NADY0520 from Frequency Domain Techniques /G=5/ NADY0520/ Exp/ K = Table B.3/ INA + DNA/ D + P/ ± 20% F/ N/ 292

6.12 Experimental Dynamic Controller NADY0530 from Frequency Domain Techniques /G=5/ NADY0530/ Exp/ K = Table B.3/ INA + DNA/ D + P/ ± 20% F/ N/ 293

FIGURE PAGE

6.13 Experimental Dynamic Controller NADY0540 from Frequency Domain Techniques /G=5/ NADY0540/ Exp/ K = Table B.3/ INA + DNA/ D + P/ ± 10% F/ N/ 294

6.14 Experimental Setpoint Change Using Dynamic Controller NADY0520 from Frequency Domain Techniques /G=5/ NADY0520/ Exp/ K = Table B.3/ INA + DNA/ D + P/ ± 10% C_2/ N/ 295

6.15 Experimental Proportional Controller FD0520 from Frequency Domain Techniques /G=3,5/ FD0520/ Exp/ K = Table B.1/ INA + DNA + CL/ P/ ± 20% F/ N/ 296

6.16 Experimental Proportional Controller FD0530 from Frequency Domain Techniques /G=3,5/ FD0530/ Exp/ K = Table B.1/ INA + DNA + CL/ P/ ± 20% F / N/ 297

6.17 Experimental Setpoint Change Using Proportional Controller FD0520 from Frequency Domain Techniques /G=3,5/ FD0520/ Exp/ K = Table B.1/ INA + DNA +CL/ P/ ± 20% F/ N/ 298

6.18 Experimental Optimal Proportional Controller OP0501 /G=5/ OP0501/ Exp/ K = (6.19)/ OPT/ P/ ± 20% F/ N/ 299

6.19 Experimental Optimal Proportional Controller OP0300 /G=3/ OP0300/ Exp/ K = (6.13)/ OPT/ P/ ± 20% F/ O/ 300

6.20 Experimental Optimal Proportional Controller OP0300 /G=3/ OP0300/ Exp/ K = (6.13)/ OPT/ P/ ± 20% FC/ O/ 301

6.21 Experimental Optimal Proportional-integral Controller OP1300 /G=3/ OP1300/ Exp/ K = (6.15)(6.16)/ OPT/ P + I/ ± 20% F/ O/ 302

6.22 Experimental Optimal Proportional Controller OP0500 /G=5/ OP0500/ Exp/ K = (6.19)/ OPT/ P/ ± 20% F/ N/ 303

FIGURE PAGE

6.23 Experimental Optimal Proportional-integral Controller OP1500 /G=3/ ML0200/ Exp/ K = Table 6.1/ MUL/ P/ ± 20% F/ 0/ 304

6.24 Experimental Multiloop Proportional Controller ML0200 /G=3/ ML0200/ Exp/ K = Table 6.1/ MUL/ P/ ± 20% F/ 0/ 305

6.25 Experimental Multiloop Proportional Controller ML0200 /G=3/ ML0200/ Exp/ K= Table 6.1/ MUL/ P/ ± 20% FC/ 0/ 306

6.26 Experimental Multiloop Proportional-integral Controller ML1200 /G=3/ ML1200/ Exp/ K = Table 6.1/ MUL/ P/ ± 20% F/ 0/ 307

6.27 Experimental Proportional Controller DNA0520 from Nyquist Array Method /G=5/ DNA0 20/ Exp/ K = Table B.4/ DNA/ P/ ± 20% F/ 0/ 308

6.28 Experimental Proportional Controller DNA0520 from Nyquist Array Method /G=5/ DNA0520/ Exp/ K = Table B.4/ DNA/ P/ ±20% FC/ 0/ 309

6.29 Experimental Setpoint Change Using Proportional Controller DNA0520 from Nyquist Array Method /G=5/ DNA0520/ Exp/ K = Table B.4/ DNA/ P/ ± 10% C_2/ 0/ 310

7.1 Nyquist Array of the Distillation Column /G=DISC/ 0.1 to 3.0/ Q(s)/ K = 1/ 311

7.2 Diagonal Elements of the Distillation Column With Their Gershgorin Bands /G=DISC/ 0.1 to 3.0/ Q(s)/ K = 1/ 312

7.3 Nyquist Array of the OLTFM $Q_1(s)$ /G=DISC/ 0.1 to 3.0/ $Q_1(s)$/ K_1 = (7.2)/ 313

7.4 Diagonal Elements of $Q_1(s)$ With Their Gershgorin Bands /G=DISC/ 0.1 to 3.0/ $Q_1(s)$/ K_1 = (7.2)/ 314

FIGURE PAGE

7.5 Nyquist Array of the OLTFM $Q_2(s)$
/G=DISC/ 0.1 to 3.0/ $Q_2(s)$/ $K_1K_2 = (7.9)$/ 315

7.6 Diagonal Elements of $Q_2(s)$ with their Gershgorin Bands
/G=DISC/ 0.1 to 3.0/ $Q_2(s)$/ $K_1K_2 = (7.9)$/ 316

7.7 Nyquist Array of the OLTFM $Q_2(s)$ When a Second Order Pade Approximation is Used in Controller $K_2(s)$
/G=DISC/ 0.1 to 3.0/ $Q_2(s)$/ $K_1K_2 = (7.9)$/ 317

7.8 Diagonal Elements of $Q_2(s)$ when a Second Order Pade Approximation is Used in Controller $K_2(s)$
/G=DISC/ 0.1 to 3.0/ $Q_2(s)$/ $K_1K_2 = (7.9)$/ 318

7.9 Diagonal Elements of Non-interacting OLTFM $Q_2^1(s)$
/G= DISC/ 0.1 to 3.0/ $Q_2^1(s)$/ $K_1K_2^1 = (7.14)$/ 319

7.10 Simulated Response of the Distillation Column for a 14% Increase in Feed Flow Using a Multiloop Control 320

7.11 Simulated Response of the Distillation Column for a 14% Increase in Feed Flow Using a Diagonally Dominant Control System (Equation (7.9)) 321

7.12 Simulated Response of the Distillation Column for a 14% Increase in Feed Flow Using a Non-interacting Control (Equation (7.14)) 322

A.1 Schematic Diagram of the Double Pilot Plant Evaporator used for this work. 336

CHAPTER ONE

INTRODUCTION

During the last two decades considerable attention has been given to the design of multivariable control systems. Most of this attention has been focused on the development of new techniques which are based on the concepts of modern control theory and use a state-variable formulation. Unfortunately many of the state-variable methods have been found [16,26] to be of limited practical value in the design of multivariable control systems for chemical processes. The main reason for the limited success with these methods is due to the fact that modern control theory has arisen from the study of systems with significantly different characteristics than chemical processes. Because of this, these methods solve only a small portion of the total design requirements of these complex processes and the design usually requires measurements (or estimates) of the state variables which often are not available because of physical or economical constraints.

Furthermore, controllers designed using methods based on linear theory, but applied to systems that are inherently non-linear, usually require tuning when they are implemented in the field. The state-variable methods do not offer any guidance to the designer in the way the controller must be altered if an unsatisfactory solution is obtained. With most of these methods, the only alternative if a controller is found to be unsatisfactory is to redesign and retest it in the field.

On the other hand single-variable frequency-domain techniques have been found to be very effective in designing controllers for single-input, single-output systems. These techniques are applicable to systems that contain time delays which are commonly found in chemical processes and they provide the designer with information such as the gain margin, phase margin, crossover frequency, etc. which are very useful for the tuning of the controller in the field.

In spite of the success of single-variable frequency domain techniques, the extension of these techniques to multivariable control has received relatively little attention. Only in the last decade has this trend been redirected. It began with Rosenbrock [65] who developed the inverse Nyquist array method in the 1960's. Since then several techniques, which are essentially generalizations of the stability criteria introduced by Bode [7] and Nyquist [54] for single-variable systems, have been proposed [4,36,44,58]. Because of their recent development the experience with most of these methods is limited and, with the exception of the inverse Nyquist array method, experimental applications based on these methods have not been reported in the literature. Since most of these methods provide information similar to the single-variable techniques and produce a controller which is easily tuned in the field, it is foreseeable that they will play as important a role in the design of multivariable control systems as the single-variable frequency domain techniques did with single-variable processes. However there is still a need for additional study of these methods in order to improve them or to develop more practical methods which will make the design of control systems even easier. There is also a need for more applications of these methods to practical systems in order to encourage their use in industrial processes.

1.1 Objectives of This Study

Based on these considerations the study of the multivariable frequency domain design techniques was selected as the objective of this investigation. Because of the vastness of this field this study was limited, after a general review of this area, to a detailed evaluation of the methods which were considered to be the most promising techniques. This study has evaluated the inverse Nyquist array [65] and the characteristic locus method [4,42]. It has also developed and evaluated the "direct" Nyquist array method. Although the "direct" technique has been suggested [38,68,70,71] in the literature it has not been fully developed or applied. The direct Nyquist array method was derived, in this study, by two different approaches. First by modification and extension of the same theory that underlies the inverse Nyquist array and characteristic locus methods and secondly by extension of the single-variable frequency domain techniques using an intuitive approach. The evaluation of these methods has been concerned with several different features of the method: the theoretical aspects, their computer implementation and the application of these techniques to the design of a control system for the double-effect evaporator pilot plant located in the Department of Chemical Engineering at the University of Alberta.

Although it is not included as part of ~~this~~ thesis this study has also included the development of a computer-aided design package [29,30,31,32]. This program assists with the design of controllers based on the inverse Nyquist array, characteristic locus and direct Nyquist array methods. The package has been written in a user oriented form and the controller can be designed in an interactive way using a CRT computer terminal. This package has been incorporated as a part of the GEMSCOPE [14] package which operates on an IBM 360 series computer under the University of Michigan time-sharing system (MTS).

This investigation has also covered the comparison of these techniques with the optimal control method and the multiloop design approach based on the experimental results obtained by applying these methods to the double-effect evaporator pilot plant.

1.2 Structure of the Thesis

This thesis is divided in eight chapters. Chapter Two contains a survey of the frequency-domain design procedures which have been proposed to date. The inverse Nyquist array method is discussed in Chapter Three and two design examples are included which illustrate the use of this method. Chapter Four deals with the characteristic locus method and presents a design example using this technique.

In Chapter Five the attention is focused on the development and application of the direct Nyquist array method. This chapter is divided in three main parts. In the first part the direct Nyquist array method is derived based on concepts which were introduced in the development of the inverse Nyquist array [65] and the characteristic locus method [4,42]. In the second part the direct Nyquist array method is shown to be a direct and intuitive extension of single-input single-output design techniques. This is a self contained section and it is based on a report written by Fisher and Kuon [15]. In the last part the direct Nyquist array method is applied to design a control system for the double effect evaporator pilot plant.

The experimental evaluation of the controllers designed using frequency domain techniques is presented in Chapter Six and includes a comparison with controllers designed using the optimal control method and the multiloop design approach.

In Chapter Seven the direct Nyquist array method is used to design a control system for a multivariable process which contains time delays. A model [79] which represents the distillation column located at the Department of Chemical Engineering of the University of Alberta has been used in this example. Finally, in Chapter Eight, the overall conclusions of this work are summarized.

1.3 Comments on Thesis Format and Use

The following comments are included to assist the reader in identifying those parts of the thesis that are most directly applicable to his particular interests and needs:

1) The description of the inverse Nyquist array, characteristic loci, and direct Nyquist array methods in Chapters Three, Four and Five respectively, were written so that they could be read, or referred to, either sequentially or independently. This required some redundancy in discussing certain basic concepts and was the reason why material, such as the description of the evaporator, was placed in appendices. Specific comments were included, where appropriate, to point out the similarities and/or relationships between the different methods but these are not normally necessary to an understanding of any one method.

2) All the frequency domain techniques are interactive and require decisions and input at each step in the design procedure. These decisions are often subjective and each user would probably make different decisions and follow a slightly different path in designing a controller for a given application. Chapters Three, Four and Five contain rather detailed presen-

tations of the steps that the author took and comments about why these steps seemed appropriate. Each example is presented in a similar format to facilitate comparison of the "mechanics" of each method. If the computer aided design system is available locally some readers may prefer to skip over the details of each example and evaluate the methods by doing the examples themselves. The description of the examples is illustrative and not essential to the presentation of the theory and/or methods.

3) The main conclusion of this work is that the direct Nyquist array method is the preferred design technique and should be used in place of the other methods. This conclusion is subjective and application dependent, but readers willing to accept it may prefer to consider Chapters One through Four as primarily historical and theoretical background to Chapter Five.

4) Readers familiar with conventional single variable frequency domain techniques might prefer to read Section 5.3 before considering the details contained in the other chapters. (Section 5.3 is an intuitive explanation of the extension of single variable Nyquist techniques to the direct, multivariable Nyquist array approach.)

5) In order to handle practical problems, multivariable frequency domain design techniques require the use of interactive computer facilities to do the numerical calculations and plotting. This thesis is concerned with the design methods and the results of applying them to specific problems. The description of the computer programs, and instructions about how to use them, are contained in separate reports. (They are written so the user can apply them to practical problems without being familiar with all the theory and the "whys" discussed in this thesis.)

6) All of the figures discussed in Chapters Two through Seven are located in the section of the thesis immediately preceeding the bibliography. This was done to facilitate multiple references to the same figure and comparisons between figures. The figures showing Nyquist diagrams etc. are direct, electronic copies of the display on the CRT of the computer terminal.

CHAPTER TWO

LITERATURE SURVEY OF MULTIVARIABLE FREQUENCY DOMAIN TECHNIQUES

2.1 INTRODUCTION

Frequency domain techniques have proven to be efficient and effective design techniques for single variable feedback control problems since they were first introduced by Bode [7] and Nyquist [54]. However it was not until the 1960's that any significant progress was made in the application of frequency domain techniques to multivariable control problems. A very important contribution was the development of the inverse Nyquist array method by Rosenbrock [65]. Other important techniques for the design of multivariable control systems using frequency domain techniques include: the commutative controller [33,36], the characteristic locus method [4,5,41,42], and the sequential return-difference method [45,46,47]. Several modifications and extensions of these techniques have also been proposed in the literature [e.g. 57,58].

Development of frequency domain techniques for the design of multivariable control systems has proceeded along two main paths. First, a number of investigators have tried to modify the problem formation, or develop a design approach, to permit the use of classical single variable design techniques. Secondly, others have assumed a true multivariable formulation and developed new design techniques. However, almost all of the techniques can be interpreted as extensions and generalizations of the original work done by Bode and Nyquist.

The following sections contain a review of frequency domain techniques presented in an order intended to emphasize the progressive development and inter-relation of the various techniques. This survey is primarily concerned with the multivariable regulator problem and is restricted to techniques that can be used to assist with the design of linear feedback control systems which can be represented as shown in Figure 2.1. Unless it is otherwise stated the feedback transducer matrix will be considered to be an identity matrix since there is no loss of generality as far as the problem of determining system stability is concerned. All of the developments and equations are presented in terms of discrete systems but the analysis is also valid for continuous systems and most of them can be applied to systems represented by both square, and non-square, transfer function matrices. The theory of some of the approaches can also handle the inclusion of a post compensator matrix, L(z), (which comes immediately after G(z) in Figure 2.1) but this is not usually of practical importance because it implies control is exercised over a combination of the real plant output variables.

2.2 MULTILOOP CONTROL SYSTEM DESIGN

A common practice in the design of controllers for multivariable systems is to neglect the interactions that occur between the system input and output variables and to proceed on the basis of a number of single variable control loops each of which can be designed independent of all the others. This approach has been widely used and is frequently referred to as multiloop control. The main place that the multivariable aspects of the problem are considered is in the pairing of the system input and output variables and/or in the field tuning of the loops. A technique to assist with this problem of pairing system variables has been proposed [e.g. 8,9] and in most cases it can be interpreted as a simplification or special case of the more general multivariable techniques discussed later. The actual controller design step is completed using any applicable design technique such as the classical Bode or Nyquist frequency domain methods.

However in many systems the interactions between process variables are too severe to be neglected entirely. In such cases the application of conventional single variable techniques results in unsatisfactory control of the overall system. In some cases control engineers have intuitively designed controllers based on their previous experience followed by a tuning of all control loops in the field.

The main reason for this lack of success is interaction i.e. the way in which a reference input $r_i(z)$ applied to input i affects the set of outputs $(y_j(z), j\neq i)$ [42]. Because of the interaction in a multivariable system the transfer function between the input $r_i(z)$ and the output $y_i(z)$ will change when the other loops are closed and also when there are changes in the controller constants in the other loops. Thus in order for a single-loop technique to produce a suitable controller for loop i, the design must be based on the system transfer function of loop i that applies when loop i is open and the rest are closed. From a design point of view this is not very convenient since the transfer function involved in the design of loop i is a function of the controller designed and parameters in all other loops of the system. Thus, in the general case there is no obvious starting point and several assumptions must be made in order to proceed with the design of the first loop.

Sequential Return-difference Method

The Sequential Return-difference method developed by Mayne [44,45,46] in its most elementary form represents an efficient algebraic implementation of the approach that an experienced control engineer would probably take in applying single variable techniques to multivariable problems. In this approach a controller $k_1(z)$ is designed for the first loop based on the transfer function $g_{11}(z)$ between the input $r_1(z)$ and the output $y_1(z)$ using a single-loop frequency domain technique. Then a new process transfer function matrix $G^1(z)$ is calculated with this first loop closed and the rest open. A controller $k_2(z)$ for the second loop is then designed based on the transfer function $g^1_{22}(z)$ (element of $G^1(z)$ between input $r_2^{\,1}(z)$ and output $y_2(z)$) using the same single loop design technique. A new process transfer function matrix $G^2(z)$ is then calculated, this time with the first and second loops closed and the rest open. The procedure continues in a similar way for the rest of the loops. A schematic representation is shown in Figure 2.2. Mayne [44,45] has shown that a sufficient condition for stability of the overall multivariable system is that each of the individual control loops developed in this approach be stable.

The algebraic updating of the transfer function is done in the following way:

Let the controller matrix with loop i closed be K^i = diag $(k_1(z), k_2(z), \dots k_i(z), 0 \dots 0, 0)$ and assume that the first i controllers have already been obtained. The original process transfer function matrix G(z) is defined by:

$$y(z) = G(z)\, u(z) \tag{2.1}$$

By closing the first i loops, and using negative feedback, u(z) is given by

$$u(z) = -K^i(z)y(z) + r^i(z) \tag{2.2}$$

where $r^i = K^i[r_1(2), r_2(2) \ldots r_m(2)]$. The new input-output relationship becomes

$$y(z) = (I_m + G(z)K^i(z))^{-1}\ G(z)\ r^i(z) \tag{2.3}$$

or

$$y(z) = F_i^{-1}\ G(z)\ r^i(z) = G^i(z)\ r^i(z) \tag{2.4}$$

The transfer function matrix $G^i(z)$ can also be easily calculated using one of Mayne's relationships [45,46] i.e.

$$G^i(z) = [I_m - \bar{k}_i(z)\ g_i^{i-1} e_i^T]\ G^{i-1}(z) \tag{2.5}$$

where:

$$\bar{k}_i(z) = k_i(z)/f_i(z) \tag{2.6}$$

$$f_i(z) = 1 + k_i(z)\ g_{ii}^{i-1}(z) \tag{2.7}$$

g_i^{i-1} = i column of $G^{i-1}(z)$

e_i^T = vector whose ith element is unity and the remaining elements are zero.

The selection of the controller for loop i is always based on the transfer function $g_{ii}^{i-1}(z)$ which is the (i,i) element of $G^{i-1}(z)$.

This is a very straightforward technique but it does not solve the basic problems associated with the design of multivariable systems. Specifically it does not provide a means of determining the best pairing of input-output variables, nor does it give directions about the order in which the individual loops should be treated in the design procedure. Obviously the final controller will be influenced by both decisions. More generally the technique does not provide a means for designing individual control loops (or picking individual controller constants) such that a performance criterion based on the overall multivariable system will be optimized. Thus while it might provide a convenient means of dealing with simple multivariable problems there is obviously a need for more rigorous multivariable techniques.

2.3 MULTIVARIABLE CONTROL SYSTEM DESIGN

Another approach to the application of single variable design techniques to multivariable problems has been to augment or modify the system by a pre- or post-compensator. If the compensator reduces the interactions between the input and output variables of the augmented plant then it will be possible to complete the actual controller design step using classical single variable techniques. The controller for the multivariable system then consists essentially of two parts: the multivariable compensator and a set of single variable controllers. The concept of non-interaction is very appealing in some applications, but unfortunately in most problems it cannot be shown that non-interaction is a necessary condition for the design of an optimal controller. In fact in some cases it can be shown that a non-interacting controller will give poorer performance than other alternatives. [64] Thus in general terms one is trading off a guarantee of overall optimality for design convenience.

2.3.1 Non-interacting Design Techniques

In this scheme the design of the controller is done in two steps. In the first step a pre-compensator K(z) is chosen so that the open loop transfer function matrix of the augmented plant, G(z)K(z) is diagonal. Since interaction has been eliminated by the compensator K(z), single-loop theory may be used to design each loop separately. This design technique has not been widely used, especially on complex processes, because it often produces a very complicated controller which is expensive or impractical to implement. Also the selection of the pre-compensator matrix K(z) to make the system diagonal restricts the form of compensation that can be applied to each loop using single-loop theory. When the determinant of G(z) has zeros outside the unit circle this procedure gives a poor or unstable control [64]. This is easily shown by the following analysis. In order to obtain a diagonal open loop transfer function matrix for the system G(z), the pre-compensator matrix K(z) has to have the following form:

$$K(z) = G^{-1}(z) \operatorname{diag} (q_1(z), q_2(z) \ldots q_m(z) \qquad (2.8)$$

where

q_1, q_2, q_3 = diagonal elements of the augmented plant G(z)K(z)

The controller will then be unstable if the plant has right half plane zeros.

Non-interactive design techniques have been discussed by Tsien [75], Rae [62] and more recently by MacFarlane [40] and Berry [6].

2.3.2 Inverse Nyquist Array Technique

The non-interacting design technique described above was a rigorous mathematical approach which could only be applied if the system met some specific mathematical condition so that the interaction could be eliminated completely. One would expect that if the objective was simply to reduce interactions rather than to eliminate them entirely then the "non-interacting" design approach could be applied to a wider range of problems and would involve compensators that were more practical to implement. The inverse Nyquist array method developed by Rosenbrock [65,67] essentially gives the control engineer a means of reducing the system interactions to a point where a controller design and overall stability analysis can proceed on the basis of classical single variable techniques.

The inverse Nyquist array [65,67] is based on an extension of the Nyquist stability criterion for multivariable systems. The stability criterion is developed from the basic equation presented by McMorran [47], but which is equivalent to the relationship obtained earlier by Popov [61]

$$\frac{|R^{-1}(z)|}{|Q^{-1}(z)|} = \frac{\text{CLCP}}{\text{OLCP}} \tag{2.9}$$

where:

$R(z) = (I + Q(z))^{-1}\,Q(z)$ = closed-loop transfer function matrix (CLTFM)

$Q(z) = G(z)K(z)$ = open-loop transfer function matrix (OLTFM)

CLCP = closed-loop characteristic polynomial

OLCP = open-loop characteristic polynomial

The inverse Nyquist array works with the inverses of the open-loop and closed-loop transfer function matrices because of the simplicity of the transformation between these two matrices and hence can only be used to design control systems for square plants.

The design of the controller with this method is done in two major steps. The first step is to design a compensator which makes the inverse of the open-loop and the closed-loop transfer function matrices "diagonally dominant".(Diagonal dominance is defined later but in general terms it means that the off-diagonal elements in the transfer function matrix for the augmented plant are small with respect to the diagonal elements.) A compensator, K(z), that will produce diagonal dominance can be developed in a systematic, interactive manner using the inverse Nyquist array. (The inverse Nyquist array is a set of m^2 Nyquist diagrams representing every element of the inverse of the OLTFM, where m is the number of the plant outputs or inputs.) Once a satisfactory degree of diagonal dominance has been obtained the next step is to use single variable frequency domain techniques to design a stable controller for each pair of input-output variables in the augmented plant. This method is discussed more fully in Chapter Three.

2.3.3 Commutative Controller Method

Another method which makes use of single-loop design techniques to design a multivariable control system is the commutative controller. This method, proposed by MacFarlane [33,36], can be very useful in the design of a control system for square plants which can be expanded into the following dyadic form:

$$G(z) = \sum_{j=1}^{m} g_j(z)\, w_j v_j^T \qquad (2.10)$$

where

$g_j(z)$ = jth eigenvalue or characteristic value of $G(z)$

w_j = linearly independent, frequency independent, real eigenvectors of $G(z)$

$w_j v_j^T$ = dyadic matrix, $v_j^T w_k = \delta_{jk}$

Single-loop techniques can be used to design a multivariable control system for this kind of plant. The design of the controllers is done in the modal or eigenvalue framework of the plant matrix $G(z)$. Then by transforming back to the original basis the controller matrix is obtained.

In this method the controller matrix is assumed to be equal to:

$$K(z) = \sum_{j=1}^{m} k_j(z)\, w_j v_j^T \qquad (2.11)$$

Then, the transfer function matrix for the controller plus plant will then be equal to:

$$Q(z) = G(z)K(z) = \sum_{j=1}^{m} g_j(z)\, k_j(z)\, w_j v_j^T \qquad (2.12)$$

and the closed-loop transfer function matrix will be

$$R(z) = (I+G(z)K(z))^{-1}\, G(z)K(z) = \sum_{j=1}^{m} \frac{g_j(z)k_j(z)}{1+g_j(z)k_j(z)} w_j v_j^T \qquad (2.13)$$

The closed loop stability and transient response characteristic of the overall system are governed by the properties of the m modally non-interacting closed-loop subsystems, $g_j(z)k_j(z)/(1+g_j(z)\ k_j(z))$. Therefore each subsystem can be designed independently and treated as a single-loop system.

Unfortunately most systems cannot be expanded in the dyadic form given by Equation 2.10 because their eigenvectors are frequency dependent. The use of single-loop techniques is not suitable for these systems because the closed-loop stability and transient response will be governed not only by their eigenvalues but also by their eigenvectors. However the commutative controller method can still be applied to these systems if its transfer function matrix is approximated by a dyadic transfer function matrix using the procedure recommended by Owens [56].

2.3.4 Characteristic Locus Method

A very important contribution in the design of multivariable control systems using multivariable frequency domain methods has been the generalization of the scalar return-difference quantity introduced by Bode [7] to a "return difference matrix". (This approach makes the design of multivariable systems equivalent to the design of single-loop systems.) The return-difference and the return-ratio matrices can be calculated [38] by assuming that all the loops are broken at one point as shown in Figure 2.3. If a signal transform vector $\alpha(z)$ is injected into the feedback control system, as in Figure 2.1, the transform of the returned signal at α' is given by $-G(z)\ K(z)\ H(z)\ \alpha(z)$. The return difference matrix $F(z)$ is defined as the coefficient matrix of the difference between the injected and return-signal i.e.

$$\alpha'(z) - \alpha(z) = (I + G(z)K(z)H(z))\ \alpha(z) = F(z)\ \alpha(z) \quad (2.14)$$

where:

F(z)= return-difference matrix = I + G(z)K(z)H(z)

The return-ratio matrix is defined by

$$T(z) = G(z)K(z)H(z) \tag{2.15}$$

It follows directly that

$$F(z) = I + T(z) \tag{2.16}$$

and when the feedback transducer matrix H(z) is unity

$$T(z) = Q(z) \tag{2.17}$$

Two of the methods proposed to date are based on the use of the return-difference matrix to determine the stability of the system. These are the characteristic locus method [4,5,41,42] and the sequential return-difference method [44,45]. The extended Nyquist stability criterion used by these techniques is based on the following relationship proved by Popov [61].

$$|F(z)| = \frac{CLCP}{OLCP} \tag{2.18}$$

The development of the characteristic locus method by Belletruti and MacFarlane [4] is based on the use of the *characteristic values* (analogous to the eigenvalues of a matrix of numeric constants) of the *return-difference* matrix. They also developed a more practical approach using the characteristic values of the *return-ratio* matrix [4,42].

This method is more general than the inverse Nyquist array method [65] since it does not require the system to be diagonally dominant to determine its stability. But the selection of the controller matrix is much more difficult because the stability of the system is established from the characteristic loci of the return-ratio matrix and it is extremly difficult to find a relationship between the elements of the controller and the characteristic values of the return-ratio matrix that can be used as a guide in the design stage. The design of the controller matrix could be done in a more systematic way if a scheme recently developed by Owens [59.60] or Kouvaritakis [508] is used. With the characteristic locus method it is possible to reduce interactions at high frequencies by aligning the characteristic directions or eigenvectors [41,42], of the OLTFM with the standard basis set of vectors. At low frequencies interaction is reduced by increasing the magnitude of the characteristic loci of the OLTFM [41, 42]. The method has a provision to check the integrity of the control to measurement transducer, error monitoring and actuator failures [4]. (Earlier it was pointed out that the performance of a conventional single variable feedback loop when applied to a specific input-output pair of variables on a multivariable system is a function of the controllers and the other elements in other parts of the multivariable system. Thus it is possible that a component failure or other change in one part of a multivariable system could effect the performance and stability of a controller applied to other input-output variable pairs in the same interacting system.) A system is said to have high integrity if it remains stable under all likely failures [4]. The commutative controller can be considered as a special case of the characteristic locus method that arises when a controller is designed to change the *characteristic values* of a system without changing its characteristic directions (eigenvectors).

In the characteristic locus approach the controller is calculated in stages. At each stage a controller is specified to modify the characteristic loci and the characteristic directions of the return-ratio matrix or the OLTFM so that it will have the desired properties. The final controller is equal to the product of the controllers used in each stage.

It should be pointed out that prior to the development of the characteristic locus method by Belletrutti and MacFarlane [4] the characteristic values of the return-ratio matrix were also used by Bohn [502,503] to determine the stability and to design a multivariable control system.

The characteristic locus method is discussed in more detail in Chapter Four.

2.3.5 Direct Nyquist Array Method

One approach that has not been fully discussed in the literature [36,38,70,71] to date is the "direct Nyquist array method". This is another technique which gives the control engineer a means of reducing the system interaction to a point where a controller design can proceed on the basis of classical single variable techniques. This method can be considered as a combination of the characteristic locus and the inverse Nyquist array techniques. The stability criterion is derived from the theory associated with the former method and with the concept of diagonal dominance and Nyquist arrays introduced in the latter technique.

This method requires that the return-difference matrix, i.e.

$$F(z) = I + Q(z) \tag{2.19}$$

be diagonally dominant. However it only uses the Nyquist diagrams of of the open-loop transfer function matrix, Q(z).

The design procedure is similar to the inverse Nyquist array method, i.e. the selection of the controller is done in two major steps. In the first step a simple controller is design to make the return-difference matrix diagonally dominant. In the final step a single-loop controller is designed for each loop in the system. This method is discussed in more detail in Chapter Five.

2.3.6 Sequential Return-difference Method

The sequential return-difference method [44,45,46,51,57] in its general form is not much different from the sequential method discussed in section 2.1 to design a multiloop control system. The main difference is that in the general case it is possible to design a pre-compensator at each step simultaneously with the controller for each loop. The pre-compensator is restricted to perform elementary column operations and, at the ith stage of the design procedure, has the following form:

$$G_c^i(z) = \begin{bmatrix} I_{i-1} & 0 \\ 0 & X \end{bmatrix} \qquad |G_c^i(z)| = 1 \tag{2.21}$$

where X defines the column operation to be performed. Then the input vector when the first i loops are closed is equal to:

$$u(z) = -G_c(z)\, K^i(z)\, y(z) + r^i(z) \tag{2.22}$$

and the closed-loop transfer function matrix is given by

$$y(z) = (I_m + G(z)\, G_c(z)\, K^i(z))^{-1}\, G(z)\, r^i(z) \qquad (2.22)$$

or

$$y(z) = F_i^{-1}\, G(z)\, r^i(z) = G^i(z)\, r^i(z) \qquad (2.23)$$

In this case the stability of the system is established from the return-difference matrix

$$F_i(z) = I_m + G(z)\, G_c(z)\, K^i(z) \qquad (2.24)$$

or:

$$F_i(z) = I_m + G(z)[G_c^1\, G_c^2 \,\dots\, G_c^i]\, K^i(z) \qquad (2.25)$$

The sequential choice of G_c^j does not affect $F_i(z)$ for $j > i$. The design procedure is as follows. On the ith step the controller $k_i(z)$ is designed based on the $g_{ii}^{i-1}(z)$ element of $G^{i-1}(z)$. Then a new transfer function matrix $G^i(z)$ is calculated with a new compensator matrix G_c^j and the first i loops closed. A new controller $k_{i+1}(z)$ is designed for the i+1 loop based on the $g_{i+1,i+1}^{i}(z)$ element of $G^i(z)$ such that this loop is stable. The procedure continues in a similar way for the rest of the loops. The matrix $G^i(z)$ at the ith step can be calculated using an algorithm developed by Mayne [45,46].

The use of a pre-compensator does not solve the main problem of the sequential return-difference method which is the order of loop closing. Any arbitrary choice of ordering may limit the achievable performance of the control systems. Owens [57] has proposed a scheme to solve this problem by expanding the plant transfer function into a dyadic form. However his scheme requires the use of a post-compensator which is highly undesirable in most practical cases.

The sequential return-difference method has flexibility in that it can be used in combination with any other design method. Any method can be used to design the pre-compensator $G_c(z)$ and the sequential return-difference method can be applied to select the final controllers in each loop. A very practical combination appears to be the direct Nyquist array and the sequential design method.

A modification of the sequential design method has been proposed by Owens [58]. The main difference between these two schemes is that Mayne's method [44,45] produces control signals $u_1(z)$, $u_2(z)$, ... $u_i(z)$ based on the feedback error $e_1(z)$, $e_2(z)$ ... $e_i(z)$ respectively.

2.3.7 Owen's Modification of the Sequential Return-difference Method

Owen's modification [58] introduces sequentially at each stage the effect of each controller $u_1(z)$, $u_2(z)$ ... $u_m(z)$ while retaining full output feedback. A schematic diagram of this method is presented in Figure 2.4. Using the latter approach the plant and the controller are expressed in the following form:

$$G^i(z) = \sum_{j=1}^{i} g_{\cdot j}(z)\, e_j^T \tag{2.26}$$

$$K^i(z) = \sum_{j=1}^{i} e_j k_{j\cdot}(z) \tag{2.27}$$

where

$g_{\cdot j}(z)$ = jth column of the plant transfer function matrix

$k_{j.}(z)$ = jth row of the controller matrix

e_j = column vector whose jth element is unity and the remaining elements are zero.

For the ith step, let $r^i(z) = K^i[r_1(z), r_2(z) \ldots r_i(z), 0 \ldots 0]$ then the plant transfer function matrix is given by

$$y(z) = G^i(z)\, u(z) \tag{2.28}$$

For a negative feedback control:

$$u(z) = -K^i(z)\, y(z) + r^i(z) \tag{2.29}$$

and the closed loop transfer function matrix is

$$y(z) = (I_m + G^i(z)\, K^i(z))^{-1}\, G^i(z)\, r^i(z) \tag{2.30}$$

The stability of the system is determined from the return-difference matrix, i.e.

$$F_i(z) = I_m + G^i(z)\, K^i(z) \tag{2.31}$$

or

$$F_i(z) = F_{i-1}(z) + g_{.i}(z)\, k_{i.}(z) = F_{i-1}(z)(I_m + F_{i-1}^{-1} g_{.i}(z) k_{i.}(z)) \tag{2.32}$$

Thus the determinant of the return-difference matrix is equal to:

$$|F_i(z)| = |F_{i-1}(z)|\; |I_m + F_{i-1}^{-1}(z)\, g_{.i}(z)\, k_{i.}(z)| \tag{2.33}$$

and applying some formulas for partitioned determinants given in Gantmacher [19]:

$$|F_i(z)| = |F_{i-1}(z)| \; |1 + k_{i.}(z) \, F_{i-1}^{-1} g_{.i}(z)| \qquad (2.34)$$

Owens' method is based on Equation (2.34). It is similar to Mayne's method [44,45] in that the design of the controller is done sequentially. At each step the m components of the row vector $k_{i.}(z)$ are chosen by examining the scalar term $(1 + k_i(z) \, F_{i-1}^{-1} g_{.i}(z))$ which must satisfy the Nyquist stability criterion. The weakness of this method is that it does not solve the basic problems of the sequential return-difference method i.e. order of loop closing, and selection of the controller constants to satisfy an overall system performance criterion. The modification introduces extra design flexibility but it also makes the selection of the controller much more difficult. The only guideline the user has is that the scalar term $(1 + k_{i.}(z) \, F_{i-1}^{-1}(z) \, g_{.i}(z))$ must satisfy the Nyquist stability criterion.

2.3.8 Another Modification of the Sequential Return-difference Method

When comparing Owen's modification to Mayne's Sequential Return-difference method [44,45] it becomes obvious that instead of using the full output to generate sequentially $u_i(z)$, $u_2(z)$ ... $u_m(z)$, the feedback error $e_i(z)$ ($i=1$, ... m) can be used to simultaneously generate all the control signals. Since the sequential methods are not discussed elsewhere in this thesis the modification is presented here. A schematic diagram of this modification is shown in Figure 2.5. The control signals generated by every feedback error are sequentially accumulated.

For this case the controller matrix can be represented in the following form

$$K^{i}(z) = \sum_{j=1}^{i} k_{.j}(z)\, e_j^T \qquad (2.35)$$

where:

$k_{.j}$ = jth column of the controller matrix.

At the ith stage the closed loop system is given by

$$u(z) = K^{i}(z)\,(y(z) - r(z)) + u^{i}(z) \qquad (2.36)$$

and

$$y(z) = (I_m + G(z)\,K^{i}(z))^{-1}\,G(z)\,u^{i}(z) + (I_m + G(z)\,K^{i}(z))^{-1}$$
$$G(z)\,K^{i}(z)\,r(z) \qquad (2.37)$$

The stability of the system will depend upon the return-difference matrix i.e.

$$F_i(z) = I_m + G(z) \sum_{j=1}^{i} k_{.j}(z)\, e_j^T \qquad (2.38)$$

or

$$F_i(z) = F_{i-1}(z)\,(I_m + F_{i-1}^{-1}\,G(z)\,k_{.i}\,e_i^T) \qquad (2.39)$$

The determinant of the return-difference matrix is

$$|F_i(z)| = |F_{i-1}(z)|\;|I_m + F_{i-1}^{-1}\,G(z)\,k_{.i}\,e_i^T| \qquad (2.40)$$

Similarly applying some formulas for partitioned determinants [19]:

$$|F_i(z)| = |F_{i-1}(z)|\;|1 + e_i^T\,F_{i-1}^{-1}\,G(z)\,k_{.i}| \qquad (2.41)$$

This modification can be developed from Equation (2.41). The design is done sequentially. At the ith stage the m elements of column i are chosen such that the scalar term $1 + e_i^T F_{i-1}^{-1} G(z) k_{.i}$ satisfies the Nyquist stability criteria. This modification has the same flexibility as the Owen's approach [58] but it also has the same problems.

2.4 CONCLUSIONS

Of all the methods discussed in this study the following appear to be the more promising ones: the inverse Nyquist array [65], the characteristic locus method [4,5,41,42] and the direct Nyquist array method [developed in Chapter Five]. (With the exception of the inverse Nyquist array method, these methods can also be used to design a control system for non-square plants but the selection of the controller is more difficult.) Because of their flexibility and convenience it appears that these multivariable frequency domain design techniques will be widely used in the future. Therefore these techniques are described more fully in the following chapters.

CHAPTER THREE

THE INVERSE NYQUIST ARRAY METHOD

3.1 INTRODUCTION

The inverse Nyquist array method first proposed by Rosenbrock [65] has received considerable attention recently [1,17,20,21,22,23,40, 50,67] and several applications of this method have been presented in the literature [3,41,48,49,52]. Experience with experimental implementations using this method is very limited and only a very small number of experimental cases have been reported in the literature [3,39]. For these reasons and in order to compare this method with other multivariable frequency-domain techniques, the evaluation of the inverse Nyquist array method was undertaken as part of this study and included:

- the theoretical aspects
- the computer implementation of this method
- the design of an actual control system using this technique
- the implementation of the resulting controller on process equipment.

This chapter deals specifically with the theoretical aspects of the inverse Nyquist array method and with the design of a control system for a double-effect evaporator pilot plant. The experimental results are presented in Chapter Six.

The inverse Nyquist array method for continuous systems has been discussed in detail by Rosenbrock [65]. This chapter discusses the most important aspects of the inverse Nyquist array method for discrete systems. The inverse Nyquist array method is considered here to be a special case of a more general method: the inverse Nyquist method. The objective in doing this is to emphasize the similarities with the characteristic locus method [4,42] and especially with the direct Nyquist array method discussed in Chapters Four and Five respectively.

Control systems for the double-effect evaporator pilot plant were designed using two different order state-space models of the same pilot plant. The results of the experimental implementation of the resulting controller in this chapter are discussed in Chapter Six.

3.2 THE INVERSE NYQUIST METHOD

The inverse Nyquist method and its special case the inverse Nyquist array method can be applied to the design of a multivariable control system of the form shown in Figure 2.1. Since the feedback matrix H(z) can always be made part of plant transfer function matrix G(z), without loss of generality, it will be assumed that the feedback matrix, H(z) is a unity matrix.

McMorran [47] has proved that for systems which can be represented by Figure 2.1 the following relationship holds:

$$\frac{|R^{-1}(z)|}{|Q^{-1}(z)|} = \frac{\text{CLCP}}{\text{OLCP}} \tag{3.1}$$

where:

CLCP = closed-loop characteristic polynomial

OLCP = open-loop characteristic polynomial

$Q(z)$ = open-loop transfer function matrix = $G(z)K(z)$

$R(z)$ = closed-loop transfer function matrix = $(I + Q(z))^{-1}Q(z)$

This was developed independently by McMorran [47] but it is equivalent to an equation derived earlier by Popov [61] and later by

Hsu and Chen [24]. The main reason for using the inverses of the open- and closed-loop transfer function matrices is the simplicity of the transformation between these two matrices i.e.

$$R^{-1}(z) = I_m + Q^{-1}(z) \tag{3.2}$$

The use of Equation (3.2) instead of the equation which relates the open- and closed-loop transfer function matrices i.e.

$$R(z) = (I_m + Q(z))^{-1}Q(z) \tag{3.3}$$

simplifies, as will be seen later, the design of a control system because the eigenvalues of $R^{-1}(z)$ may be obtained by simply "shifting" the eigenvalues of $Q^{-1}(z)$.

A general design method can be developed in terms of the determinants of the inverses of the closed and open loop transfer function matrices by using the following result. Let D be a contour in the complex z-plane as shown in Figure 3.1 consisting of a unit circle and a circle of radius α which is large enough to ensure that any zero of $|Q^{-1}(z)|$ and $|R^{-1}(z)|$ outside the unit circle is inside the contour D. Let also $|Q^{-1}(z)|$ map D into $\hat{\Gamma}_o$ and $|R^{-1}(z)|$ map D into $\hat{\Gamma}_c$ encircling the origin counterclockwise n_o and n_c times respectively (clockwise encirclements are assumed to be positive). Using Equation (3.1), the principle of the argument [66] and the well known fact that a closed loop multivariable discrete system is stable if and only if the closed-loop characteristic polynomial does not contain any zero outside the unit circle centered at the origin it can be shown [47] that the system is closed loop stable if and only if

$$n_c - n_o = -p_o \tag{3.4}$$

where p_o is the number of zeros outside the unit circle of the open-loop characteristic polynomial.

Although Equation (3.4) can theoretically be used to design a multivariable regulator it has no value as a practical design method. The controller cannot be designed in a systematic way because of the difficulty of predicting the effect of specific elements of the controller on the values of $|Q^{-1}(z)|$ and $|R^{-1}(z)|$.

A more practical approach can be developed by using the eigenvalues or the characteristic values of $Q^{-1}(z)$ and $R^{-1}(z)$ to determine the stability of the system instead of their determinants. The term "characteristic values" has been used by MacFarlane [38] to emphasize the fact that they are not constant values (as the familiar eigenvalue is) but are functions of z. In this case if every characteristic value of $Q^{-1}(z)$ and $R^{-1}(z)$ maps D into $\hat{\Gamma}_{oi}$ and $\hat{\Gamma}_{ci}$ (i=1,2 ... m) encircling the origin counterclockwise n_{oi} and n_{ci} times respectively, it can be shown [4] that

$$n_o = \sum_{i=1}^{m} n_{oi} \tag{3.5}$$

and

$$n_c = \sum_{i=1}^{m} n_{ci} \tag{3.6}$$

Then the system is closed-loop stable if and only if:

$$\sum_{i=1}^{m} n_{ci} - \sum_{i=1}^{m} n_{oi} = -p_o \tag{3.7}$$

The approach based on Equation (3.7) can be simplified further because the stability of the system can be determined by using only the characteristic values of the inverse of the open-loop transfer function matrix ($\hat{q}_i(z)$, i = 1 ... m). By applying the eigenvalue shift theorem [35] to Equation (3.2), the characteristic values of the inverse of the closed-loop transfer function matrix ($\hat{r}_i(z)$: i = 1 ... m) can be expressed as:

$$\hat{r}_i(z) = 1 + \hat{q}_i(z) \qquad (3.8)$$

Then, using Equation (3.7) it can be stated that a necessary and sufficient condition for the closed-loop system to be stable is that the number of encirclements of the critical point (-1,0) minus the number of encirclements of the origin by the characteristic loci (Nyquist diagrams of the characteristic values) of matrix $Q^{-1}(z)$ *be equal to* $-p_o$.

This stability criterion is the basis of a design method which is equivalent to the characteristic loci method proposed by Belletrutti and MacFarlane [4] and discussed in Chapter Four. The main difference between these two methods is that the characteristic loci method uses the characteristic values of the open-loop transfer function matrix or in general of the return-ratio matrix while this approach uses the characteristic values of the inverse of the open-loop transfer function matrix. Both methods have similar properties and similar disadvantages. These are discussed in more detail in Chapter Four.

3.3 THE INVERSE NYQUIST ARRAY METHOD

Rosenbrock's inverse Nyquist array (INA) method [65] is a simplification of the general inverse Nyquist method. The INA method is based on a more practical stability criterion which can be obtained for systems represented by Figure 2.1 when the inverses of the open-loop, $Q^{-1}(z)$

and the closed-loop, $R^{-1}(z)$, transfer function matrices are row or column diagonally dominant. The matrix $Q^{-1}(z)$ is said to be row dominant if for all the z on the contour D the following equation is satisfied:

$$|\hat{q}_{ii}(z)| - \sum_{\substack{j=1\\ j\neq i}}^{m} |\hat{q}_{ij}(z)| > 0 \tag{3.9}$$

where $[\hat{q}_{ij}]$ is the (i,j) element of $Q^{-1}(z)$. Similarly the matrix $R^{-1}(z)$ is row dominant if Equation (3.10) is satisfied, i.e.

$$|\hat{r}_{ii}(z)| - \sum_{\substack{j=1\\ j\neq i}}^{m} |r_{ij}(z)| > 0 \tag{3.10}$$

where $[\hat{r}_{ij}]$ is the (i,j) element of $R^{-1}(z)$. Equivalent equations can be written when $Q^{-1}(z)$ and $R^{-1}(z)$ are column dominant.

When matrices $Q^{-1}(z)$ and $R^{-1}(z)$ are diagonally dominant the stability of the closed-loop system can be established using only the diagonal elements of matrix $Q^{-1}(z)$. Rosenbrock [65] has shown, using Gershgorin's theorem [43] that if the *diagonal elements*, $\hat{q}_{ii}(z)$, of $Q^{-1}(z)$ (not the characteristic values as in the general case) map D into $\hat{\Gamma}_{oii}$ and the diagonal elements, $\hat{r}_{ii}(z)$, of $R^{-1}(z)$, map D into $\hat{\Gamma}_{cii}$ encircling the origin counterclockwise n_{oii} and n_{cii} times respectively, then

$$n_o = \sum_{i=1}^{m} n_{oii} \tag{3.11}$$

and

$$n_c = \sum_{i=1}^{m} n_{cii} \tag{3.12}$$

Thus using Equations (3.4), (3.10) and (3.11) it can be shown that *a* *sufficient and necessary condition for a diagonally dominant closed-loop system to be stable is*

$$\sum_{i=1}^{m} n_{cii} - \sum_{i=1}^{m} n_{oii} = -p_o \qquad (3.13)$$

Because $\hat{r}_{ii}(z) = 1 + \hat{q}_{ii}(z)$, the only difference between the Nyquist diagrams of $\hat{r}_{ii}(z)$ and $\hat{q}_{ii}(z)$ is a shift in the imaginary axis. Thus the system is closed-loop stable if the number of encirclements of the (-1,0) point minus the number of encirclements of the origin by the Nyquist diagrams of $\{\hat{q}_{ii}: i=1, 2 \ldots m\}$, $\hat{r}_{oii}$, is equal to $-p_o$.

Based on this stability criterion Rosenbrock [65] has developed a very practical technique to design a multivariable control system. Rosenbrock [65] has also introduced the concept of the inverse Nyquist array which is a set of m^2 Nyquist diagrams (m is the number of inputs or outputs in the system) that correspond to every element of $Q^{-1}(z)$. The inverse Nyquist array is a very useful graphical tool to observe the effect of each controller matrix in the control system and to select the type of control which is necessary.

Diagonal dominance in the system can also be established graphically by drawing circles for different frequencies on the Nyquist diagrams of the diagonal elements of $Q^{-1}(z)$. The centres of these circles are located on the Nyquist loci of the diagonal elements, $\hat{q}_{ii}(z)$, of $Q^{-1}(z)$ and their radii are equal to the sum of the magnitudes, for a given frequency, of the off-diagonal elements in a row or in a column depending whether row or column dominance is to be established. For row dominance the radii of the circles are equal to

$$d_i = \sum_{\substack{j=1 \\ j \neq i}}^{m} |\hat{q}_{ij}(z)| \tag{3.14}$$

and for column dominance the radii of these circles are given by

$$\delta_i = \sum_{\substack{j=1 \\ j \neq i}}^{m} |\hat{q}_{ji}(z)| \tag{3.15}$$

The bands formed by these circles are usually referred as the Gershgorin bands. The inverse of the open-loop and the closed-loop transfer function matrices are diagonally dominant if the Gershgorin circles do not enclose the origin and the (-1,0) point respectively. The Gershgorin bands have two more important properties. The first one has been proved by Gershgorin [43] and states that the characteristic values of the matrices $Q^{-1}(z)$ and $R^{-1}(z)$ are located inside the Gershgorin bands. This property was used by Rosenbrock [65] to prove the stability criterion on which the inverse Nyquist array method is based. It is because of this property that the Gershgorin bands are also used to determine the stability of the system.

The second property is a very important one because it gives some physical insight into this method. Rosenbrock [67,69] has proved using a theorem due to Ostrowski [55] that when the inverse of the open-loop transfer function matrix $Q^{-1}(z)$ is diagonally dominant the Gershgorin bands are the limiting bounds of a narrower band which is usually referred as the Ostrowski band. This latter band also has the property of being a limiting bound of the region where the inverse of the transfer function between input i and output i, when loop i is open and the rest are closed, is located. The Ostrowski bands are generated by circles whose centers are located in the Nyquist diagram of the diagonal elements, $\hat{q}_{ii}(z)$ of $Q^{-1}(z)$ and whose radii are equal to the radii of the Gershgorin circles multiplied by a factor α_i or α_i^1. These factors are equal to

$$\alpha_i = \max_{\substack{j \\ j \neq i}} \frac{d_j}{|1 + \hat{q}_{jj}|} \tag{3.16}$$

if row dominance is used, or

$$\alpha_i^1 = \max_{\substack{j \\ j \neq i}} \frac{\delta_j}{|1 + \hat{q}_{jj}|} \tag{3.17}$$

if column dominance is used.

The latter property of the Ostrowski bands can be represented by the following equations:

$$|\hat{q}_{ii}(z) - h_i^{-1}(z)| < \alpha_i d_i < d_i \tag{3.18}$$

or

$$|\hat{q}_{ii}(z) - h_i^{-1}(z)| < \alpha_i^1 \delta_i < \delta_i \tag{3.19}$$

where, $h_i(z)$ is the transfer function between input i and output i when the loop i is open and the rest of the loops are closed.

Since the width of the Ostrowski bands depends upon the values of the controller constants in the other loops they are not generally used in the design of the controller except when it is necessary to define more precisely the region of stability of each loop. Its use requires a trial and error procedure. However the property of the

Ostrowski bands of being located inside the Gershgorin bands is very useful because once the system is diagonally dominant the design of the controller can be done using single-variable techniques on each of the Gershgorin bands of the inverse of the open-loop transfer function matrix.

The Gershgorin bands can also be considered as a measure of the degree of interaction in the system. The narrower these bands are the less interacting the system is.

The design of a multivariable regulator using the inverse Nyquist array method involves three steps:

1) Pairing of the input-output plant variables.

2) Design of a pre-compensator to make the inverse of the open-loop, $Q^{-1}(z)$, and the closed-loop, $R^{-1}(z)$, transfer function matrices diagonally dominant.

3) Design of a multiloop control system using single-variable frequency domain techniques.

In the first step the inputs are reordered in such a way that the interaction between the input-output systems $\{u_i(z): y_i(z)\ i=1 \ldots m\}$ is minimized or that the control of the output $y_i(z)$ is done by the input that has the greatest influence on it, $u_i(z)$. This step is usually done by graphical comparison using the plant inverse Nyquist array which is also useful to determine if a compensator is required to make the system diagonally dominant.

In the second step a pre-compensator is selected in order to make matrices $Q^{-1}(z)$ and $R^{-1}(z)$ diagonally dominant. This compensator is usually designed by performing successive elementary row operations on the inverse of the plant transfer function matrix. Most of these operations can be selected by visual inspection of the corresponding inverse Nyquist array.

The final control matrix will be equal to the product of the control matrices found in each step. Each step is an iterative and interactive process. However the design of the control matrix is always done in a systematic way.

Once the matrix $Q^{-1}(z)$ is diagonally dominant a multiloop control system is designed by using the single-variable frequency domain techniques which apply to inverse polar plots. The only difference between the design of single-loop control systems and the design of a controller for each loop in this step is that the Nyquist diagram of the inverse transfer function of each loop is replaced here by a band (Gershgorin band).

This three step procedure also allows the designer to solve several of the control system requirements like stability, reduction of interactions, integrity against transducer and error-monitoring failures and the performance of the system. In the first two steps a system is given good non-interacting and high integrity properties against transducer and error monitoring failures by selecting a controller which makes the inverse of the open-loop and closed-loop transfer function matrices diagonally dominant. For example, if a failure in the transducer of any loop in the system occurs all the remaining loops in the system will remain stable. Although such a failure will affect the transfer function of each loop when it is open and the remaining loops are closed, the Nyquist plots of these transfer functions will still be located inside their respective Gershgorin bands. Since the design was based on the Gershgorin bands the stability of the loops will not be affected (although the gain margins may be changed). The same occurs when there is an error-monitoring failure.

In the last step of the design the feedback gains $\{k_i, i=1,..m\}$ are chosen so that the closed-loop system is made stable and the performance of the system is satisfactory. This makes the inverse Nyquist array method a very useful and practical technique.

There are however some shortcomings in the use of the inverse Nyquist array method. These are:

1. It is not always possible to find a simple controller matrix which will make $Q^{-1}(z)$ and $R^{-1}(z)$ diagonally dominant. For the case when the matrix $R^{-1}(z)$ has been made diagonally dominant and an analytical expression of $G(z)$ (or $Q(z)$) is given it is possible to overcome the requirement that $Q^{-1}(z)$ be diagonally dominant at the cost of additional calculations. It is always possible to go back to the general stability criterion given by Equation (3.4), i.e.

$$n_c - n_o = p_o \tag{3.4}$$

Since the inverse closed-loop transfer function matrix, $R^{-1}(z)$, is diagonally dominant, n_c will still be given by Equation (3.12) ($n_c = \sum_{i=1}^{m} n_{cii}$). The encirclements of the origin, n_o, can be obtained directly by examining the Nyquist diagrams corresponding to the mapping of the contour D by $|Q(z)|$ or $|G(z)|$.

There is also the alternative of modifying Equation (3.4) by taking into consideration the fact that $n_o = p_o - z_o$ where z_o is the number of zeros of $|Q(z)|$ outside the unit circle. Equation (3.4) then will be equal to:

$$\sum_{i=1}^{m} n_{cii} - p_o + z_o = -p_o$$

or

$$\sum_{i=1}^{m} n_{cii} = z_o$$

From this equation it can be seen that the closed-loop system will be stable if and only if the number of encirclements of the (-1,0) point by the Nyquist diagrams of $\{q_{ii}(z), i=1,..m\}$ is equal to the number of zeros of $|Q(z)|$ outside the unit circle.

In some cases $Q^{-1}(z)$ can be made diagonally dominant by designing a post-compensator, $L(z)$, in combination with a pre-compensator, $K(z)$, such that $Q^{-1}(z)$ is equal to:

$$Q^{-1}(z) = K^{-1}(z)G^{-1}(z)L^{-1}(z) \tag{3.20}$$

From the practical point of view this alternative is questionable because the control would then be exercised over a combination of the output variables instead of the output themselves.

Another alternative has been used by Hawkins [501,505]. A feedback controller, $K(z)$, can always be found that will make the closed-loop sytem containing $Q(z)$, diagonally dominant. This closed-loop system can then be treated as the new system matrix $Q_1(z)$ and the design continued using the standard inverse Nyquist array method.

2. Since diagonal dominance is not a necessary condition for

non-interaction [42] or good control, some design feedom (and/or control energy) may be wasted making the system diagonally dominant.

3. Integrity against actuator failures cannot be checked in this method.
4. It can only be applied to plants which have a square transfer function matrix.

3.4 USE OF A BILINEAR TRANSFORMATION

Although all the results presented here for discrete systems have been obtained using the z-transform, the design of a multivariable regulator for a discrete system is, for practical reasons, usually done using a w- or r-bilinear transformation, i.e.

$$z = \frac{1 + w}{1 - w} \tag{3.21}$$

or

$$z = \frac{r + 1}{r - 1} \tag{3.22}$$

A bilinear transformation maps the unit circle in the z-plane into the left half plane in the w- or r-plane. Its use makes the computation of the Nyquist diagram easier because the Nyquist contour used in the w- or r-plane is identical to the Nyquist contour used for continuous systems in the s-plane as it is shown in Figure 3.2. This also simplifies the programming to implement this technique because the same programs can be used to design a continuous or a discrete control system. The Nyquist diagrams obtained using a bilinear transformation are exactly the same as the ones obtained using a z-transform.

In this study the w-transformation was arbitrarily chosen.

3.5 AN ALTERNATIVE TO THE INVERSE NYQUIST METHOD

Similar stability criteria can be obtained using the open- and closed-loop transfer function matrices instead of their inverses by rewriting Equation (3.1) in the following form:

$$\frac{|Q(z)|}{|R(z)|} = \frac{\mathrm{CLCP}}{\mathrm{OLCP}} \tag{3.23}$$

Using this equation equivalent stability criteria can also be obtained in terms of the eigenvalues of $Q(z)$ and $R(z)$ and in terms of their diagonal elements when these matrices are diagonally dominant. However the methods based on these stability criteria are less practical than the inverse Nyquist array discussed in this chapter and the direct Nyquist array methods discussed in Chapter Five. This is because the methods based on Equation (3.23) require the calculation of the closed-loop transfer function matrix using Equation (3.3) to determine the stability of the closed-loop system. This calculation is not necessary in the inverse and the direct Nyquist array methods.

3.6 DESIGN OF A MULTIVARIABLE REGULATOR FOR THE THIRD ORDER EVAPORATOR MODEL

In this section a multivariable regulator for the double-effect evaporator pilot plant, described in appendix A, is designed using the inverse Nyquist array method. The evaporator was represented by a a discrete, three state, linear, time-invariant model with normalized perturbated variables. (The coefficient matrices for the state-space model are shown in Table A.3) This model was obtained by reduction, using Marshall's method [77], of a ten-state linear, time-invariant model derived by Wilson [76].

The z-transform of this model can be represented by the following equation:

$$\begin{bmatrix} W_1(z) \\ W_2(z) \\ C_2(z) \end{bmatrix} = \begin{bmatrix} \\ G(z) \\ \\ \end{bmatrix} \begin{bmatrix} S(z) \\ B_1(z) \\ B_2(z) \end{bmatrix} \qquad (3.24)$$

The outputs of the system are the first-effect hold up, W_1, the second-effect hold up, W_2, and the product concentration, C_2, The inputs are the steam to the first-effect, S, the bottoms flow from the first-effect B_1, and the bottoms flow from the second-effect, B_2. The plant z-transfer function matrix G(z) was obtained from the state space model using the algorithm of Souriau-Frame-Faddeev [66]. G(z) is presented in Table 3.1. For reasons explained earlier the design was carried out using the w-bilinear transformation of G(z). The plant w-transfer function matrix of the third order evaporator model, G(w), is shown in Table 3.2.

The poles of the z- and w-transfer function matrices or the zeros of the open-loop characteristic polynomial of the third order double-effect evaporator are shown in Table 3.3.

The evaporator model is marginally stable since it has two

TABLE 3.1

z-transfer Function Matrix Derived from the Third Order Evaporator Model

$$G(z) = \frac{1}{d(z)} \begin{bmatrix} -0.03255\ (z-1.0)(z-0.9602) & -0.08110\ (z-1.0)(z-0.9602) & 0 \\ -0.03779\ (z-1.0)(z-0.9602) & 0.08540\ (z-1.0)(z-0.9602) & -0.04063\ (z-1.0)(z-0.9602) \\ 0.05290\ (z-1.0)^2 & -0.04415\ (z-1.0)^2 & 0 \end{bmatrix}$$

$$d(z) = (z-1.0)^2(z-0.9602)$$

TABLE 3.2

w-transfer Function Matrix Derived from the Third Order Evaporator Model

$$G(w) = (1-w) \begin{bmatrix} \frac{-0.01628}{w} & \frac{-0.04055}{w} & 0 \\ \frac{-0.01890}{w} & \frac{0.04275}{w} & \frac{-0.02031}{w} \\ \frac{0.02690}{(w+0.0203)} & \frac{-0.02252}{(w+0.0203)} & 0 \end{bmatrix}$$

TABLE 3.3

Poles of the Third Order Evaporator Model

z-plane	w-plane
1.0	0.0
1.0	0.0
0.9602	-0.0203

TABLE 3.4

Inverse of the w-transfer Function Matrix Based on the Third Order Evaporator Model

$$G^{-1}(w) = \frac{1}{(1-w)} \begin{bmatrix} -15.444\,w & 0 & 27.811(w+0.0203) \\ -18.508\,w & 0 & -11.650(w+0.0203) \\ -24.518\,w & -49.150\,w & -49.225(w+0.0203) \end{bmatrix}$$

poles located on the unit circle in the z-plane.

Since the inverse Nyquist array works with the inverse of the plant transfer function matrix, $G^{-1}(w)$ is presented in Table 3.4.

Step one: Pairing the input-output variables of the evaporator

The inverse Nyquist array of G(w) is shown in Figure 3.3 for the frequency range of 0.1 - 10.0 radians/second. The labels in this figure indicate the numerical value at the end of each axis. The pairing of variables has been done by graphical comparison between the elements of the Nyquist array of $G^{-1}(w)$. It can be seen in Figure 3.3 that none of the rows or columns of $G^{-1}(w)$ are diagonally dominant. This can be seen more clearly in Figure 3.4 where the diagonal elements of $G^{-1}(w)$ with the Gershgorin bands for row dominance are displayed. Thus the plant in its present form is highly interactive.

In order to reduce interaction and to have more effective control of the outputs a renumbering of the inputs is necessary. From Figure 3.3 it can be seen that the best configuration is obtained when:

row 2 is made row 1

row 3 is made row 2

row 1 is made row 3

This operation is accomplished by pre-multiplying $G^{-1}(w)$ by the controller matrix K_1^{-1}

$$K_1^{-1} = \begin{bmatrix} 0 & 1 & 0 \\ 0 & 0 & 1 \\ 1 & 0 & 0 \end{bmatrix} \tag{3.25}$$

Note, when using the interactive design program developed at the University of Alberta the user simply identifies what elementary operations he wants done and the computer generates the appropriate compensator, e.g. K_1^{-1} in Equation (3.25).

This means physically that if a *multiloop* control system is to be designed the least interacting scheme occurs when the first effect hold up, W_1, is controlled by B_1, the second effect hold up, W_2, is controlled by B_2 and the product concentration C_2 is controlled by steam flow, S. This is in agreement with previous results obtained by Newell [53] and Jacobson [27] when designing a multiloop control system for the evaporator using conventional techniques and experimental data.

The new open-loop transfer function matrix $Q_1(w)$ is given by

$$Q_1^{-1}(w) = K_1^{-1}G^{-1}(w) \tag{3.26}$$

Its inverse Nyquist array is shown in Figure 3.5. The diagonal elements of $Q_1^{-1}(w)$ with their Gershgorin bands are presented in Figure 3.6. From these figures it can be observed that only rows 1 and 3 of $Q_1^{-1}(w)$ are diagonally dominant.

Because row 2 of $Q_1^{-1}(w)$ is not diagonally dominant there is a need to proceed further with the design procedure, i.e. to design a controller which makes the system diagonally dominant in all three rows.

Step two: Design of a pre-compensator to make matrices $Q^{-1}(w)$ and $R^{-1}(w)$ diagonally dominant

The Nyquist array of $Q_1^{-1}(w)$ in Figure 3.5 helps in the design of compensator $K(z)$ that will make $Q(z)$ diagonally dominant. For example, by comparison of the magnitude $q_{11}(z)$ with $q_{21}(z)$ (and/or by trial and error) it can be seen that subtracting from row 2 1.325 times row 1 will make row 2 diagonally dominant. Simultaneously, diagonal dominance can be improved in row 3 by subtracting from it 0.830 times row 1. Then the inverse controller is given by:

$$K_2^{-1} = \begin{bmatrix} 1.0 & 0.0 & 0.0 \\ -1.325 & 1.0 & 0.0 \\ -0.830 & 0.0 & 1.0 \end{bmatrix} \qquad (3.27)$$

The inverse Nyquist array of $Q_2(w)$ (where $Q_2^{-1}(w) = K_2^{-1}Q_1^{-1}(w)$) is presented in Figure 3.7 and the diagonal elements of $Q_2^{-1}(w)$ with the Gershgorin bands are shown in Figure 3.8. All the rows in $Q_2^{-1}(w)$ are now diagonally dominant. However diagonal dominance can still be improved in row 1 and 2. This can be done simultaneously by adding 0.3 times row 3 to row 1 and 0.930 times row 3 to row 2 respectively, i.e. $Q_2^{-1}(w)$ must be pre-multiplied by:

$$K_3^{-1} = \begin{bmatrix} 1.0 & 0.0 & 0.300 \\ 0.0 & 1.0 & 0.930 \\ 0.0 & 0.0 & 1.0 \end{bmatrix} \qquad (3.28)$$

to obtain $Q_3^{-1}(w)$. From the inverse Nyquist array of $Q_3^{-1}(w)$ shown in Figure 3.9 it can be observed that the compensated system is almost diagonal, i.e. almost totally non-interacting.

Since the system is diagonally dominant the stability of the closed-loop system can be investigated using the inverse Nyquist array method. If the open-loop system is assumed to be stable (poles at the origin assumed to be stable), then the contour shown in Figure 3.2 can be used and p_0, the number of zeros of the open loop characteristic polynomial in the right half plane is equal to zero. According to Rosenbrock's [65] stability criteria the closed-loop system will be stable if the diagonal elements of the inverse of the open-loop transfer function matrix encircle the origin counterclockwise the same number of times as they encircle the point (-1,0).

To satisfy this encirclement criterion it is necessary to change the signs in loops 1 and 2. This can be done using the following controller:

$$K_4^{-1} = \begin{bmatrix} -1.0 & 0 & 0 \\ 0 & -1.0 & 0 \\ 0 & 0 & 1.0 \end{bmatrix} \tag{3.29}$$

The open loop transfer function matrix at this stage is $Q_4(w)$, where $Q_4^{-1}(w) = K_4^{-1}\ Q_3^{-1}(w)$. The inverse Nyquist diagrams of its diagonal elements are shown in Figure 3.10. The pre-compensator which has been used to make the open-loop transfer function matrix diagonally dominant and stable is given by K_B, where:

$$K_B^{-1} = K_4^{-1}\ K_3^{-1}\ K_2^{-1}\ K_1^{-1} \tag{3.30}$$

and

$$K_B^{-1} = \begin{bmatrix} -0.300 & -0.751 & 0.0 \\ -0.930 & 2.096 & -1.0 \\ 1.000 & -0.830 & 0.0 \end{bmatrix} \tag{3.31}$$

or

$$K_B = \begin{bmatrix} -0.830 & 0.0 & 0.751 \\ -1.000 & 0.0 & -0.300 \\ -1.324 & -1.0 & -1.327 \end{bmatrix} \qquad (3.32)$$

Step three: Design of a multiloop control system for the open-loop transfer function matrix

The final step in the design procedure is the selection of the final controllers in each loop. Because the transfer function between the output and the input for each loop is represented by a first order system the use of only proportional plus integral controller in each loop should be sufficient to produce good control. Physically, this means that a controller matrix $K_C(z)$ should be selected such that the final multivariable regulator is given by

$$K(z) = K_B\ K_C(z) \qquad (3.33)$$

where $K_C(z)$ is given by Equation (3.34). If only proportional control is to be used:

$$K_C = \begin{bmatrix} k_1 & 0 & 0 \\ 0 & k_2 & 0 \\ 0 & 0 & k_3 \end{bmatrix} \qquad (3.34)$$

When proportional and integral control is desired $K_C(z)$ is given by Equation (3.35) i.e.

$$K_C(z) = \begin{bmatrix} k_1 + \frac{1}{\tau_1}\ \frac{1}{1-z^{-1}} & 0 & 0 \\ 0 & k_2 + \frac{1}{\tau_2}\ \frac{1}{1-z^{-1}} & 0 \\ 0 & 0 & k_3 + \frac{1}{\tau_3}\ \frac{1}{1-z^{-1}} \end{bmatrix} \qquad (3.35)$$

The selection of the controller constants of matrix K_C can be either done using simulated runs or by direct tuning of the controller constants in the field. Although the selection of the controller constant was, in this case, done by experimental tuning, the use of simulated runs could be helpful in some cases.

A very useful piece of information to guide the selection of the the final controller constants in matrix K_C is the estimation of the stability gain region for each loop (i.e. the gain margins). This can be obtained graphically from the diagonal elements of the inverse of the open-loop transfer function matrix, $Q_4(w)$ in Figure 3.10. The closed-loop system will be stable and diagonally dominant for the following gains:

$$\text{Loop 1:} \quad \infty > 1/k_1 > 1/18.5 \quad \text{or} \quad 0 < k_1 < 18.5 \qquad (3.36)$$

$$\text{Loop 2:} \quad \infty > 1/k_2 > 1/49.2 \quad \text{or} \quad 0 < k_2 < 49.2 \qquad (3.37)$$

$$\text{Loop 3:} \quad \infty > 1/k_3 > 1/37.0 \quad \text{or} \quad 0 < k_3 < 37.0 \qquad (3.38)$$

Note that this system has "high integrity" against measurement transducer or error monitoring component failures because it remains stable and diagonally dominant for a wide range of gains (including zero or "open-loop"). According to the Ziegler-Nichols rules the recommended value for the controller constants k_1, k_2 and k_3 is 50% of the ultimate gains given in Equation (3.36), (3.37) and (3.38) respectively. These values were found to be too high when the regulator was experimentally implemented although the simulated runs had indicated the opposite. For this reason a decision was made to tune the loops in the field.

Figure 3.11 presents a simulated response of the closed-loop third order, evaporator model for a 20% step change in the feed flow disturbance using different gains for k_1, k_2 and k_3. The values used for these gains are 50% (controller: FD0350), 30% (controller: FD0330) 20% (FD0320) and 10% (FD0310) of their respective ultimate gains. It can be seen that there is an improvement of the closed-loop system response when the gains are increased. This improvement is mainly in the control of the first-effect hold-up, W_1.

Figure 3.12 presents the response of the controlled system for a 20% step change in the feed flow when the gains used in each loop are equal to their ultimate gains. As expected the evaporator is on the verge of instability.

In order to evaluate the degree of interaction in the control system Figure 3.13 presents the response of the control system for a 10% step change in the setpoint of the product concentration, C_2, when the controller constants k_1, k_2, κ_2 are 50% (controller: FD0350) and 20% controller: FD0320) of their respective ultimate gains. In this case there is not much improvement in the response of the double-effect evaporator when the gains k_1, k_2 and k_3 are increased. However the system is, for all practical cases, non-interacting regardless of the gains used. The use of the controller (FD0350) for this step change violates the physical constraints in variable B_2.

The selection of the controller constants for the proportional-integral control case was also done by experimental tuning. In this case it was not possible to apply the Ziegler-Nichols' rules to select the integral constants because the crossover frequency for each loop is zero.

The results of the experimental tuning of the controller obtained in this section are presented in Chapter Six.

3.7 DESIGN OF A MULTIVARIABLE REGULATOR FOR THE FIFTH ORDER EVAPORATOR MODEL

The design of a multivariable regulator for the double-effect evaporator pilot plant, described in appendix A and represented by a fifth order model, is presented in this section.

The z-transform of the system used in this example is also given by Equation (3.24). The only difference with respect to the example presented in the last section is that in this example G(z), which is shown in Table 3.5, was obtained from a discrete, five-state (rather than three state) linear, time-invariant model with normalized perturbation variables. This model was obtained by Wilson [76] and it is shown in Table A.2 in Appendix A. As in the previous example the design was carried out using the w-bilinear transformation of G(z). The w-plant transfer function matrix, G(w), is shown in Table 3.6.

The poles of G(z) and G(w) or the zeros of the open-loop characteristic polynomial of the fifth order double-effect evaporator model are shown in Table 3.7.

TABLE 3.7

Poles of the Fifth Order Evaporator Model

z-plane	w-plane
1.0	0.0
1.0	0.0
0.9604	-0.0202
0.9216	-0.0408
0.4328	-0.3905

The inverse of the w-plant transfer function matrix is presented

TABLE 3.5

z-transfer Function Matrix Derived from the Fifth Order Evaporator Model

$$G(z) = \begin{bmatrix} \dfrac{-0.01191\ (z+0.7628)}{(z-1.0)(z-0.4384)} & \dfrac{-0.08169}{(z-1.0)} & 0 \\[2ex] \dfrac{-0.01375\ (z+0.7628)}{(z-1.0)(z-0.4384)} & \dfrac{0.08474}{(z-1.0)} & \dfrac{-0.04957}{(z-1.0)} \\[2ex] \dfrac{0.01373\ (z+0.7628)(z-0.8898)}{(z-0.9603)(z-0.9216)(z-0.4384)} & \dfrac{-0.04328}{(z-0.9603)} & 0 \end{bmatrix}$$

The characteristic polynomial of this transfer function matrix is given by:

$$\text{OLCP} = (z-1.0)^2(z-0.9603)(z-0.9216)(z-0.4384)$$

TABLE 3.6

w-transfer Function Matrix Derived from the Fifth Order Evaporator Model

$$G(w) = (w-1.0)\begin{bmatrix} \dfrac{0.000982\ (w+7.432)}{w(w+0.3905)} & \dfrac{0.04085}{w} & 0 \\ \dfrac{0.001134\ (w+7.432)}{w(w+0.3905)} & -\dfrac{0.04237}{w} & \dfrac{0.02029}{w} \\ -\dfrac{0.001142\ (w+7.432)(w+0.0583)}{(w+0.3905)(w+0.0408)(w+0.0202)} & \dfrac{0.02208}{(w+0.0202)} & 0 \end{bmatrix}$$

in Table 3.8. The plant in this example is also marginally stable since it contains two poles on the unit-circle in the z-plane.

Step one: Pairing the input-output variables of the evaporator

The inverse Nyquist array of $G(w)$ presented in Figure 3.14 shows that there is a strong interaction between the loops in the system. This is also shown in Figure 3.15 which presents the diagonal elements of $G^{-1}(w)$ with their Gershgorin bands. In this example interaction can be reduced by an appropriate pairing of variables or by renumbering the inputs.

As in the previous example the best combination is obtained if W_1 is controlled by B_1, W_2 is controlled by B_2 and C_2 is controlled by S. This change can be implemented by pre-multiplying the matrix $G^{-1}(w)$ by K_1^{-1} where:

$$K_1^{-1} = \begin{bmatrix} 0 & 1 & 0 \\ 0 & 0 & 1 \\ 1 & 0 & 0 \end{bmatrix} \tag{3.39}$$

The inverse Nyquist array of $Q_1^{-1}(w) = K_1^{-1}\, G^{-1}(w)$ is shown in Figure 3.16 and its diagonal elements with their Gershgorin bands are shown in Figure 3.17. From these figures it can be observed that the matrix $Q^{-1}(w)$ is not diagonally dominant. Therefore it is necessary to continue with the second step in the design procedure.

Step two: Design of a pre-compensator to make the matrices $Q^{-1}(w)$ and $R^{-1}(w)$ diagonally dominant

TABLE 3.8

Inverse of the w-transfer Function Matrix Derived from the Fifth Order

Evaporator Model

$$G^{-1}(w) = \frac{1}{(w-1.0)} \begin{bmatrix} \dfrac{323.2\ w(w+0.3905)(w+0.0408)}{(w+7.430)(w+0.0527)} & 0 & \dfrac{-\text{[illegible]}.8\ (w+0.3905)(w+0.0408)(w+0.0202)}{(w+7.430)(w+0.0527)} \\ \dfrac{16.71\ w(w+0.0583)}{(w+0.0527)} & 0 & \dfrac{14.37\ (w+0.0408)(w+0.0202)}{(w+0.0527)} \\ \dfrac{16.83\ w(w+0.0774)}{(w+0.0527)} & 42.29\ w & \dfrac{63.45\ (w+0.0408)(w+0.0202)}{(w+0.0527)} \end{bmatrix}$$

Step 2a) Design of a constant pre-compensator

From the Nyquist array of $Q^{-1}(w)$ in Figure 3.16 it can be observed that rows 1 and 3 of $Q_1^{-1}(w)$ are slightly diagonally dominant at low frequencies. Row 2 can be made diagonally dominant at low frequencies by subtracting from this row 2.0 times row 1 and by adding 0.3 times row 3 to row 2. This operation can be performed by pre-multiplying $Q_1^{-1}(w)$ by the following controller:

$$K_2^{-1} = \begin{bmatrix} 1 & 0 & 0 \\ -2.0 & 1 & 0.3 \\ 0 & 0 & 1.0 \end{bmatrix} \tag{3.40}$$

The new open-loop transfer function matrix is given by

$$Q_2^{-1}(w) = K_2^{-1}\, Q_1^{-1}(w) \tag{3.41}$$

The Nyquist array and the diagonal elements with the Gershgorin bands of $Q_2^{-1}(w)$ are shown in Figures 3.18 and 3.19 respectively. Diagonal dominance can still be improved in row 3 of $Q_2^{-1}(w)$ by subtracting 2.0 times row 1 from row 3, i.e. $Q_2^{-1}(w)$ must be pre-multiplied by

$$K_3^{-1}(w) = \begin{bmatrix} 1 & 0 & 0 \\ 0 & 1 & 0 \\ -2.0 & 0 & 1 \end{bmatrix} \tag{3.42}$$

The improvements on diagonal dominance in $Q_3^{-1}(w) = K_3^{-1}\, Q_2^{-1}(w)$ can be observed from Figure 3.21 which shows the diagonal elements of $Q_3^{-1}(w)$ with the Gershgorin bands. The Nyquist array of Q_3^{-1} is also presented in Figure 3.20.

Diagonal dominance can be improved marginally in row 1 or $Q_2^{-1}(w)$ by adding to this row 0.15 times row 3, or by pre-multiplying

$Q_3^{-1}(w)$ by the controller:

$$K_4^{-1} = \begin{bmatrix} 1.0 & 0 & 0.15 \\ 0 & 1 & 0 \\ 0 & 0 & 1 \end{bmatrix} \qquad (3.43)$$

The Nyquist array of the new open-loop transfer function matrix $Q_4^{-1}(w) = K_4^{-1} Q_3^{-1}$ is shown in Figure 3.22 and the diagonal elements of this matrix with their Gershgorin bands are presented in Figure 3.23.

In order to satisfy the stability criterion in each loop the sign has to be changed in rows 1 and 2 by pre-multiplying Q_4^{-1} by the controller matrix:

$$K_5^{-1} = \begin{bmatrix} -1 & 0 & 0 \\ 0 & -1 & 0 \\ 0 & 0 & 1 \end{bmatrix} \qquad (3.44)$$

The diagonal elements of $Q_5^{-1}(w)$ are shown in Figure 3.24 for a frequency range of 0.01 - 1.0, in Figure 3.25 for a frequency range of 0.01 - 0.5 and in Figure 3.26 for a frequency range of 0.1 - 5.0. From these figures it can be concluded that the OLTFM and the CLTFM are only diagonally dominant at low frequencies. Consequently the closed-loop stability and the stability region cannot be determined at this stage and the design cannot be continued. In order to make the inverses of the open-loop and closed-loop transfer function matrices diagonally dominant a dynamic pre-compensator has to be used.

Several proportional-integral controllers were tested but none of them make the inverses of the OLTFM and CLTFM diagonally dominant. Thus a more complicated controller was necessary to complete the design of a control system for the double-effect evaporator. This is discussed in the next section.

This example is a good illustration of one of several pitfalls of the inverse Nyquist method. It is not always possible to find a simple controller which will make the inverses of the OLTFM and the CLTFM diagonally dominant. Furthermore if diagonal dominance is not obtained the design cannot be completed using this design method. (In Chapter Five it will be shown that the *direct* Nyquist array method can be applied to this example, to design a proportional control matrix.)

Step 2b) Design of a dynamic pre-compensator

From the Nyquist array of $Q_1^{-1}(w)$ and the Nyquist diagrams of its diagonal elements in Figures 3.16 and 3.17 it was observed that only row 3 was diagonally dominant. It is obvious from Figure 3.16 that diagonal dominance at low frequencies could be obtained in row 2 by subtracting row 1 from row 2, i.e. by pre-multiplying the matrix $Q_1^{-1}(w)$ by

$$(K_2^1)^{-1} = \begin{bmatrix} 1 & 0 & 0 \\ -1 & 1 & 0 \\ 0 & 0 & 1 \end{bmatrix} \qquad (3.45)$$

The Nyquist array of $(Q_2^1(w))^{-1} = (K_2^1)^{-1}\ Q_1(w)$ is shown in Figure 3.27 and the Nyquist diagrams of its diagonal elements with their respective Gershgorin bands are shown in Figure 3.28. A careful examination of the poles and zeros of the matrix $(Q_2^1(w))^{-1}$ and of Figure 3.27 shows that row 3 could be made perfectly diagonally dominant if a phase-lag compensator is used and the following elementary row operation is performed:

$$\text{row } 3 = \text{row } 3 - 19.2\ \left(\frac{w + 0.390}{w + 7.400}\right) \times \text{row } 1 \qquad (3.46)$$

This operation can be accomplished if $(Q_2^1(w))^{-1}$ is pre-multiplied by:

$$(K_3^1(w))^{-1} = \begin{bmatrix} 1 & 0 & 0 \\ 0 & 1 & 0 \\ -19.2\ (\frac{w + 0.390}{w + 7.400}) & 0 & 1 \end{bmatrix} \qquad (3.47)$$

The new OLTFM is given by:

$$(Q_3^1(w))^{-1} = (K_3^1(w))^{-1}\ (Q_2^1(w))^{-1} \qquad (3.48)$$

The Nyquist array of $(Q_3^1(w))^{-1}$ and the Nyquist diagrams of its diagonal elements with their Gershgorin bands are shown in Figure 3.29 and 3.30 respectively. Figure 3.29 and an analysis of the poles and zeros of $(Q_3^1(w))^{-1}$ indicates that row 1 can be made perfectly diagonally dominant if a phase-lead compensator is used and the following operation is performed:

$$\text{row 1} = \text{row 1} + 0.0165\ (\frac{w + 7.400}{w + 0.390}) \times \text{row 3} \qquad (3.49)$$

This operation can be accomplished by using the following controller matrix:

$$(K_4^1(w))^{-1} = \begin{bmatrix} 1 & 0 & 0.0165\ (\frac{w + 7.400}{w + 0.390}) \\ 0 & 1 & 0 \\ 0 & 0 & 1 \end{bmatrix} \qquad (3.50)$$

The Nyquist array of $(Q_4^1(w))^{-1} = (K_4^1(w))^{-1}\ (Q_3^1(w))^{-1}$ and the Nyquist diagrams of its diagonal elements with their Gershgorin bands in Figures 3.31 and 3.32 show that rows 1 and 3 are almost diagonal.

However row 2 is only diagonally dominant at low frequencies. An improvement in the diagonal dominance of row 2 can be obtained if another phase-lead compensator is used and the following operation is performed:

$$\text{row } 2 = \text{row } 2 + 0.056\left(\frac{w + 7.400}{w + 0.390}\right) \times \text{row } 3 \tag{3.51}$$

To perform this operation it is necessary to use the following controller matrix:

$$(K_5^1(w))^{-1} = \begin{bmatrix} 1 & 0 & 0 \\ 0 & 1 & 0.056\left(\frac{w + 7.400}{w + 0.390}\right) \\ 0 & 0 & 1 \end{bmatrix} \tag{3.52}$$

The Nyquist diagrams of the diagonal elements of matrix $(Q_5^1(w))^{-1} = (K_5^1(w))^{-1}\ (Q_4^1(w))^{-1}$ in Figure 3.33 indicate that this matrix is almost diagonal. The Gershgorin circles are very small but the diagonal elements (loops) 1 and 2 are unstable. To correct this situation it is necessary to pre-multiply $(Q_5^1(w))^{-1}$ by

$$(K_6^1)^{-1} = \begin{bmatrix} -1 & 0 & 0 \\ 0 & -1 & 0 \\ 0 & 0 & 1 \end{bmatrix} \tag{3.53}$$

The Nyquist diagrams of the diagonal elements with their Gershgorin bands of the OLTFM $(Q_6^1(w))^{-1} = (K_6^1)^{-1}\ (Q_5^1(w))^{-1}$ are presented in Figure 3.34.

The pre-compensator used to make the inverses of the open- and closed-loop transfer function matrices diagonally dominant is then given by:

$$K_B^{-1}(w) = (K_6^1)^{-1} \times (K_5^1)^{-1} \times (K_4^1)^{-1} \times (K_3^1)^{-1} \times (K_2^1)^{-1} \times K_1^{-1} \tag{3.54}$$

or

$$K_B(w) = \begin{bmatrix} -19\left(\frac{w + 0.390}{w + 7.400}\right) & 0 & 0.668 \\ -1 & 0 & -0.0165\left(\frac{w + 7.400}{w + 0.390}\right) \\ -1 & -1 & -0.0725\left(\frac{w + 7.400}{w + 0.390}\right) \end{bmatrix} \qquad (3.55)$$

The z-transform of pre-compensator $K_B(w)$ is equal to:

$$K_B(z) = \begin{bmatrix} -3.144\left(\frac{z - 0.4383}{z + 0.7619}\right) & 0 & 0.668 \\ -1 & 0 & -0.0997\left(\frac{z + 0.7619}{z - 0.4383}\right) \\ -1 & -1 & -0.438\left(\frac{z + 0.7619}{z - 0.4383}\right) \end{bmatrix} \qquad (3.56)$$

Step three: Design of a multiloop control system for the open-loop transfer function matrix: $Q_6^1(w)$

In this step the controller matrix K_C must be selected such that the multivariable regulator is equal to:

$$K = K_B\, K_C \qquad (3.57)$$

If only proportional control is desired K_C will be given by:

$$K_C = \begin{bmatrix} k_1 & 0 & 0 \\ 0 & k_2 & 0 \\ 0 & 0 & k_3 \end{bmatrix} \qquad (3.58)$$

When proportional plus integral control is required K_C is given by Equation (3.35).

In order to select the final gains in each loop it is very useful to obtain the gain margins of each loop for which the system will remain closed-loop stable. This piece of information can be graphically obtained from Figure 3.34. The control system will be stable for the following set of gains:

$$\text{Loop 1: } \frac{1}{15.6} < k_1 < \infty \quad \text{or} \quad 0 < k_1 < 17.9 \tag{3.59}$$

$$\text{Loop 2: } \frac{1}{49.2} < k_2 < \infty \quad \text{or} \quad 0 < k_2 < 49.2 \tag{3.60}$$

$$\text{Loop 3: } \frac{1}{50.9} < k_3 < \infty \quad \text{or} \quad 0 < k_3 < 50.9 \tag{3.61}$$

These gain margins are almost the same as the gain margins obtained in Section 3.6 using the third order model with the exception of the third loop in which there is a difference of less than 20%. This makes the comparison between the controller matrices obtained in this section and Section 3.6 easier.

The simulated response of the fifth order model for a 20% step change in the feed flow and using the controller obtained in this section (continuous line) and the controller obtained from the third order model (broken lines) are presented in Figures 3.35, 3.36 and 3.37. The final gains used for each controller in Figures 3.35, 3.36 and 3.37 are approximately 10% (controllers FD0310, NADY0510), 20% controllers FD0320, NADY0520) and 30% (controllers FD0330, NADY0530) respectively of the corresponding ultimate gain of each loop. As expected, in every case the dynamic regulator gives slightly better results than the proportional controller designed based on the third order model.

Figure 3.38 presents the simulated response of the fifth order model for a 10% step change in the product concentration, C_2, set-point when the dynamic compensator obtained in this section (continuous line) and the constant compensator obtained from the third order model (broken lines) are used. The final gains used for each loop in this case are approximately 20% of their corresponding ultimate gain. It can be observed that the dynamic compensator produces a less interacting control system than the controller obtained from the third order model.

Since similar problems to those described in the previous section were expected in the experimental implementation of the dynamic regulator no decision about the final proportional and proportional-integral constants was made at this point. The selection of the final gains was done by experimental tuning and the results are presented in Chapter Six.

3.8 CONCLUSIONS

From the examples presented in the chapter and from the experience obtained in implementing and applying this method the following conclusions were drawn:

1) The inverse Nyquist array is a simple technique which provides a systematic means of incorporating several typical control system design requirements, e.g. stability, interaction, integrity against transducer and error monitoring failures, and a satisfactory transient response.

2) A direct and easy interpretation of one of the theorems due to Ostrowski [55] is possible when using this method. This theorem permits the determination of the location of the inverse of a transfer function of a loop when it is open and the rest are closed [67]. With this theorem it is possible to determine the exact stable gain space more accurately [69] and to find out when the system is under tight control.

3) The requirement of diagonal dominance is the most severe short-

coming of this method. Some design freedom could be wasted in making the system diagonally dominant. (Conversely, changes to the design method that would generate a narrower band than the Gershgorin band would mean greater accuracy and, in many cases, less control action to produce diagonal dominance.) In some cases, like in the fifth order evaporator model, it is not possible to fulfill this requirement with a proportional or proportional plus integral controller and consequently it is not possible to design a simple controller for this type of system. In other cases this problem can be overcome at the cost of additional calculations using the procedure indicated in Section 3.3.

4) Since it is the controller matrix and not its inverse which will be implemented there is no direct indication in the inverse Nyquist array method of the complexity of the controller when a dynamic compensator is being designed. This problem is more critical for discrete systems where as a matter of convenience it is desirable to use a bilinear transformation.

5) The method does not have the flexibility to design a control system of high integrity for actuator failures.

CHAPTER FOUR

THE CHARACTERISTIC LOCUS METHOD

4.1 INTRODUCTION

Most of the frequency domain design methods for multivariable control systems which have been proposed recently [e.g. 41,45,57,58] are based on a generalization of the scalar return-difference quantity introduced by Bode [7]. Included in this group is the characteristic locus method [4,5,41,42] which was developed by Belletrutti and MacFarlane [4] and has been discussed in detail by MacFarlane and Belletrutti [5,41,42].

Because of its more recent development the experience with this method is more limited than with the inverse Nyquist array method [65]. Only a very limited number of examples using this method have been presented in the literature [e.g. 4,42]. However this method is receiving more attention recently [60,72,76].

In order to compare the characteristic locus method with the inverse and direct Nyquist array methods the former method has also been included in this study. The investigation of the characteristic locus method has covered the same aspects covered in the study of the inverse Nyquist array method presented in Chapter Three.

Since the characteristic locus method for continuous systems has been discussed in detail by MacFarlane and Belletrutti [4,5,41,42] the discussion of theoretical aspects of this method in Section 4.2 of this chapter is restricted to the design of discrete control systems. In Section 4.3 an example of the design of a multivariable regulator for a double-effect evaporator pilot plant represented by a discrete three-state linear time-invariant model is presented. The results of the experimental implementation of the controller developed in this chapter are presented in Chapter Six. In the final section of this chapter some conclusions about the characteristic locus method based on the experience obtained in using this method are presented.

4.2 THE CHARACTERISTIC LOCUS METHOD

4.2.1 Basic Theory

The characteristic locus method was developed to design multivariable feedback control systems of the type represented by Figure 2.1. For this type of system Popov [61] and later Hsu and Chen [24] have proven that

$$|F(z)| = \frac{CLCP}{OLCP} \tag{4.1}$$

where:

$F(z) = I_m + T(z)$ = return-difference transfer function matrix

$T(z)$ = return-ratio transfer function matrix

CLCP = closed-loop characteristic polynomial

OLCP = open-loop characteristic polynomial

The return-ratio matrix T(z) will depend on the way the loops are broken in the control system represented by Figure 2.1. When the loops are broken after the plant transfer function matrix, T(z), is equal to

$$T(z) = G(z)\ K(z)\ H(z) \tag{4.2}$$

If the loops are broken before or after the control matrix K(z) the return-ratio matrix T(z) is given by $T_e(z)$ or $T_u(z)$ respectively where

$$T_e(z) = H(z)\ G(z)\ K(z) \tag{4.3}$$

and

$$T_u(z) = K(z)\ H(z)\ G(z) \tag{4.4}$$

Since the feedback transducer matrix, $H(z)$, can always be made part of the plant or control matrix without loss of generality it will be assumed that the matrix $H(z)$ is equal to a unity matrix. In this case Equation (4.2) is equal to the open-loop transfer function matrix, $Q(z)$.

Using Equation (4.1) and the principle of the argument, Belletrutti and MacFarlane [4] have shown that, for systems represented by Figure 2.1, if the determinant of the return-difference matrix $|F(z)|$ maps the contour D, shown in Figure 3.1, into Γ_f encircling the origin n_f times clockwise, then the closed-loop multivariable system will be stable if and only if

$$n_f = -p_o \tag{4.5}$$

where p_o is the number of zeros outside the unit circle of the OLCP.

The use of this stability criterion as a basis for a design method is impractical because it is not possible to design a multivariable regulator in a systematic way, i.e., it is not possible to correlate the values of $|F(z)|$ with the elements of the controller matrix.

A more useful stability criterion has been obtained in terms of the characteristic values or the eigenvalues of the return-difference matrix, $F(z)$. It has been shown [4] that if the characteristic values $f_i(z)$ $(i=1,2\ \dots\ m)$ of $F(z)$ map D into Γ_{fi} encircling the origin n_{fi} times clockwise then

$$n_f = \sum_{i=1}^{m} n_{fi} \qquad (4.6)$$

and the system will be stable with all its loops closed if and only if:

$$\sum_{i=1}^{m} n_{fi} = -P_0 \qquad (4.7)$$

Although this stability criterion is more useful than the previous one its use as a basis for a design technique is still very limited because it does not provide a systematic way to design the control matrix.

A more practical method can be obtained if the characteristic values, $t_i(z)$ ($i=1,2 \ldots m$) of the return-ratio matrix $T(z)$, of the system shown in Figure 2.1 are used. Since the return-difference matrix, $F(z)$, and the return-ratio matrix, $T(z)$, are related by the following equation:

$$F(z) = I_m + T(z) \qquad (4.8)$$

the relationship between the eigenvalues of $F(z)$ and $T(z)$, by applying the eigenvalue shift theorem [35], is given by:

$$f_i(z) = 1 + t_i(z) \quad (i=1 \ldots m) \qquad (4.9)$$

From Equation (4.9) it can be observed that the difference between the Nyquist diagram of $f_i(z)$ (characteristic locus of $F(z)$) and the Nyquist diagram of $t_i(z)$ (characteristic locus of $T(z)$) is simply a shift in the imaginary axis. Consequently, if $t_i(z)$ maps the contour D, shown in Figure 3.1, into Γ_{ti} encircling the point (-1,0), n_{ti} times clockwise it follows that:

$$n_{fi} = n_{ti} \tag{4.10}$$

and the multivariable system shown in Figure 2.1 will be stable with all its loops closed if and only if:

$$\sum_{i=1}^{m} n_{ti} = -p_o \tag{4.11}$$

Any of the return-ratio matrices given by Equations (4.2), (4.3) and (4.4) can be used to determine the stability of the closed-loop system using Equation (4.11). However the return-ratio matrix given by Equation (4.2) is usually preferred because the return-ratio matrix is equal to the open-loop transfer function matrix, Q(z).

4.2.2 Design Objectives: Stability, integrity, non-interaction and accuracy

Based on the stability criterion given by Equation (4.11) Belletrutti and MacFarlane [4] have developed the characteristic locus method. This is a general method which includes provision for taking the following design objectives into consideration: stability, integrity, interaction and accuracy.

A control system is said to have good integrity if it remains stable under all combinations of a stipulated set of failure conditions [4]. A control system of high integrity, against the failure in the output transducer of one loop, can be designed using the characteristic locus method by ensuring that the characteristic loci (Nyquist diagrams of the characteristic values) of the principal sub-matrix obtained by deleting the corresponding column and row from the return-ratio matrix given by Equation (4.2) satisfy the stability criterion given by Equation (4.11). Other types of failures can also be considered with this method by requiring that the respective principal sub-matrix of the appropriate return-ratio matrix satisfy the stability criterion given by Equation (4.11) [4].

For systems represented by Figure 2.1 the closed-loop transfer function matrix, R(z), is expressed in the following form:

$$R(z) = [I + Q(z)]^{-1}Q(z) \qquad (4.12)$$

where:

$$Q(z) = T(z) = G(z)\ K(z)$$

When the eigenvalues or characteristic values of Q(z) are distinct and are associated with linearly independent characteristic vectors or directions denoted by $w_i(z)$, $(i=1,2 \ldots m)$ the open-loop transfer function matrix can be expressed in the following way [42]:

$$Q(z) = W(z)[\mathrm{diag}\{t_i(z)\}]\ V(z) \qquad (4.13)$$

where:

$$W(z) = [w_1(z),\ w_2(z)\ \ldots\ w_m(z)] \qquad (4.14)$$

$$V(z) = W^{-1}(z) \qquad (4.15)$$

$t_i(z)$ = ith characteristic value of Q(z) or T(z)

Then from Equation (4.12) it can be shown [42] that the closed-loop transfer function matrix is equal to:

$$R(z) = W(z)[\mathrm{diag}\,(\frac{t_i(z)}{1 + t_i(z)})]\ V(z) \qquad (4.16)$$

It can be observed from Equation (4.16) that the characteristic values, $r_i(z)$, of the closed-loop transfer function matrix are given by:

$$r_i(z) = \frac{t_i(z)}{1 + t_i(z)} \qquad i=1,2 \ldots m \qquad (4.17)$$

and by comparing Equations (4.16) and (4.13) the characteristic directions (eigenvectors) of the closed-loop transfer function matrix are equal to the characteristic directions of the open-loop transfer function matrix, Q(z).

Using this information the characteristic locus method can be used to design a control system of low interaction by aligning the eigenvectors of the open-loop or return-ratio matrix with the standard basis set of vectors, i.e., by designing $Q(z) = G(z)\ K(z)$ such that the matrix W(z) approaches the identity matrix.

At low frequencies interaction can be reduced when using the characteristic locus method [42] by ensuring that the gain of the characteristic loci, $t_i(z)$, of Q(z) are high enough such that:

$$\frac{t_i(z)}{1 + t_i(z)} \simeq 1 \qquad i=1 \ldots m \qquad (4.18)$$

From Equation 4.16 it can be seen that both approaches will tend to make the closed-loop transfer function matrix, R(z), diagonal.

The accuracy of the control system, defined as the degree to which the actual outputs follow the desired outputs [42], can also be considered when using the characteristic locus method. High accuracy can be obtained in a system when the magnitudes of the characteristic loci of the open-loop transfer function matrix are relatively large at low frequencies. When this is the case Equation (4.18) will be satisfied and the closed-loop TFM will tend to be equal to a unity matrix. Consequently the output will follow closely any change in the setpoints.

4.2.3 Design Procedure

The characteristic locus method can be applied to square as well as non-square plants but it is relatively easier to apply to square plants.

The design procedure using the characteristic locus method involves four phases whose order depends upon the relative importance of each property. These four phases are

- stability phase
- integrity phase
- interaction phase
- performance phase

In each phase a basic controller, $K_i(z)$, is designed in an interactive and iterative way to give the system the desired properties. The final controller is given by the product of the basic controller matrices found during the different phases, i.e.

$$K(z) = \prod_{i=1}^{P} K_i(z) \tag{4.19}$$

Three types of diagrams are commonly used with this method. The most important ones are the characteristic loci diagrams (part a of Figures 4.1 through 4.15) which are the Nyquist diagrams of the characteristic values (eigenvalues) of the open-loop or return-ratio transfer function matrix, Q(z). These diagrams are used to determine graphically the stability of the closed-loop system by applying to them the stability criterion represented by Equation (4.11). Another diagram (part b of Figures 4.1 through 4.15) used is the magnitude of the characteristic loci as a function of frequency. This plot is useful to select the gains which are desirable in order to have low interaction and high accuracy at low frequencies. From this diagram it can be readily observed when Equation (4.18) will be satisfied and consequently when the system will have non-interacting and high accuracy properties. The third diagram (part c of Figures 4.1 through 4.15) plots the alignment of the characteristic directions (eigenvectors) of the matrix Q(z) or R(z) with the standard basis vectors as a function of frequency. These diagrams are useful to determine the degree of interaction of the closed-loop and open-loop system at any frequency. When the characteristic directions are properly aligned they will be orthogonal, i.e., matrices W(z) and R(z) in Equation (4.16) will be diagonal. Consequently the closed-loop system will be non-interacting.

4.2.4 General Comments

Different types of basic controller matrices have been suggested [5,42] to give the control system specific properties. Several of these controllers have also been recommended for use with the inverse Nyquist array method [65,67]. The idea of the commutative controller can be incorporated as part of this method. The commutative controller method [36] can be used when it is required to change the characteristic values without changing the characteristic directions (eigenvectors) of the open-loop transfer function matrix.

Unfortunately the design of a controller using the characteristic locus method, at least as originally proposed, is a difficult task especially for a plant whose transfer function matrix is of order greater than two. In higher order systems it is difficult to establish the relationship between the characteristic loci and the elements of the controller matrix and hence the systematic selection of a controller becomes the major problem. The designer also does not get any physical insight into the system because the characteristic loci do not have a "physical meaning" such as can be attributed to the direct Nyquist diagrams.

Recent papers have proposed more systematic approaches to the to the design of controllers using the characteristic locus method [60, 508] One approach proposed by Owens [60] involves the selection of a controller such that the characteristic values of the open-loop matrix, $Q(z)$, take specified values at a given frequency. This is done by expanding the transfer function matrix in a dyadic form [59]. The other scheme developed by Kouvaritakis [508] designs the controller by breaking the frequency range of interest into three regions: low, intermediate and high. At high frequencies a real controller, K_h, is designed to improve the aligment between the eigenvectors of $G(z)$ and the standard basis vectors. The resulting open-loop transfer function matrix $Q_1(z) = G(z)K_h$ is then considered as the new plant transfer function matrix. At intermediate frequencies a new controller, $K_m = W_m \mathrm{diag}(k_i(z))\ V_m$ is designed to compensate (about the critical point) the characteristic values of $Q_1(z)$ (where W_m and V_m approximate at intermediate frequencies the eigenvector and the reciprocal eigenvector structure of $Q_1(z)$). The controller K_m must tend to a unity matrix at high frequencies so that it does not upset the eigenvector alignment affected in the first stage of the design. The new open-loop transfer function matrix $Q_2(z)=G(z)K_hK_m(z)$ now becomes the new plant transfer function matrix. Finally at low frequencies a proportional-integral controller, K_1, is designed. The proportional matrix will be a unity matrix and the integral matrix will be equal to $\alpha W_1 \mathrm{diag}(k_i)V_1$, where W_1 and V_1 approximate, at low frequencies, the eigenvector and the reciprocal eigenvector structure of $Q_2(z)$. The gains, k_i, are selected to adjust the magnitude of the characteristic values of $Q_2(z)$ and α determines the duration of the integral action as the frequency increases. This controller must also tend to the unity matrix at high frequencies.

The design of multivariable control systems using the characteristic values of the return-difference and return-ratio matrix to determine the stability of the system was proposed by Bohn [502,503] previous to the development of the characteristic locus method by Belletrutti and MacFarlane [4]. In his work [503] which was mainly directed toward the diagonalization of the return-ratio matrix, Bohn pointed out some of the difficulties of working with characteristic values. These difficulties have also been commented on more recently by Rosenbrock and Cook [72] and by MacFarlane [506]. The difficulties arise because the characteristic values (eigenvalues) of the return-difference matrix are not necessarily rational polynomials as in the case when the closed-loop characteristic polynomial is factored by conventional methods. Therefore the characteristic values may not be single-valued analytical functions of z at all point within the closed contour D. If the characteristic values are not single-valued then the Nyquist criterion cannot be applied directly to each individual characteristic value unless branch cuts are introduced in the Nyquist contour [503]. These branch cuts are important in determinig the number of encirclements of the critical point of each individual characteristic value. However, they do not need to be considered when determining the total number of encirclements, $n_f = \sum_{i=1}^{m} n_{ti}$, of the deteminant of the return-difference matrix because the branch cut locus is always traced through in opposite directions for each conjugate pair of characteristic values [503]. Thus, in practical applications, the test for system stability based on the total number of encirclements, n_f, is not changed by the (possible) existence of irrational characteristic values.

One important restriction in the characteristic locus method arises because the characteristic values are a property of the system matrix rather than being associated with individual feedback gains $\{k_i, i=1,..m\}$. Therefore, the use of characteristic values to determine the stability region of a system requires that the same gain be used for each loop in the system [503]. Recently Rosenbrock and Cook [72] have examined the characteristic locus method for the case when different gains, k_i, are used in each loop. It has been found [72] that if different gains, $\{k_i, i=1,..m\}$, are used then further restrictions are required on the return-ratio or open-loop transfer function matrix, More specifically, when different feedback gains $\{k_i, i=1,..m\}$ are used the characteristic locus method is valid only when:

1. The open-loop matrix Q(z) is a normal matrix for all values of z around the contour D, i.e.

$$Q(z)\ Q^T(z) = Q^T(z)\ Q(z) \tag{4.20}$$

   where $Q^T(z)$ is the transpose of Q(z). Then the stability of the closed-loop system can be determined by application of a theorem due to Freeman et al. [18].
2. The return-difference matrix, F(z), is diagonally dominant. The stability of the system in this case can be determined using a theorem due to Rosenbrock [70] and Cook [11] (This theorem is the basis of the direct Nyquist array method discussed in next chapter.).

The same restrictions apply for the case discussed in Chapter Three when the characteristic loci of the inverse of the open-loop transfer function matrix are used to design a control system.

4.3 DESIGN OF A MULTIVARIABLE REGULATOR FOR THE THIRD ORDER EVAPORATOR MODEL

A design of a multivariable regulator for the double-effect evaporator, described in Appendix A, using the characteristic locus method is developed in this section. The model used in this example is a discrete, three state, linear, time-invariant model with normalized perturbation variables. This model has been obtained from a tenth order model using the discrete Marshall's reduction technique [78]. The tenth order model has been obtained by Wilson [77]. This same model has also been used in Section 3.6 to design a multivariable regulator using the *inverse* Nyquist array method [65].

The z-transform of the model is given by:

$$\begin{bmatrix} W_1(z) \\ W_2(z) \\ C_2(z) \end{bmatrix} = \begin{bmatrix} G(z) \end{bmatrix} \begin{bmatrix} S(z) \\ B_1(z) \\ B_2(z) \end{bmatrix} \tag{4.21}$$

where G(z) is the plant z-transfer function matrix and is shown in Table 3.1. The outputs of the double-effect evaporator are the first effect hold up, W_1, the second effect hold-up, W_2, and the product concentration, C_2. The inputs of the system are the steam flow to the first effect, S, the bottoms flow from the first effect, B_1, and the bottoms flow from the second effect B_2.

For reasons explained in Section 3.4 the design of the multivariable regulator for the double-effect evaporator has been carried out using a w-bilinear transformation of the z-plant transfer function matrix. Thus G(w) has been used instead of G(z), where $w = \frac{z-1}{z+1}$. The w-transfer function matrix, G(w) is presented in Table 3.2. The poles of this transfer function matrix are shown in Table 3.1.

The system is marginally stable because two of its poles are at the origin in the w-plane. To determine the stability of the system the Nyquist contour shown in Figure 3.2 has been used. Using this contour the number of right-half-plane zeros of the open loop characteristic polynomial is equal to zero, i.e.

$$p_o = 0 \tag{4.22}$$

The design of the controller is based on the characteristic loci diagrams of the open-loop or return-ratio transfer function matrix. The three characteristic loci of G(w) are shown in Figures 4.1, 4.2 and 4.3. Each figure consists of three graphs. Graph (a) shows a characteristic locus of G(w). The labels indicate the numerical value at the end of each axis. The magnitude of this characteristic locus for different frequencies is shown in graph (b). The magnitudes are given in decibels and the frequency in radian/sec. Finally the alignment of the corresponding eigenvector with a standard basis vector at different frequencies is presented in graph (c). In this graph the angles are given in degrees. From these figures it can be observed that the closed-loop system without compensator will be unstable since they do not satisfy the stability criterion given by Equation (4.11). It also shows that there is a considerable amount of interaction in the open-loop transfer function matrix because eigenvectors 2 and 3 are both aligned with the same standard basis vector.

The most important design factor is the absolute stability followed by the interaction of the system. The performance and integrity of the system are considered later in the design.

The characteristic loci diagrams in Figures 4.1, 4.2, and 4.3 provide an indication of how well the control system will perform but they do not give any specific idea about the type of controller which must be used.

The selection of the controller is usually done by trying a specific type of controller matrix which is known to give the system certain properties. Then a decision about the value of this type of control is made by observing the characteristic loci diagrams.

A controller to reorder the inputs of the system was tried first. This could reduce the interaction and improve the relative stability of the system. From previous experience with the double-effect evaporator the best control scheme has been found to be when first effect hold up, W_1 is controlled by bottoms flow B_1, the second effect hold up, W_2, is controlled by bottoms flow, B_2 and the product concentration, C_2, is controlled by steam flow, S. This can be accomplished by using the following control matrix:

$$K_1 = \begin{bmatrix} 0 & 0 & 1.0 \\ 1.0 & 0 & 0 \\ 0 & 1.0 & 0 \end{bmatrix} \qquad (4.23)$$

The new OLTFM is then given by

$$Q_1(w) = G(w)\ K_1 \qquad (4.24)$$

The effect of K_1 on the characteristic loci of $Q_1(w)$ is difficult to predict but can be observed in Figures 4.4, 4.5 and 4.6 which show the three characteristic loci of $Q_1(w)$. Although two eigenvectors of $Q_1(w)$ are aligned with the same standard vector the system is less interacting in this case as shown by Figures 4.4c, 4.5c and 4.6c. The second eigenvector is perfectly aligned with the second standard vector as shown by Figure 4.5c. The system is however unstable because it does not satisfy the stability criterion given by Equation (4.11). It is necessary to change the signs in the characteristic loci 1 and 2 to make the system stable. This is done by using the following control matrix

$$K_2 = \begin{bmatrix} -1 & 0 & 0 \\ 0 & -1 & 0 \\ 0 & 0 & 1 \end{bmatrix} \qquad (4.25)$$

From the characteristic loci of $Q_2(w) = Q_1(w)\,K_2$ in Figures 4.7, 4.8 and 4.9 it can be observed that the closed-loop system is stable. This suggests that the characteristic loci 1 and 2 are strongly influenced by columns 1 and 2 respectively. In this case the three eigenvectors of $Q_2(w)$ are aligned with the second standard basis vector which indicates that $Q_2(w)$ is more interacting than $Q_1(w)$.

The closed-loop system is already stable. However the system does not have the desired properties, i.e., interaction, integrity, performance with the controller matrix K_1K_2. Therefore the controller matrix K_1K_2 was eliminated and another control matrix was tested instead.

One type of controller which is very useful and very often recommended [5,42,67] is one which makes the open loop system diagonal at very low and/or at very high frequencies. At very low frequencies the recommended [42] controller is given by:

$$K_0 = G^{-1}(0) \tag{4.26}$$

For the double-effect evaporator $G^{-1}(0)$ does not exist because it has two poles at the origin. However the controller which makes the system diagonal at high frequencies [42] is equal to:

$$K_\infty = G^{-1}(\infty)$$

or

$$K_\infty = \begin{bmatrix} 15.444 & 0.0 & -27.811 \\ 18.508 & 0.0 & 11.650 \\ 24.518 & 49.150 & 49.225 \end{bmatrix} \tag{4.27}$$

In order to apply this controller to the plant it is necessary to adjust the gains in each column. Then the control matrix will be given by

$$K_1^{\,1} = K_\infty D_1 \tag{4.28}$$

where D_1 is a diagonal matrix that can be chosen arbitrarily. In this case D_1 was chosen to be equal to:

$$D_1 = \begin{bmatrix} 1/24.5 & 0 & 0 \\ 0 & 1/49.15 & 0 \\ 0 & 0 & 1/27.8 \end{bmatrix} \tag{4.29}$$

so that the controller designed in this section is equal to the controller obtained using the direct Nyquist array in Section 5.4.

Then the new open-loop transfer function matrix is equal to

$$Q_1^{\,1}(w) = G(w)K_1^{\,1} \tag{4.30}$$

The characteristic loci of $Q_1^{\,1}(w)$ are presented in Figures 4.10, 4.11 and 4.12. From these figures it can be observed that the system is almost diagonal (the eigenvectors are properly aligned and consequently orthogonal) not only at very high frequencies but it also is diagonal for all the frequency spectrum. For this reason the characteristic loci can be used without any problem. From these diagrams it can also be observed that the system is unstable. This can be easily corrected by using the following controller:

$$K_2^{\,1} = \begin{bmatrix} -1 & 0 & 0 \\ 0 & -1 & 0 \\ 0 & 0 & -1 \end{bmatrix} \tag{4.31}$$

Figures 4.13, 4.14 and 4.15 show the characteristic loci of the new open-loop transfer function matrix $Q_2^1(w) = Q_1^1(w)K_2^1$. The closed-loop system with the controller $K_B = K_1^1 K_2^1$, i.e.

$$K_B = \begin{bmatrix} -0.630 & 0.0 & 1.000 \\ -0.755 & 0.0 & -0.420 \\ -1.000 & -1.0 & -1.777 \end{bmatrix} \qquad (4.32)$$

has very good properties besides stability. It is almost non-interacting and has high integrity against different transducer and error-monitoring failures.

The final phase in the design is the performance phase. It is a requirement in the design that the system must possess good performance characteristics. Good accuracy (in the sense of following changes in the setpoints) is achieved for setpoint changes whose frequency content is in the range in which the moduli of all the characteristic loci of the open-loop transfer function matrix are large. These moduli can be increased by increasing the final gain for each column.

From the characteristic loci of $Q_1^1(w)$ in Figures 4.10a, 4.11a and 4.12a it can be observed that the system can be represented by three first-order sub-systems. Thus the offsets of the system can be reduced by increasing the moduli of the characteristic values in Figure 4.10b, 4.11b and 4.12b. This means that proportional control only is sufficient to have a good control system. In this case the final control will be

$$K = K_B K_C \qquad (4.33)$$

where, K_B is given by Equation (4.32) and K_C is equal to

$$K_C = \begin{bmatrix} k_1 & 0 & 0 \\ 0 & k_2 & 0 \\ 0 & 0 & k_3 \end{bmatrix} \tag{4.34}$$

Before selecting the final gains in each loop it is convenient to determine the stability region or the stability margins of the closed-loop system. In general this is done by selecting the controller K_C such that:

$$K_C = kI_3 \tag{4.35}$$

where I_3 is the identity matrix and k is a parameter which is used to study the stability of the system. From Figures 4.13a, 4.14a and 4.15a it is found that the system will remain stable for the following values of k

$$0 < k < \frac{1}{0.0407} = 24.5 \tag{4.36}$$

In this particular example it is possible to expand this stability region by using different gains in each loop, i.e. by using Equation (4.34). This is because the system has very good diagonal dominance (almost diagonal) as will be seen in the next chapter (cf. Figure 5.12) and the Gershgorin bands are disjoint [72]. This ensures that the characteristic values of $Q_2^1(w)$ are single-valued for every value of w on the contour D and that a different gain can be applied to each characteristic value [72]. The expanded stability region for which the closed-loop system will remain stable can also be obtained from Figures 4.13a, 4.14a and 4.15a and it given by:

$$0 < k_1 < \frac{1}{0.0407} = 24.5 \tag{4.37}$$

$$0 < k_2 < \frac{1}{0.0203} = 49.15 \qquad (4.38)$$

$$0 < k_3 < \frac{1}{0.0360} = 27.8 \qquad (4.39)$$

Once the stability region has been determined the design procedure can be continued by selecting the final gain in each loop. The selection, in this case, was also done based on the stability margin of each loop. However for reasons similar to the ones explained in Section 3.6 the selection of the final gains was done by experimental tuning.

By selecting k_1, k_2 and k_3 in Equation (4.34) to be 50%, 30%, 20% and 10% of their respective ultimate gain the controllers FD0350, FD0330, FD0320 and FD0310 were obtained respectively. These control matrices are almost equal to the ones obtained in Section 3.6 using the inverse Nyquist array method. The simulated responses of the evaporator when these controllers are used and a 20 % step change in the feed flow is introduced in the system are presented in Figure 3.11. The simulated responses of the evaporator for a 10% step change in the setpoint of the product concentration when controller FD0350 and FD0320 are used are shown in Figure 3.13.

Integral action can also be added to the control system by designing, in this case, the matrix K_C given by Equation (3.35). The selection of this controller was also done by experimental tuning.

The experimental results obtained by implementing the controllers designed in this section are presented in Chapter Six.

4.4 CONCLUSIONS

The characteristic locus method [4,42] is a technique which can be used to design a stable control system with good integrity properties, low interaction and good performance. This method is more general than the inverse Nyquist array method [65] since it does not require the system to be diagonally dominant.

On the other hand the characteristic locus method is a less practical method than the inverse Nyquist array technique. The design of simple control matrices with the characteristic locus method is very difficult because the characteristic loci show how good the control is but they do not give any specific indication about the way the controller must be modified to improve the control system. This means that the design of the controller with this method cannot always be done in a systematic way. However the characteristic loci diagrams are a very good tool in the analysis of a control system. A controller can be easily accepted or rejected according to inspection of the characteristic loci diagrams of the open-loop transfer function. Nevertheless it is also possible to design a control system in a systematic way with the characteristic locus method if a scheme recently developed by kouvaritakis [508] is used.

CHAPTER FIVE

THE DIRECT NYQUIST ARRAY METHOD

5.1 INTRODUCTION

A very practical and powerful design technique which has been suggested [38,68,70,71] but not fully developed or discussed in the literature is what can be called the "direct" Nyquist array method. This method arises from the combination of principles from the inverse Nyquist array [65] and the characteristic locus methods [4,42]. More specifically, it combines the requirement of diagonal dominance used in the inverse Nyquist array method [65] with a stability criterion based on the encirclements generated by the return-difference transfer function matrix used in the characteristic locus method [4,42]. The direct Nyquist array method can also be derived by intuitive extension [15] of the conventional single-input, single-output Nyquist design procedures to the design multivariable control systems.

The direct Nyquist array method has been evaluated in this study and the following discussion focuses attention on the development and applications of this method.

The following discussion of the direct Nyquist array method is restricted to discrete systems. However, this discussion also applies directly to continuous systems. The basic theoretical aspects of the direct Nyquist array method are presented in Section 5.2 and they build upon what has been said about the characteristic locus method in Chapter 4. In Section 5.3 the development of the direct Nyquist array method by extension of conventional techniques is presented as a self-contained section. The application of the direct Nyquist array method to the design of a control system based on discrete three- and five-state, linear, time invariant double-effect evaporator models is presented in Sections 5.4 and 5.5, respectively. The models used in these examples are the same as the ones used in Chapters Three and Four.

In the final section of this chapter some conclusions about this method are presented based on the experience obtained in applying this method and from comparing this technique with the inverse Nyquist array method and the characteristic locus method.

5.2 THE DIRECT NYQUIST ARRAY METHOD

5.2.1 Stability Criterion

The characteristic locus method which has been discussed in Chapter Four is based on the Nyquist criterion of encirclement of the origin by the characteristic values of the return-difference matrix, F(z). It has been shown [4,42] that if the characteristic values $\{f_i(z), i=1, \ldots m\}$ of the return-difference transfer function matrix of a system represented by Figure 2.1 map the contour D, shown in Figure 3.1, into Γ_{fi} encircling the origin n_{fi} times clockwise then the multivariable system will be stable with all its loops closed if and only if

$$\sum_{i=1}^{m} n_{fi} = -p_o \tag{5.1}$$

where p_o is the number of zeros outside the unit circle of the open-loop characteristic polynomial.

It has also been mentioned in Chapter Four that this stability criterion was not very practical because it did not allow the design of the controller to proceed in a systematic way. However if the concept of diagonal dominance used in the inverse Nyquist array method [65] is used then a more practical stability criterion can be obtained. By requiring the return-difference matrix, F(z) to be diagonally dominant, i.e. that

$$|f_{ii}(z)| > \sum_{\substack{j=1 \\ j\neq i}}^{m} |f_{ji}(z)| \tag{5.2}$$

for column dominance or

$$|f_{ii}(z)| > \sum_{\substack{j=1 \\ j\neq i}}^{m} |f_{ij}(z)| \tag{5.3}$$

for row dominance, where f_{ij} represents element (i,j) of F(z), a stability criterion, which involves only the diagonal elements, $f_{ii}(z)$, of F(z) can be obtained. Using a theorem due to Gershgorin and a proof similar to the one used by Rosenbrock [65] in the inverse Nyquist array method it can be shown [11,38,70] that if the return-difference matrix is diagonally dominant for all the z on the contour D and the diagonal elements $f_{ii}(z)$ map D into Γ_{fii} encircling the origin n_{fii} times clockwise, then the system will be stable with all its loops closed if

$$\sum_{i=1}^{m} n_{fii} = -p_o \tag{5.4}$$

Since the return-difference matrix, when the transducer feedback matrix is an identity matrix, is equal to

$$F(z) = I_m + Q(z) \tag{5.5}$$

the relationship between the elements of F(z) and the open-loop transfer function matrix, Q(z), is given by:

$$f_{ii}(z) = 1 + q_{ii}(z) \tag{5.6}$$

and

$$f_{ij}(z) = q_{ij}(z) \qquad i \neq j \tag{5.7}$$

From Equation (5.6) it can be observed that the difference between the Nyquist diagram of $f_{ii}(z)$ and $q_{ii}(z)$ is a shift in the imaginary axis. Thus using Equation (5.4) it can be shown [38,70,71] that, when the return-difference matrix of a system represented by Figure 2.1 is diagonally dominant for all the z on the contour D, the closed-loop system will be stable if and only if the number of encirclements of the critical point (-1,0) by the Nyquist diagrams of the diagonal elements, $\{q_{ii}, i=1,..m\}$, of Q(z) is equal to $-p_o$, where p_o is the number of poles of Q(z) outside the unit circle in the complex plane. The direct Nyquist array method is based on this stability criterion.

5.2.2 Design Procedure

The design procedure used in the direct Nyquist array method is very similar to the one used in the inverse Nyquist array method.

The direct Nyquist array method makes use of the Nyquist array concept introduced by Rosenbrock [65] in the development of the inverse Nyquist array method. The Nyquist array of Q(z), which is a mxm set of Nyquist diagrams corresponding to each element in the matrix Q(z), is a very useful graphical tool for determining the effect of the controller matrix on the controlled system and for selecting the type of control which is necessary to satisfy the design requirements.

Diagonal dominance of the return-difference matrix can also be determined graphically by drawing the Gershgorin circles with their centers located on the Nyquist loci of the diagonal elements, $q_{ii}(z)$, of $Q(z)$. The radii, d_i, of the Gershgorin circles are equal to the sum of the magnitudes of the off-diagonal elements, i.e.

$$d_i = \sum_{\substack{j=1 \\ j \neq i}}^{m} |q_{ji}(z)| \tag{5.8}$$

if column dominance is used. When row dominance is used the radii of the Gershgorin circles, are equal to

$$d_i = \sum_{\substack{j=1 \\ j \neq i}}^{m} |q_{ij}(z)| \tag{5.9}$$

The return-difference matrix is diagonally dominant if the Gershgorin circles do not include the point (-1,0).

Rosenbrock [69] has shown that these Gershgorin bands have the property of containing a narrower band, the Ostrowski band, which is the boundary of a region where the transfer function between input i and output i is located, when loop i is open and the rest are closed. The Ostrowski circles have their centers on the Nyquist loci of $\{q_{ii}(z), i=1, \ldots m\}$ and their radii are equal to the radius of the Gershgorin circles multiplied by the factor α_i, where

$$\alpha_i = \max_{\substack{j \\ j \neq i}} \frac{d_j}{|1 + q_{jj}|} \qquad j = 1 \ldots m \tag{5.10}$$

The design of a control system using the direct Nyquist array method involves three steps:

1) Pairing the input-output plant variables.
2) Design of a simple pre-compensator which makes the return-difference matrix, F(z), diagonally dominant and gives Q(z) the desired properties.
3) Design of a multiloop control system based on the diagonal elements of the open-loop transfer function matrix, with their respective Gershgorin and Ostrowski bands.

5.2.3 Advantages of the Direct Nyquist Array Method

In this three step procedure the designer can take into account in an interactive and iterative way the following design requirements: stability,interaction, integrity against different failures, accuracy and the transient response of the closed-loop system. The design of the controller using this method is done in a systematic way and at each step the designer has some indication as to how the controller should be modified to achieve the desired performance.

The main difference between the direct and the inverse Nyquist array methods is that the direct method is based on the "conventional" Nyquist diagrams of Q(z) with which the practicing control engineer is familiar, while the inverse Method is based on the Nyquist diagrams of $Q^{-1}(z)$. Another major difference is that the inverse method requires the inverses of the closed- and open-loop transfer function matrices to be diagonally dominant while the direct method requires only the return-difference matrix to be diagonally dominant. This means that in the inverse method in order to determine the stability of the system the Gershgorin circles must not include neither the origin nor the critical point (-1,0) while in the direct method it is only necessary that the Gershgorin circles do not enclose the critical point (-1,0). As can be seen there is more flexibility and freedom in the selection of the controller with the "direct" approach. When Q(z) is known algebraically it is also possible to design a control system with the inverse Nyquist array method without requiring diagonal dominance from the inverse of the open-loop transfer function matrix. However this requires some additional calculations.

It is also possible to derive the direct Nyquist array design procedure based on an intuitive extension of conventional single-input, single-output Nyquist design procedures. Such an approach has the advantage of requiring no new theory and all the concepts and mathematical operations involved are familiar to most control engineers. Furthermore the intuitive development provides greater insight into the physical meaning of each step in the design procedure and also results in a more practical and more powerful design technique than has been obtained to date. This development is presented in the next section.

5.3 DEVELOPMENT OF THE DIRECT NYQUIST ARRAY METHOD BY EXTENSION OF CONVENTIONAL DESIGN TECHNIQUES

The problem of interest is feedback control of a multi-input multi-output, linear system such as shown in Figure 2.1. It is assumed that the system of interest is fully described by the $m \times \ell$ transfer function matrix, G(z), and that the compensator matrix, K(z), is to be designed to give stable, closed-loop control. In order to emphasize the two main steps in the proposed design procedure the feedback system will be treated as shown in Figure 5.1 in which the compensator is divided into two parts:

1) the dynamic component $\overline{K}(z)$ which is designed first so that the augmented plant $\overline{Q}(z) = G(z)\overline{K}(z)$ is square and has the desired dynamic characteristics.
2) the static component, K, which is a diagonal matrix of constant controller gains $\{k_{ii}, i=1 \ldots m\}$. As shown later, K can be designed on the basis of approximations which bound the true value of the system transfer functions and permit a modified Nyquist stability analysis to be completed.

The final step in the proposed design procedure generates m conventional Nyquist diagrams each of which is an exact representation of the relationship between one input-output pair of the augmented system when all the other loops are closed. The necessary and sufficient condition for stability of the closed-loop multivariable system, when the return-difference matrix is diagonally dominant for all the z on the contour D, is simply that these diagrams all satisfy the Nyquist criterion (cf. Appendix D).

For the sake of completeness the following discussion includes some concepts and definitions that have been discussed elsewhere or are already familiar to most control engineers.

5.3.1 Formulation of the Design Problem

System Model

Multivariable frequency domain design techniques assume that a suitable mathematical model of the system of interest can be derived and expressed in the form:

$$y(z) = G(z)u(z) \qquad (5.11)$$

Equation (5.11) shows that the relationship between the m-dimensional vector of plant output variables, $y(z)$, and the ℓ-dimentional vector of plant input variables, $u(z)$ is defined by the system transfer function matrix, $G(z)$. It is written in z transform notation because multivariable control systems are normally implemented using digital computers and hence the discrete formulation is most appropriate. However, the following development also applies directly to continuous systems which can be represented by Equation (5.11) written as a function of the Laplace transform variable s.

Control Strategy

It is assumed that the system described by Equation (5.11) is to be controlled by the multivariable feedback control system shown in Figure 2.1 where:

$$u(z) = K(z)[r(z) - y(z)] \tag{5.12}$$

$K(z)$ = ℓxm compensator matrix

$r(z)$ = an mx1 vector of setpoints or inputs.

It is easily shown that the controller matrix $K(z)$ can be expanded, without loss of generality into the form

$$K(z) = \overline{K}(z)\, K \tag{5.13}$$

where:

K is a mxm diagonal matrix of constant controller gains, k_{ii}

$\overline{K}(z)$ is a ℓxm matrix of dynamic elements

It will be seen that the use of a general controller matrix $K(z)$ as defined in Equation (5.13):

1) is frequently necessary to make the design procedure practical.
2) provides flexibility in the pairing of input-output variables.
3) permits non-square systems, $G(z)$, to be handled.
4) permits the specification of dynamic feedback controllers.
5) provides a means of achieving specific design objectives such as non-interaction, or specified system dynamics.
6) allows the designer to consider properties that are unique to multivariable systems such as the "integrity" (e.g. stability of each loop when one or more components in the other loops fail).
7) implies no loss of simplicity since setting $\overline{K}(z)$ equal to the identity matrix is equivalent to working directly with $G(z)$.

Figure 5.1 shows the general feedback control system of Figure 2.1 with the controller $K(z)$ broken into two parts: the static component, K, and the dynamic component, $\overline{K}(z)$. The following discussion will be concerned first with determining the elements k_{ij} of K and hence it will be assumed that the design of the dynamic part of the controller is complete and that it has been included as part of the augmented system $\overline{Q}(z)$ where

$$\overline{Q}(z) = G(z)\,\overline{K}(z) \tag{5.14}$$

The specification of the dynamic compensator, $\overline{K}(z)$, such that the augmented system $\overline{Q}(z)$ has the desired properties is discussed later. (Note that in Section 5.3 $q_{ij}(z)$ refers to an element of $\overline{Q}(z)$ while in the rest of the thesis it refers to an element of $Q(z) = G(z)\overline{K}(z)\,K =$

$\overline{Q}(z)K$. The use of $\overline{Q}(z)$ rather than $Q(z)$ emphasizes the role of the feedback gain elements k_{ii} of the matrix K but in latter sections it will be seen that the usual practice is to use $Q(z)$ to define the augmented plant at all stages in the design procedure regardless of how $K(z)$ is defined. The meaning is normally clear from context.)

The above approach implies that although $G(z)$ and $\overline{K}(z)$ may be non-square, $\overline{Q}(z)$ is always square and that the diagonal elements of the K matrix can be interpreted as constant feedback proportional controller gains, k_{ii}, associated with the control of the input/output pair $u_i'(z):y_i(z)$. One of the advantages of this approach is that it associates a single gain element, k_{ii} with each output, y_i, which is convenient both in the design stage and for field tuning of the resulting control system.

The specification of the individual controller gains, k_{ii}, obviously depends on the transfer functions relating each input-output pair of the augmented system. Therefore the following section discusses the derivation of these transfer functions.

5.3.2 Development of the Transfer Function Relating Each Input-Output Pair

The "open-loop" relationship between the input to the augmented plant, u_i', and output y_i, when the proportional feedback control loops are closed around all the other input-output pairs, is defined as:

$$y_i(z) = h_i(z)\, u_i'(z) \tag{5.15}$$

This relationship is illustrated in Figure 5.2 where the large shaded block represents the augmented system $\overline{Q}(z)$ with inputs u_i' and outputs

$y_i(z)$. Obviously $h_i(z)$ must be derived from the OLTFM of the augmented plant and the following subsections consider four cases in order of increasing generality (and complexity).

Diagonal OLTFM

The simplest case is when $\overline{Q}(z)$ is diagonal since $h_i(z)$ is then equal to the diagonal element $q_{ii}(z)$ and the selection of the feedback controller gains reduces to m independent, single-input single-output design problems. The design can be completed using any applicable design approach such as conventional Nyquist stability analysis.

2 x 2 OLTFM

In the more general case where the off-diagonal elements of $\overline{Q}(z)$ are non-zero there are interactions between the components of the input and output vectors, and in general $h_i(z)$ in Equation (5.15) becomes a function of several elements of $\overline{Q}(z)$ and also of the feedback controller gains, k_{ii}, in all the other loops. This is readily apparent when the general feedback system shown in Figures 5.1 and 5.2 is expanded into the more familiar block diagram form. Figure 5.3 shows the block diagram representation of a 2 x 2 system of the type shown in Figure 5.1 from which it follows directly that the transfer function relating the second input-output pair (assuming that the other loop is closed) is given by:

$$h_2(z) = q_{22}(z) + \left[\frac{-k_{11}q_{21}(z)}{1 + k_{11}q_{11}(z)}\right] q_{12}(z) \qquad (5.16)$$

which illustrates the dependence or interaction, between loop 2 and loop 1. This approach to the analysis of a 2 x 2 system is developed more fully in a separate research report [30].

3 x 3 OLTFM

The analysis of higher order systems is considerably more complicated but a straightforward block diagram analysis of a 3 x 3 system will show that $h_2(z)$ is as shown in Equation (5.17).

m x m OLTFM

The transfer functions defined by Equation (5.16) and (5.17) consist of the appropriate diagonal element $q_{ii}(z)$ plus m-1 terms which represent the effect of interactions with the other feedback control loops. Each of these "interaction terms" has the form of a coefficient multiplying an off-diagonal element in column i of $\overline{Q}(z)$. This representation generalizes to the form given by Equation (5.18). The relationship given by Equation (5.18) was derived independently and has a different structure, but gives the same $h_i(z)$ (when the m^{th} loop is open and the other m-1 loops are closed) as given by Rosenbrock [60]. Once the relationship between each input-output pair has been determined it is possible to proceed with the specification of the gains, k_{ii}.

$$h_2(z) = q_{22}(z) + \left[\frac{1}{1 - \left(\frac{k_{11}q_{31}(z)}{1 + k_{11}q_{11}(z)}\right)\left(\frac{k_{33}q_{13}(z)}{1 + k_{33}q_{33}(z)}\right)}\right]$$

$$\times \left\{ \left(\frac{-k_{11}q_{21}(z)}{1 + k_{11}q_{11}(z)}\right)[q_{12}(z)] \right.$$

$$+ \left(\frac{k_{33}q_{23}(z)}{1 + k_{33}q_{33}(z)}\right)\left(\frac{k_{11}q_{31}(z)}{1 + k_{11}q_{11}(z)}\right)[q_{12}(z)]$$

$$+ \left(\frac{-k_{33}q_{23}(z)}{1 + k_{33}q_{33}(z)}\right)[q_{32}(z)]$$

$$\left. + \left(\frac{k_{11}q_{21}(z)}{1 + k_{11}q_{11}(z)}\right)\left(\frac{k_{33}q_{13}(z)}{1 + k_{33}q_{33}(z)}\right)[q_{32}(z)] \right\} \qquad (5.17)$$

$$h_i(z) = q_{ii}(z) + L_i(z) \qquad (5.18a)$$

$$L_i^{col.}(z) = \sum_{\substack{j=1 \\ j\neq i}}^{m} \phi_{ji}(z)\, q_{ji}(z) \qquad (5.18b)$$

$$L_i^{row}(z) = \sum_{\substack{j=1 \\ j\neq i}}^{m} \phi_{ij}(z)\, q_{ij}(z) \qquad (F(z) \text{ row dominant}) \qquad (5.18c)$$

$$\phi_{ji}^{col.}(z) = \frac{\text{cofactor of element } (j,i) \text{ of } F^n(z)}{\text{cofactor of element } (i,i) \text{ of } F^n(z)} \qquad (5.18d)$$

$$\phi_{ij}^{row}(z) = \frac{\text{cofactor } (i,j)^T \text{ of } (F^n(z))^T}{\text{cofactor } (i,i) \text{ of } (F^n(z))^T} \qquad (5.18e)$$

$F(z)$ = Return Difference Matrix = $(I + Q(z))$ (5.18f)

$F^n(z)$ = Normalized Return Difference matrix obtained by dividing each column/row of $F(z)$ by the diagonal element in that column/row (5.18g)

5.3.3 Development of the Multivariable Frequency Domain Design Method

5.3.3.1 Direct Application of Nyquist Techniques to Each Input-Output

The design problem reduces to the specification of the individual feedback gain k_{ii} associated with each input-output pair of the augmented plant. Equation (5.18) can be used to *analyse* the system stability directly, but even with the use of computers, this approach is impractical for *design* purposes and hence resort is made to graphical techniques analogous to conventional Nyquist analysis.

Assuming the availability of an interactive computer program based on Equation (5.18) and a CRT terminal with graphic capability it is a relatively simple matter to display the Nyquist loci of the transfer function $\{h_i(z): i=1 \dots m\}$, relating each input-output pair. The gains k_{ii} can then be adjusted such that each of the loci satisfies the Nyquist stability criteria and has the characteristics that imply satisfactory closed-loop performance. This approach represents an intuitive extension of frequency domain analysis techniques from single-input single-output (SISO) to multiple-input multiple-output (MIMO) systems. However it is only valid when the return-difference matrix, F(z), is diagonally dominant for all the z on the contour D (cf. Appendix D). NOTE THAT NO MODIFICATION OF THE "SISO" NYQUIST STABILITY ANALYSIS IS SUGGESTED, OR REQUIRED. THE ONLY DIFFERENCE BETWEEN "SISO" SYSTEMS AND "MIMO" SYSTEMS FOR MOST PRCTICAL APPLICATIONS IS IN THE DERIVATION OF THE TRANSFER FUNCTION RELATING EACH INPUT-OUTPUT PAIR.

The stability analysis procedure outlined above is NOT practical for design purposes because, for example, a careful analysis of Equation (5.18) will shown that in addition to the requirement of diagonal dominance it is necessary to have specific numeric values for m-1 of the control parameters k_{ii} in order to evaluate any one transfer function, $h_i(z)$. In general, Equations (5.16), (5.17) or (5.18) are too complicated to give much guidance for the selection of a feasible set of control parameters. Similarly even if the designer comes up with an initial estimate for each controller gain, k_{ii}, Equation (5.18) and its associated Nyquist diagram, provide little practical guidance about how the controller gains should be modified to improve the overall system performance. The next section will show how a practical, convenient design method can be developed from the application of Nyquist analysis to modified forms of Equation (5.18).

5.3.3.2 Development of a Practical Frequency Domain Design Method

The form of Equation (5.18) is relatively simple but the coefficients $\phi_{ji}(z)$ are in general functions of the controller gains in all the other loops and hence it is difficult to design the first m-1 loops. The following subsections discuss various approximations for the interaction terms, $L_i(z)$, in Equation (5.18) which can be used to make the application of Nyquist techniques more practical.

Cases with Zero Interaction ($L_i(z) = 0$)

A common, and practical approach for systems with very weak interactions, is simply to complete the control system design assuming that $h_i(z) = q_{ii}(z)$, which implies that the interactions are neglected. The same effect could obviously be obtained by setting $L_i(z) = 0$ in Equation (5.18).

An alternative approach is to specify $\overline{K}(z)$ such that the OLTFM, $\overline{Q}(z)$ is diagonal. This approach is normally referred to as "the non-interacting design approach" and in terms of Equation (5.18) would result in values of zero for all the interaction terms $L_i(z)$.

Using Limiting Values for $L_i(z)$

Instead of simply neglecting the interactions or specifying $\overline{K}(z)$ so that $h_i(z) = q_{ii}(z)$ it is possible to find limiting values of $L_i(z)$ which can be used in Equation (5.18). For example if it were possible to define an upper limit, $L_i^{max}(z)$ on the magnitude of the interaction term $L_i(z)$, then it follows that the magnitude of the transfer function relating the i^{th} input-output pair would be bounded by:

$$\left\{|q_{ii}(z)| - L_i^{max}(z)\right\} \leq |h_i(z)| < \left\{|q_{ii}(z)| + L_i^{max}(z)\right\} \qquad (5.19)$$

In terms of a Nyquist diagram, Equation (5.19) shows that the Nyquist locus of the transfer function $h_i(z)$ lies within a band centered on the locus of $q_{ii}(z)$, and including the region defined by adding and subtracting, at each frequency, the value $L_i^{max}(z)$. More specifically the band is defined by circles, with radii equal to $L_i^{max}(z)$ centered on the loci of $q_{ii}(z)$, for all frequencies. An example is shown in Figure 5.5. Although this approach may sound awkward it leads to a very practical design procedure which is in fact equivalent to the Direct Nyquist Array (DNA) Method discussed earlier in this chapter. The following sections deal with concepts such as Gershgorin circles that are familiar from the proceeding development of the DNA method. This is followed by extensions based on Equation (5.18).

Gershgorin Circles: It can be shown (see Appendix C) that if the return difference matrix, F(z), is diagonally dominant, (as defined below) then $\phi_{ij}(z) \leq 1$ for all values of controller gains and for all frequencies. Thus it follows from Equation (5.18) and (5.19) that the Nyquist locus of $h_i(z)$ lies within a band centered on the locus of $q_{ii}(z)$ and with a width defined by circles with the following radi:

$$\text{radius of Gershgorin circles} = L_i^{max}(z) = \sum_{\substack{j=1 \\ j\neq i}}^{m} |q_{ij}(z)| \qquad (5.20)$$

This band is in fact the "Gershgorin band" defined in Equations (5.8) and (5.9). ($q_{ij}(z)$ does not contain k_{ii} and is defined the same in all equations) It has the obvious advantage of being independent of the controller gains and hence once the OLTFM is defined the Nyquist plots with the Gershgorin bands can be plotted for all diagonal elements, $q_{ii}(z)$. Since the locus of the exact transfer function, $h_i(z)$, must lie within the Gershgorin band the stability analysis can proceed as in the conventional Nyquist procedure but using the band in place of the locus. However if the critical point falls within the Gershgorin band then no decision can be made concerning the closed loop stability of that input-output pair.

This approach clearly shows that the Gerhsgorin band represents a region that will contain the locus of $h_i(z)$ regardless of what gains k_{ii} are used in the other loops - a fact that will be important to the understanding of system integrity. Also it is clear that the width of the band is a direct indication of the potential interactions of loop i with all the other loops in the multivariable system.

Diagonal Dominance: By analogy to the definitions used in the INA method, the return-difference matrix F(z) is said to be (columnwise) diagonally dominant if:

$$|f_{ii}(z)| > \sum_{\substack{j=1\\ j\neq i}}^{m} |f_{ji}(z)| \qquad i = 1,2 \ldots m \qquad (5.21)$$

where $f_{ij}(z)$ represents element (i,j) of F(z). Since $f_{ji}(z) = q_{ji}(z)$ for non-diagonal elements it follows directly from the physical significance of Equations (5.20) and (5.18b) that diagonal dominance is a guarantee that the critical point will not lie within the Gershgorin band and hence that this design approach is feasible. In practice the most convenient way of checking a system for diagonal dominance is to display the Gershgorin band associated with the Nyquist loci of the diagonal elements of $\overline{Q}(z)$ and see for what range of gain they satisfy the Nyquist stability criteria with respect to the critical point $(^{-1}/k_{ii}, 0)$.

Ostrowski Circles: As shown earlier in this chapter derivation of the direct Nyquist array method using theorems of linear algebra leads to the definition of the Ostrowski band. In terms of Equation (5.18) and (5.19) the Ostrowski band implies that when F(z) is diagonally dominant:

$$L_i^{max}(z) = \max_p \left\{ \frac{k_{pp}}{1 + k_{pp}q_{pp}(z)} \right\} \sum_{\substack{j=1\\ j\neq i}}^{m} q_{ji}(z) \qquad \begin{matrix} p = 1 \ldots m \\ p \neq i \end{matrix} \qquad (5.22)$$

The Ostrowski band defined by Equations (5.19) and (5.22) can be deduced from Equations (5.16) through (5.18). It is narrower than the Gershgorin band but requires values of the gains, k_{ii}, in all the other loops. As discussed later it is recommended that the "exact" relationship defined by Equation (5.18) be used rather than the Ostrowski approximation and hence Equation (5.22) is not discussed further.

5.3.4 Extensions to the Direct Nyquist Array Method

The DNA equivalent of the INA method developed by Rosenbrock involves a Nyquist analysis based on the diagonal elements of the augmented plant, $q_{ii}(z)$, plus the bands defined by the Gershgorin and Ostrowski circles. However the intuitive development that led to Equation (5.18) gives greater insight into the physical significance of the DNA method and permits several extensions which make the method more practical as well as more accurate.

For example once (m-1) of the gain elements k_{ii} have been determined, the m^{th} transfer function $h_i(z)$ can be evaluated directly from Equation (5.18) rather than using Gershgorin, Ostrowski, or other approximations. Also Equation (5.18) makes it easier to recognize cases where the interaction terms, $L_i(z)$, are zero and to calculate limiting values $L_i^{max}(z)$ that are more accurate than the Gershgorin circles. Some of these are discussed in the following sections.

Cases with Zero Interaction

If the augmented system, $\overline{Q}(z)$, is *diagonal* then, as pointed out previously, the radius of the Gershgorin circles is zero and the Nyquist analysis can be done ~~on the~~ basis of $q_{ii}(z)$.

A less demanding approach is to design the matrix $\overline{K}(z)$ so that the augmented system OLTFM is *triangular* in form. This would mean that all the interactions, $L_i(z)$, as defined in Equation (5.18) would be zero and hence the Nyquist analysis could again proceed on the basis of $q_{ii}(z)$.

The importance, to the design procedure, of zero elements in $\overline{Q}(z)$ does not seem to have been fully realized or utilized in previous proposals or implementations. Since $\overline{Q}(z) = G(z)\ \overline{K}(z)$, it is possible in many practical applications to generate zero elements in specific elements of $\overline{Q}(z)$ by proper specification of $\overline{K}(z)$ (Note that $\overline{K}(z)$ must be physically realizable and its poles and the zeros of det $\overline{K}(z)$ must be located inside the unit circle in the complex plane). If some of the interaction terms, $L_i(z)$, in Equation (5.18) can be made zero then this reduces the number of loops that must be designed by approximation and/or iteration. If enough zeros are introduced to make $\overline{Q}(z)$ triangular then the design of the MIMO system reduces to that of m SISO problems.

The Gershgorin circles, as defined previously, can be an overly conservative and misleading bound on system interactions because they do not take into account the existence of zero elements in $\overline{Q}(z)$. For example, most triangular OLTFM would result in Gershgorin circles of nonzero radius which would imply uncertainty, or interactions, when in fact none exists. Therefore it is desirable to develop better limiting values.

Limiting Values for the Interactions, $L_i(z)$

The Gershgorin circles result from the fact that the magnitude of the coefficients, $\phi_{ji}(z)$, as defined by Equation (5.18d) is always less than one when F(z) is diagonally dominant. However when $\overline{Q}(z)$ contains zeros then some of the terms that contribute to the interactions, $L_i(z)$, will be zero regardless of the gains, k_{ii}, in the other loops. In many cases a more accurate value of $L_i^{max}(z)$ can be derived if these zeros are taken into account.

G° Circles

From Equation (5.18d) it is obvious that $\phi_{ji}(z) = 0$ whenever the cofactor of element (j,i) of $F^n(z)$ (or equivalently of F(z) or Q(z)) contains the equivalent of a row or column of zeros. This condition is obvious to the designer from the structure of Q(z) and can be defined formally as:

$$\text{radius G° circles} = L_i^{max}(z) = \sum_{\substack{j=1 \\ j\neq i}}^{m} \phi^\circ_{ji} \, |q_{ji}(z)| \qquad (5.23)$$

where:

$\phi^\circ_{ji} = 0$ when the cofactor of $q_{ji}(z)$ is zero or $|q_{ji}(z)| = 0$
$= 1$ when $\phi_{ji}(z) \neq 0$

In the general case when all the $\phi_{ji}(z)$ are non-zero the G° and Gershgorin circles are equivalent. On the other hand the G° circles are more accurate when some of the coefficients are zero and can be used whenever F(z) is diagonally dominant.

5.3.5 Conclusions

The most significant result of the preceding development of the direct Nyquist array method is the insight it gives to the physical problem. It is also important, from the point of view of the examples discussed in the following sections, that Equation (5.18) could be used as an "exact" Nyquist plot of $h_i(z)$ as opposed to using the Ostrowski circles.

5.4 DESIGN OF A MULTIVARIABLE REGULATOR FOR THE THIRD ORDER EVAPORATOR MODEL

This section presents the design of a multivariable regulator for the double-effect evaporator pilot plant described in Appendix A using the direct Nyquist array method. The model of the system is the same as the one used in Sections 3.6 and 4.3 and it consists of a discrete, three state, linear, time invariant model with normalized perturbation variables. The model was obtained from the tenth order model, derived by Wilson [77], using the Marshall's reduction technique [78] and is presented in Table A.3.

The z-transform of the model is represented by the following equation:

$$\begin{bmatrix} W_1(z) \\ W_2(z) \\ C_2(z) \end{bmatrix} = \begin{bmatrix} \\ G(z) \\ \\ \end{bmatrix} \begin{bmatrix} S(z) \\ B_1(z) \\ B_2(z) \end{bmatrix} \qquad (5.24)$$

where G(z) has been obtained from the state space model shown in Table A.3 by using an algorithm of Souriau-Frame-Faddeev [66]. G(z) is presented in Table 3.1.

The outputs of the system are the first effect holdup, W_1, the second effect holdup, W_2, and the product concentration, C_2. Similarly the inputs are the steam flow to the first effect, S, the bottoms flow from the first effect, B_1, and the bottoms flow from the second effect, B_2.

For reasons explained before, the design has been carried on using w-transfer function matrices instead of z-transfer function matrices so the procedure will appear to the user as identical to that used for continuous systems. (w is a bilinear transformation of z such that $z = {}^{(1+w)}/(1-w)$.) The plant w-transfer function matrix is presented in Table 3.2. The poles of the third order evaporator model (i.e. the zeros of the open-loop characteristic polynomial) are shown in Table 3.3. The system has two poles at the origin in the w-plane. However, if the Nyquist contour used to determine the stability of the system is the one shown in Figure 3.2 then the number of right-half-plane zeros (p_0) of the open-loop characteristic polynomial is zero.

The direct Nyquist array is more convenient to the user than its counterpart the inverse Nyquist array because of the information it provides. For example, the Nyquist array of G(w), shown in Figure 5.4, for the range of frequencies, $0.15 \le w \le 10.0$, indicates that:

1) The first effect holdup, W_1, is affected mainly by the bottoms flow B_1, followed by the steam flow to the first effect, S.
2) The second effect holdup, W_2, is affected mainly by the bottoms flow B_1. However, the steam flow S and the bottoms flow B_2 also affect W_2 significantly.
3) The product concentration, C_2, is mainly by the steam flow, S, followed by the bottoms flow B_1.
4) The bottoms flow B_2 does not affect C_2 and W_1.

This information is not easily available from the inverse Nyquist array shown in Figure 3.3. The system in its present form is highly interacting. This can also be observed from Figure 5.5 which shows the diagonal elements of G(w) with their respective Gershgorin bands. In each case the Gershgorin bands include the origin. (The labels in each diagram indicate the scale at the end of each axis.)

Step one: Pairing the output-input variables of the evaporator

Interaction in the evaporator can be reduced by proper pairing of the variables. From the four points noted above, it can be concluded that the least interacting scheme is obtained when W_1 is controlled by B_1, W_2 is controlled by B_2 and C_2 is controlled by S. This means that column 1 must be made column 3, column 2 must be made column 1 and column 3 must be made column 2. This operation can be accomplished mathematically by post-multiplying the plant transfer function matrix by

$$K_1 = \begin{bmatrix} 0 & 0 & 1 \\ 1 & 0 & 0 \\ 0 & 1 & 0 \end{bmatrix} \tag{5.25}$$

It should also be noted in passing that this first step of the Nyquist array approach can be regarded as an alternative to the method recommended by Bristol [8,9] to select the different control loops in a multiloop scheme.

The Nyquist array of the new open loop transfer function matrix $Q_1(w) = G(w)\ K_1$, is presented in Figure 5.6. The diagonal elements of $Q_1(w)$ with their respective Gershgorin bands are shown in Figure 5.7. Only the second column of the system $Q_1(w)$ is diagonally dominant. Therefore, it is necessary to proceed with another step in the design.

Step two: Design of a pre-compensator to make the return-difference matrix, F(w), diagonally dominant

The objective in this step is to design the simplest controller which will make the return-difference matrix, F(z), diagonally dominant. The use of the Nyquist array plots is very helpful in this step. The Nyquist array of $Q_1(w)$ in Figure 5.6 suggests that:

-column 1 can be made diagonally dominant by adding to this column 2.1 times column 2.

-column 3 can be made diagonally dominant by subtracting from this column 0.93 times column 2.

These two elementary column operations can be done by post-multiplying $Q_1(w)$ by the following controller:

$$K_2 = \begin{bmatrix} 1.0 & 0.0 & 0.0 \\ 2.1 & 1.0 & 0.93 \\ 0.0 & 0.0 & 1.0 \end{bmatrix} \tag{5.26}$$

The new open-loop transfer function matrix is then equal to

$$Q_2(w) = Q_1(w)\ K_2 = Q(w)\ K_1 K_2 \tag{5.27}$$

Every column in $Q_2(w)$ is now diagonally dominant as can be seen from the Nyquist array of $Q_2(w)$ in Figure 5.8 and from the diagonal elements of $Q_2(w)$ with their Gershgorin bands in Figure 5.9. However, the diagonal dominance of column 3 can be improved further by subtracting 0.4 times column 1 from this column 3, i.e. by post-multiplying matrix $Q_2(w)$ by:

$$K_3 = \begin{bmatrix} 1 & 0 & -0.4 \\ 0 & 0 & 0 \\ 0 & 0 & 1 \end{bmatrix} \tag{5.28}$$

Figure 5.10 shows the Nyquist array of the new open loop transfer function matrix $Q_3(w) = Q_2(w) K_3$ and Figure 5.11 shows its diagonal elements, with their respective Gershgorin bands. It can be seen from these figures that columns two and three are almost perfectly diagonally dominant (i.e. imply "non interaction") and that diagonal dominance can be improved in column 1 by adding 0.63 times column 3 to column 1, i.e. by using the controller:

$$K_4 = \begin{bmatrix} 1 & 0 & 0 \\ 0 & 1 & 0 \\ 0.63 & 0 & 1 \end{bmatrix} \tag{5.29}$$

The Nyquist diagrams of the diagonal elements of $Q_4(w) = Q_3(w) K_4$ in Figure 5.12 indicate that $Q_4(w)$ is strongly diagonally dominant, i.e. the Gershgorin bands can hardly be noticed in this figure.

Having obtained a controller matrix which makes the OLTFM diagonally dominant the stability of the closed-loop system can now be determined. Using the Nyquist contour shown in Figure 3.2, $p_o = 0$ and hence the closed-loop system will be stable if none of the loci of the diagonal elements encircles the critical point (-1,0). In order to satisfy the stability criterion the sign in columns 1 and 2 must be changed. Thus it will be necessary to post-multiply $Q_4(w)$ by:

$$K_5 = \begin{bmatrix} -1 & 0 & 0 \\ 0 & -1 & 0 \\ 0 & 0 & 1 \end{bmatrix} \tag{5.30}$$

The diagonal elements of $Q_5(w) = Q_4(w) K_5$ are presented in Figure 5.13 and it is obvious that none of them encircle the critical point. Therefore the system is stable. Thus the controller that will make the OLTFM diagonally dominant and simultaneously make the closed-loop system stable is given by:

$$K_B = K_1K_2K_3K_4K_5 \tag{5.31}$$

or

$$K_B = \begin{bmatrix} -0.630 & 0.0 & 1.0 \\ -0.748 & 0.0 & -0.400 \\ -0.985 & -1.00 & -1.777 \end{bmatrix} \tag{5.32}$$

Step three: Design of individual controllers for each loop

Each loop in the system (i.e. the diagonal elements of the OLTFM) can be adequately represented by a first order transfer function. Thus the use of simple proportional, or proportional plus integral control in each loop should be sufficient to provide very good control.

The gain margins of each loop can be estimated graphically from Figure 5.13 using the same approach as in the design of single variable control systems. The system will be closed-loop stable if

Loop 1 $\quad 0 < k_1 < \frac{1}{0.0406} = 24.6 \qquad (5.33)$

Loop 2 $\quad 0 < k_2 < \frac{1}{0.0203} = 49.2 \qquad (5.34)$

Loop 3 $\quad 0 < k_3 < \frac{1}{0.0360} = 27.8 \qquad (5.35)$

The final controller matrix will be given by:

$$K = K_BK_C \tag{5.36}$$

where for proportional control K_C will be equal to

$$K_C = \text{diag}\ (k_1, k_2, k_3) \tag{5.37}$$

and for a proportional-integral control K_C will be given by Equation (3.35).

It should be noticed that the controller K_B and the stability margins given by Equations (5.32),(5.33),(5.34) and (5.35) are almost identical to the controller obtained using the characteristic locus method in Section 4.3. Also for the third order model it is possible to calculate a controller which will give a "perfectly" non-interacting system. This was done in Appendix E and the controller was almost identical to Equation (5.32). Thus in this example the "graphical" frequency domain design procedures led to essentially the same result as the analytical calculation. Another interesting result is obtained by letting $k_1 = 1.337$, $k_2 = 1.0$ and $k_3 = 0.751$ in Equation (5.37); the new controller matrix is then equal to:

$$K = K_B K_C = \begin{bmatrix} -0.842 & 0.0 & 0.751 \\ -1.000 & 0.0 & -0.300 \\ -1.317 & -1.0 & -1.329 \end{bmatrix} \tag{5.38}$$

and the new stability region will be given by:

Loop 1 $\quad 0 < k_1 < \frac{24.6}{1.337} = 18.4 \quad$ (5.39)

Loop 2 $\quad 0 < k_2 < \frac{49.2}{1.0} = 49.2 \quad$ (5.40)

Loop 3 $\quad 0 < k_3 < \frac{27.8}{0.751} = 37.0 \quad$ (5.41)

This is the same basic controller matrix with the same stability region obtained for the third order evaporator model using the inverse Nyquist array and the characteristic locus method in Sections 3.6 and 4.3 respectively. Thus the simulated runs shown in Figures 3.11, 3.12

and 3.13 in Section 3.6 also applies for the controller matrix given by Equation (5.32). The application of the Ziegler-Nichols settings rule to select the final gains produced excellent control in the simulated runs but they were found to be too high when these gains were used in the pilot plant. For this reason a decision was made to tune the loops experimentally for the proportional and proportional plus integral case. The selection of the matrix K_C by experimental tuning is presented in Chapter Six.

5.5 DESIGN OF A MULTIVARIABLE REGULATOR FOR THE FIFTH ORDER EVAPORATOR MODEL

In this example a multivariable regulator is designed using the direct Nyquist array for the double-effect evaporator plant described in Appendix A. The model used in this example is the same as the one used in Section 3.7, i.e. a discrete, five-state, linear, time invariant model as presented in Table A.2. The evaporator is represented in the z-domain by:

$$\begin{bmatrix} W_1(z) \\ W_2(z) \\ C_2(z) \end{bmatrix} = \begin{bmatrix} \\ G(z) \\ \\ \end{bmatrix} \begin{bmatrix} S(z) \\ B_1(z) \\ B_2(z) \end{bmatrix} \qquad (5.42)$$

where the plant z-transfer function G(z) is shown in Table 3.5. The design of the multivariable regulator, as in the previous cases and for reasons explained before has been done using a w-bilinear transformation of the plant z-transfer function matrix. Thus G(w) has been used instead of G(z), where $z = (1+w)/(1-w)$. G(w) is shown in Table 3.6.

The poles of the plant transfer function matrix or the zeros of the open-loop characteristic polynomial are shown in Table 3.7. The plant has two poles at the origin in the w-plane. The Nyquist contour used to determine the stability of the system is shown in Figure 3.2. Using this contour the number of right-half-plane zeros (p_0) of the open-loop characteristic polynomial is equal to zero. The Nyquist array of G(w) for a range of frequencies $0.1 < w < 5.0$ is shown in Figure 5.14. (Different ranges of frequencies have been used in the different examples in this thesis in order to have an appropriate scale in each diagram.) It can be observed from Figure 5.14 that:

1) the first effect holdup, W_1, is mainly affected by the bottoms flow B_1, followed by the steam flow, S.
2) the second effect holdup, W_2, is mainly influenced by the bottoms flow B_1 and followed, at high frequencies, by the bottoms flow B_2 and finally by the steam flow S. Note that at low frequencies the steam flow S has a greater effect than B_2 in controlling W_2.
3) the product concentration C_2 is affected almost equally by the steam flow S and the bottoms flow B_1.
4) the bottoms flow B_2 does not affect C_2 or W_1.

This is essentially the same information obtained in the previous example which gives an indication of the accuracy of the third order model. This information also indicates that the present configuration of the double-effect evaporator is highly interacting. This can also be observed in Figure 5.15 which shows the Nyquist diagrams of the diagonal elements of G(w) with their corresponding Gershgorin bands.

Interaction can be reduced in this case, without the use of a compensator by properly pairing the input-output variables.

Step one: Pairing the evaporator input-output variables

From the information obtained from the Nyquist array of G(w) in Figure 5.14 it can be concluded that the least interacting configuration is obtained when B_1 controls W_1, B_2 controls W_2 and S controls C_2.

This first step in the design involves a renumbering in the columns of G(w). This is obtained by post-multiplying the OLTFM by:

$$K_1 = \begin{bmatrix} 0 & 0 & 1 \\ 1 & 0 & 0 \\ 0 & 1 & 0 \end{bmatrix} \tag{5.43}$$

In Figures 5.16 and 5.17 the Nyquist array of $Q_1(w) = G(w)\ K_1$ and its diagonal elements with their Gershgorin bands are presented, respectively. Only column 2 is diagonally dominant. Consequently it is necessary to design a pre-compensator to make the system diagonally dominant.

Step two: Design of a pre-compensator to make the return-difference matrix F(w) diagonally dominant

Step 2a) Design of constant pre-compensator

This step involves the selection of the simplest controller that will make the return-difference matrix diagonally dominant, i.e. the selected controller must produce an open-loop system in which the Gershgorin circles of its diagonal elements do not enclose the critical point (-1,0). The use of the Nyquist array is again very helpful in this selection.

From Figure 5.16 it can be seen that column 1 can be made diagonally dominant if 2.0 times column 2 is added to column 1, i.e. if the following control matrix is used:

$$K_2 = \begin{bmatrix} 1.0 & 0.0 & 0.0 \\ 2.0 & 1.0 & 0.0 \\ 0.0 & 0.0 & 1.0 \end{bmatrix} \qquad (5.44)$$

Gershgorin bands are shown in Figures 5.18 and 5.19 respectively. Columns 1 and 2 of $Q_2(w)$ are now diagonally dominant. However the diagonal elements are unstable. These loops can be made stable by changing the signs in these two columns, i.e. by using the following controller matrix:

$$K_3 = \begin{bmatrix} -1 & 0 & 0 \\ 0 & -1 & 0 \\ 0 & 0 & 1 \end{bmatrix} \qquad (5.45)$$

The new OLTFM is equal to

$$Q_3(w) = Q_2(w)\ K_3 \qquad (5.46)$$

and its Nyquist array and diagonal elements are shown in Figures 5.20 and 5.21. Column 3 is still not diagonally dominant. However, it is obvious from Figure 5.20 that interaction can be reduced in this column by adding 0.4 times column 1 to column 3, i.e. by postmultiplying $Q_3(w)$ by the controller matrix:

$$K_4 = \begin{bmatrix} 1 & 0 & 0.4 \\ 0 & 1 & 0 \\ 0 & 0 & 1 \end{bmatrix} \qquad (5.47)$$

Figures 5.22 and 5.23 present the Nyquist array of $Q_4(w) = Q_3(w)\ K_4$ and its diagonal elements with their respective Gershgorin bands. Diagonal dominance in column 1 can slightly be improved by subtracting 0.6 times column 3 from column 1. This operation can be accomplished with the controller matrix:

$$K_5 = \begin{bmatrix} 1.0 & 0.0 & 0.0 \\ 0.0 & 1.0 & 0.0 \\ -0.6 & 0.0 & 1.0 \end{bmatrix} \qquad (5.48)$$

The Nyquist diagrams of the elements of $Q_5(w) = Q_4(w)\ K_5$ are shown in Figure 5.24 and the Nyquist diagrams of the diagonal elements with their Gershgorin bands are shown in Figure 5.25. The open-loop transfer function matrix $Q_5(w)$ is not diagonally dominant in column 3. A careful examination of Figure 5.24 suggests that the diagonal dominance can be improved in columns 1 and 3 but it will not be possible to make column 3 of the OLTFM, $Q_5(w)$ diagonally dominant using a constant pre-compensator. However it can be noticed in Figure 5.25 that the return-difference matrix, i.e.

$$F(w) = I + Q_5(w) \qquad (5.49)$$

is diagonally dominant. (The Gershgorin circles do not enclose the critical point (-1,0)). Thus it is possible, using a constant compensator, to continue in this case with the design. *This was not the case when the inverse Nyquist array method was used to design a static regulator for this system.*

The pre-compensator used so far to make the return-difference matrix diagonally dominant is given by:

$$K_A = K_1K_2K_3K_4K_5 \tag{5.50}$$

or

$$K_A = \begin{bmatrix} -0.600 & 0.0 & 1.0 \\ -0.760 & 0.0 & -0.400 \\ -1.520 & -1.0 & -0.800 \end{bmatrix} \tag{5.51}$$

From the Nyquist array of $Q_5(w)$ in Figure 5.24 it can be noticed that diagonal dominance of $F(w)$ could be improved a little in column 1 by subtracting 0.5 times column 2 from column 1. Similarly diagonal dominance in column 3 could also be improved by adding column 2 to column 3. This operation can be accomplished by post-multiplying $Q_5(w)$ by matrix K_6, where

$$K_6 = \begin{bmatrix} 1 & 0 & 0 \\ -0.5 & 1 & 1 \\ 0 & 0 & 1 \end{bmatrix} \tag{5.52}$$

The Nyquist array of $Q_6(w) = Q_5(w)\, K_6$, and the Nyquist diagrams of its diagonal element with their respective Gershgorin bands are shown in Figures 5.26 and 5.27, respectively. The new pre-compensator matrix, K_B, used to make the return-difference matrix diagonally dominant is then given by:

$$K_B = K_AK_6$$

or

$$K_B = \begin{bmatrix} -0.600 & 0.0 & 1.0 \\ -0.760 & 0.0 & -0.400 \\ -1.020 & -1.0 & -1.800 \end{bmatrix} \qquad (5.53)$$

The compensator K_B given by Equation (5.54) is approximately the same as the one obtained in Section 5.3 using the direct Nyquist array method and the third order model. (This is another indication of the accuracy of the third order model.)

The degree of diagonal dominance obtained in the return-difference matrix F(w) using the pre-compensator K_B is about the best that can be obtained when a constant pre-compensator is used. If better diagonal dominance is desired in the return-difference and in the open-loop transfer function matrix a dynamic compensator has to be designed. In order to investigate the effect of diagonal dominance in the performance of the control system a dynamic pre-compensator was also designed as part of this example to improve the degree of diagonal dominance in the open-loop transfer function matrix.

Step 2b: Design of a dynamic pre-compensator

It was observed from the Nyquist array of the OLTFM $Q_2(w)$ and from the Nyquist diagrams of its diagonal elements in Figures 5.18 and 5.19 respectively that columns 1 and 2 of $Q_2(w)$ were diagonally dominant. A careful examination of the poles and zeros of the plant transfer function matrix and the Nyquist array of $Q_2(w)$ in Figure 5.18 suggested that column 3 could be made diagonally dominant if a phase-lead compensator is used and the following elementary operation is performed.

$$\text{column } 3 = \text{column } 3 - 0.0559 \left(\frac{w + 7.400}{w + 0.390}\right) \times \text{column } 2 \qquad (5.54)$$

This operation can be realized if the matrix $Q_2(w)$ is post-multiplied by the following controller matrix:

$$K_3^1(w) = \begin{bmatrix} 1 & 0 & 0 \\ 0 & 1 & -0.0559\left(\frac{w + 7.400}{w + 0.390}\right) \\ 0 & 0 & 1 \end{bmatrix} \tag{5.55}$$

The new open-loop transfer function matrix, $Q_3^1(w)$ will be given by:

$$Q_3^1(w) = Q_2(w)\ K_3^1(w) \tag{5.56}$$

The Nyquist array of $Q_3^1(w)$ and the Nyquist diagrams of its diagonal elements with their Gershgorin bands are presented in Figures 5.28 and 5.29 respectively. It can be observed from Figure 5.29 that the three columns are diagonally dominant. However columns 1 and 3 are weakly diagonally dominant. The Nyquist array of $Q_3^1(w)$ in Figure 5.28 and an analysis of the zeros and poles of this matrix suggests that column 3 can be made almost diagonal if a phase-lead compensator is used and the following operation is performed:

$$\text{column 3} = \text{column 3} - 0.024\left(\frac{w + 7.400}{w + 0.390}\right) \times \text{column 1} \tag{5.57}$$

This operation can be accomplished if the matrix $Q_3^1(w)$ is post-multiplied by

$$K_4^1(w) = \begin{bmatrix} 1 & 0 & -0.0240\left(\frac{w + 7.400}{w + 0.390}\right) \\ 0 & 1 & 0 \\ 0 & 0 & 1 \end{bmatrix} \tag{5.58}$$

The Nyquist array of the new OLTFM $Q_4^1(w) = Q_3^1(w)\ K_4^1(w)$, is presented in Figure 5.30. The Nyquist diagrams of the diagonal elements of $Q_4^1(w)$ with their respective Gershgorin bands are shown in Figure 5.31. From this figure it can be observed that only column 1 of $Q_4^1(w)$ does not have very good diagonal dominance. However an analysis of the Nyquist array of $Q_4^1(w)$ in Figure 5.30 and of the poles and zeros of this matrix suggests that diagonal dominance in column 1 can be drastically improved if a phase-lag compensator is used and the following operation is performed on $Q_4^1(w)$:

$$\text{column 1} = \text{column 1} + 13.2\left(\frac{w + 0.390}{w + 7.400}\right) \times \text{column 3} \tag{5.59}$$

This operation can be realized if the matrix $Q_4^1(w)$ is post-multiplied by:

$$K_5^1(w) = \begin{bmatrix} 1 & 0 & 0 \\ 0 & 1 & 0 \\ -13.2\left(\frac{w + 0.390}{w + 7.400}\right) & 0 & 1 \end{bmatrix} \tag{5.60}$$

The new open-loop transfer function matrix, $Q_5^1(w)$ is given by

$$Q_5^1(w) = Q_4^1(w)\ K_5^1(w) \tag{5.61}$$

The Nyquist array of $Q_5^1(w)$ and Nyquist diagrams of their diagonal elements with their Gershgorin bands are presented in Figures 5.32 and 5.33 respectively. From Figure 5.33 it can be observed that $Q_5^1(w)$ has a high degree of diagonal dominance (it is almost diagonal). However two of its diagonal elements are unstable. To correct this situation it is necessary to post-multiply $Q_5^1(w)$ by

$$K_6^1 = \begin{bmatrix} -1 & 0 & 0 \\ 0 & -1 & 0 \\ 0 & 0 & 1 \end{bmatrix} \tag{5.62}$$

The Nyquist diagrams of the diagonal elements of the new open-loop transfer function matrix $Q_6^1(w) = Q_5^1(w)\ K_6^1$ are presented in Figure 5.34.

The dynamic compensator designed in this section to make the open-loop transfer function matrix diagonally dominant will be given by

$$K_B^1(w) = K_1 K_2 K_3^1(w)\ K_4^1(w)\ K_5^1(w)\ K_6^1 \tag{5.63}$$

or

$$K_B^1(w) = \begin{bmatrix} -13.2\ (\frac{w + 0.390}{w + 7.400}) & 0 & 1 \\ -0.683 & 0 & -0.024\ (\frac{w + 7.400}{w + 0.390}) \\ -0.629 & -1 & -0.1039\ (\frac{w + 7.400}{w + 0.390}) \end{bmatrix} \tag{5.64}$$

The z-transform of this controller is equal to

$$K_B^1(z) = \begin{bmatrix} -2.18\left(\frac{z - 0.4383}{z + 0.7619}\right) & 0 & 1 \\ -0.683 & 0 & -0.145\left(\frac{z + 0.7619}{z - 0.4383}\right) \\ -0.629 & -1.0 & -0.628\left(\frac{z + 0.7619}{z - 0.4383}\right) \end{bmatrix} \qquad (5.65)$$

Step three: Design of individual controllers for each loop

Step 3a. Stability analysis for the constant compensator

The controller matrix K_B given by Equation (5.53) was designed to produce diagonal dominance in the return-difference matrix and is typical of the best results that can be obtained using a compensator of constants. The design can be continued by selecting the individual controllers in each loop such that the final controller matrix is given by:

$$K = K_B K_C \qquad (5.66)$$

where K_C is diagonal. It has the following form when only proportional control is desired:

$$K_C = \begin{bmatrix} k_1 & 0 & 0 \\ 0 & k_2 & 0 \\ 0 & 0 & k_3 \end{bmatrix} \qquad (5.67)$$

The main objective in this step is the selection of the constant k_1 , k_2 , k_3 . In order to select these constants it is very useful to first determine the stability region for which the closed-loop system will remain stable, i.e. the gain margin of each loop. A conservative stability region can be obtained from the Nyquist diagrams of the diagonal elements of the OLTFM $Q_6(w)$ containing the respective Gershgorin bands in Figure 5.27. The closed-loop system in this case will remain stable for the following combination of gains.

$$\text{Loop 1:} \qquad 0 < k_1 < \frac{1}{0.0693} = 14.4 \qquad (5.68)$$

$$\text{Loop 2:} \qquad 0 < k_2 < \frac{1}{0.0231} = 49.2 \qquad (5.69)$$

$$\text{Loop 3:} \qquad 0 < k_3 < \frac{1}{0.116} = 8.62 \qquad (5.70)$$

The stability region given by Equations (5.68), (5.69) and (5.70) can be graphically represented by Figure 5.35. The closed-loop system will remain stable for any combination of gains inside the parallelopiped. Each side of this stability region can be expanded by making use of the Nyquist diagram of the exact transfer function of each loop when the rest of the loops are closed as given by Equation (5.18). However the determination of the expanded stability region involves a very complicated procedure and its complexity increases with the order of the system. The new region which is irregular has to be determined pointwise and each point has to be found by a trial and error procedure. In addition the use of Equation (5.18) will produce a discontinuous stability region since it is only possible to find the expanded stable space for the region which opposes each side of the parallelopiped, as shown in broken lines in Figure 5.35. This is because the use of the transfer function $\{h_i(z), i=1,..m\}$ given by Equation (5.18) only guarantees stability when the return-difference matrix is diagonally dominant, i.e. only one value of k_i can be varied in each trial and error attempt and the values of the other gains must be within the region defined by Equation (5.68)-(5.70). Because the benefits of obtaining an expanded stability region are marginal the calculation of the expanded gain space is not recommended and it was not done in this example.

Once the stability region has been obtained it is possible to select the final gains in each loop. In this example a direct application of the Ziegler-Nichols controller setting rules is not feasible since the gain margins obtained do not represent the ultimate gain of each loop. Therefore the selection of the final gains has to be done in a somewhat arbitrary way. One logical way to make this selection is by choosing the gains based on the conservative gain margins given by Equations (5.68), (5.69) and (5.70) and by using higher percentages of these values when the uncertainty is greater i.e. when the Gershgorin circles are larger. Additional tuning of the loops may be required for these cases.

An arbitrary selection in this example of a gain which is 34% of the gain margin for the first loop, 20% for the second loop and 65% for the third loop will produce the controller FD0320 shown in Table B.1 in the Appendix B. Controllers FD0310 and FD0330 can be obtained by using different percentages of the gain margins. Figures 3.36 and 3.38 present in broken lines the simulated response of the evaporator using controller FD0320 for a 20% step change in the feed flow and 10% step change in the setpoint of the product concentration, respectively.

The experimental tuning of the compensator given by Equation (5.54) is presented in Chapter Six.

Step 3b. Stability analysis for the dynamic compensator

Note that the dynamic compensator given by Equation (5.65) is very similar to the compensator for "perfect" non-interacting control (cf. Appendix E). The stability region can be determined using the Nyquist diagrams of the diagonal elements of $Q_6^1(w)$ in Figure 5.34. From this figure it can be established that the closed-loop system will be stable for the following combinations of gains:

Loop 1: $$0 < k_1 < \frac{1}{0.0395} = 24.1 \qquad (5.74)$$

Loop 2: $$0 < k_2 < \frac{1}{0.0212} = 50.6 \qquad (5.75)$$

Loop 3: $$0 < k_3 < \frac{1}{0.0415} = 31.5 \qquad (5.76)$$

The final control matrix in this case will be given by:

$$K^1(z) = K_B^1(z)\, K_C \qquad (5.78)$$

where K_C is also given by Equation (5.67) when only proportional control is desired.

It should be noted that if K_C in Equation (5.67) is selected, such that $k_1 = 1.464$, $k_2 = 1.0$ and $k_3 = 0.668$, the controller $K^1(z)$ given by Equation (5.78) and its stability region will be approximately equal to the dynamic compensator and the stability region obtained in Section 3.7 using the inverse Nyquist array and the fifth order model.

The selection of the final gains in this case was also done by experimental tuning. However the simulated responses of the evaporator for a 20% step change in the feed flow, when the gains used in each loop are 10% (controller NADY0510), a 20% (controller NADY0520) and 30% (controller NADY0530) of its corresponding ultimate gain, are also represented by the continuous line in Figures 3.35, 3.36 and 3.37 respectively. In this case there is also an improvement in the control system when the gains in each loop are increased. This improvement is mainly reflected in the first effect level.

Figure 3.38 presents the simulated response (continuous lines) of the evaporator when controller NADY0520 is used for a 10% step change in the setpoint of the product concentration, C_2. Since the system is non-interacting when the dynamic compensator is used only the product concentration is affected in this case.

Effect of Improving the Diagonal Dominance in the Evaporator

In the previous example it is possible to invesigate the effect of improving the diagonal dominance in the system. Three compensators were obtained that make the open-loop and return-difference matrices diagonally dominant to different degrees. These compensators were K_A given by Equation (5.51), K_B given by Equation (5.53) and K_B^1 given by Equation (5.64). The degree of improvement in the diagonal dominance of the system can be observed in Figures 5.25, 5.27 and 5.34 by comparing the radii of the Gershgorin circles. The compensator K_B^1 makes the system almost diagonal while K_A gives the poorest diagonal dominance.

Figure 5.36 presents the response of the open-loop compensated plant for a step change in the input corresponding to C_2. As expected, improving the diagonal dominance of a system makes it less interacting.

Figure 5.37 and 5.38 present the simulated response of the evaporator for a step change in feed flow and in the setpoint of the product concentration using controllers DNA0520, FD0320 and NADY0520. These controllers are based on the compensators K_A, K_B and K_B^1 respectively and have gains which are of the same magnitude. The controller NADYQ520 was used as a base case and its gains are 20 % of the corresponding ultimate gains. It can be observed from these figures that the performance of the evaporator improves slightly by improving the diagonal dominance in the OLTFM not only for a setpoint change but also for a step change in a load disturbance. It should also be noted that the improvement is smaller for a step change in the setpoint of C_2 than for a step change in the feed flow.

The effect of improving diagonal dominance in the system is also shown in Figures 3.35, 3.36, 3.37 and 3.38 which compare the performance of the evaporator using constant versus dynamic controllers. It can be noticed that when the gains are approximately the same for the dynamic and the constant compensators the response when using the dynamic compensator is slightly better than when the constant compensator is used. This is the case not only for a step change in a setpoint but also for a step change in a disturbance variable.

5.6 CONCLUSIONS

The direct Nyquist array method has been found to be a very practical and powerful design technique which arises intuitively by extending the conventional single-input, single-output Nyquist design procedure. This method has the advantage of requiring no new theory and all the concepts and mathematical operations involved are familiar to most control engineers. The direct Nyquist array method provides a systematic means of implementing control system design objectives such as: stability, reduction of interactions, high system integrity against component failures, good steady-state accuracy and acceptable transient responses.

The direct Nyquist array method is more practical than the characteristic locus method [4,42], because the Nyquist array plots provide more insight into the performance of the system and an indication of how to design a controller to produce a particular closed-loop characteristic rather than simply providing a test of whether or not the the desired result has been obtained. It must be noted that a procedure for the characteristic locus method has been developed recently by Kouvaritakis [508] to design a control system in a more systematic way.

The *direct* Nyquist array method is more practical than the *inverse* [65] method because the designer specifies the controller elements directly (rather than specifying elements of the inverse of the control matrix and having the computer calculate the actual values later). Thus the designer has a better "feel" of the complexity of the actual controller he is developing. Also the direct Nyquist array consists of "standard" Nyquist diagrams that represent components of the actual physical system (rather than their inverses) so most users would get a better physical insight than with the inverse method. With the *direct* method it is also possible to relax the requirement of diagonal dominance required by the *inverse* method and hence is applicable to a broader class of applications. From the computational point of view the direct Nyquist array method is more efficient than the inverse method since one extra operation is required in the latter method, i.e. the inversion of the plant transfer function matrix.

CHAPTER SIX

EXPERIMENTAL RESULTS AND COMPARISON WITH OTHER METHODS

6.1 INTRODUCTION

This chapter discusses the experimental evaluation of the multivariable regulators, designed in Chapters Three, Four and Five using the inverse Nyquist array [65], the characteristic locus [4,42] and the direct Nyquist array methods respectively. All of the controllers were designed for, and applied to the double effect evaporator described in Appendix A. These methods are also compared with an optimal-quadratic multivariable controller and a multiloop control scheme that have been applied previously to the same evaporator [27,53,77].

Each control system was evaluated by introducing a step change in one of the disturbance variables of the system. Three different disturbances can be used to upset the pilot plant evaporator: feed flow, feed concentration and feed temperature. Only the first two have been used in this study. Feed flow has been found to be the most severe disturbance in the system and this was the main reason for using it. The feed concentration disturbance has been used to evaluate the degree of interaction in the control system. The degree of interaction of the closed-loop system was also tested by introducing a step change in the setpoint of the product concentration in the double effect evaporator.

The experimental runs described in this chapter were done in two sets separated by several months during which the evaporator was operated almost continuously and underwent a major overhaul. The second set of runs was done primarily to evaluate a dynamic compensator that was designed in the last stages of this investigation but also included some other runs for comparison. It should be noted that in the second set of runs a slightly lower (i.e. 80%) effective gain was used in the C_2 measurement transducer and also that there is slightly less noise evident in the system. For these reasons comparisons are made only between experimental runs from the same set. However both sets of runs lead to the same general conclusions.

The controllers were implemented on an IBM 1800 digital data acquisition and control computer, which is interfaced to the pilot plant evaporator, using a computer control package developed by Newell [53].

There were a number of factors that had to be considered when evaluating the different design methods and the performance of the controllers produced by each method. These included:

1) Design method
    - inverse Nyquist array
    - direct Nyquist array
    - characteristic locus method
    - optimal quadratic regulator
    - conventional single variable, multiloop control
2) Model used as the basis for the controller design
    - third order state space evaporator model
    - fifth order state space evaporator model
3) Control modes
    - proportional
    - proportional plus integral
    - open-loop

4) Control performance
    - under load changes
    - under setpoint changes
5) Augmented plant
    - compensator of constant elements
    - dynamic compensator
6) Method of evaluation
    - simulated runs
    - experimental runs

It was not feasible to investigate all possible combinations of these different factors but the controllers evaluated as part of this study and the figure numbers that present the corresponding dynamic response of the evaporator variables, are summarized in Table 6.1.

After the experimental results have been presented and discussed, the conclusions regarding the most important of the above factors are summarized. Unfortunately there is no single, quantitative performance criterion that adequately applies under all conditions. Therefore in most cases the conclusions are derived by careful, qualitative comparison of the runs as grouped in Table 6.1.

The first sections of this chapter discuss the experimental tuning that was required to determine the final gains in the controllers designed using the inverse Nyquist array, the direct Nyquist array and the characteristic locus methods. This is followed by the experimental results using an optimal multivariable controller and a multiloop control scheme.

TABLE 6.1

EXPERIMENTAL RUNS PERFORMED IN THIS STUDY

MODEL	CONTROLLER	LOAD		SETPOINT
		ΔF	ΔC_F	ΔC_2
Third Order	P	FD0310 (6.1) FD0320 (6.2) FD0330 (6.3) FD0520* (6.15) FD0530* (6.16) ML0200 (6.24) OP0300 (6.10)	FD0320 (6.4) ML0200 (6.25) OP0300 (6.20)	FD0320 (6.5) FD0320 (6.6) FD0520* (6.17)
	P + I	FD1320 (6.7) FD1315 (6.8) FD1315.1 (6.9) OP1300 (6.21) ML1200 (6.26)		
Fifth Order	P	DNA0520 (5.26) FD0310 (6.1) FD0320 (6.2) FD0330 (6.3) FD0520* (6.15) FD0530* (6.16) OP0500 (6.22) OP0501 (6.18)	DNA0520 (5.27) FD0320 (6.4)	DNA0520 (5.28) FD0320 (6.5) FD0520* (6.17)

. . . continued

TABLE 6.1 (continued)

MODEL	CONTROLLER	LOAD		SETPOINT
		ΔF	ΔC_F	ΔC_2
Fifth Order	P + I	FD1320 (6.7) FD1315 (6.8) FD1315.1 (6.9) OP1500 (6.23)		
	Dynamic with Proportional Action	NADY0510* (6.10) NADY0520* (6.11) NADY0530* (6.12) NADY0550* (6.13)		NADY0520* (6.14)

DNA = direct Nyquist array

FD = INA + CL + DNA

ML = multiloop

NADY = INA + DNA with dynamics

OP = optimal

* = last set of runs

6.2 EXPERIMENTAL TUNING OF THE CONSTANT COMPENSATOR OBTAINED FOR THE THIRD AND FIFTH ORDER MODEL USING THE INVERSE, THE DIRECT NYQUIST ARRAY, AND THE CHARACTERISTIC LOCUS METHODS

For the third order evaporator model it was noticed that the static compensator designed with the inverse Nyquist array method [65] in Chapter Three and with the characteristic locus method [4,42] in Chapter Four were practically the same as the one obtained using the direct Nyquist array method in Chapter Five. Furthermore it was pointed out also in Chapter Five that the constant compensator obtained for the fifth order evaporator model using the direct Nyquist array method was almost equal to the one obtained for the third order model. Since the same basic compensator was obtained in all these cases this section covers the tuning of the constant compensator for all these cases.

6.2.1 Selection of the Proportional Gains

The use of the Ziegler-Nichols setting rules [12] to select the final proportional gains in each loop produce a set of gains which were found to be relatively high when they were applied in the field. The response of the evaporator was not as good as the simulated runs had indicated. Therefore the proportional gains in each loop were obtained by experimental tuning. This was done in a systematic way. Starting with the basic information obtained in Chapters Three, Four and Five. The tuning of the constant compensator for the third order model proceeded as follows (For the fifth order model a more conservative stability region was obtained so different percentages than the ones indicated below have to be used to produce the results presented in this section.)

Given the basic controller:

$$K_B = \begin{bmatrix} -0.630 & 0.0 & 1.0 \\ -0.748 & 0.0 & -0.400 \\ -0.985 & -1.0 & -1.777 \end{bmatrix} \tag{6.1}$$

and the gain space for which the system remains stable:

Loop 1: $0 < k_1 < 24.6$ (6.2)

Loop 2: $0 < k_2 < 49.2$ (6.3)

Loop 3: $0 < k_3 < 27.8$ (6.4)

The objective was to find the matrix K_C.

$$K_C = \begin{bmatrix} k_1 & 0 & 0 \\ 0 & k_2 & 0 \\ 0 & 0 & k_3 \end{bmatrix} \tag{6.5}$$

such that the control system

$$K = K_B K_C \tag{6.6}$$

gave the best response for a step change in the setpoints of the controlled variables or for a step change in the disturbance variables.

The procedure followed to choose k_1, k_2 and k_3 was very similar to the Ziegler-Nichols approach [12] commonly used to select the controller settings in single-loop systems. The chosen gain in each loop (k_1, k_2, k_3) was always based on its respective ultimate gain. The gains used in each loop to control the evaporator were 10% (controller FD0310), 20% (controller FD0320) and 30% (controller FD0330) percent of the corresponding ultimate gain of each loop. The numerical values of these controllers are presented in Table B.1.

Figures 6.1, 6.2 and 6.3 present the experimental response of the closed loop system using the controllers FD0310, FD0320, and FD0330 respectively for a step change of 20% in the feed flow. As expected by increasing the gains in each loop the offsets are reduced but the system becomes more oscillatory. The effect of increasing the gains can be clearly noticed in the three output variables which are being controlled: first effect level, W_1, second effect level, W_2, and the product concentration, C_2. When using controller FD0330 in this set of runs there was a sustained cycling in the system (Figure 6.3), indicating that the evaporator is on the verge of instability.

From these runs it was concluded that a reasonable set of gains are the ones used in controller FD0320, which produced the results plotted in Figure 6.2. (A later run with a gain equal to 16% of the ultimate value for the C_2-S loop and done when there was less noise evident in the evaporator system, is plotted in Figure 6.15 and has an even better response.)

The fact that the basic multivariable controller can be tuned experimentally using procedures similar to the ones used for single-loop controllers is probably one of the most important advantages of the frequency domain techniques studied here. With these methods if the process response is unsatisfactory there is usually no need to completely redesign the controller. A satisfactory control system can usually be obtained by increasing or decreasing the gains in each feedback loop. This is not the case with many of the multivariable time domain methods, since if the design criterion is to be maintained an unsatisfactory controller has to be redesigned, re-evaluated and finally re-implemented experimentally.

Another important advantage of the frequency-domain methods discussed in this study is that with these methods it is always clear to the control engineer how the controller should be modified if it is not satisfactory. With other methods it is not always clear what must be modified, or how to obtain a satisfactory control system.

The proportional controller FD0320 was also tested for a 20% step change in feed concentration with the results shown in Figure 6.4. In this run there is no significant change in any of the output variables. Because the feed concentration affects only the product concentration this run is a measure of the interaction in the controller. The system is almost non-interactive as expected. (An unexplained disturbance in the steam flow, at T=104 minutes affected all the output and control variables.)

The degree of interaction of the control system using the proportional controller FD0320 can also be observed in Figures 6.5 and 6.6. These figures show the response of the evaporator to a 10% step change in the setpoint of the product concentration, C_2. The response of the system is fast and the interaction between loops is low. For a 10% change in the product concentration, C_2, there is a disturbance of only 4.5% and 6.0% in the levels of the first and second effect respectively and they recover after a relatively short period of time. The system is a little more oscillatory for a step-up than for a step-down in the setpoint.

From the previous experimental runs it can be noticed that the ultimate gains obtained experimentally do not agree with the theoretical ones obtained from the Nyquist diagram of the third and fifth order models. The experimental ultimate gains (see run FD0330 in Figure 6.3) are approximately 30% of the theoretical ones. The difference is attributed to modelling errors. However the simulated results presented in Chapter Three (Figures 3.11, 3.13, 3.35-3.38) are qualitatively consistent with the experimental results. In both cases the main effect of increasing the gains in the controller is to reduce the offset in the first-effect level, W_1. The increase of gains in each loop does not affect the second-effect level, W_2, and the product concentration, C_2, very much.

6.2.2 Selection of the Integral Constants

In the previous section the most reasonable proportional gains were found to be the ones used in the controller FD0320. Consequently these gains were used as a starting point in the selection of the proportional plus integral controller constants. In the third order model (cf. Tables 3.1 and 3.2) and to a lesser extent in the fifth order model, every open-loop transfer function in the system behaved approximately like a first-order system. Thus it was not possible, in this case, to use the crossover frequencies to estimate the integral constants. Therefore they were arbitrarily chosen to be 1/64 of the gains used in controller FD0320. This integral controller FD1320 shown in Table B.2 was used to control the evaporator for a 20% step change in feed flow. The response of the system is presented in Figure 6.7. It can be observed from this figure by comparing with the response of controller FD0320 in Figure 6.2 that the main effect of the integral action has been to eliminate the offsets. However in this case the maximum deviations are slightly higher than when using proportional control only. This indicated that the level of integral action was satisfactory and that the oscillatory behaviour of the evaporator was probably due to too high a proportional gain.

Since the system was on the verge of instability when the proportional controller FD0330 was implemented on the evaporator, a new set of proportional gains was selected for the proportional-integral controller FD1315, given in Table B.2. They were chosen to be 50% of the gains used in controller FD0330 since it is common practice to use 50% of the gain that produces sustained oscillations. The response of the pilot plant using controller FD1315 is shown in Figure 6.8 in which it can be observed that the oscillatory behaviour of controller FD1320 (Figure 6.7) has been almost eliminated. In controller FD1315.1 the integral constants were increased by a factor of 1.5 while keeping the same proportional constants as in controller FD1315. The response of the system with this controller is shown in Figure 6.9. The effect of increasing the integral action deteriorates the control. The maximum deviations are higher and the system is more oscillatory than in Figure 6.8.

From these results it can be concluded that a reasonable set of values for a proportional-integral controller are given by proportional-integral controller FD1315 defined in Table B.2.

6.3 EXPERIMENTAL TUNING OF THE DYNAMIC COMPENSATOR FOR THE FIFTH ORDER MODEL OBTAINED USING THE INVERSE AND DIRECT NYQUIST ARRAY METHODS

The selection of the proportional gains for the dynamic compensator was done in the same way as for the static compensator in the previous section. However since this compensator was design significantly later in this study than the other controllers a new set of runs was done to evaluate and select the proportional gains for this dynamic compensator. All the experimental runs presented in this section are from this recent set of runs.

The basic dynamic compensators obtained for the fifth order evaporator model using the inverse and the direct Nyquist array methods were essentially the same as the one given by Equation (3.56). The stability margins for which the closed-loop will remain stable when using this compensator are given by Equations (3.59), (3.60) and (3.61).

Figures 6.10, 6.11, 6.12 and 6.13 present the responses of the evaporator for a 20% step change in the feed flow when the gains used in each loop are 10% (controller NADY0510). 20% (controller NADY0520), 30% (controller NADY0530) and 50% (controller NADY0550) of their corresponding ultimate gain, respectively. The gain used in the concentration loop is actually 80% of the values indicated above. The numerical values of these controllers are presented in Table B.3. There is a low level of noise in the response of the system in each case. The experimental results are in this case, in close agreement with the simulated results (see Figures 3.35, 3.36 and 3.37). The effect of increasing the gains in each loop is reflected mainly in the reduction of the offset in the first effect level, W_1. However the response of the system also becomes more oscillatory by increasing the gains. The product concentration, C_2, and the second effect level, W_2, are not affected significantly when the gains in each loop are increased.

From these results it was concluded that a suitable set of gains will be the ones used in controllers NADY0520 or NADY0530.

Figure 6.14 presents the response of the evaporator for a 10% step change in the setpoint of the product concentration using controller NADY0520. Although the dynamic compensator makes the system model almost non-interacting the experimental response shows that there is still some interaction in the system as evidenced by the small perturbations in W_1 and W_2.

The use of the dynamic compensator with only proportional control action produced very good results. Therefore integral action was not applied in this case.

During the second set of runs it was observed that there was less noise in the system and a slightly lower (i.e. 80%) effective gain had been used in the C_2 measurement transducer. For these reasons and in order to make a more fair comparison among different controllers some additional runs were performed using the constant compensator discussed in the previous section and the optimal multivariable control discussed in Section 6.5.1.

In the recent set of runs the pilot plant evaporator was also operated using controllers FD0520 and FD0530 which are based in the static compensator given by Equation 6.1. These controllers, defined in Table B.1, are almost identical to controllers FD0320 and FD0330, respectively. The only difference is that the effective gain in the loop corresponding to the product concentration, C_2, is 80% of the value of the gain used in the latter controllers. Figure 6.15 and 6.16 present the responses of the pilot plant for a 20% step change in the feed flow when the controllers FD0520 and FD0530 are used. The performance of the system was in this case much better than with controllers FD0320 and FD0330. This was mainly due to the lower level of noise in the system and lower gain in product concentration measurement system.

As in the previous runs when controllers FD0320 (Figure 6.2) and FD0330 (Figure 6.3) were used the main effect of increasing the gains in the loops is to decrease the offset in W_1. The response of the system was more oscillatory when controller FD0530 was used which confirms that the gains used in controller FD0520 or in FD0320 are the most suitable ones.

In Figure 6.17 controller FD0520 has been used to control the evaporator during a 10% step change in the setpoint of C_2. Since the controller is only diagonally dominant (as opposed to non-interacting) some interactions are present in the responses of W_1 and W_2 as they were in Figure 6.5.

An optimal multivariable controller, OP0501, given by Equation 6.19 and discussed in Section 6.5.1 was also used in this set of runs to control the evaporator during a 20% step change in the feed flow disturbance. The experimental response of the evaporator is presented in Figure 6.18.

6.4 EXPERIMENTAL RESULTS WITH THE OPTIMAL REGULATOR CONTROL METHOD AND THE THIRD ORDER EVAPORATOR MODEL

The Optimal quadratic regulator control method is probably the most widely known of the so-called multivariable time domain methods. This technique has been studied extensively at the University of Alberta by Newell [53]. The method can be summarized in the following way:

Given the discrete state space model

$$x(n + 1) = Ax(n) + Bu(n) + Dd(n) \tag{6.7}$$

$$y(n) = Cx(n) \tag{6.8}$$

and the discrete linear quadratic performance index:

$$J = \sum_{n=1}^{N-1} (x(n) - x_d)^T Q(x(n) - x_d) + u(n - 1)^T Ru(n - 1) \quad (6.9)$$

where:

x_d is the desired state vector

Q is a positive semi-definite symmetric matrix

R is a symmetric positive definite matrix (but since this is a discrete formulation it can be made arbitrarily small)

N is a large integer such that at n = N the process has reached steady state the recursive relations which define the control matrices have converged to constant values.

The optimal control method involves minimization of the quadratic performance index and produces a discrete law of the form:

$$u(n) = Kx(n) \quad (6.10)$$

The matrix K is defined by a recursive relationship [73] which converges to constant values after a few interactions. Note that under this scheme the control is exercised over the system states rather than the outputs as in the frequency domain methods.

The design freedom in this method is in the selection of the weighting matrices Q and R. In this study an exhaustive search was not made to determine the best values for these matrices. The values used in these experiments are the best ones found in previous work by Newell [53] and Wilson [77].

For the third order model the state variables are the same as the output variables. Consequently there is no need to estimate any of the state variables.

6.4.1 Proportional Control

The values of the Q and R matrices used to calculate the optimal proportional control for the third order evaporator model are given by:

$$Q = \mathrm{diag}[10,10,100] \tag{6.11}$$

$$R = \mathrm{diag}[0.05,0.05,0.05] \tag{6.12}$$

The proportional controller matrix for a sampling interval of 64 seconds is given by

$$K_{OP0300} = \begin{bmatrix} 4.904 & -0.401 & -11.920 \\ 5.784 & -1.600 & 4.425 \\ 4.093 & 9.685 & 9.357 \end{bmatrix} \tag{6.13}$$

Figure 6.19 shows the response of the evaporator, using controller OP0300, for a step change of 20% in the feed flow disturbance. The gains of this controller seem to be high. There are small oscillations in all the controlled variables but the offsets are very small. The response of the same controller for a 20% step change in feed concentration is shown in Figure 6.20. The control is very good in all the output variables.

This proportional controller generates a system which is diagonally dominant and it is probably because of this property that the system is non-interacting.

6.4.2 Proportional-Integral Control

The state vector was augmented, as described by Newell [53], to generate integral action on each output variable. The R matrix used in this case is the same as Equation (6.12) while Q matrix is given by:

$$Q = \text{diag}[10,10,100,1,1,1] \tag{6.14}$$

For a sampling interval of 64 seconds the proportional-integral control, OP1300, is equal to

$$K_{P_{OP1300}} = \begin{bmatrix} 5.490 & -0.190 & 12.0 \\ 6.429 & -1.386 & 4.487 \\ 5.519 & 12.26 & 11.810 \end{bmatrix} \tag{6.15}$$

$$K_{I_{OP1300}} = \begin{bmatrix} 0.989 & -0.050 & -1.175 \\ 1.156 & -0.325 & 0.437 \\ 0.825 & 1.935 & 1.090 \end{bmatrix} \tag{6.16}$$

The response of the evaporator, using controller OP1300, to a 20% step change in feed flow is shown in Figure 6.21. The effect of adding integral action can be appreciated by comparing it with the proportional control OP0300 in Figure 6.19. With integral action the small offsets are eliminated, the system is a little more oscillatory and has larger overshoots. Other work [27,53] has shown that optimal proportional and proportional-integral controllers can give much better control of the evaporator than shown in Figure 6.19 and 6.21.

6.5 EXPERIMENTAL RESULTS WITH THE OPTIMAL REGULATOR CONTROL METHOD AND THE FIFTH ORDER EVAPORATOR MODEL

In the fifth order model the number of states is greater than the number of outputs. The implementation of the fifth order optimal control requires the estimation of the unmeasured first effect concentration, C_1. In previous studies this estimation was done using a Kalman-Bucy filter estimator [2,25] or a Luenberger observer [34,74]. However in this study a procedure programmed by Newell [53] was used, because of its simplicity and convenience.

6.5.1 Proportional Control

The proportional controller OP0500, was calculated for a sampling interval of 64 seconds and using the following matrices in the quadratic performance index:

$$Q = \text{diag}[10,1,1,10,100] \tag{6.17}$$

$$R = \text{diag}[0.05,0.05,0.05] \tag{6.18}$$

The calculated optimal control, OP0500, is equal to

$$K^P_{OP0500} = \begin{bmatrix} 6.511 & -1.226 & -3.234 & -0.0873 & -13.13 \\ 3.822 & 0.368 & 0.689 & -1.377 & 9.707 \\ 3.054 & 1.056 & 0.0178 & 9.75 & 11.570 \end{bmatrix} \tag{6.19}$$

The response of the evaporator using proportional controller OP0500 for a 20% step change in feed flow, is shown in Figure 6.22. The control of the product concentration, C_2, and the second effect holdup, W_2, is very good. There is only a small offset in the first effect holdup, W_1. (During the most recent set of runs this controller was also used to control the evaporator. The response of this controller (OP0501) was presented in Figure 6.18. The results in Figure 6.18 are very similar to the one presented in Figure 6.22 and they are typical of the better results obtained with optimal quadratic controllers by previous workers [53,77]. It can be noticed also that there is evidence of less noise in Figure 6.18.)

6.5.2 Proportional-Integral Control

For this case the state vector was also augmented as described by Newell [53] to generate integral action on each output variable. The R matrix used in this run was given by Equation 6.18 and the Q matrix was defined by:

$$Q = \mathrm{diag}[10,1,1,10,100,1,1,1] \tag{6.20}$$

The calculated control matrices for a sampling interval of 64 seconds are:

$$K^P_{OP1500} = \begin{bmatrix} 8.209 & -1.239 & -3.640 & 0.139 & -15.44 \\ 4.542 & 0.371 & 0.553 & -1.284 & 9.07 \\ 4.238 & 1.166 & -0.059 & 12.26 & 14.22 \end{bmatrix} \tag{6.21}$$

$$K^I_{OP1500} = \begin{bmatrix} 1.277 & 0.027 & -1.432 \\ 0.793 & -0.298 & 0.895 \\ 0.648 & 1.936 & 1.306 \end{bmatrix} \tag{6.22}$$

The response of the evaporator, using the proportional-integral controller OP1500, for a 20% step change in feed flow is shown in Figure

6.23. This is more oscillatory than the response of the system with only proportional control. However the offsets are eliminated by the integral action.

6.6 EXPERIMENTAL RESULTS USING A MULTILOOP CONTROL SCHEME

The multiloop case was implemented by using diagonal matrices in the multivariable proportional plus integral control algorithms. This makes it equivalent to single variable control and also provides a "base case" for comparison with multivariable techniques. When the control parameters are the same as the diagonal elements in the multivariable controllers then a comparison of the two cases gives an indication of the effect of the off-diagonal elements in the controller matrices.

The pairing of the input and output variables for the multiloop evaporator control scheme was obtained by analyzing the direct Nyquist array (see Chapter Five). It was found that the configuration which is the least interacting is given by the following loops:

- product concentration, C_2, controlled by steam flow, S,
- first effect holdup, W_1, controlled by bottoms flow B_1.
- second effect holdup, W_2, controlled by bottoms flow B_2.

Similar results were obtained by Newell [53] using Bristol's approach [8,9].

An exhaustive search for the best proportional and proportional-integral constants was not made. Instead the selection of the controller constants was made mainly to illustrate the effect on the evaporator response of the off-diagonal elements in the controller matrices discussed in the preceeding sections (i.e. to illustrate the advantage of multivariable versus multiloop control).

6.6.1 Multiloop Proportional Control

The proportional gains used in the multiloop proportional control are shown in Table 6.2 for the run ML0200. These constants are equal to the corresponding diagonal entries of the best control matrix (FD0320) found using the third order evaporator model and the inverse or direct Nyquist array method. In this way a direct comparison can be made between multivariable proportional control FD0320 and multiloop proportional control ML0200. The response of the latter controller for a 20% step change in feed flow is shown in Figure 6.24. Comparing this response with the response of proportional control FD0320 in Figure 6.2 it can be observed that the multiloop system produces higher offsets and higher maximum deviations in the three output variables. Figure 6.25 shows the response of control ML0200 to a 20% step change in feed concentration. Since this disturbance affects only the product concentration, C_2, its effect in the control system is very small. These responses under multiloop control are typical of the best results obtained in other studies [27].

6.6.2 Multiloop Proportional-Integral Control

The proportional and integral constants used in the multiloop proportional-integral controller were equal to the corresponding entries of the best proportional-integral matrix (FD1315) found using the third order evaporator model and the inverse or direct Nyquist array method. The controller constants used in this controller are the ones shown in Table 6.1 for run ML1200. The response to a 20% step change in feed flow is shown in Figure 6.26. The addition of integral action to the proportional controller eliminates the offsets. The negative aspects of introducing integral action are that some of the maximum deviations are slightly higher especially for the product concentration, C_2. The comparison of the response of the multiloop proportional-integral control ML1210 of Figure 6.26 with the response of the multivariable proportional-integral control FD1315 of Figure 6.8 shows that the multivariable control reduces considerably the maximum deviations in the output variables and makes the system respond faster.

TABLE 6.2

CONTROL SETTINGS FOR MULTILOOP RUNS

Run	Loop		Control Interval (Sec.)	Proportional Constant	Integral Constant (Min^{-1})
ML0200	B_1	W_1	64	3.68	
	B_2	W_2	64	9.84	
	S	C_2	64	-5.56	
ML1210	B_1	W_1	64	2.76	0.115
	B_2	W_2	64	7.38	0.205
	S	C_2	64	-4.17	-0.173

6.7 COMPARISON AND CONCLUSIONS OF THE EXPERIMENTAL RESULTS

6.7.1 Proportional Versus Proportional-Integral Control

The addition of integral action in the multiloop control scheme improved the response of the control system dramatically. The severe offsets associated with the proportional controller were eliminated with the integral action. An analogous improvement was not observed with the multivariable control systems. The addition of integral action to the multivariable controllers produced no significant improvement in the response of the evaporator. The response of the system using only proportional control was very good and the offsets were very small due to the relatively high proportional gains. Thus there was little room for improvement. For the controller designed using the inverse and direct Nyquist array the only noticeable effect of adding integral action was to reduce the offset in the first effect level. When the optimal control method was used the performance of the system with integral action was more oscillatory than when only proportional action was used. However this could probably be corrected by proper choice of the Q and R matrices.

Thus, it was concluded that a good multivariable design method would produce a proportional controller that would give at least as good control of the evaporator as a multiloop proportional plus integral controller.

6.7.2 About the Control System Design Method

When applied to the third order evaporator model the inverse Nyquist array [65], the characteristic locus [4,42] and the direct Nyquist array method produce essentially identical proportional or proportional plus integral controllers. These methods lead naturally to similar controllers whenever a constant controller matrix exists which makes the system almost diagonal. The response of the double-effect evaporator with these controllers is very good. The main advantage of these methods is that they produce a controller which is very easy to tune in the field. Once the basic controller and gain stability region has been obtained, the final controller can be chosen by tuning of the basic controller in the field in a manner similar to the tuning of single-loop systems.

For the fifth order model the inverse Nyquist array method was unable to produce a constant compensator which would make the CLTFM diagonally dominant. Thus it was not possible to design a proportional controller for the fifth order model with this method. On the other hand the *direct* Nyquist array method did produce a proportional controller for the same model which was almost the same as the one obtained for the third order model.

When dynamic elements were used in the compensator the inverse and the direct Nyquist array methods both produced essentially the same dynamic controller for the fifth order model. The response of the double effect evaporator with this dynamic controller was excellent.

Another important feature of the inverse Nyquist array [65], the characteristic locus [4,42] and the direct Nyquist array method is that the control system design produced by these methods is capable of handling set point changes as well as rejecting any type of unwanted disturbances. This is not the case with the optimal control method where different control matrices are required for "optimal" setpoint control and to regulate the system against undesirable disturbances.

The optimal control method also produced very good control. The use of the fifth order model gave much better results than using the third order model. The critical step in this method is the selection of the matrices Q and R of the quadratic performance index and unfortunately the method includes no direct means of estimating what Q and R should be to produce a specified type of response. Another disadvantage of the method is that the control is based on the state variables instead of the outputs. In many cases this requires the estimation of the states which increases the complexity of the control system.

Of all the methods studied here the multiloop design approach produced the worst control system and one would expect the performance to be even worse for processes with larger interactions. However this scheme is the simplest and most familiar approach for designing control systems.

The controller which gave the best experimental performance was the tuned dynamic compensator obtained with the direct and the inverse Nyquist array methods using the fifth order model. The second best performance was obtained using the optimal control method and the fifth order model. (This was a 3 x 5 controller matrix.) The third best performance was obtained using the tuned constant compensator designed with direct Nyquist array method and the fifth order model or the third order model or using the inverse Nyquist array and the characteristic locus method with the third order model.

6.7.3 About the Order of the Model

It is a significant fact that the same constant compensator was obtained for the third and fifth order models when using the direct Nyquist array method. In both cases the compensator represented the best that could be obtained when a constant compensator was used. However it was not possible to obtain the same high degree of diagonal dominance (i.e. non-interaction) with the fifth order model as had been obtained when using the third order model. This is obviously because the third order model is less complicated (and hence less representative of the real evaporator) than the fifth order model. With the inverse Nyquist array method [65] it was not possible to design a constant compensator that would produce a diagonally dominant system when using the fifth order model. This may indicate that the direct Nyquist array method is less sensitive to reductions in the model order or accuracy and also less restrictive.

In general, with the inverse Nyquist array [65] the characteristic locus [4,42] and the direct Nyquist array methods the difficulty of designing a controller increases with increasing order of the model. This is because it is more difficult to visualize the type of operation or the type of controller which is required to obtain the specified design objectives. It also appears that the complexity of the controller matrix is increased (i.e. more dynamic elements are required) when the order of the model is increased even though the dimensions of the controller matrix remain the same.

The experimental work has shown that there is not a direct relationship between the complexity of the controller and the performance of the system. There is not much difference between the performance of the pilot plant evaporator using a constant controller and using a dynamic controller which requires two phase lead and one phase lag compensator. (The performance of the system, however, is slightly better when the dynamic controller is used.)

6.7.4 The Effect of Diagonal Dominance

The design of a control system for the fifth order evaporator model using the direct Nyquist array method, as described in Chapter Five, provided an opportunity to investigate the effect of diagonal dominance (of the open-loop and return-difference transfer function matrices) on the performance of the control system. In this example three compensators, K_A (Equation (5.52)), K_B (Equation (5.54)) and K_B' (Equation (5.66)), were obtained that made the open-loop and return-difference matrices diagonally dominant in different degrees. The varying degree of diagonal dominance can be observed in the Nyquist diagrams of the diagonal elements of the respective open-loop transfer function matrix with their Gershgorin bands, i.e. Figures 5.25, 5.27 and 5.34 respectively.

Experimental runs using controllers based on compensators K_B and K_B' have been discussed previously (i.e. controllers FD0320, FD0520, NADY0520). The controller based on compensator K_A given by Equation (5.52) was also implemented experimentally. The gains used with this compensator were chosen such that the elements of the resulting controller, DNA0520, were approximately of the same magnitude as the elements of controllers FD0320 and NADY0520. In this way a fair comparison could be made among controllers DNA0520, FD0320, FD0520 and NADY0520. Controller DNA0520 is presented in Table B.4. The responses of the double-effect evaporator, when using controller DNA0520, for a 20% step change in feed flow, feed concentration and for a 10% increase in the setpoint of the product concentration are presented on Figures 6.27, 6.28 and 6.29, respectively. The effect of improving diagonal dominance can be analyzed by comparing these figures with Figures 6.2, 6.4 and 6.5, respectively which present the response of controller FD0320 based on compensator K_B. All these experiments are from the same set of runs and hence can be compared directly.

For a 20% change in feed flow the improvement in the response of the system by improving the diagonal dominance of the controller is very small. The use of controller FD0320 gives smaller offsets and lower overshoots than when controller DNA0520 is used. For a 20%

decrease in the feed concentration there is no difference in the behaviour of these two controllers. The same applies for a step changed in the setpoint of the product concentration. In all three cases the controller FD0320 is a little more oscillatory which indicates that slightly higher effective gains were used in this controller.

The effect of improving diagonal dominance can also be analyzed by comparing the responses of controller FD0520, based on compensator K_B, in Figures 6.7 and 6.9 against the response of the system in Figures 6.14 and 6.17 when controller NADY0520, based on compensator K_B', is used. As in the previous case there is no significant difference in the behaviour of these controllers for a 10% step change in the setpoint of the product concentration. For a step change in the feed flow there was a marginal improvement in the response of the product concentration when controller NADY0520 is used. It was surprising to find out in these experimental runs that a marginal improvement was noticed for load disturbances and not when a setpoint change was introduced into the evaporator because one would expect diagonal dominance to be more important in setpoint changes.

From these observations it can be concluded that small improvements in the degree of diagonal dominance in the open-loop and return-difference matrices produced only a marginal improvement in the closed-loop performance of the system. This means that a non-interacting system cannot always be justified and that Nyquist array design techniques are valuable because they allow the designer to trade off controller complexity versus the degree of non-interaction produced.

The same general conclusions were obtained in Chapter Five based on simulated results.

CHAPTER SEVEN

CONTROL SYSTEM DESIGN FOR MULTIVARIABLE PROCESSES CONTAINING TIME DELAYS

7.1 INTRODUCTION

Pure time delays are very common in process systems but can only be handled by a few design techniques. The presence of a time delay in a transfer function makes it an irrational function and in most cases, unless they are approximated by rational functions, the basic Nyquist stability theorem [54] has to be modified to deal with irrational transfer functions [13,71]. Desoer and Wu [504] give sufficient conditions for the stability of multi-input, multi-output, linear, time-invariant, feedback systems which are a generalization of previous works on system stability that originally began with Nyquist. However, the design of multivariable systems with non-rational G(s) is still "not fully clarified [509]". However transfer functions with time delays have the peculiarity that the basic Nyquist stability theorem can be applied to them directly without requiring any modification. One of the main reasons for the popularity of the single-input, single-output frequency domain techniques was due to this fact. In multivariable systems with pure time delays the direct Nyquist array design method is more convenient than the inverse Nyquist array method because, in the direct method, time delays cause the Nyquist locus to "spiral into the origin" whereas in the inverse method the corresponding loci spiral out to infinity.

The direct Nyquist design approach was implemented using numerical methods to perform operations such as matrix multiplication, inversion, etc. For example Q(s) = G(s) K(s) is calculated numerically at each frequency rather than trying to multiply G(s) and K(s) analytically to produce a single matrix with each element being a complex function. It is relatively easy to incorporate time delays into the elements of G(s) and/or K(s) and since the calculations are done numerically the subsequent numerical multiplication step, plotting, etc remains unchanged. Further work would be required to determine how pure time delays could be incorporated into the inverse Nyquist array and the characteristic locus methods.

The following section presents a design example using the direct Nyquist array method to design a system, for a binary distillation column which contains time delays in each element of its transfer function matrix. The results agree with previous work by Wood and Berry [79].

7.2 DESIGN OF A CONTROL SYSTEM FOR A BINARY DISTILLATION COLUMN MODEL

In this example the direct Nyquist array method is applied to the design of a control system for a binary distillation column model. The model used was obtained by Berry [6] from an eight tray, nine inch diameter, pilot-scale distillation column by pulse testing. The column has a total condenser and a basket type of reboiler and is used to separate a binary mixture of methanol and water. The distillation column is located in the Department of Chemical Engineering and has been described in detail by Berry [6] and Wood and Berry [79]. The distillation column used in this example can be represented by the following dynamic model:

$$\begin{bmatrix} X_D(s) \\ X_B(s) \end{bmatrix} = \begin{bmatrix} \\ G(s) \\ \\ \end{bmatrix} \begin{bmatrix} R(s) \\ S(s) \end{bmatrix} \tag{7.1}$$

where the output variables are the overhead product composition, X_D, and the bottom product composition, X_B. The input variables are the reflux flow rate, R, and the steam flow rate, S. The plant transfer function matrix, G(s) is presented in Table 7.1. The design is carried out in the s domain, rather than the w domain used in previous examples to illustrate that both cases appear essentially the same to the user of the interactive design program.

As can be observed from Table 7.1 the distillation column contains a time delay term in each element of its transfer function matrix. The Nyquist array of the distillation column is presented in Figure 7.1, for a frequency range of 0.1 to 3.0 radians/min. From this figure it can be observed that:

- the reflux flow rate, R, and the steam flow rate, S, have almost the same effect on the overhead product composition, X_D.
- the bottom product composition, X_B, is affected more strongly by the steam flow rate, S, than by the reflux flow rate, R.

This indicates that the present configuration is the best one to control the distillation column under a multiloop scheme. This fact is emphasized from observing Figure 7.2 which presents the Nyquist diagrams of the diagonal element of the distillation column with their Gershgorin bands. This figure shows that the plant transfer function matrix, G(s), is already diagonally dominant. Thus there is no

TABLE 7.1

DISTILLATION COLUMN TRANSFER FUNCTION MATRIX

$$G(s) = \begin{bmatrix} \dfrac{12.8\ e^{-1s}}{16.7s + 1} & \dfrac{-18.9\ e^{-3s}}{21.0s + 1} \\[2em] \dfrac{6.6\ e^{-7s}}{10.9s + 1} & \dfrac{-19.4\ e^{-3s}}{14.4s + 1} \end{bmatrix}$$

Typical steady state operating conditions of the distillation column [79].

Stream	Flow lb/min	Composition wt. % methanol
Overhead*	1.18	96.0
Reflux**	1.95	96.0
Bottoms*	1.27	0.5
Feed	2.45	46.5
Steam**	1.71	

* Output variables: overhead composition, bottoms composition

** Input variables: reflux flow, steam flow need to reorder the variables.

From Figures 7.1 and 7.2 it is also apparent that the diagonal elements in column 2 will be unstable under negative feedback. In order to correct this situation it is necessary to change the sign in this column by post-multiplying the plant transfer function matrix, G(s), by

$$K_1 = \begin{bmatrix} 1 & 0 \\ 0 & -1 \end{bmatrix} \tag{7.2}$$

The plant matrix G(s) is replaced in the subsequent operations by the OLTFM $Q_1(s) = G(s)\ K_1$. The Nyquist array of the OLTFM $Q_1(s)$ is presented in Figure 7.3 and the Nyquist diagrams of the diagonal elements of $Q_1(s)$ are shown in Figure 7.4. The latter figure is plotted with an assumed loop gain of unity and it is clear from the plot of the second diagonal element that F(s) is NOT diagonally dominant. However F(s) can be made diagonally dominant by proper choice of the loop gains. Thus it is possible to design, in this case, a multiloop control system using the direct Nyquist array method. At this point there are two alternatives in the design. The first one is to proceed with the design of the multiloop control system and the second is to design a pre-compensator to improve the diagonal dominance of the system. Both alternatives have been evaluated in the following sections.

Design of a Multiloop Control System

Since the control of the present distillation column using a multiloop control scheme has been investigated by Wood and Berry [79] and the best controller constants have been obtained by experimental tuning by Berry [6] no attempt was made to select the final controller constants in this example. This section is presented to illustrate the information which the direct Nyquist array method provides.

From Figure 7.4 which contains the Nyquist plots of the Gershgorin bands for the diagonal elements it can be observed that the distillation column will remain stable with its loops closed for the following combination of gains:

$$\text{Loop 1:} \qquad 0 < k_1 < \frac{1}{1.08} = 0.926 \tag{7.3}$$

$$\text{Loop 2:} \qquad 0 < k_2 < \frac{1}{4.70} = 0.213 \tag{7.4}$$

This region can be expanded by using the exact Nyquist locus of each loop when it is open and the rest are closed and a trial and error procedure. However no major benefits are obtained from the expanded stablity region.

With the information provided by Equations (7.3) and (7.4) it is possible to select safely the proportional constants for each loop.

Design of a Pre-compensator to Improve the Diagonal Dominance in the System

The transfer function matrix of the distillation column shown in Table 7.1 can be considered to have the preferred structure for a system which contains time delays. This is because the greatest time delays are in the off-diagonal positions and hence the augmented system can easily be made diagonally dominant by using a dynamic compensator.

This type of transfer function matrix is not uncommon. Hydraulic models have been found [3] to have the same type of transfer function matrix.

The use of a static compensator does not significantly improve the dominance in this system. However using a dynamic compensator the following alternatives are possible:

a) make the OLTFM an upper or lower triangular matrix

b) improve the diagonal dominance of the OLTFM

c) make the OLTFM a diagonal matrix (i.e., non-interacting)

Only the last two alternatives have been investigated in this study.

i) Improving Diagonal Dominance in the OLTFM

From the transfer function matrix, G(s) in Table 7.1 it can be observed that the elements in the same row have time constants of the same magnitude. Thus it is possible to improve diagonal dominance by using only time delays in the compensator. From the matrix $Q_1(s)$ and its Nyquist array in Figure 7.3 it was found that diagonal dominance could be greatly improved in $Q_1(s)$ if the following elementary operations are performed: (With the present implementation, the use of pure time delays in the controller, K(s), requires that all the dynamic components be introduced at one time rather than in a series of steps. This limitation could be overcome by reprogramming but would reduce computing efficiency.)

$$\text{column } 2 = \text{column } 2 - 1.3 \times e^{-2s} \times \text{column } 1 \qquad (7.5)$$

and

$$\text{column } 1 = \text{column } 1 - 0.45 \times e^{-4s} \times \text{column } 2 \qquad (7.6)$$

These operations are performed by using the following compensator:

$$K_2(s) = \begin{bmatrix} 1 & -1.3\ e^{-2s} \\ -0.45\ e^{-4s} & 1 \end{bmatrix} \qquad (7.7)$$

The Nyquist array of the new OLTFM, $Q_2(s) = Q_1(s)K_2(s)$ and the Nyquist diagrams of its diagonal elements with their Gershgorin bands are presented in Figures 7.5 and 7.6 respectively. Figure 7.6 shows that the system is now strongly diagonally dominant and that a controller gain can be chosen that will make the system closed loop stable.

The final compensator used in this case is given by:

$$K_B = K_1K_2 \qquad (7.8)$$

or

$$K_B = \begin{bmatrix} 1 & -1.3\ e^{-2s} \\ 0.45\ e^{-4s} & -1 \end{bmatrix} \qquad (7.9)$$

Padé Approximations of the Time Delays

It should be pointed out here that in this example there have not been any approximations of the time delays present in the plant or the controller. However in order to investigate the use of approximations for pure time delays the controller matrix K_2 was also generated using a second order Pade approximation [10]. The Nyquist array and Nyquist diagrams of the diagonal elements with Gershgorin circles for the OLTFM $Q_2(s)$, in which a second order Pade approximation was used, are presented in Figure 7.7 and 7.8. It can be noticed by comparison of these figures with Figures 7.5 and 7.6 that the second order Pade approximations compensate for the process time delays very well at all frequencies but the difference becomes apparent at high frequencies. Hence the use of the Pade approximation will lead to a smaller stability region.

2) Designing a Non-interacting System

The OLTFM $Q_1(s)$ (which is equal to G(s) but with the signs changed in the second column) can easily be made diagonal (non-interacting) by performing simultaneously the following column operations on $Q_1(s)$:

$$\text{column } 2 = \text{column } 2 - 1.478 \times \left(\frac{16.7s + 1}{21.0s + 1}\right) \times e^{-2s} \times \text{column } 1 \quad (7.10)$$

and

$$\text{column } 1 = \text{column } 1 - 0.34 \times \left(\frac{14.4s + 1}{10.9s + 1}\right) \times e^{-4s} \times \text{column } 2 \quad (7.11)$$

The factors used in these operations were obtained by an analysis of the elements of matrix G(s). These operations are accomplished by post-multiplying $Q_1(s)$ by the following matrix:

$$K_2^1 = \begin{bmatrix} 1 & -1.478\left(\frac{16.7s + 1}{21.0s + 1}\right) e^{-2s} \\ -0.34\left(\frac{14.4s + 1}{10.9s + 1}\right) e^{-4s} & 1 \end{bmatrix} \quad (7.12)$$

The Nyquist diagrams of the diagonal elements of the OLTFM, $Q_2^1(s) = Q_1(s)K_2^1$ are shown in Figure 7.9. The Gershgorin circles in this case have a zero radius. The final controller used to make the open-loop transfer function matrix diagonal is then given by:

$$K_B^1 = K_1 K_2^1 \tag{7.13}$$

or

$$K_B^1 = \begin{bmatrix} 1 & -1.478\left(\frac{16.7s + 1}{21.0s + 1}\right) e^{-2s} \\ 0.34\left(\frac{14.4s + 1}{10.9s + 1}\right) e^{-4s} & -1 \end{bmatrix} \tag{7.14}$$

Stability Analysis

Controller matrix K_B given by Equation (7.9) and controller K_B^1 given by Equation (7.14) produce a system with similar properties. From the Nyquist diagrams of the diagonal elements of $Q_2(s)$ and $Q_2^1(s)$ in Figures 7.6 and 7.8 the stability region for which the closed-loop system will remain stable can be obtained for each controller. In both cases the distillation column will remain stable for the following combination of gains:

$$\text{Loop 1:} \qquad 0 < k_1 < \frac{1}{0.78} = 1.28 \tag{7.15}$$

$$\text{Loop 2:} \qquad 0 < k_2 < \frac{1}{3.70} = 0.27 \tag{7.16}$$

From Figures 7.6 and 7.8 the crossover frequency of each loop can also be obtained. Again, in both cases the crossover frequency obtained for each loop is the same.

Loop 1: crossover frequency : 1.5 radians/min

Loop 2: crossover frequency : 0.55 radians/min

Non-interacting control of the present distillation column has been studied previously by Wood and Berry [79]. The non-interacting control system was in this case derived directly from the transfer function representation of the distillation column and is the same as the one obtained by Wood and Berry [79]. (The same result could have been obtained by progressively increasing the diagonal dominance of the Nyquist array of Q(s).) Since they obtained the final controller constants by experimental tuning no attempt was made here to specify different constants. The following controller constants reported by Wood and Berry [79] for non-interacting control (which are the "best" values found in their experimental evaluation of conventional single variable control) were used in this study:

Loop X_D - R:

Proportional constant	$K_p = 0.35$
Integral constant	$K_I = 0.040 \text{ min}^{-1}$

Loop X_B - S:

Proportional constant	$K_p = 0.12$
Integral constant	$K_I = 0.014 \text{ min}^{-1}$

The complete distillation column including the effect of the feed flow and feed concentration disturbances as modelled by Berry [6] was simulated using IBM's Continuous System Modelling Program (CSMP). Figures 7.10, 7.11, and 7.12 present the simulated response of the distillation column for a step change of approximately 14% (+0.34 lb/min) in the feed flow, when a multiloop, a diagonally dominant and a non-interacting control system is used, respectively. As expected from the previous Nyquist analysis the control system that makes the system diagonally dominant (controller with only time delays given by Equation (7.9) behaves almost the same as the non-interacting control (given by Equation (7.9)). The only difference is that the response of the non-interacting control system leads the response of the system with the "approximate" controller slightly. The response of these two controllers is much more damped then the response of the multiloop control which is oscillatory. The overshoots in the case of the multiloop control are also higher. On an overall basis the response of the multiloop control system can be considered to be worse than the non-interacting and the diagonally dominant systems.

7.3 CONCLUSIONS

The direct Nyquist array method has been found to be a very powerful technique that can handle systems which contain time delays in the process system, G(s) and/or the controller, K(s), without requiring any approximations. The distillation column example presented in this chapter illustrates this case.

From the examples presented in this chapter and Chapter Five it can also be concluded that whenever a controller matrix exists which is physically realizable and makes the system non-interacting, it can be designed using the direct Nyquist array method. A very important advantage of the direct Nyquist array method is that with this method several alternatives can be investigated by compromising between the complexity of the controller and non-interaction in the system. In many cases, like in the distillation column example, it is possible to design a less complex system with almost the same characteristics as a non-interacting system.

CHAPTER EIGHT

CONCLUSIONS AND FURTHER RESEARCH

8.1 CONTRIBUTIONS

The main contributions of this work are:

1) Development and extension of the direct Nyquist array design method.
2) A comparison of the inverse Nyquist array, characteristic locus and the direct Nyquist array design methods.
3) Experimental implementation and evaluation of controllers designed using the inverse Nyquist array, characteristic locus, direct Nyquist array, optimal quadratic and conventional design techniques.
4) Development, documentation and demostration of a set of interactive computer programs to implement the multivariable frequency domain design techniques.

8.2 COMPARISON OF FREQUENCY DOMAIN AND STATE-SPACE METHODS

The main advantage of the frequency domain techniques over the methods based on a state variable formulation are:

1) The use of frequency domain methods obviates the need of having to determine a parametric model since frequency response data, which adequately defines the system, can be used directly.
2) They take into account the sometimes conflicting design requirements for: stability, non-interaction, integrity and overall performance of the system.
3) They produce a controller matrix which is easier to tune "on line"

because it includes a diagonal matrix of loop gains.

4) The control system involves only the output variables, i.e. it does not require measurement of the state variables.

5) Many control applications run into difficulty due to system parameters which change as a function of time and/or due to errors in estimating parameters which mean that the model on which the control system design is based is different than the actual process on which the control system is finally implemented. Multivariable frequency domain techniques can deal with this problem in some cases. For example, if the change in system parameters (or measurement errors or noise) is equivalent to a change in one or more of the feedback gains $\{k_i, i=1,..m\}$ then the range of actual k_i values can be checked against the stability limits on k_i generated during the frequency domain design. For each loop there is a range of values of k_i for which loop i is stable, and since the stability analysis is based on the Gershgorin or Ostrowski bands it is known that all the other loops will also be stable at least for the range of $\{k_i, i=1,..m\}$ for which F(z) remains diagonally dominant. It is obvious that changes on any column of G(z), which when combined do not produce any change in the diagonal dominance (i.e. radius of Gershgorin circles), would have no effect on the stability analysis and hence would not result in unstable system performance (The use of a "band" instead of a line locus during the stability analysis would normally result in conservative gain estimates).

The above result is a quantitative test. More subjectively it is known that the off-diagonal elements of $G(z)$ have only a small effect on the off-diagonal elements of a diagonally dominant $Q(z) = G(z)K(z)$. Thus one would expect that, at least for small changes in the off-diagonal elements, small parameter changes in $G(z)$ would have a smaller effect on the closed-loop performance of diagonally dominant systems than if the loops were closed around $G(z)$ directly.

Thus the multivariable frequency domain design techniques are expected to give conservative controllers that are less sensitive to parameter changes than controllers designed by other methods.

8.3 COMPARISON OF FREQUENCY DOMAIN DESIGN METHODS

The characteristic locus method [4,42] is slightly more general than the inverse [65] and the direct Nyquist array methods. However the use of characteristic values to determine the stability of the system makes the characteristic locus method a less practical procedure than the latter techniques. The characteristic loci diagrams are a very uselful tool to analyze control systems but they do not give adequate guidance about the type of controller which must be used to achieve the desired control specifications. Thus, with the characteristic locus method the selection of the controller cannot be done in a systematic way as with the inverse and the direct Nyquist array methods when designing a constant compensator. However this problem is at least partially overcome in the characteristic locus method, when designing a proportional-integral control matrix, if the procedure recently proposed by Kouvaritakis [508] is used.

The inverse [65] and the direct Nyquist array methods are very similar. Their relationship is similar to the one that exists between the single-variable frequency design procedures when using the inverse versus the direct polar plots. These methods have been found easier to use and more convenient than the characteristic locus method [4,42]. However the information provided by the Nyquist array diagrams is less exact than the information supplied by the set of the characteristic loci diagrams.

The inverse and the direct Nyquist array methods produce basically the same controller when a high degree of diagonal dominance in the open-loop transfer function matrix is required.

In spite of the similarities between the direct and inverse Nyquist array methods this study has found the direct Nyquist array method to be more convenient than the inverse Nyquist array technique for the following reasons:

1) It involves the use of the familiar "direct" Nyquist diagrams that represent the mathematical relationship between physical input/output variables and hence are more familiar and meaningful to most users than the Nyquist plots of the transfer functions of the inverse of the open-loop transfer function matrix, $Q^{-1}(z)$, used in the inverse method. This means that the information provided by the direct Nyquist array is more physically meaningful to the user than the information supplied by the inverse Nyquist array. Furthermore the DNA method can be interpreted as a direct and intuitive extension of conventional

single-input single-output (SISO) design techniques. Thus it relates more directly to the previous experience of most users.

2) The direct Nyquist array method requires only that the return-difference matrix, F(z), be diagonally dominant (which is a physically meaningful characteristic) as compared to the inverse Nyquist array method which requires that both the inverse of the closed-loop matrix, $R^{-1}(z)$, and the inverse of the open-loop matrix, $Q^{-1}(z)$, be diagonally dominant (a condition which is more difficult to interpret physically). This makes the DNA a more convenient technique because it requires only that the (-1,0) point not be enclosed by the Gershgorin circles as opposed to the INA method which requires the same condition for the (-1,0) point and the origin. However if the plant transfer function matrix is known algebraically the requirement that the origin should not be enclosed by the Gershgorin circles in the inverse Nyquist array method can be relaxed by performing some additional calculations as explained in Section 3.3

3) The DNA method can handle systems with non-square transfer function matrices directly (However, note that Q(z) is always square.).

4) The DNA method works with the control matrix, K(z), at all times (as opposed to $K^{-1}(z)$) so the user is always aware of the form, complexity and magnitude of the elements of K(z) and hence it is relatively easier to be sure that the controller is practical and physically realizable.

5) The intuitive derivation of the DNA method based on the

extension of conventional SISO techniques shows that when the return-difference matrix is diagonally dominant the Gershgorin circles and the Ostrowski circles are simply a means of approximating, or defining the limits of interaction terms in the analytical expression for $h_i(z)$ that relates the input/output pair $u_i:y_i$. This analytical expression for $h_i(z)$ can be used to derive other limiting or approximate solutions that in many problems will permit a more accurate and convenient design than is possible with the Gershgorin or Ostrowski circles. For example the Gershgorin circles for a system with a "triangular OLTFM" will, in general, have non-zero radii whereas it is obvious from physical considerations that there are no interactions which influence system stability. The use of the "G^o circles", which take into account any zero elements in the OLTFM, Q(z), show that $h_i(z)$ is equal to $q_{ii}(z)$ when Q(z) is triangular.

6) A final check on the stability and performance of the closed-loop multiple-input multiple-output (MIMO) system can be made using the Nyquist plots of $\{h_i(z),\ i=1,\ldots m\}$. If F(z) is diagonally dominant then for open-loop stable systems it is necessary and sufficient that each of the Nyquist plots of $h_i(z)$ satisfy the conventional Nyquist stability criterion. For the general case, the sum of the clockwise encirclements of the critical point (-1,0) by the Nyquist locus of $\{h_i(z),\ i=1,..m\}$ must be equal to $-p_o$, where p_o is the number of unstable poles of Q(z). (See Appendix D).

7) The DNA method provides a general procedure for pairing input/output variables of MIMO systems since the direct Nyquist array defines the relationship between each possible pair of input and output variables. In most practical applications the columns of $Q(z)$ should be interchanged so that the "linkage" or "transmission" between u_i and y_i (represented by $q_{ii}(z)$) is greater than between y_i and the other input variables. This procedure takes into consideration not only the steady state behaviour of the system but the dynamic behaviour as well.

8) The DNA is computationally more efficient than the inverse Nyquist array method since the latter method always requires an extra operation: the inversion of the plant transfer function matrix.

9) It is easier to accomodate pure time delays in the DNA method since the Nyquist plot spirals in to the origin rather than out to infinity as it does in the INA method.

The inverse Nyquist array method has also been found to have some advantages over the direct Nyquist array method, the most important of which are:

1) The Ostrowski circles in the inverse Nyquist array method become small when the gains in the other loops are increased [69]. This means that the region of uncertainty associated with the inverse of the transfer function $h_i^{-1}(z)$ is reduced when high gains are used. Note that in the limit as the radius of the Ostrowski circles approaches zero the $Q_{ii}(z$_ approaches $h_i(z)$ [69]. In the DNA method, $h_i(z)$ and $h_i^{max}(z)$

must be calculated from Equation 5.18 and plotted (where $h_i^{max}(z)$ is the value of $h_i(z)$ when all the gains, k_i, assume their maximun permissible values). The difference between the two loci shows the maximun effect on $h_i(z)$ that can be produced by increasing the other gains $\{k_l, l=1,..m, l \neq i\}$ i.e. a more exact indication of the effect of increasing the loop gains than implied by the radius of the Ostrowski circles in the INA method. Thus in the DNA method more exact information can be obtained by at the price of extra computer calculations.

2) According to Rosenbrock [69] it seems that there is a tendency, in practice, for the off-diagonal elements of the inverse of the plant transfer function matrix, G^{-1}, to be relatively smaller than those of G. In this study this tendency has not been noticed. Also it is not clear whether this difference in "sensitivity" is an advantage or disadvantage.

3) As in the single-variable case the inverse Nyquist array is more convenient to use when the transducer feedback matrix is a nonconstant matrix. However it has been pointed out earlier that in these cases, it is always possible (and desirable) to make the transducer feedback matrix part of the plant transfer function matrix.

8.4 FURTHER RESEARCH

Some natural extensions and recommendations for future investigations in this area are:

1) Development of a systematic procedure to design a control system

for non-square plants using the direct Nyquist array method (cf. work by Kontakos [507]). The research should be oriented toward the design of a non-square pre-compensator which in combination with the non-square plant will produce a square open-loop transfer function matrix that retains the most important characteristics of the plant.

2) Further research is required into the analytical expression for $h_i(z)$ in order to derive other limiting or approximate solutions which will permit a more accurate and convenient design than is possible with the Ostrowski circles.

3) Serious consideration must be given to the combination of the direct Nyquist array method and the sequential return-difference method. The use of the direct Nyquist array procedure in the first stage of the design will minimize the basic problem of the sequential return-difference method which is the order of loop closing. Similarly the use of the sequential return-difference in the final stage of the design provides the direct Nyquist array method with a systematic and exact single-loop design procedure.

4) Further work would be required to determine how pure time delays could be incorporated into the general direct Nyquist array, inverse Nyquist array, and the characteristic locus methods.

5) In order to increase the flexibility of the computer-aided design package and make the design of a control system an easier task the following programs should be incorporated into GEMSCOPE:

    a) A minimal realization algorithm to obtain the state-space model from a transfer function matrix.

b) A program to obtain the transfer function matrix from the experimental frequency response of a system. Although the availability of a transfer function matrix is not required with the frequency domain techniques, the knowledge of this TFM could be helpful in the design.

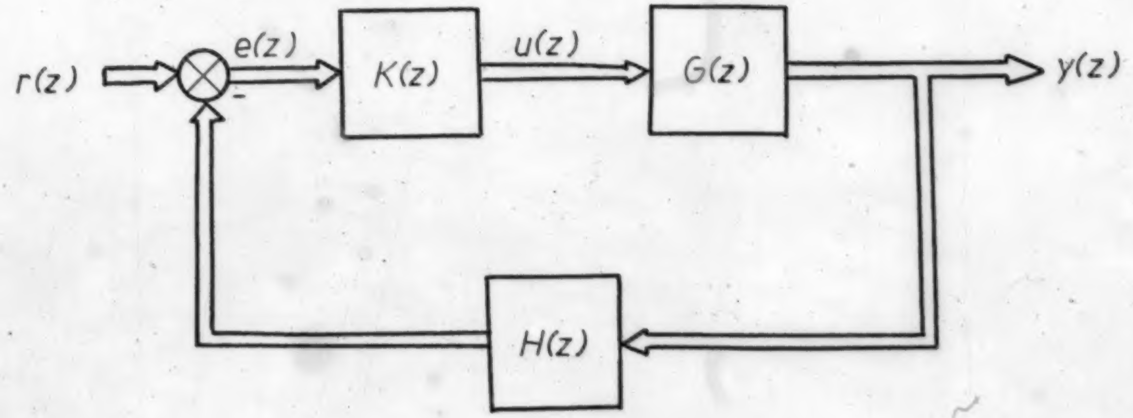
r(z)
e(z)
-
K(z)
u(z)
G(z)
y(z)
H(z)

Figure 2.1 Multivariable Feedback Control System Expressed in a Block Diagram Notation

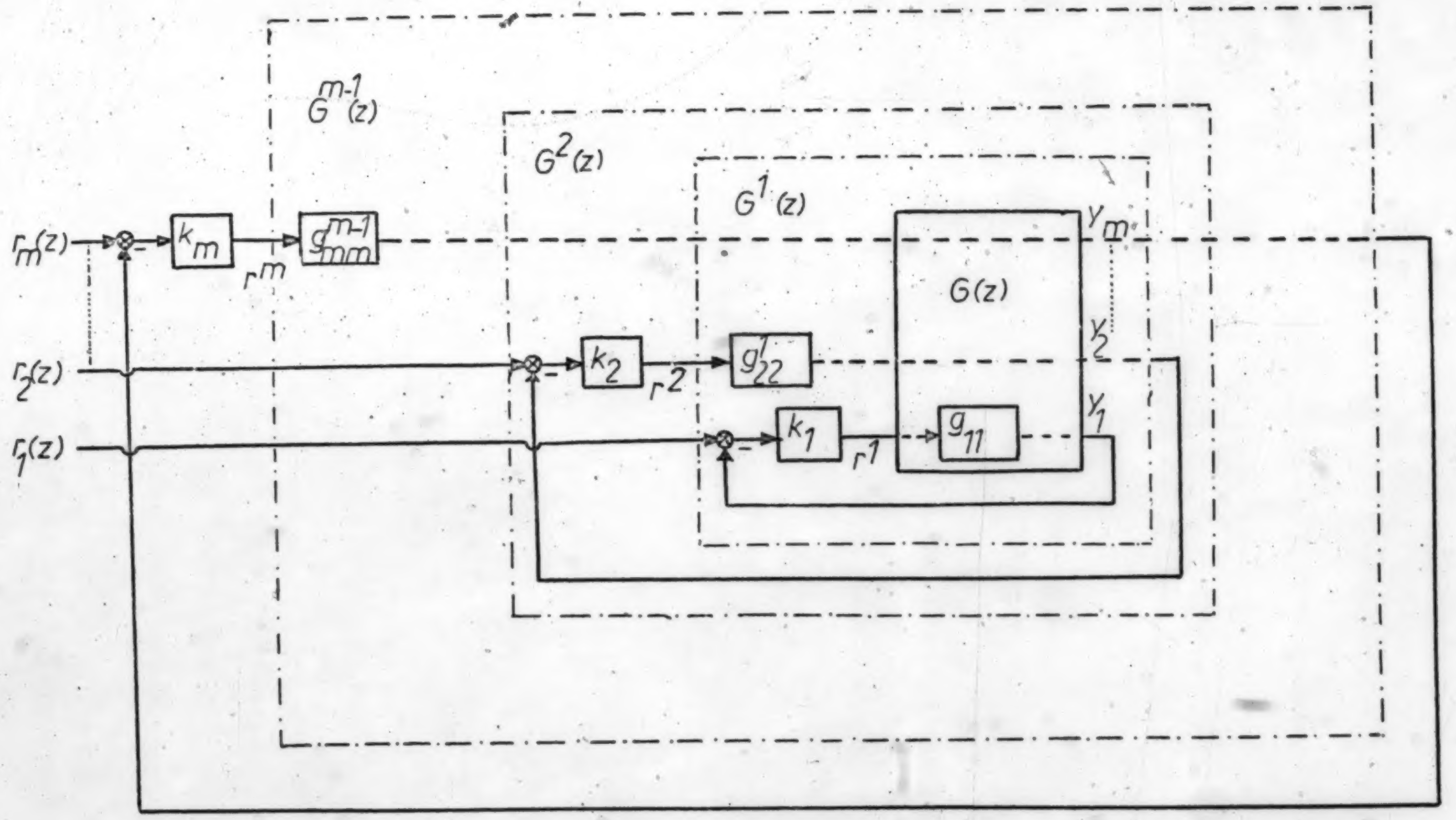

$G^{m-1}(z)$
$G^2(z)$
$G^1(z)$
$r_m(z)$
$r_2(z)$
$r_1(z)$
k_m
r^m
g_{mm}^{m-1}
k_2
r^2
g_{22}^1
k_1
r^1
g_{11}
$G(z)$
y_m
y_2
y_1

Figure 2.2 Schematic Diagram of the Sequential Return-Difference Method (Section 2.2, Reference [44,45])

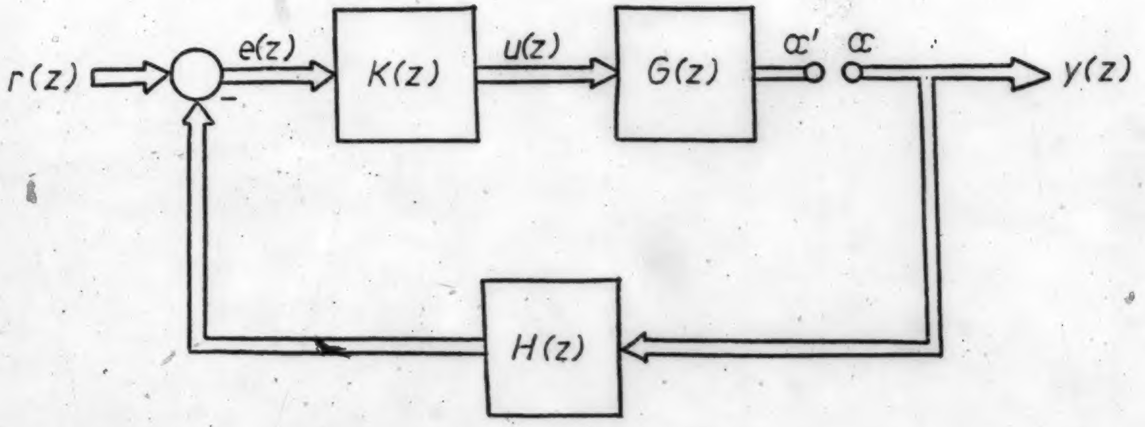
r(z)
e(z)
K(z)
u(z)
G(z)
α'
α
y(z)
-
H(z)

Figure 2.3 Multivariable Feedback Control System with all the Loop Broken
Return-Ratio: $T(z) = G(z)\ K(z)\ H(z)$
Return-Difference: $F(z) = I + G(z)\ K(z)\ H(z)$

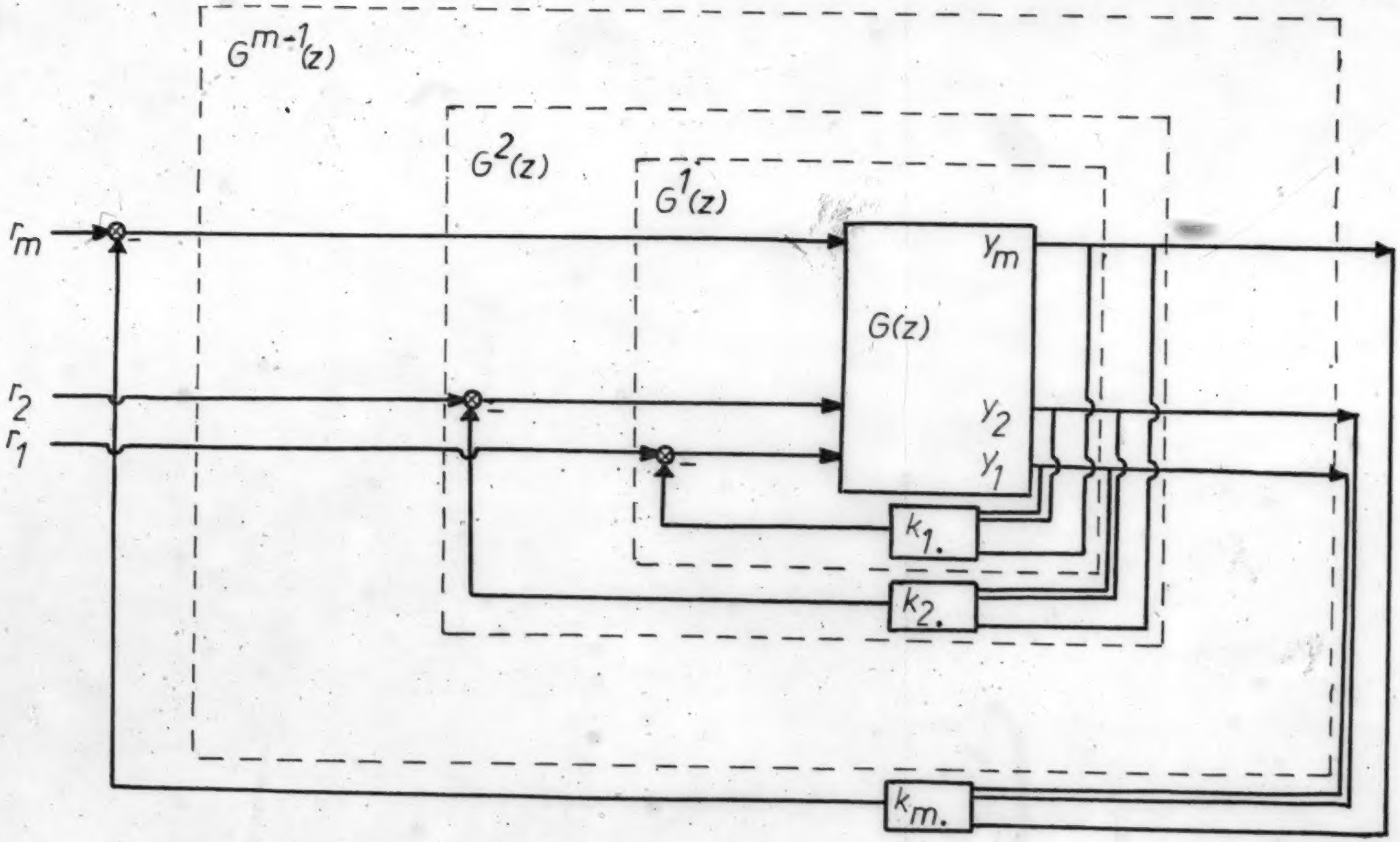
$G^{m-1}(z)$
$G^2(z)$
$G^1(z)$
r_m
r_2
r_1
$G(z)$
y_m
y_2
y_1
$k_{1.}$
$k_{2.}$
$k_{m.}$

Figure 2.4 Schematic Diagram of the Sequential Return-Difference Method Using Full Output Feedback (Section 2.3.7, Reference [58])

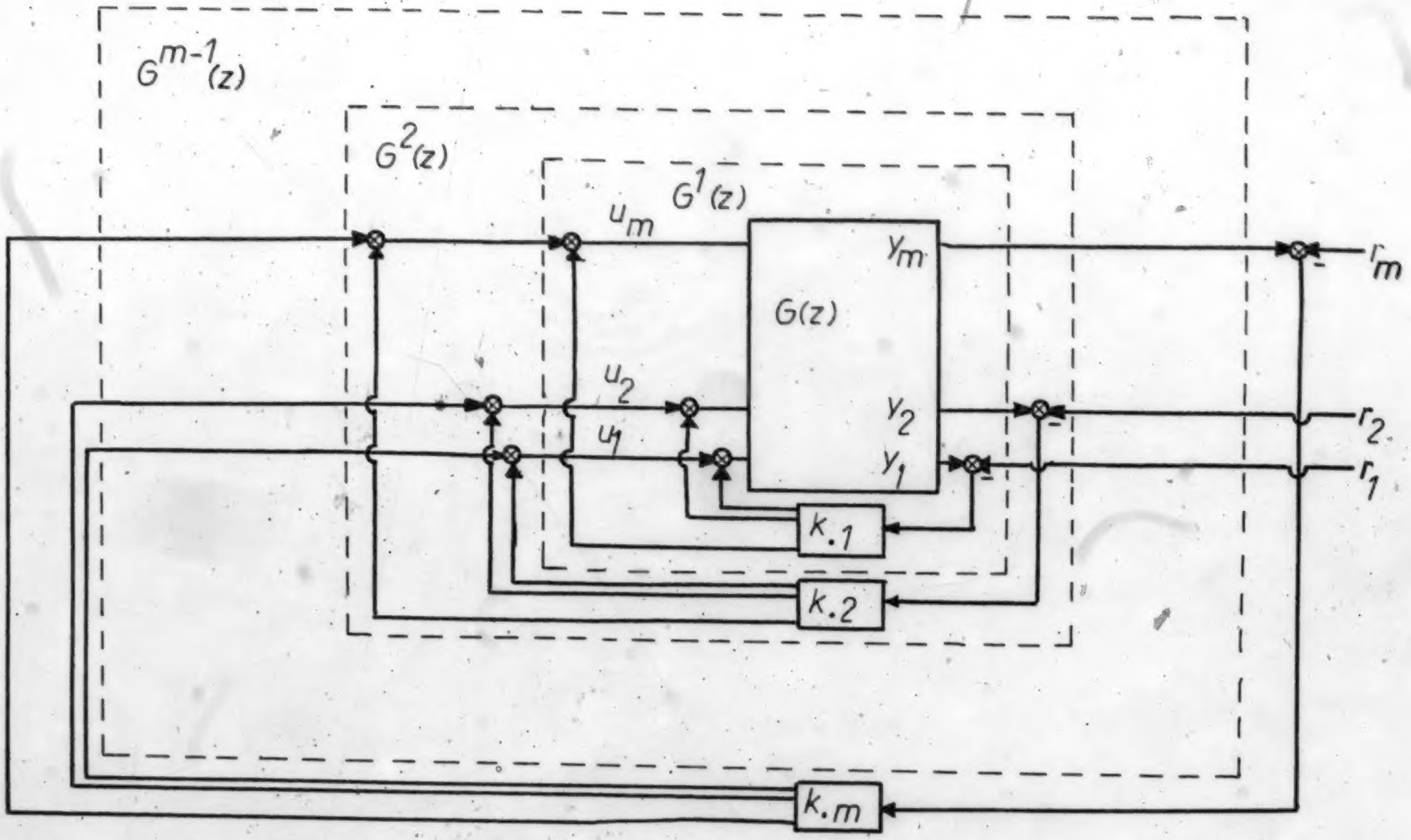
$G^{m-1}(z)$
$G^2(z)$
$G^1(z)$
u_m
u_2
u_1
$G(z)$
y_m
y_2
y_1
r_m
r_2
r_1
$k_{.1}$
$k_{.2}$
$k_{.m}$
-
-
-

Figure 2.5 Schematic Diagram of a Modification of the Sequential Return-Difference Method (Section 2.3.8)

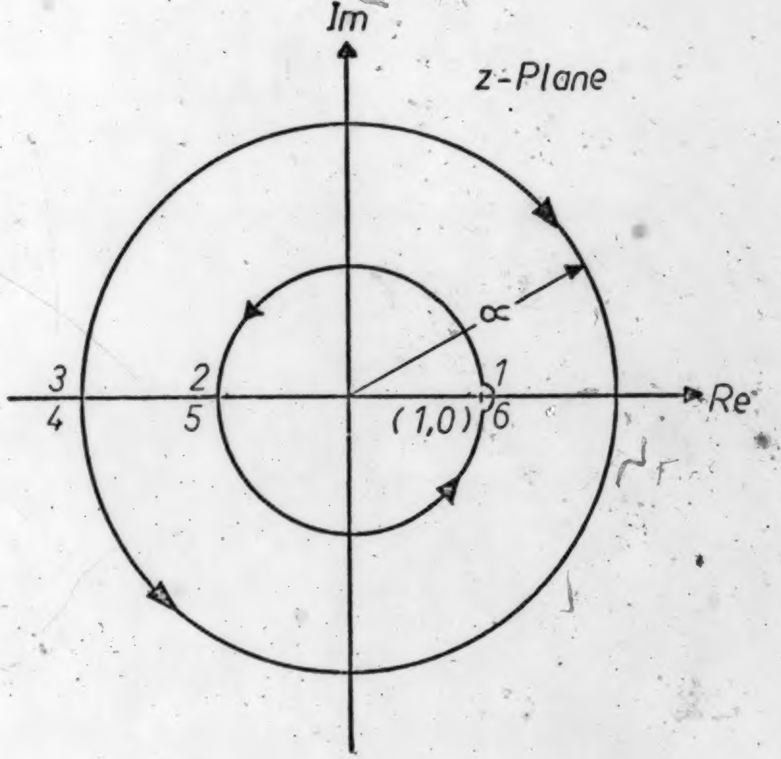
Im
z-Plane
∞
1
2
3
4
5
6
(1,0)
Re

Figure 3.1 Nyquist Contour in the z-Plane

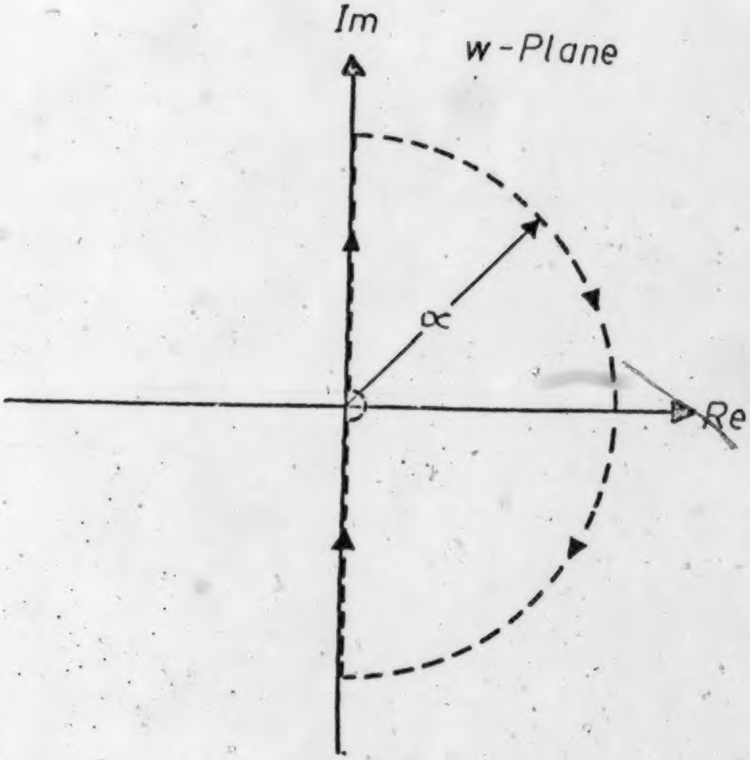
Im
w-Plane
∝
Re

Figure 3.2 Nyquist Contour in the w-Plane

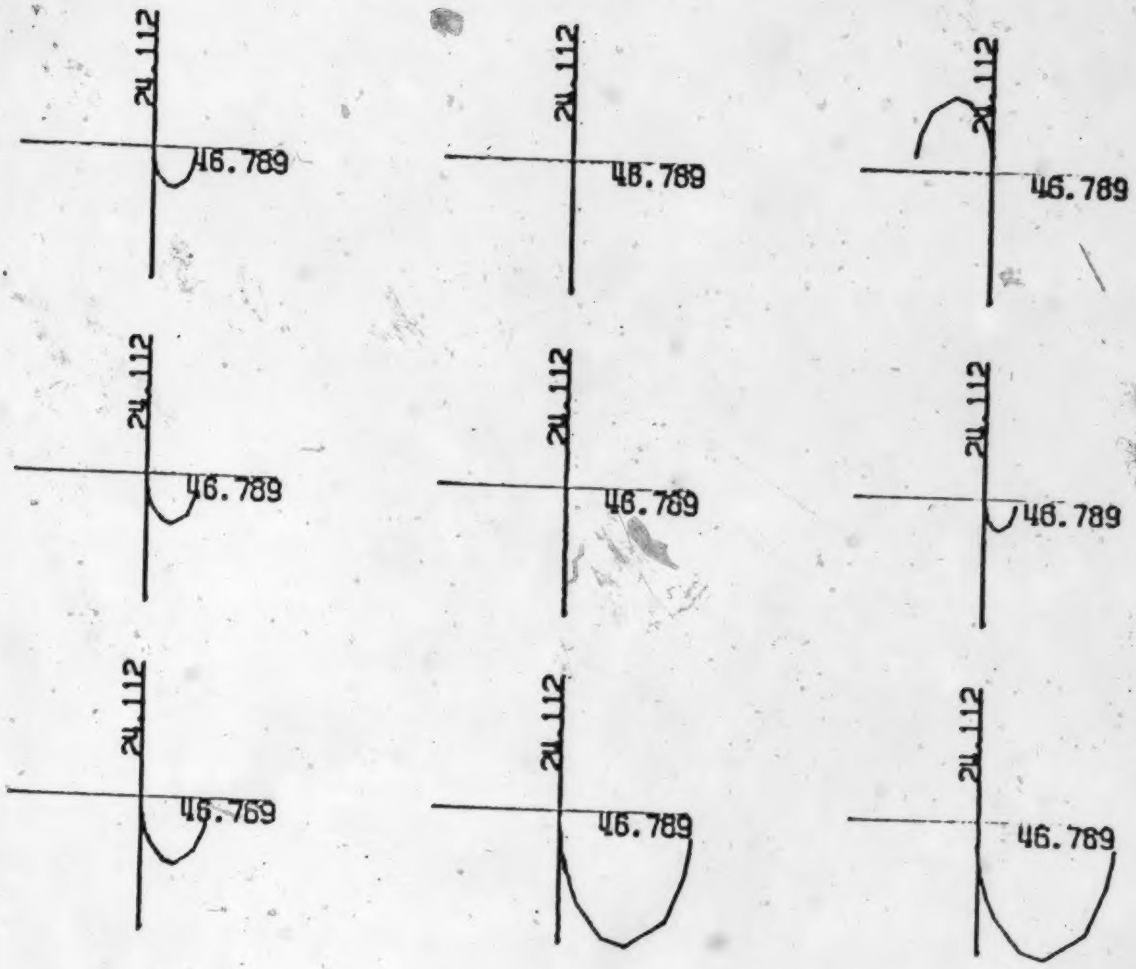

Figure 3.3 Inverse Nyquist Array of G(w)
$|G=3|$ 0.1 to 10.0 $|G^{-1}(w)|$ $K = I|$

Note: the code used to summarize the conditions used to generate this figure are defined in appendix B.

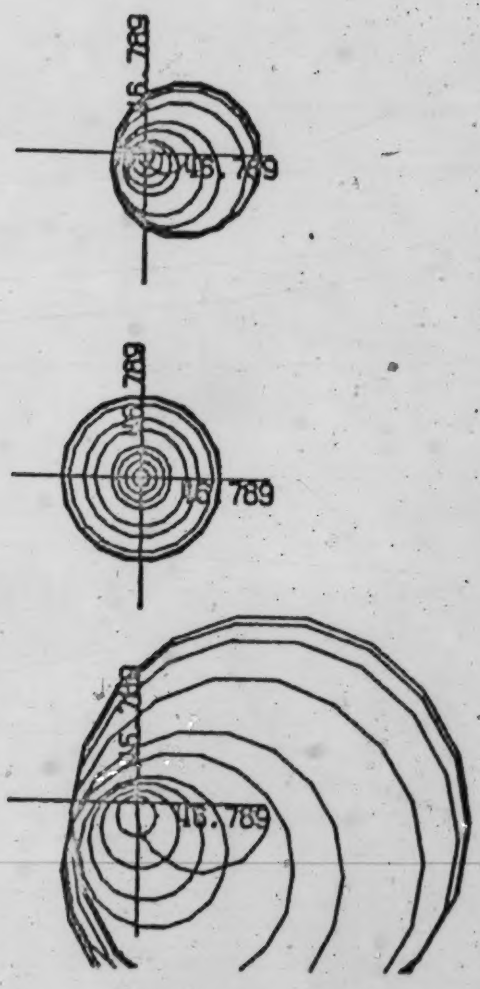

Figure 3.4 Diagonal Elements of $G^{-1}(w)$ with their Gershgorin Bands
|G=3| 0.1 to 10.0| $G^{-1}(w)$| K = I|

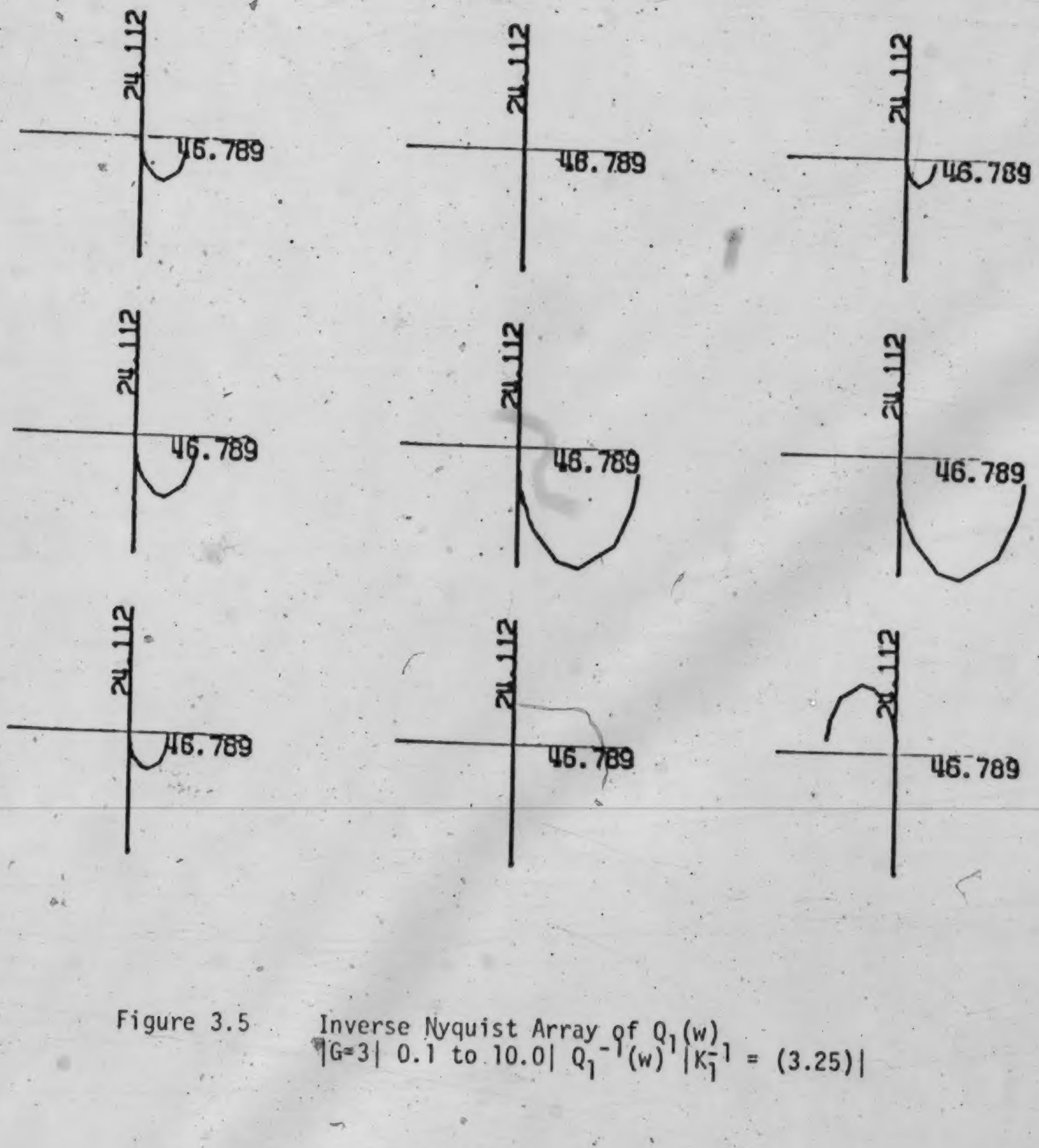

Figure 3.5 Inverse Nyquist Array of $Q_1(w)$
|G=3| 0.1 to 10.0| $Q_1^{-1}(w)$ |K_1^{-1} = (3.25)|

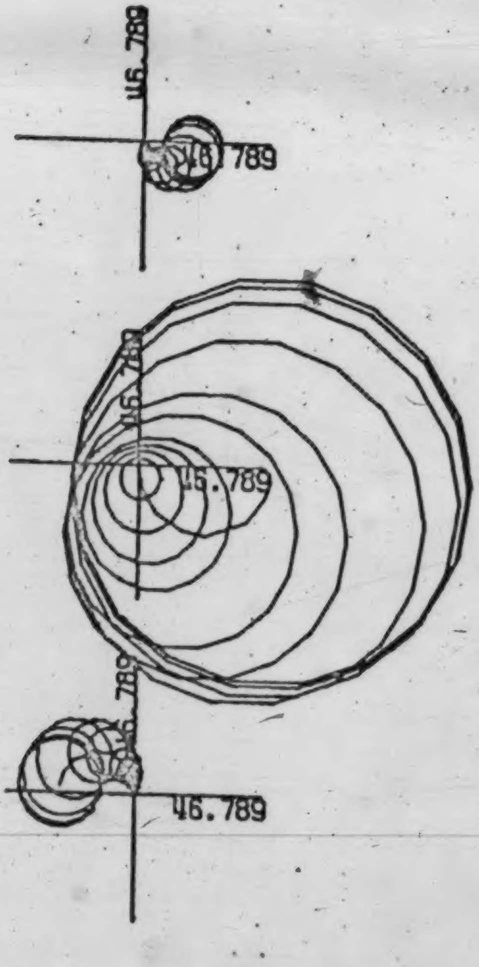

Figure 3.6 Diagonal Elements of $Q_1^{-1}(w)$ with their Gershgorin Bands
$|G=3|$ 0.1 to 10.0$|$ $Q_1^{-1}(w)$$|$ K_1^{-1} = (3.25)$|$

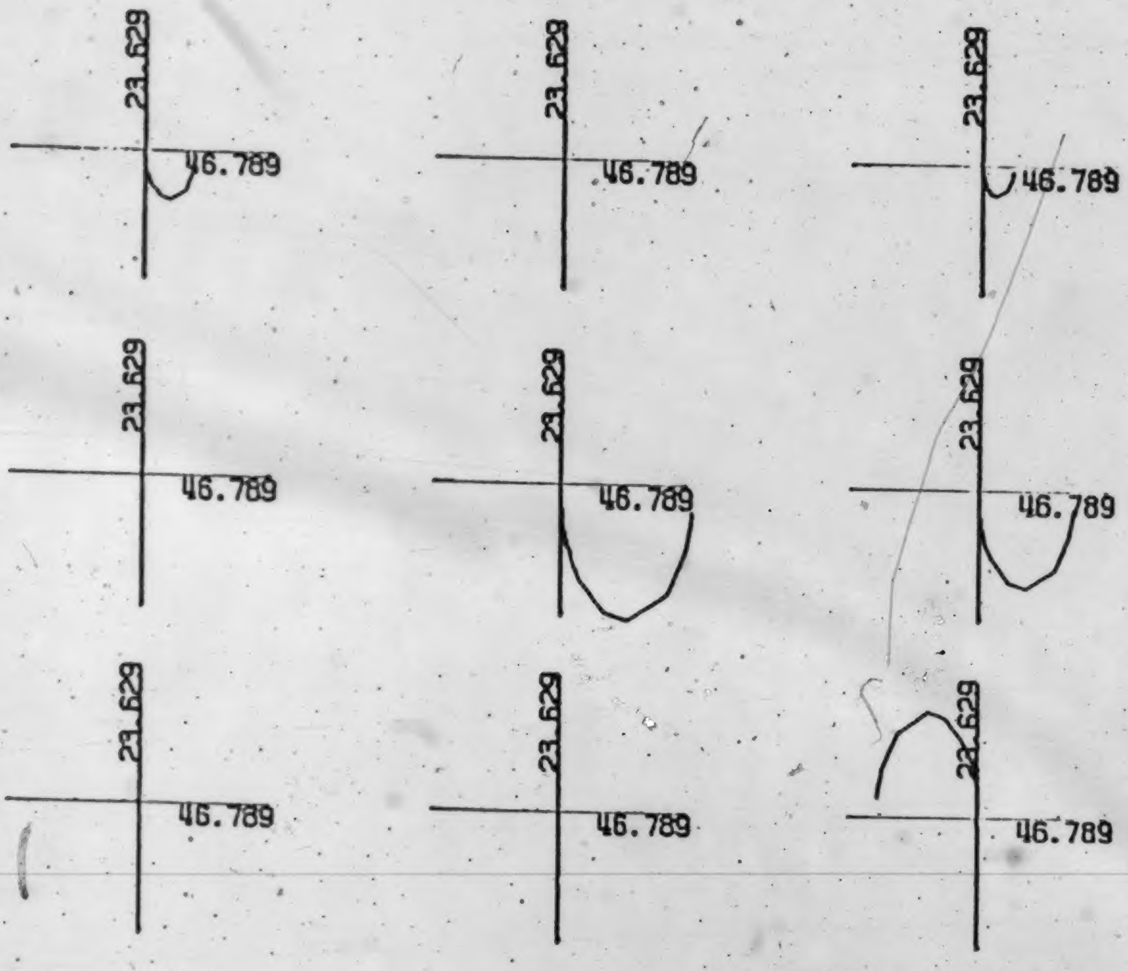

Figure 3.7 Inverse Nyquist Array of $Q_2(w)$
$|G=3|$ 0.1 to 10.0$|$ $Q_2^{-1}(w)|$ $K_2^{-1}K_1^{-1}$ = (3.27)(3.28)$|$

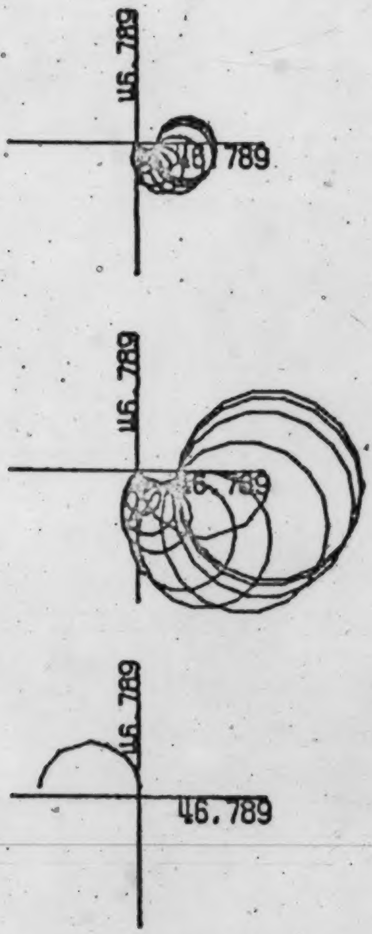

Figure 3.8 Diagonal Elements of $Q_2^{-1}(w)$ with their Gershgorin Bands
|G=3| 0.1 to 10.0| $Q_2^{-1}(w)$| $K_2^{-1}K_1^{-1}$ = (3.27)(3.28)|

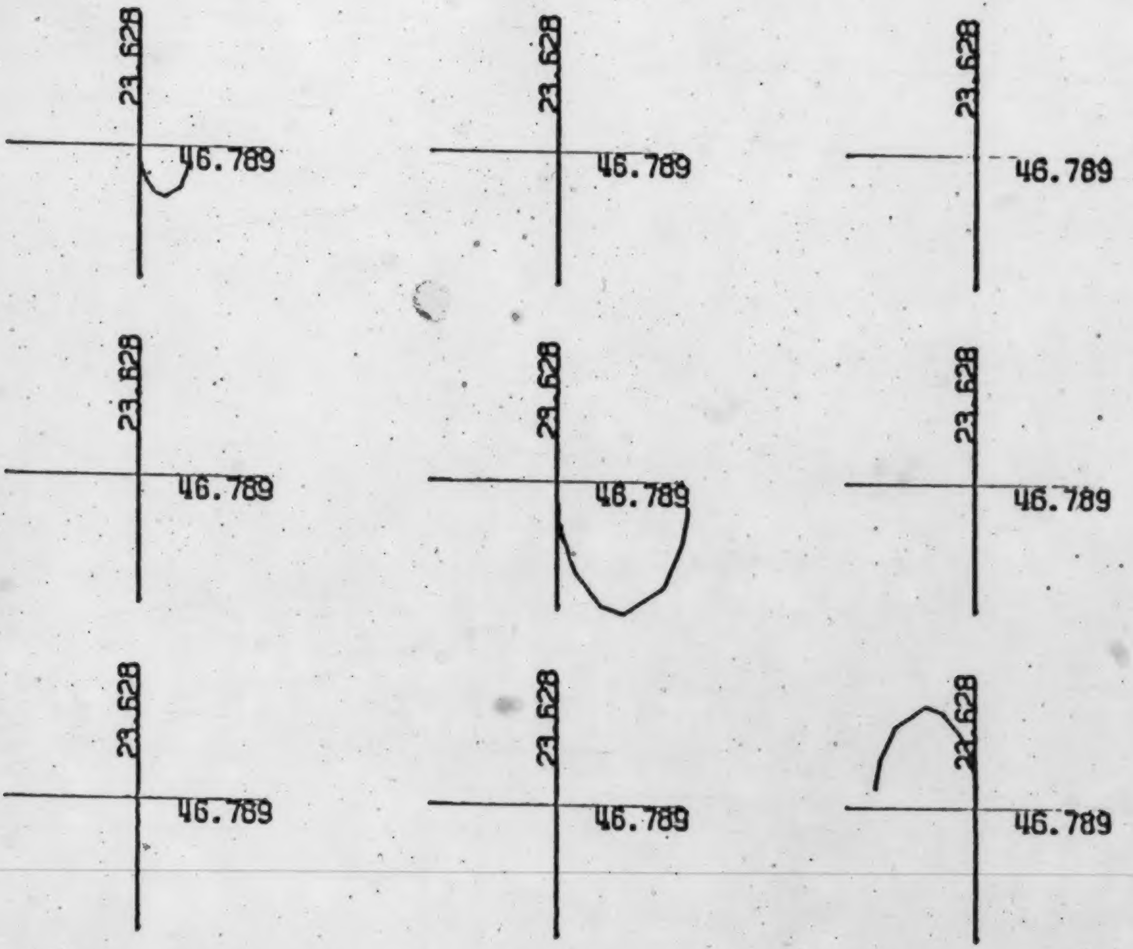

Figure 3.9 Inverse Nyquist Array of $Q_3(w)$
|G=3| 0.1 to 10.0| $Q_2^{-1}(w)$| $K_3^{-1}K_2^{-1}K_1^{-1}$ = (3.32)|

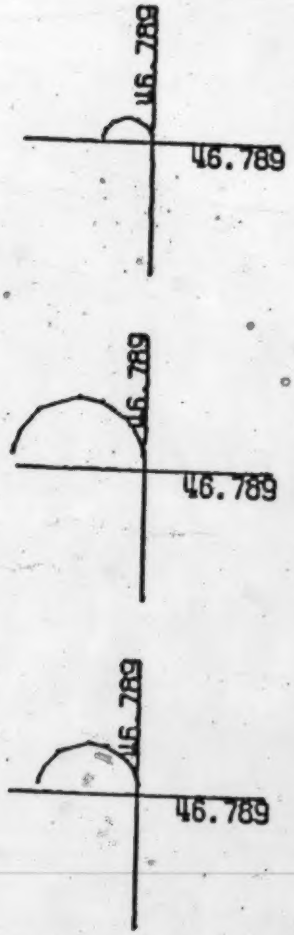

Figure 3.10 Diagonal Elements of $Q_4^{-1}(w)$ with their Gersngorin Bands
|G=3| 0.1 to 10.0| $Q_2^{-1}(w)$| $K_4^{-1}K_3^{-1}K_2^{-1}K_1^{-1}$ = (3.32)|

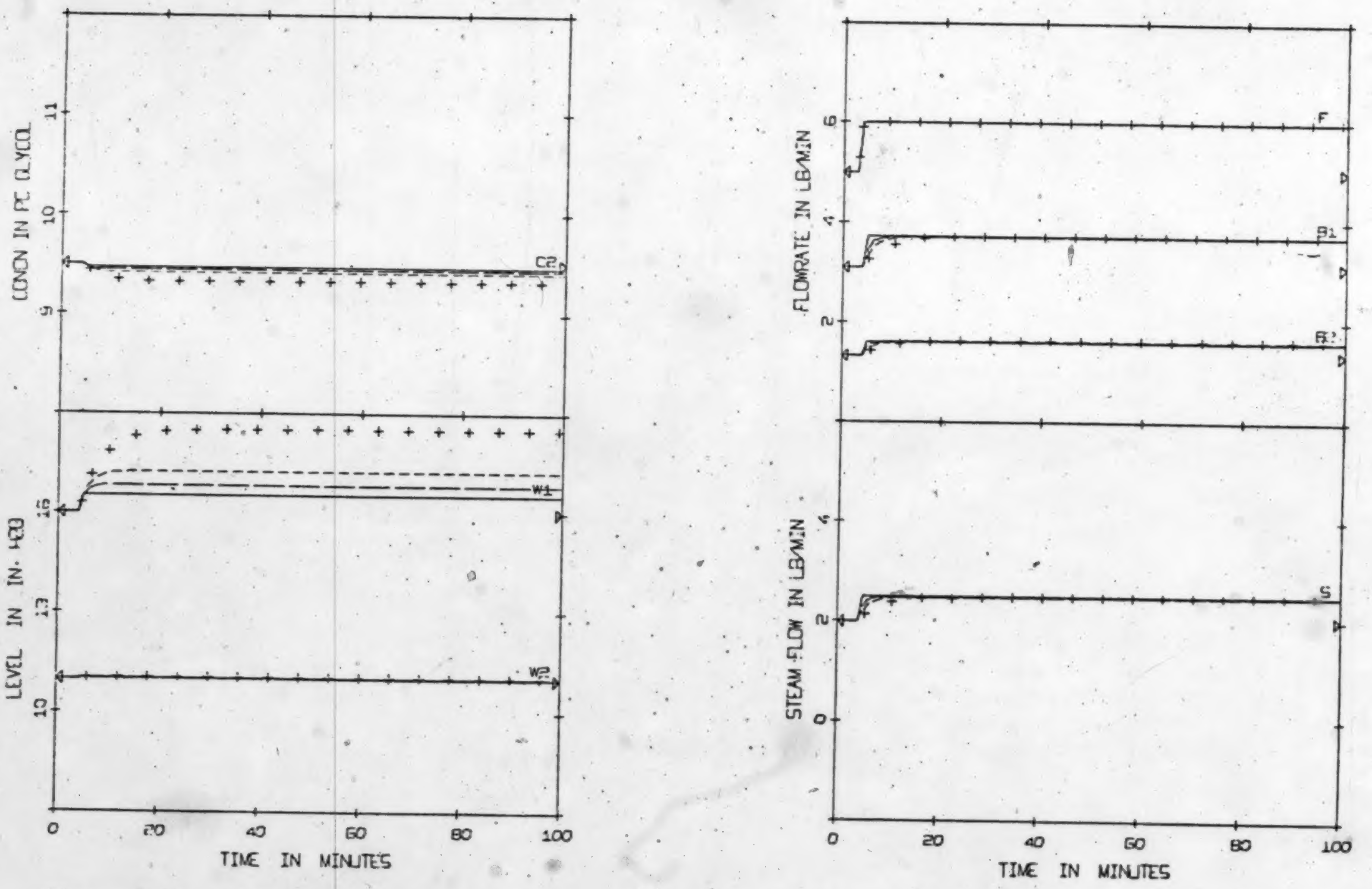

Figure 3.11 Effect of Increasing the Gains in Constant Compensator from Frequency Domain Techniques
FD0310: ++++, FD0320: ----, FD0330: — —, FD0350: ——
|G=3| FD0310| 0320| 0330| 0350| SIM 3| K = Table B.1| INA + DNA + CL| P| ± 20% F|

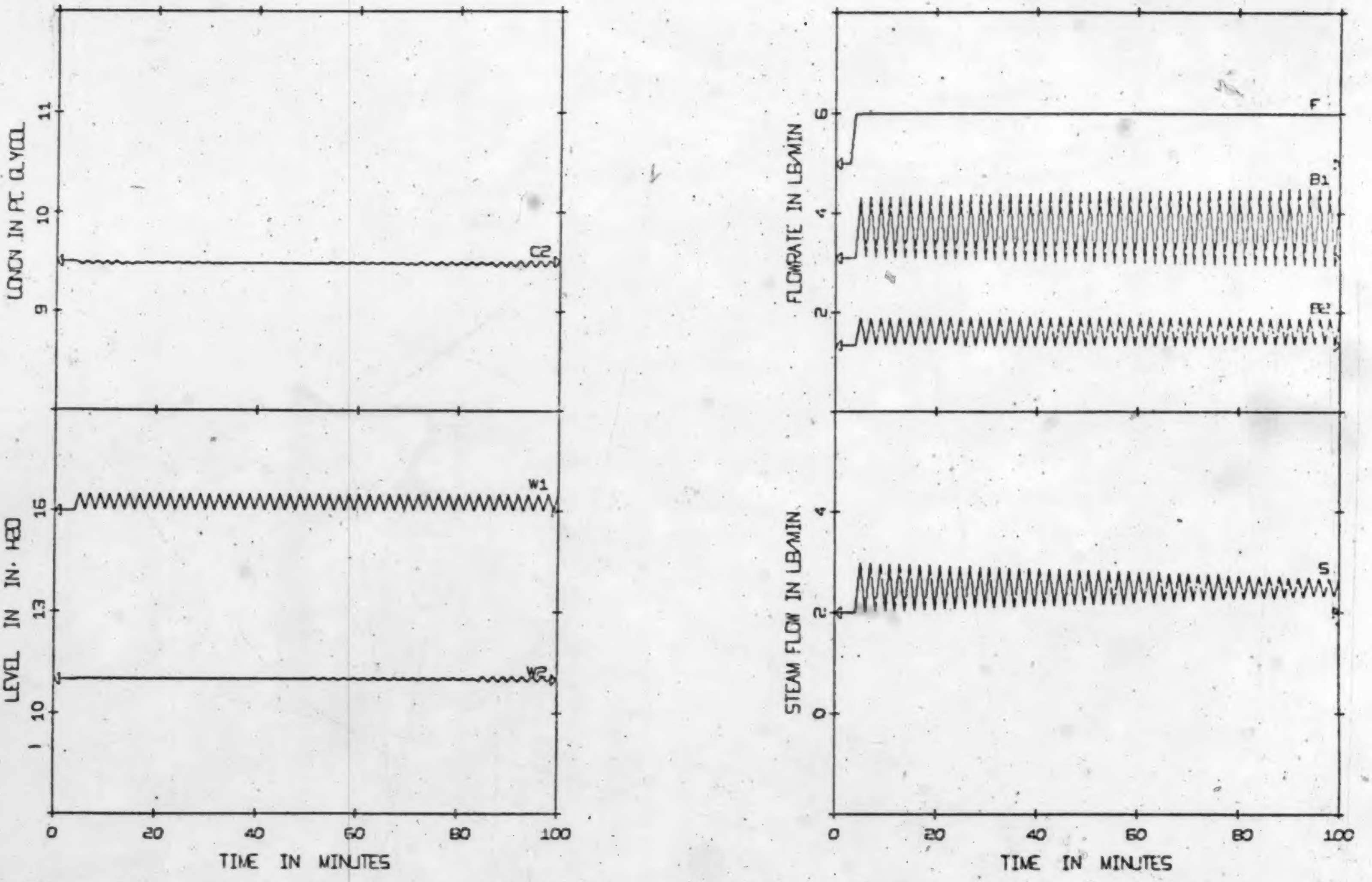

Figure 3.12 Effect of Using the Ultimate Gains in Constant Compensator from Frequency Domain Techniques |G=3| FD0390| SIM 3| K = Table B.1| INA + DNA + CL| P| + 20% F|

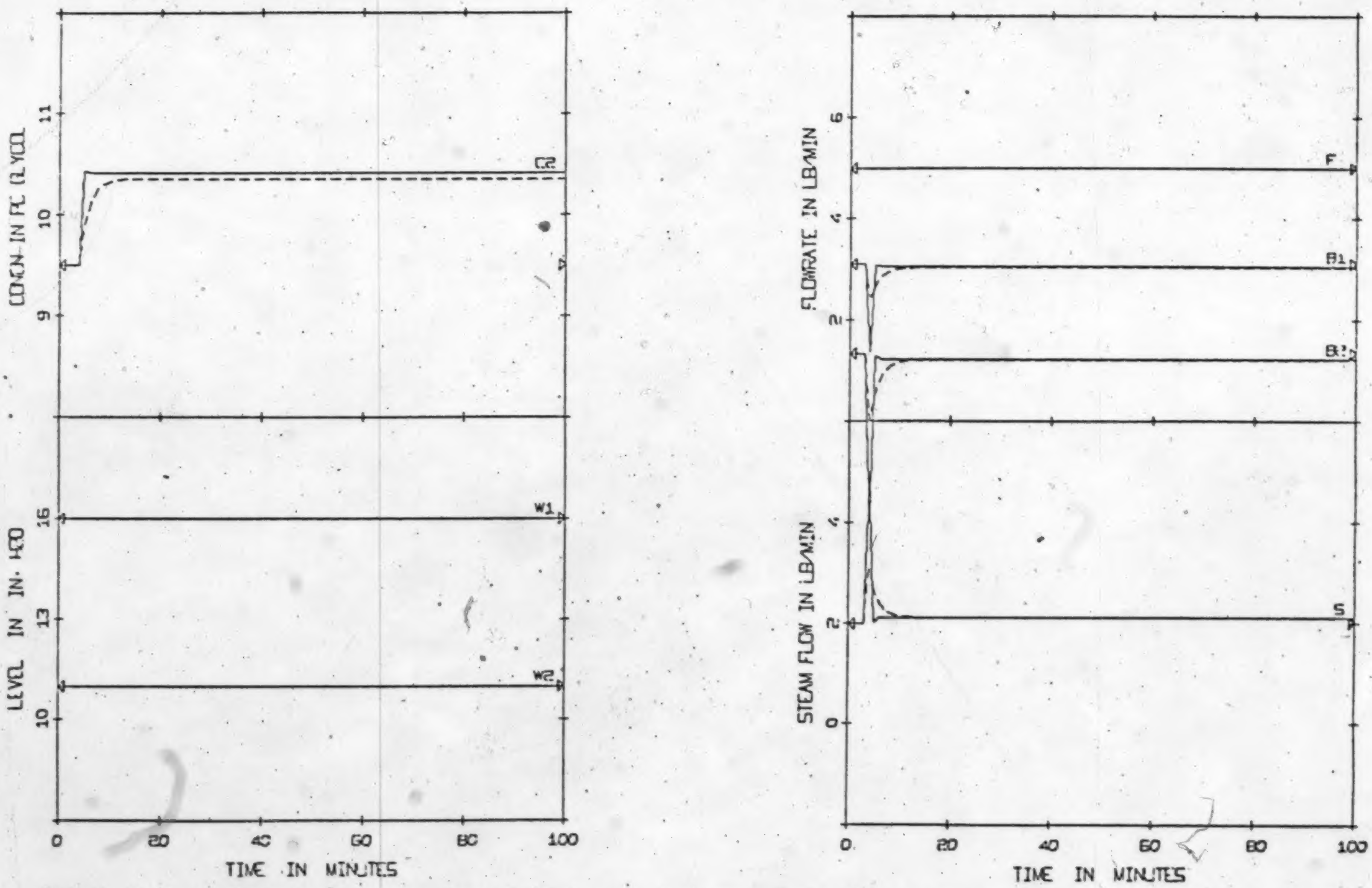

Figure 3.13 Effect of Increasing the Gains in Constant Compensator from Frequency Domain Technique for a Step Change in Setpoint of C_2
FD0320: ----, FD0350: ——
|G=3| FD0320| 0350| SIM 3| K = Table B.1| INA + DNA + CL| P| + 10% C_2|

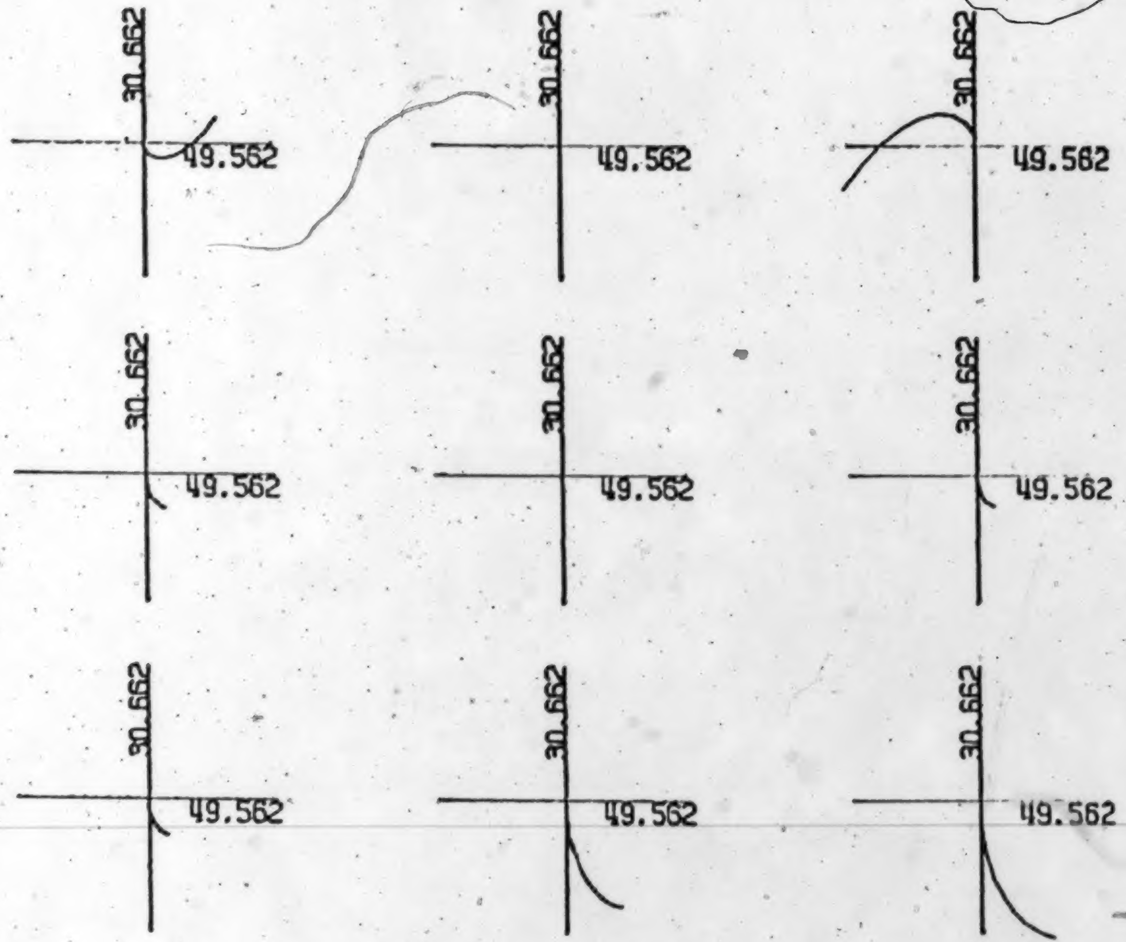

Figure 3.14 Inverse Nyquist Array of G(w)
|G=5| 0.1 to 1.0| $G^{-1}(w)$| K = I|

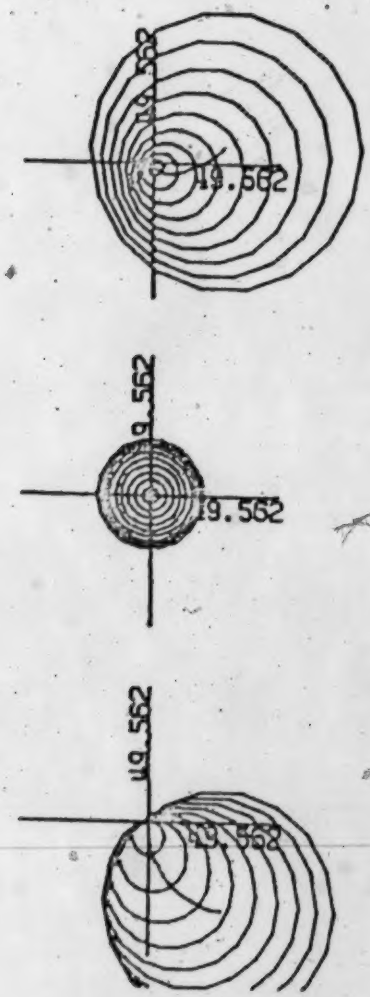

Figure 3.15 Diagonal Elements of $G^{-1}(w)$ with their Gershgorin Bands
|G=5| 0.1 to 1.0| $G^{-1}(w)$| K = I|

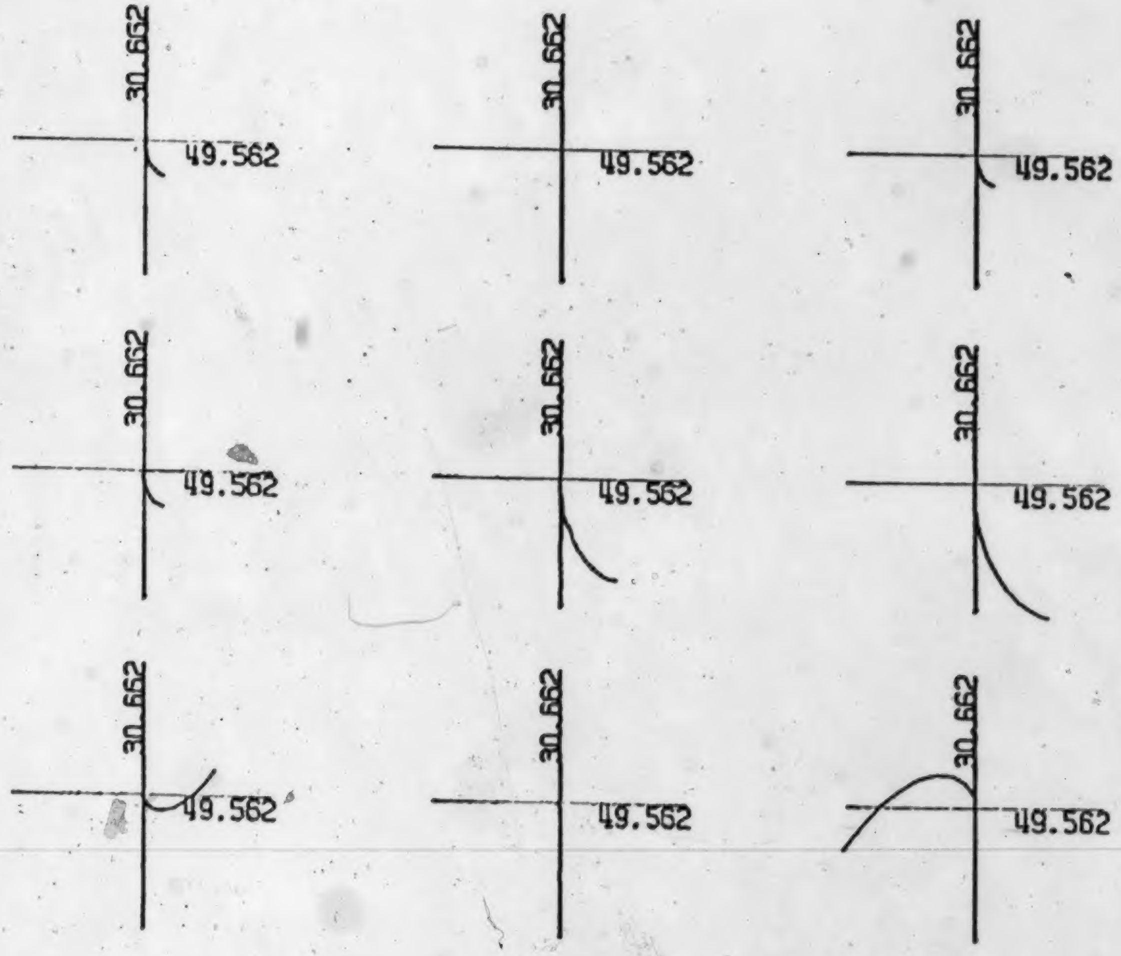

Figure 3.16 Inverse Nyquist Array of $Q_1(w)$
$|G=5|$ 0.1 to 1.0$|$ $Q_1^{-1}(w)$$|$ K_1^{-1} = (3.39)$|$

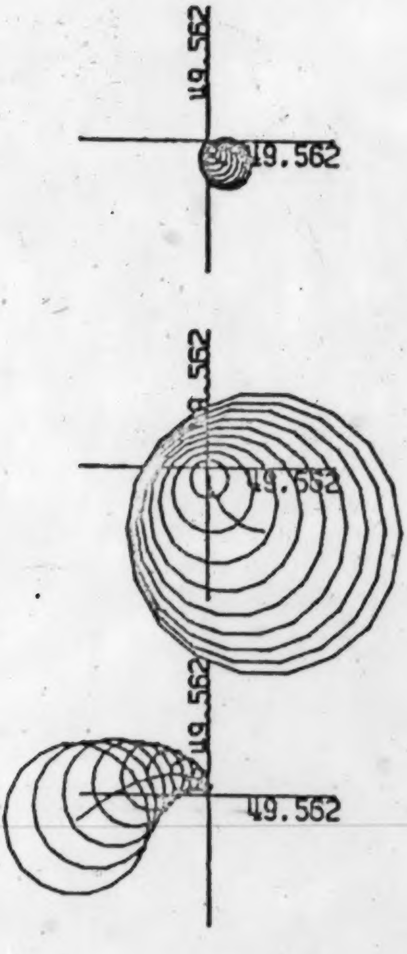

Figure 3.17 Diagonal Elements of $Q_1^{-1}(w)$ with their Gershgorin Bands
$|G=5|$ 0.1 to 1.0$|$ $Q_1^{-1}(w)$$|$ K_1^{-1} = (3.39)$|$

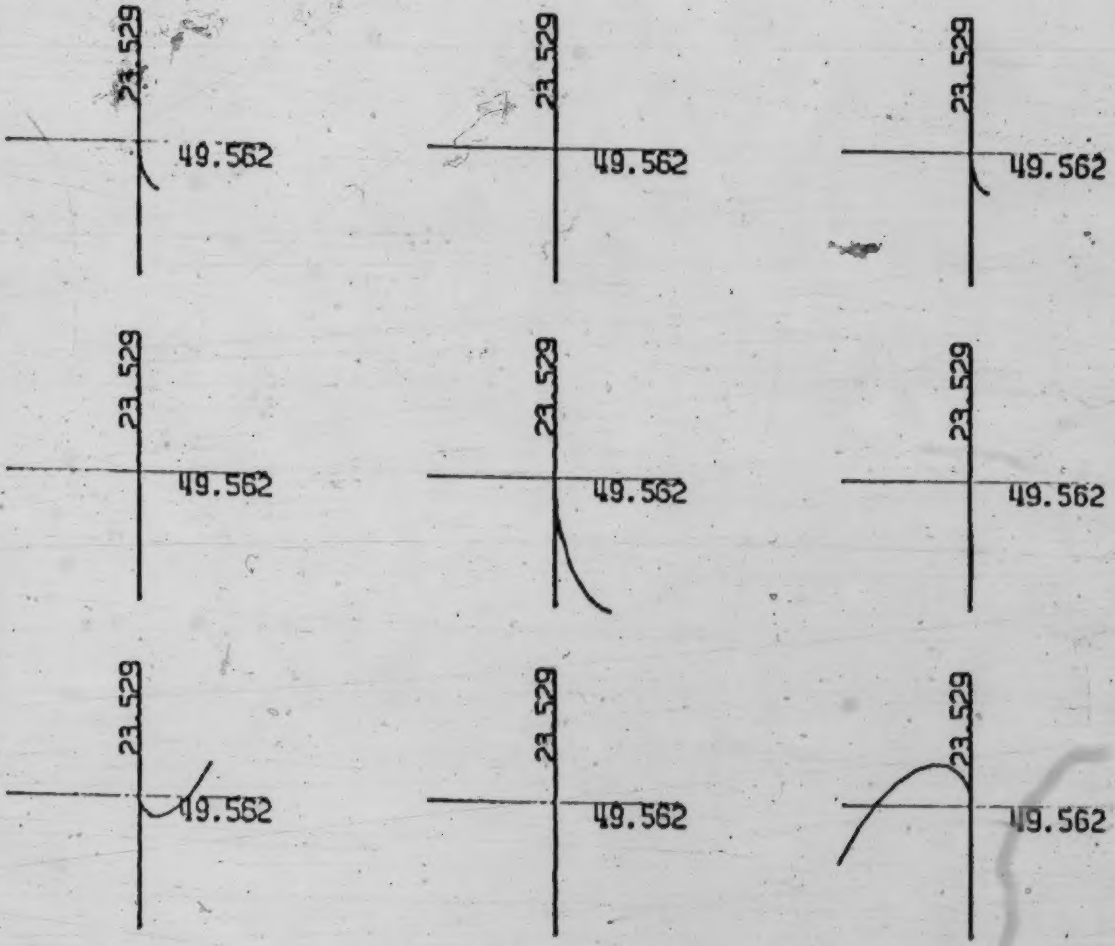

Figure 3.18 Inverse Nyquist Array of $Q_2(w)$
|G=5| 0.1 to 1.0| $Q_2^{-1}(w)$| $K_2^{-1}K_1^{-1}$ = (3.40)(3.39)|

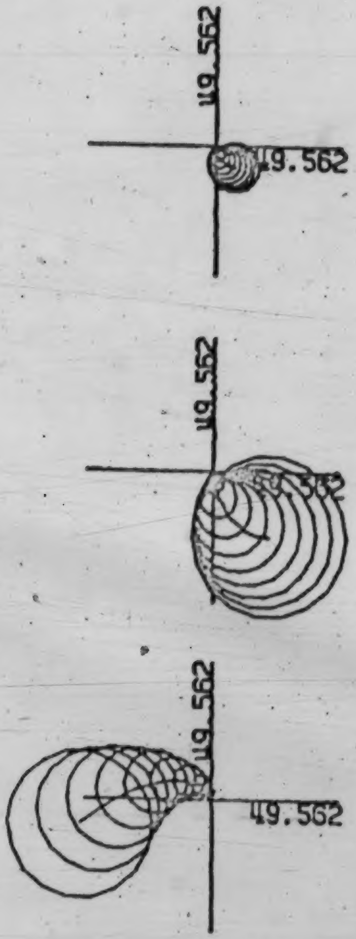

Figure 3.19 Diagonal Elements of $Q_2^{-1}(w)$ with their Gershgorin Bands
$|G=5|$ 0.1 to 1.0$|$ $Q_2^{-1}(w)|$ $K_2^{-1}K_1^{-1}$ = (3.40)(3.39)$|$

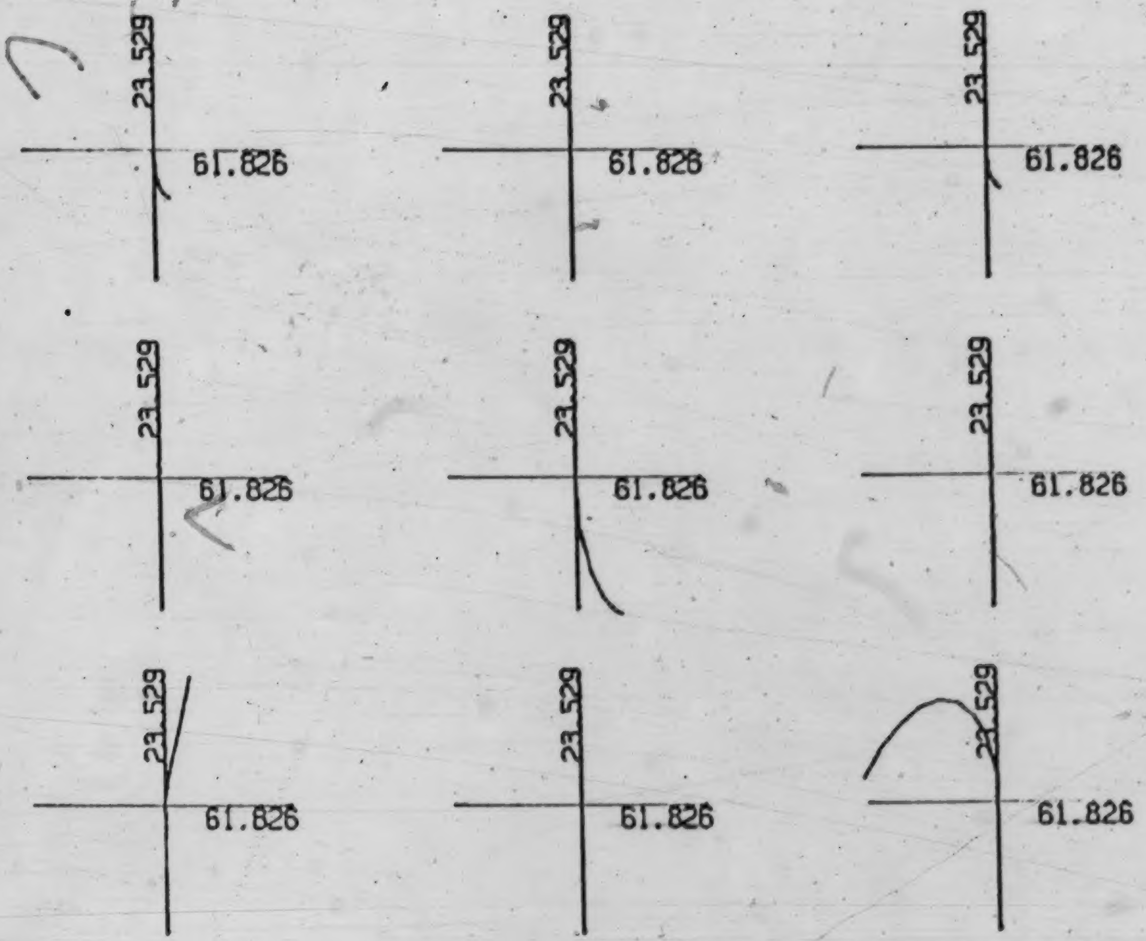

Figure 3.20 Inverse Nyquist Array of $Q_3(w)$
|G=5| 0.1 to 1.0| $Q_3^{-1}(w)$| $K_3^{-1}K_2^{-1}K_1^{-1}$ = (3.42)(3.40)(3.39)|

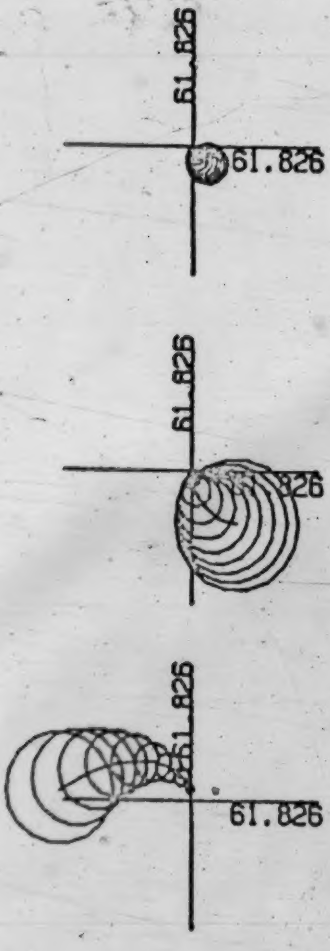

Figure 3.21 Diagonal Elements of $Q_3^{-1}(w)$ with their Gershgorin Bands
|G=5| 0.1 to 1.0| $Q_3^{-1}(w)$| $K_3^{-1}K_2^{-1}K_1^{-1}$ = (3.42)(3.40)(3.39)|

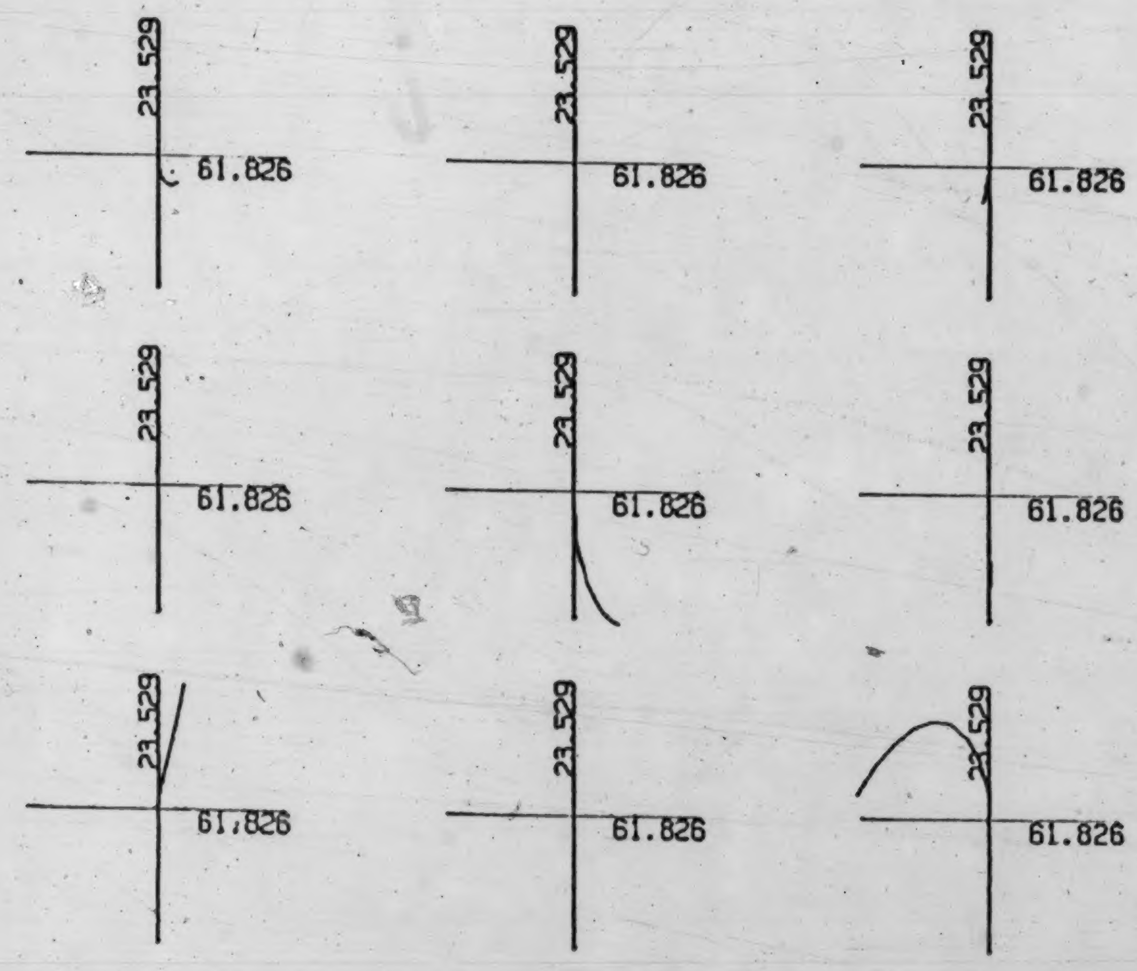

Figure 3.22 Inverse Nyquist Array of $Q_4(w)$
$|G=5|$ 0.1 to 1.0$|$ $Q_4^{-1}(w)|$ $K_4^{-1}K_3^{-1}K_2^{-1}K_1^{-1}$ = (3.43)(3.42)(3.40)(3.39)$|$

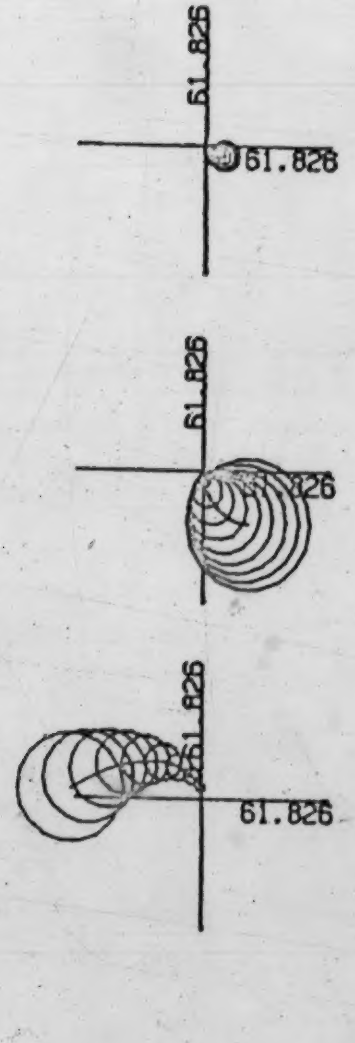

Figure 3.23 Diagonal Elements of $Q_4^{-1}(w)$ with their Gershgorin Bands |G=5| 0.1 to 1.0| $Q_4^{-1}(w)$| $K_4^{-1}K_3^{-1}K_2^{-1}K_1^{-1}$ = (3.43)(3.42)(3.40)(3.39)|

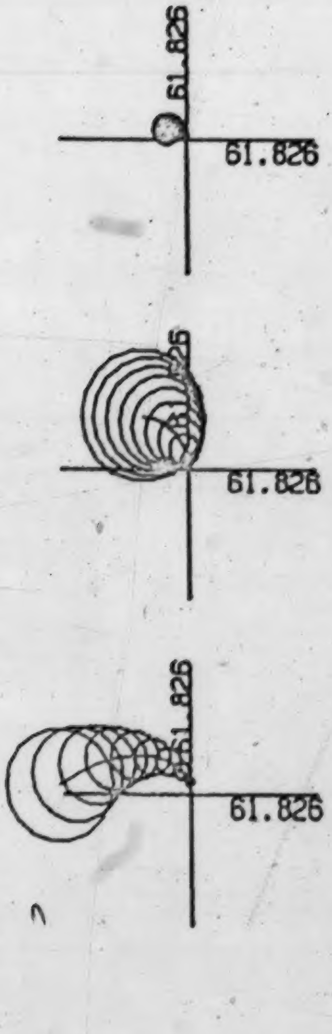

Figure 3.24 Diagonal Elements of $Q_5^{-1}(w)$ with their Gershgorin Bands
|G=5| 0.01 to 1.0| $Q_5^{-1}(w)$| K_5^{-1} ... K_1^{-1} = (3.44) ... (3.39)|

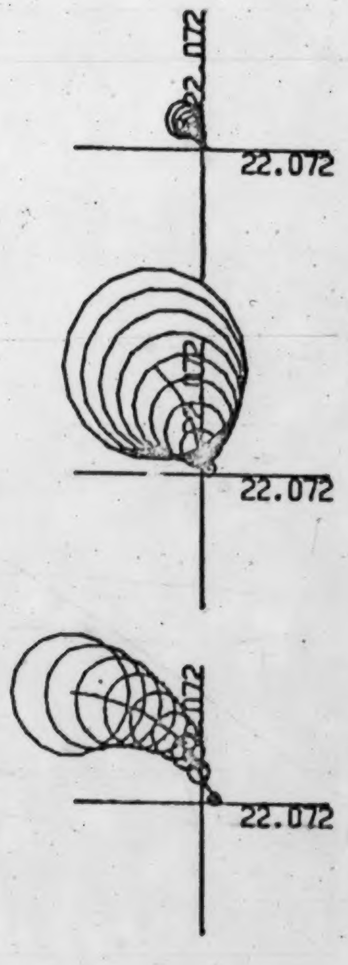

Figure 3.25 Diagonal Elements of $Q_5^{-1}(w)$ with their Gershgorin Bands
|G=5| 0.01 to 0.5| $Q_5^{-1}(w)$| K_5^{-1} ... K_1^{-1} = (3.44) ... (3.39)|

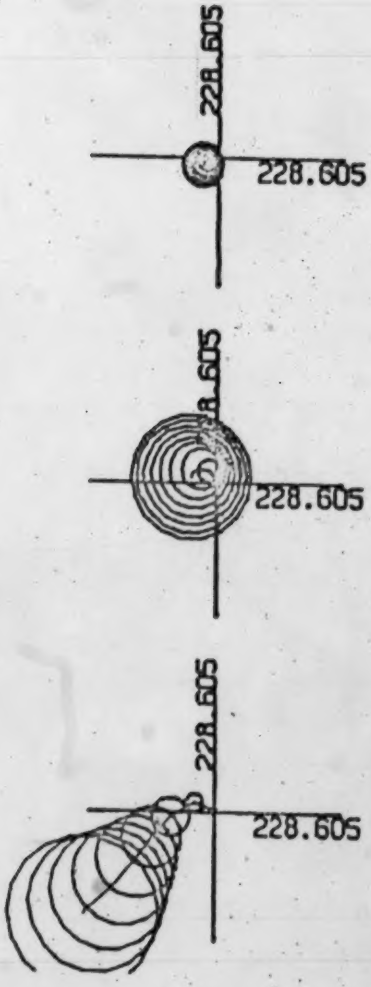

Figure 3.26 Diagonal Elements of $Q_5(w)$ with their Gershgorin Bands |G=5| 0.1 to 5.0| $Q_5^{-1}(w)$| $K_5^{-1}K_4^{-1} \ldots K_1^{-1}$ = (3.44)(3.43)...(3.39)|

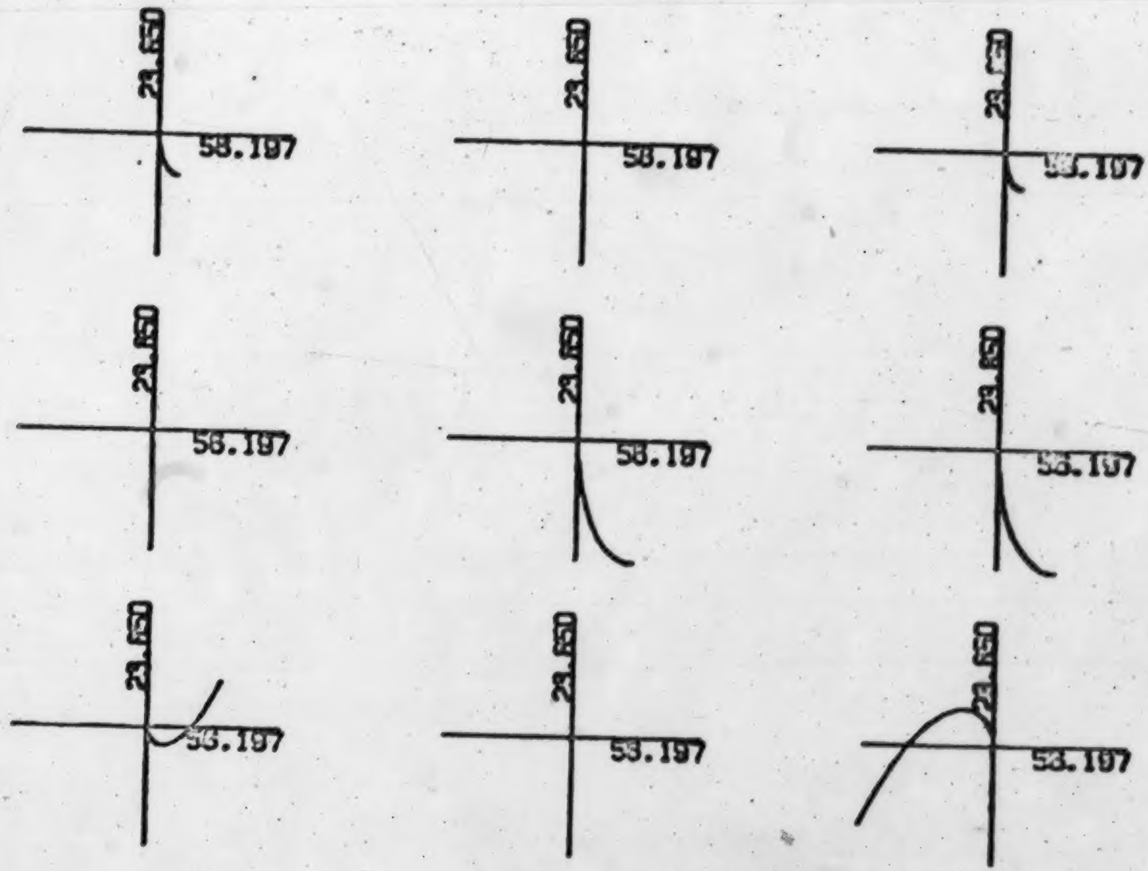

Figure 3.27 Inverse Nyquist Array of $Q_2^1(w)$
|G=5| 0.1 to 1.0| $(Q_2^1(w))^{-1}$| $(K_2^1)^{-1}K_1^{-1}$ = (3.45)(3.39)|

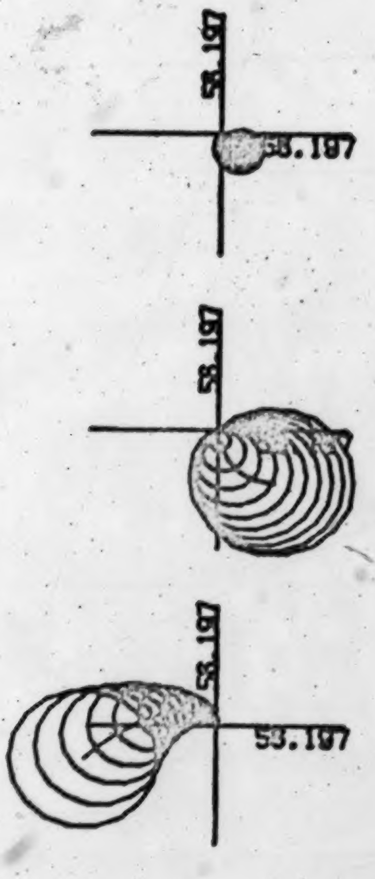

Figure 3.28 Diagonal Elements of $(Q_2^1(w))^{-1}$ with their Gershgorin Bands
|G=5| 0.1 to 1.0| $(Q_2^1(w))^{-1}$| $(K_2^1)^{-1}K_1^{-1}$ = (3.45)(3.39)|

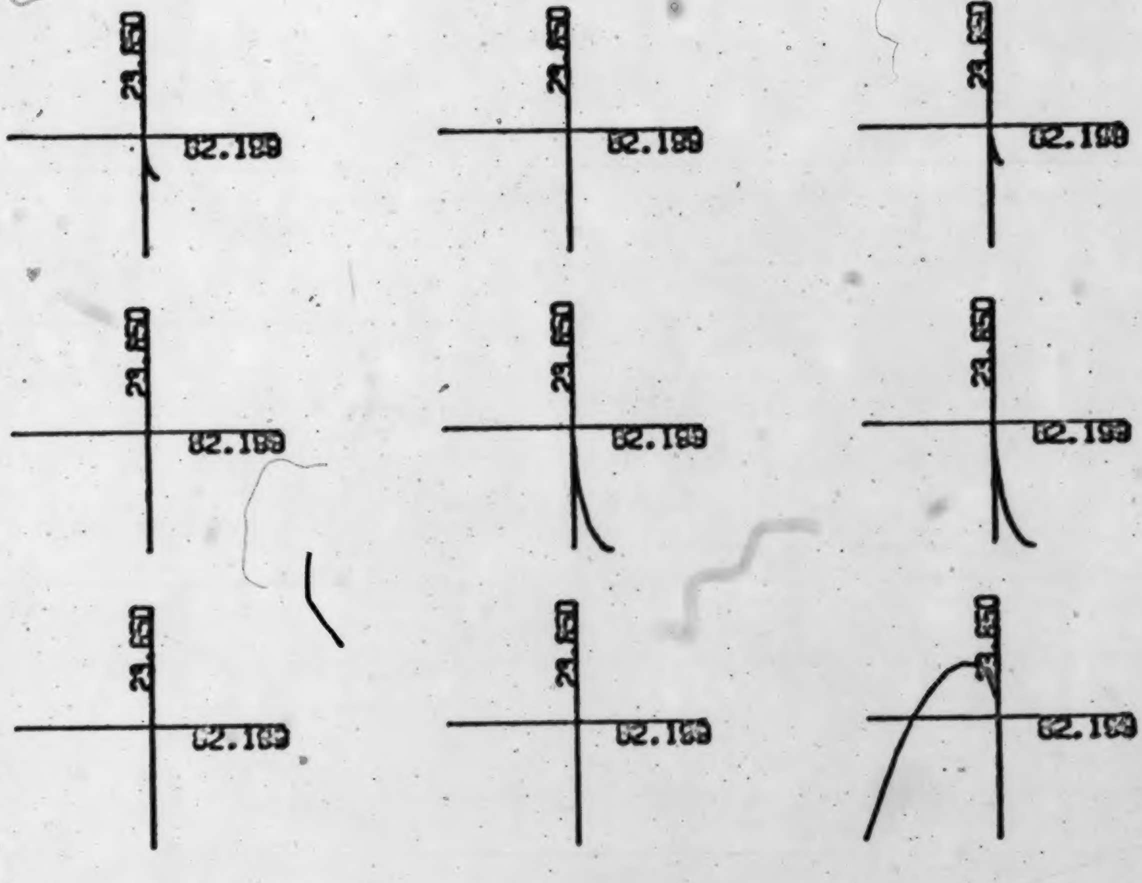

Figure 3.29 Inverse Nyquist Array of $Q_3^1(w)$
$|G=5|$ 0.1 to 1.0$|$ $(Q_3^1(w)^{-1}|$ $(K_2^1)^{-1}K_1^{-1}$ = (3.45)(3.39)$|$

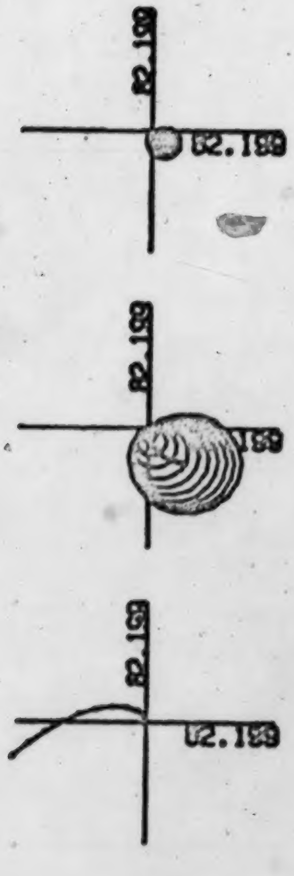

Figure 3.30 Diagonal Elements of $(Q_3^{1}(w))^{-1}$ with their Gershgorin Bands
$|G=5|$ 0.1 to 1.0$|$ $(Q_3^{1}(w))^{-1}|(K_3^{1})^{-1}(K_2^{1})^{-1}(K_1)^{-1}$ = (3.47) (3.45)(3.39)$|$

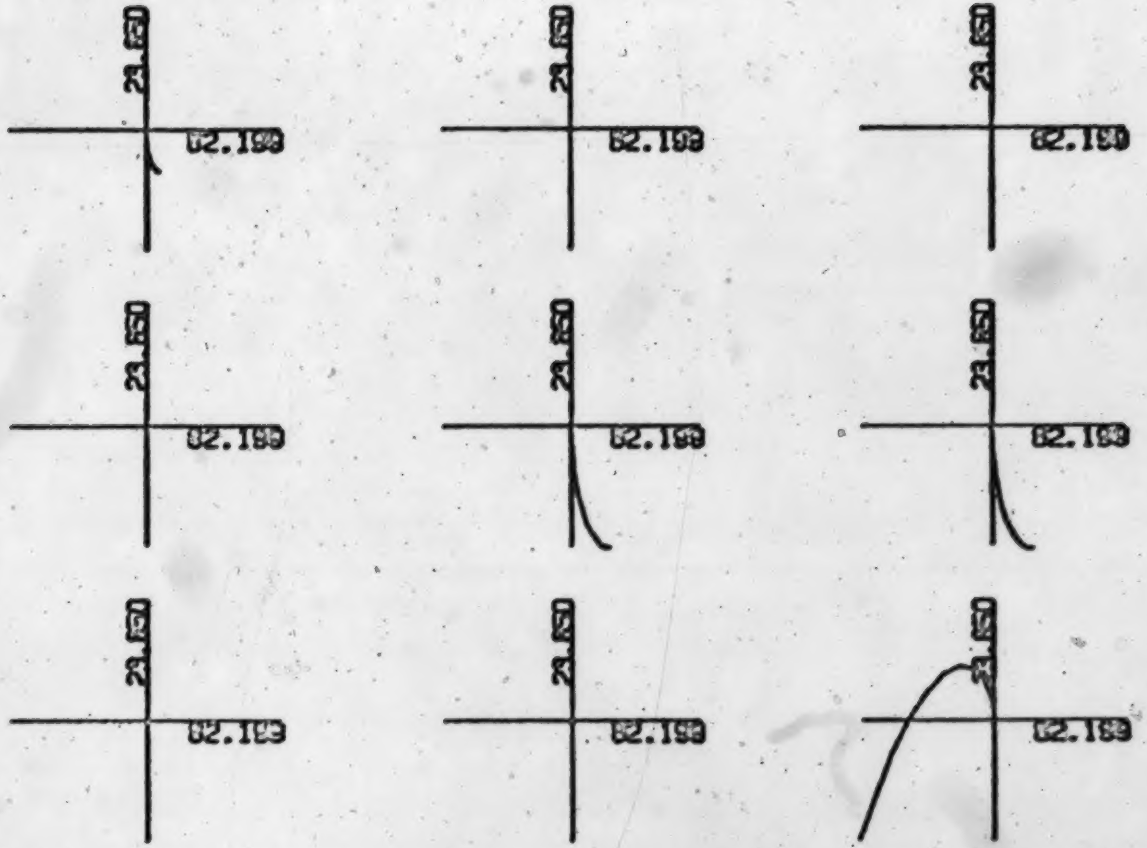

Figure 3.31 Inverse Nyquist Array of $Q_4^1(w)$
|G=5| 0.1 to 1.0| $(Q_4^1(w))^{-1}$| $(K_4^1)^{-1}(K_3^1)^{-1}(K_2^1)^{-1}(K_1)^{-1}$ =
(3.50)(3.47)(3.45)(3.39)|

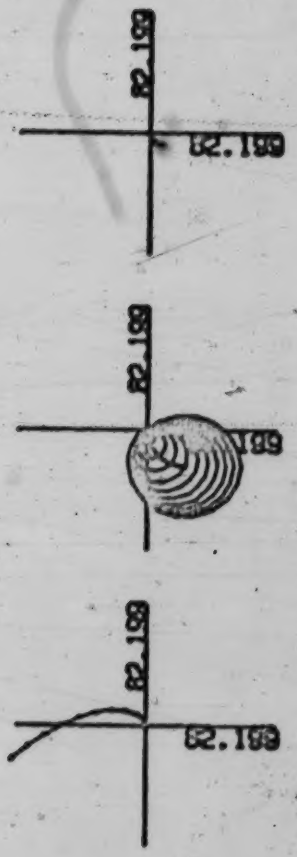

Figure 3.32 Diagonal Elements of $(Q_4{}^1(w))^{-1}$ with their Gershgorin Bands
$|G=5|$ 0.1 to 1.0| $(Q_4{}^1(w)^{-1}|$ $(K_4{}^1)^{-1}(K_3{}^1)^{-1}(K_2{}^1)^{-1}(K_1)^{-1}$ = (3.50)(3.47)(3.45)(3.39)|

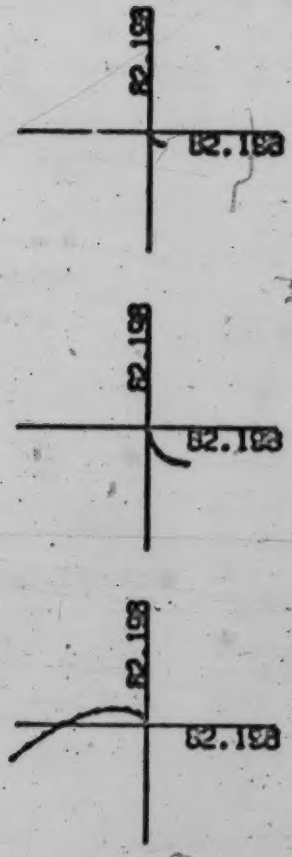

Figure 3.33 Diagonal Elements of $(Q_5^1(w))^{-1}$ with their Gershgorin Bands
|G=5| 0.1 to 1.0| $(Q_5^1(w))^{-1}$| $(K_5^1)^{-1}(K_4^1)^{-1} \dots (K_1)^{-1}$ = (3.53)(3.50) ... (3.39)|

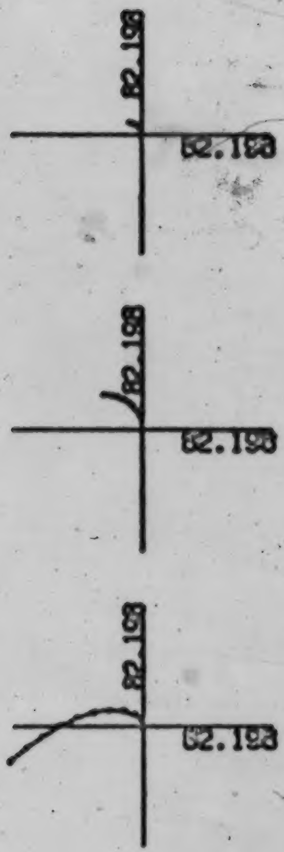

Figure 3.34 Diagonal Elements of $(Q_6^1(w))^{-1}$ with their Gershgorin Bands
$|G=5|$ 0.1 to 1.0$|$ $(Q_6^1(w))^{-1}|$ $((K_6^1)^{-1}(K_5^1)^{-1} \ldots (K_1)^{-1})^{-1}=$ (3.55)$|$

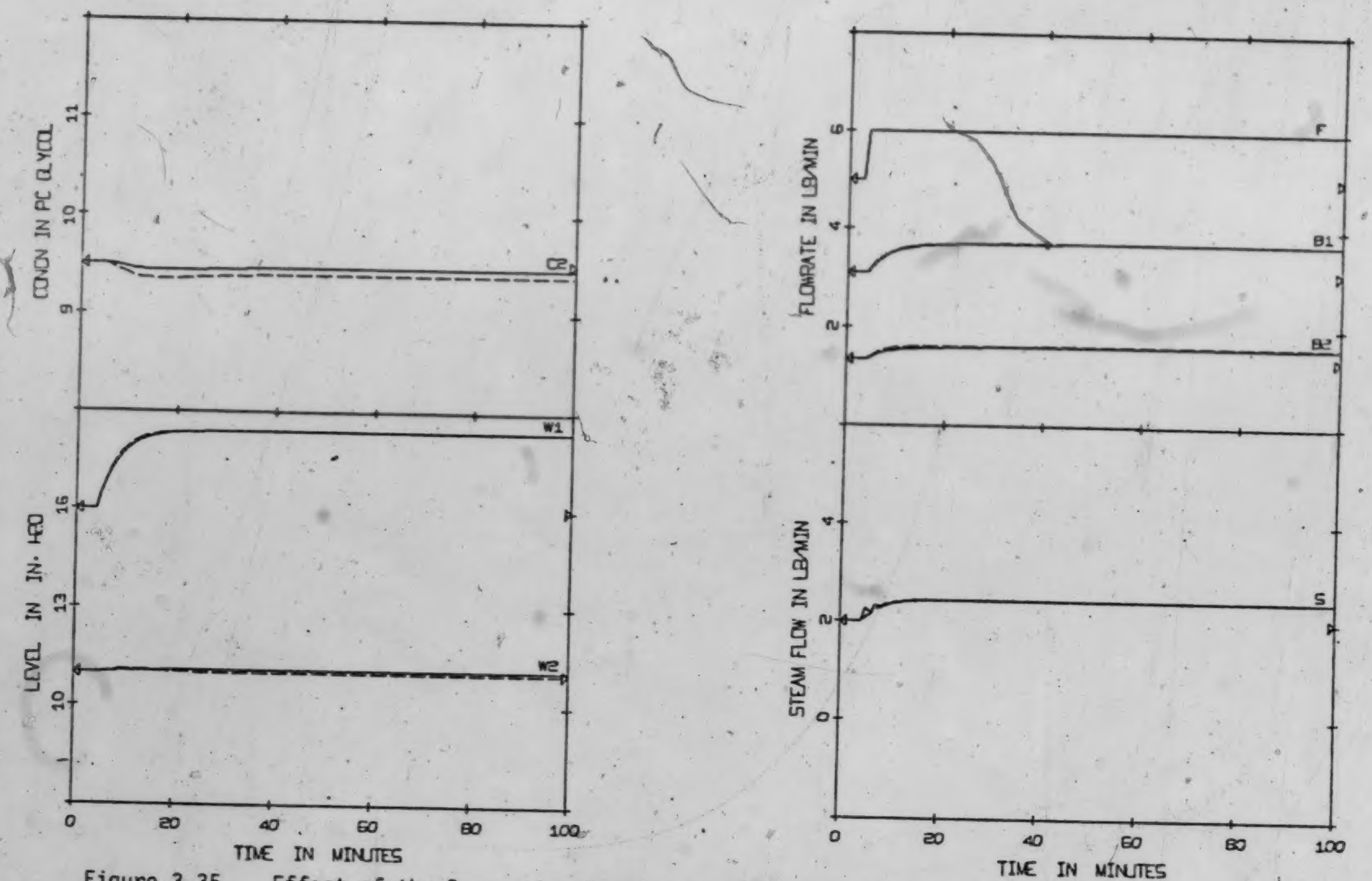

Figure 3.35 Effect of the Proportional and Dynamic Compensator from Frequency Domain Techniques
FD0310: ----, NADY0510: ——
|G=3,5| FD0310| NADY0310| SIM 5| K = Tables B.1,B.3| INA + DNA| + 20% F|

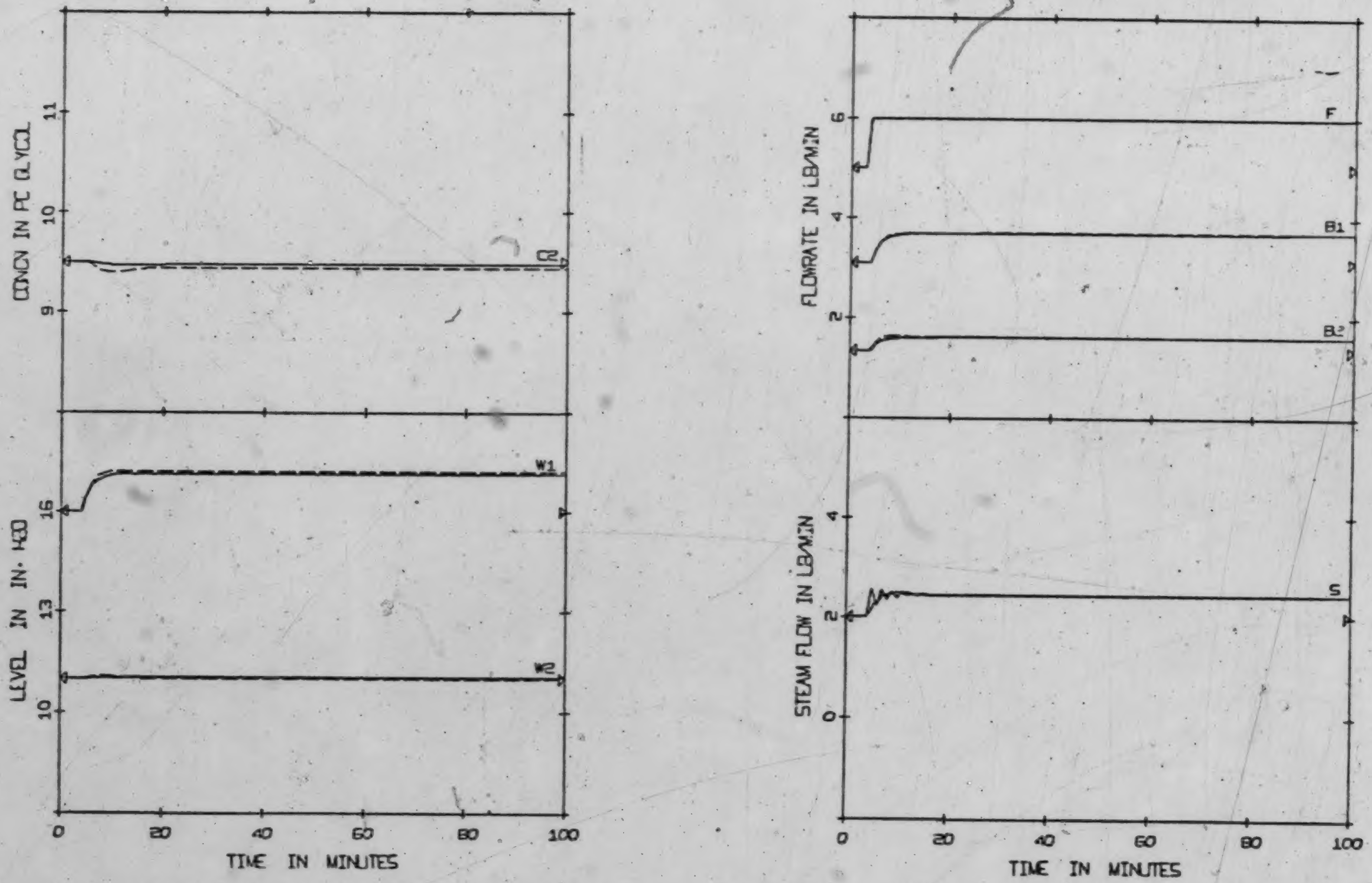

Figure 3.36 Effect of the Proportional and Dynamic Compensator from Frequency Domain Techniques
FD0320: ----, NADY0320: ——
|G=3,5| FD0320| NADY0320| SIM 5| K = Tables B.1,B.3| INA + DNA| + 20% F|

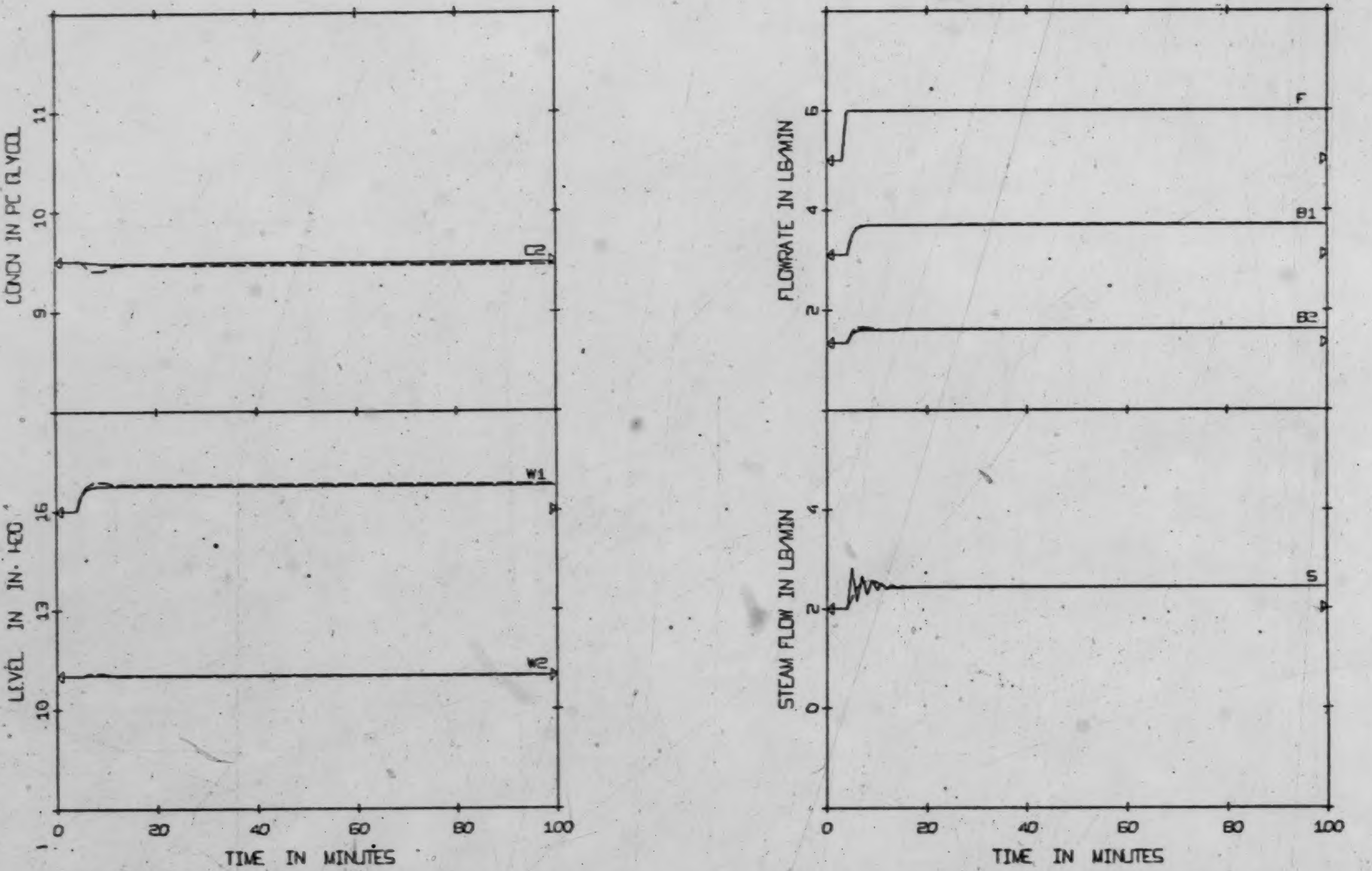

Figure 3.37 Effect of the Proportional and Dynamic Compensator from Frequency Domain Techniques
FD0330: ----, NADY0330: ——
|G=3,5| FD0330| NADY0330| SIM 5| K = Tables B.1,B.3| INA + DNA| + 20% F|

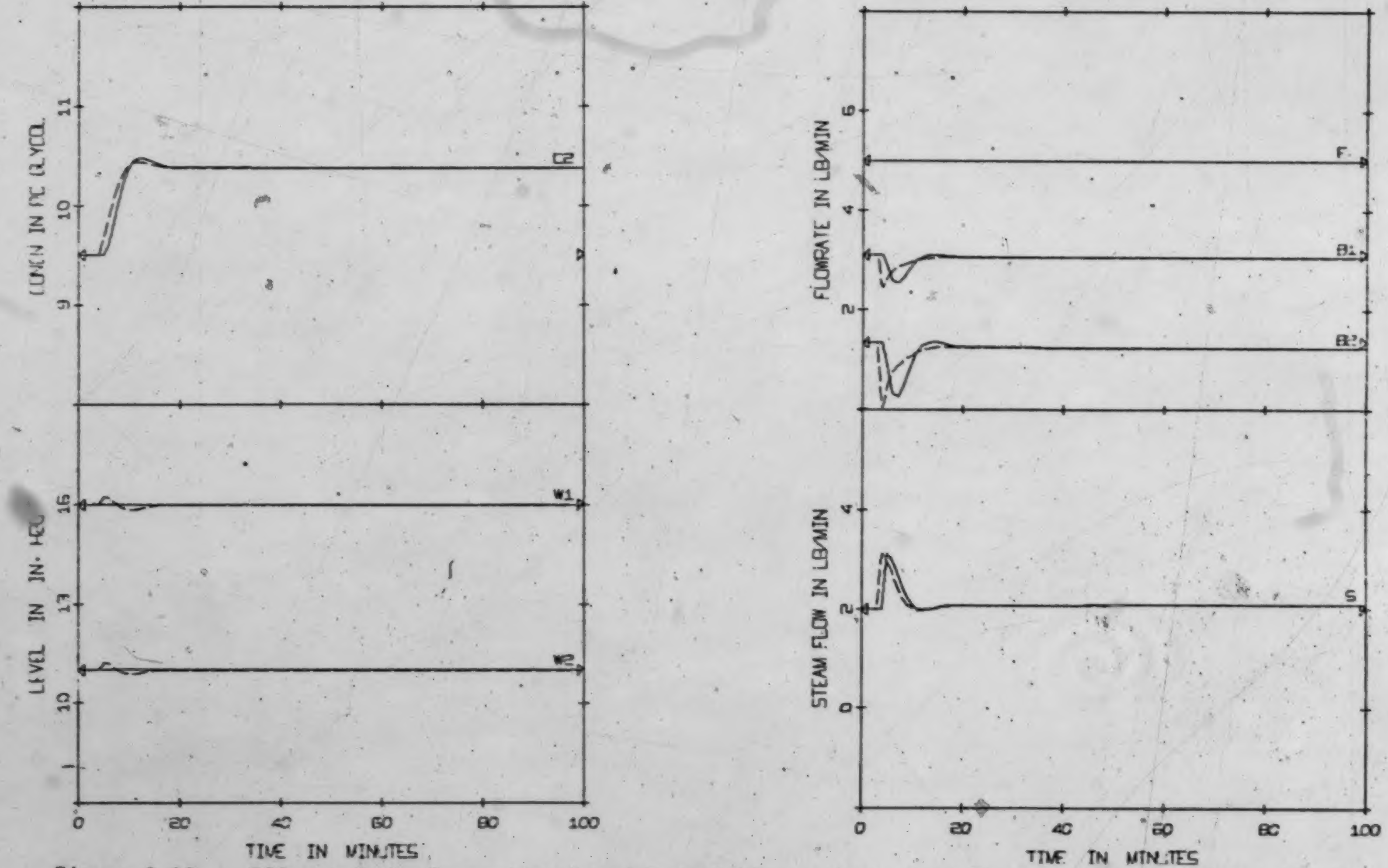

Figure 3.38 Effect of the Proportional and Dynamic Compensator from Frequency Domain Techniques for a Step Change in Setpoint of C_2
FD0320: ----, NADY0520: ——
|G=3,5| FD0320| NADY0320| SIM 5| K = Tables B.1,B.3| INA + DNA| + 10% C_2|

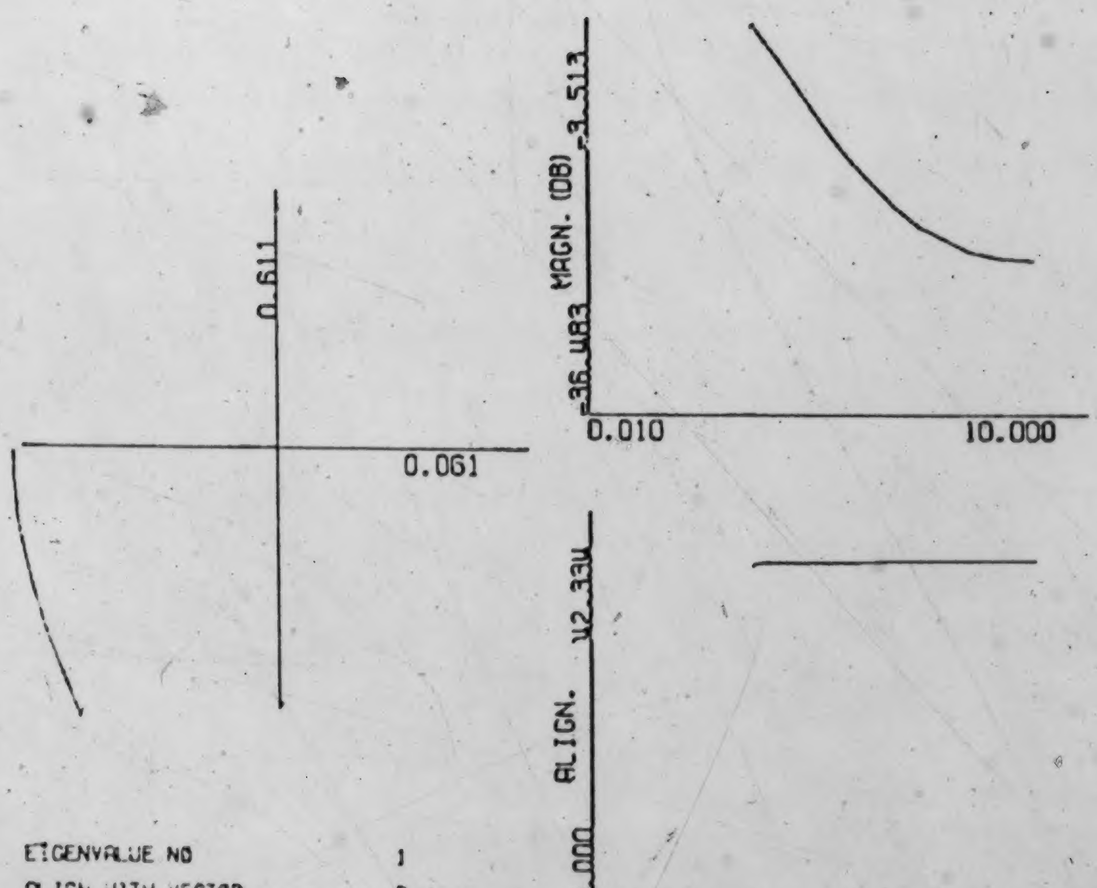

Figure 4.1 Characteristic Locus No. 1 of G(w)
|G=3| 0.1 to 10.0 |CL| G(w) |K=I|
a) Characteristic locus
b) Magnitude of characteristic locus
c) Alignment of the corresponding eigenvector

Note: the explanation of the code used is contained in appendix B

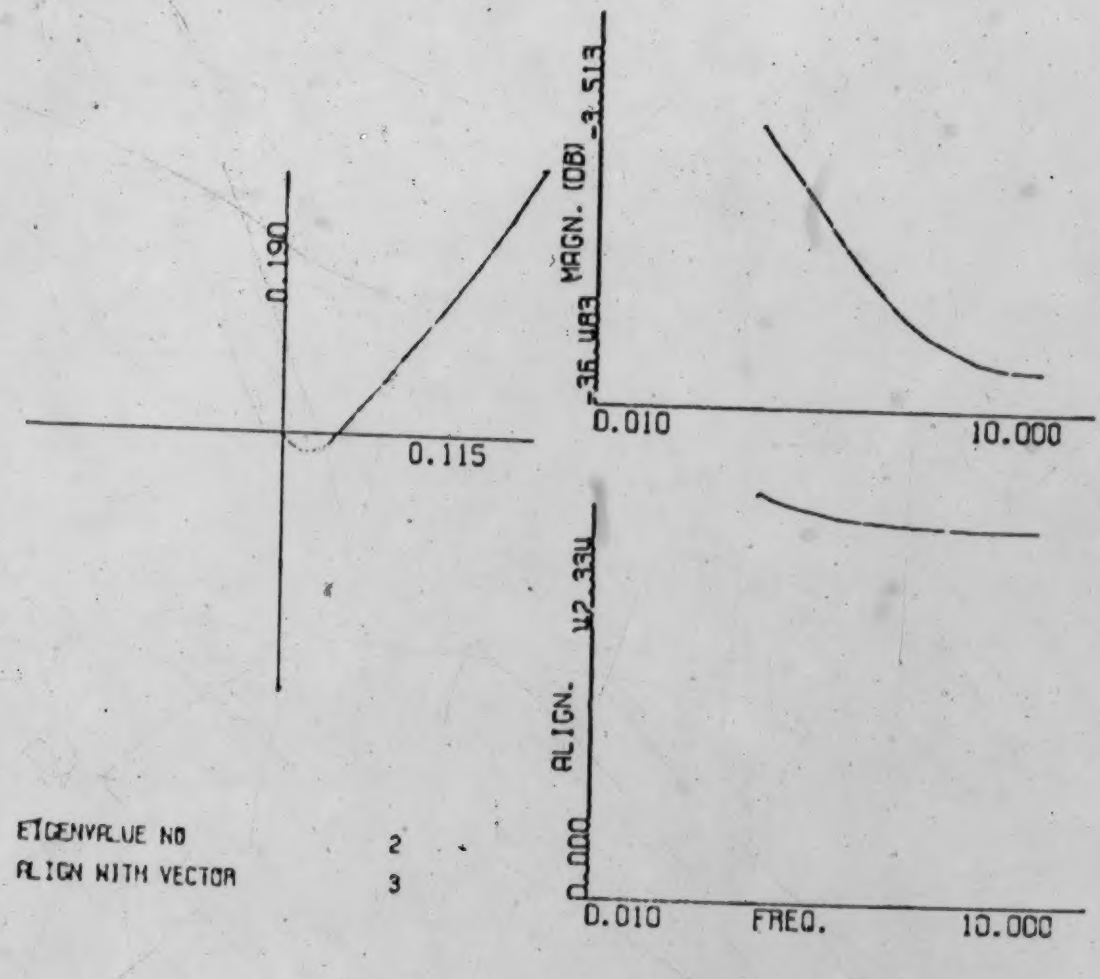

Figure 4.2 Characteristic Locus No. 2 of G(w)
|G=3| 0.1 to 10.0 |CL| G(w) |K=I|
a) Characteristic locus
b) Magnitude of characteristic locus
c) Alignment of the corresponding eigenvector

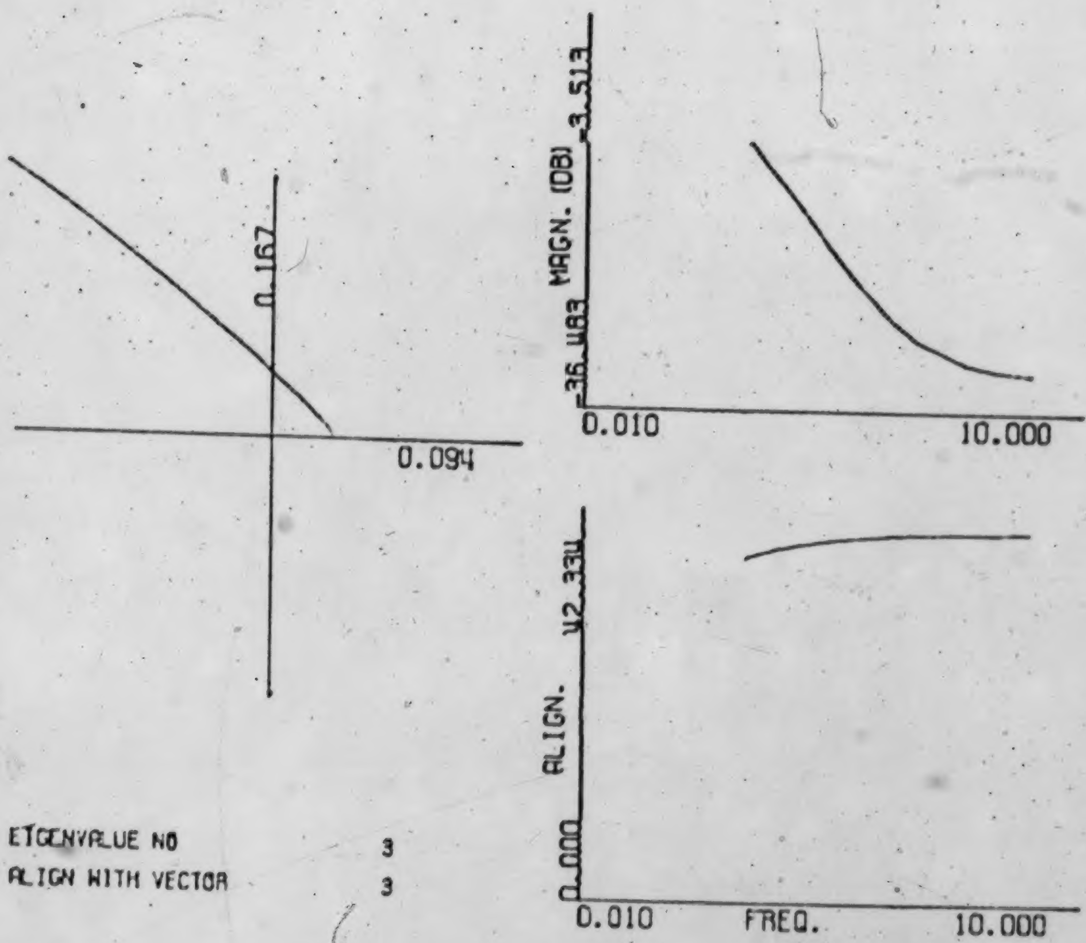

Figure 4.3 Characteristic Locus No. 3 of G(w)
|G=3| 0.1 to 10.0 |CL| G(w) |K=I|
a) Characteristic locus
b) Magnitude of characteristic locus
c) Alignment of the corresponding eigenvector

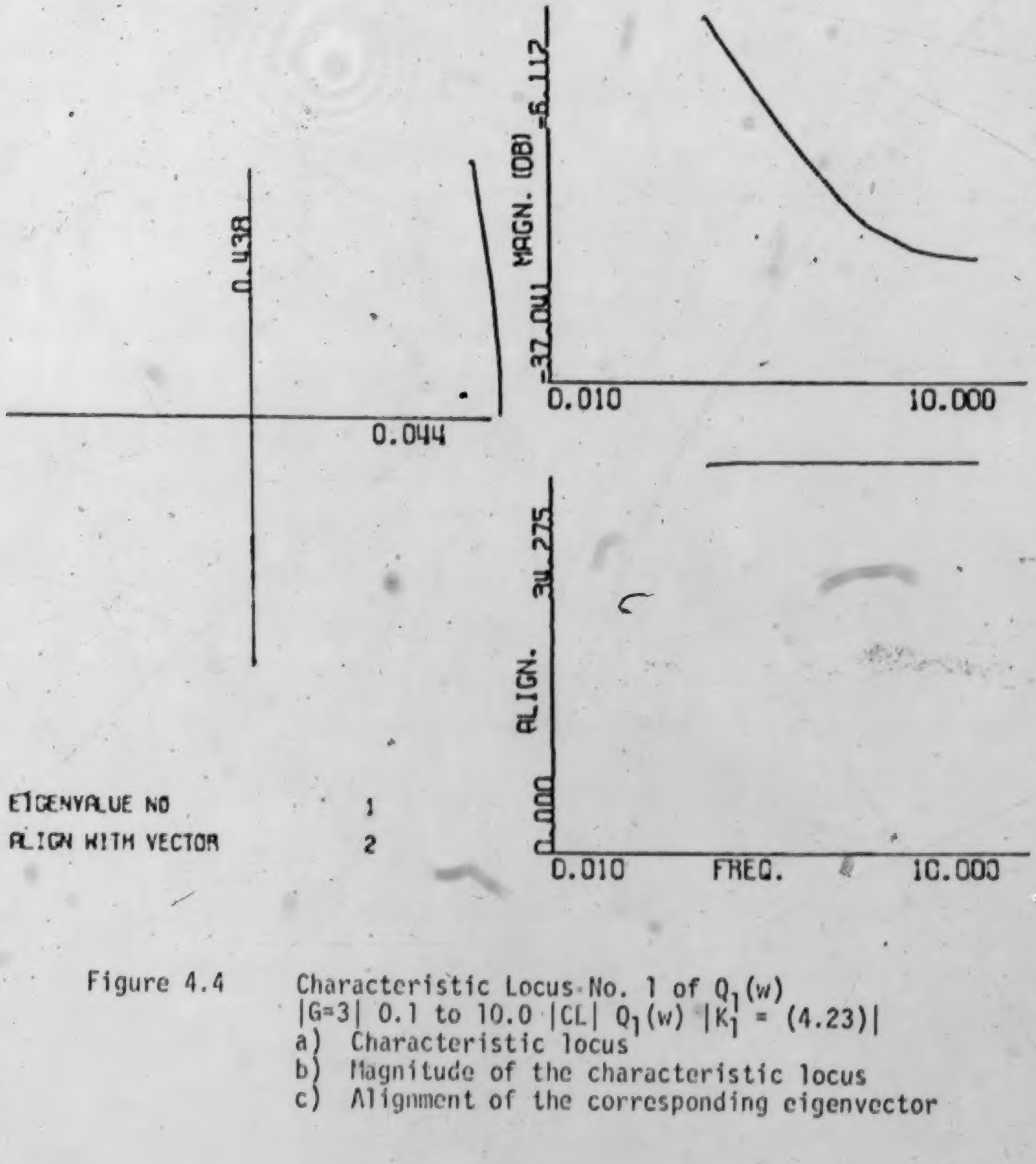

Figure 4.4 Characteristic Locus No. 1 of $Q_1(w)$
$|G=3|$ 0.1 to 10.0 $|CL|$ $Q_1(w)$ $|K_1$ = (4.23)$|$
a) Characteristic locus
b) Magnitude of the characteristic locus
c) Alignment of the corresponding eigenvector

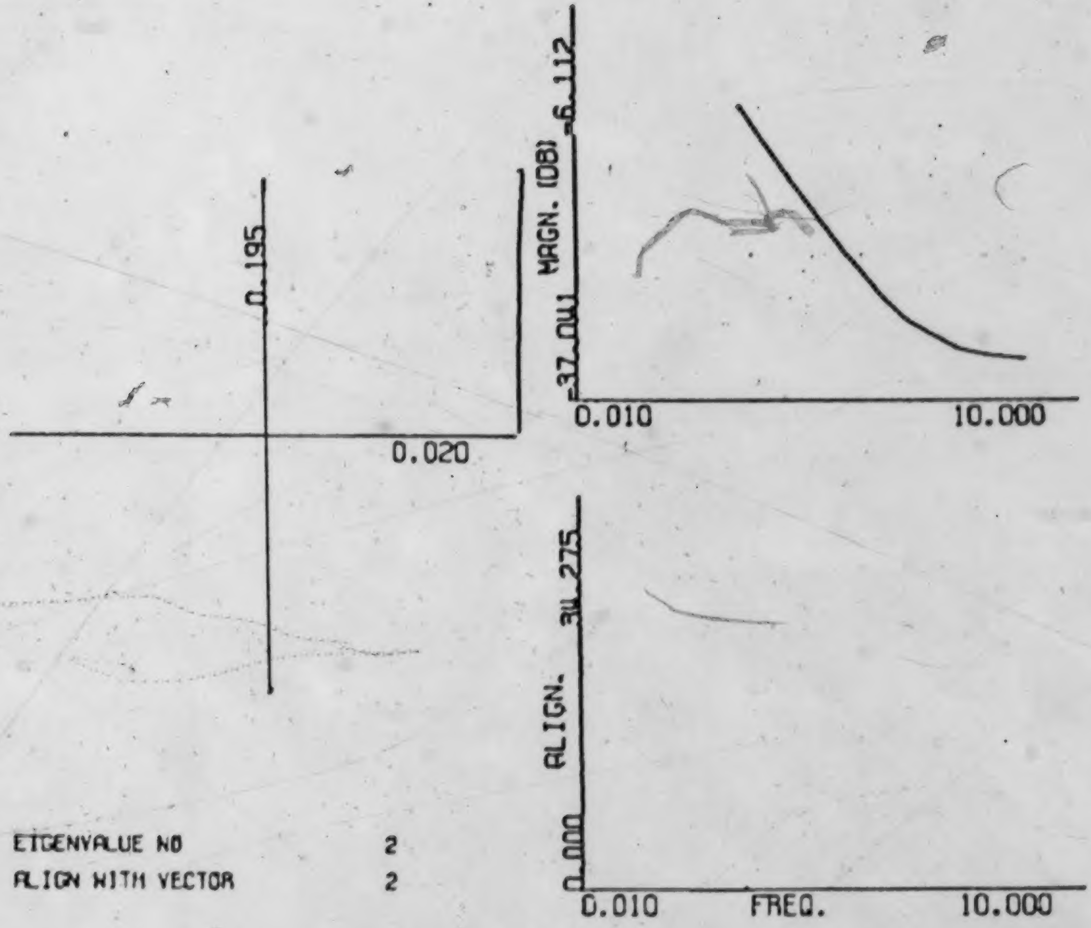

Figure 4.5 Characteristic Locus No. 2 of $Q_1(w)$
|G=3| 0.1 to 10.0 |CL| $Q_1(w)$ K_1 = |(4.23)|
a) Characteristic locus
b) Magnitude of the characteristic locus
c) Alignment of the corresponding eigenvector

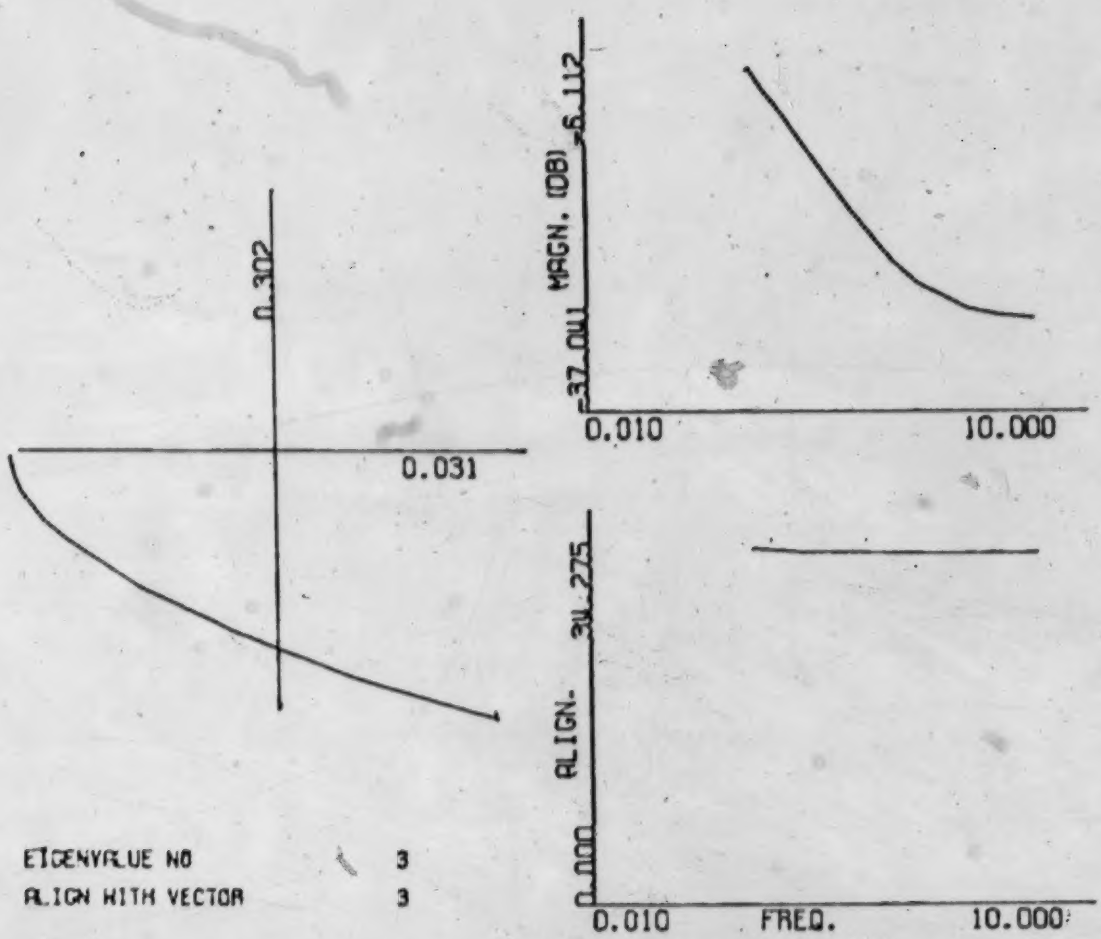

Figure 4.6 Characteristic Locus No. 3 of $Q_1(w)$
$|G=3|$ 0.1 to 10.0 $|CL|$ $Q_1(w)$ $|K_1| = (4.23)|$
a) Characteristic locus
b) Magnitude of the characteristic locus
c) Alignment of the corresponding eigenvector

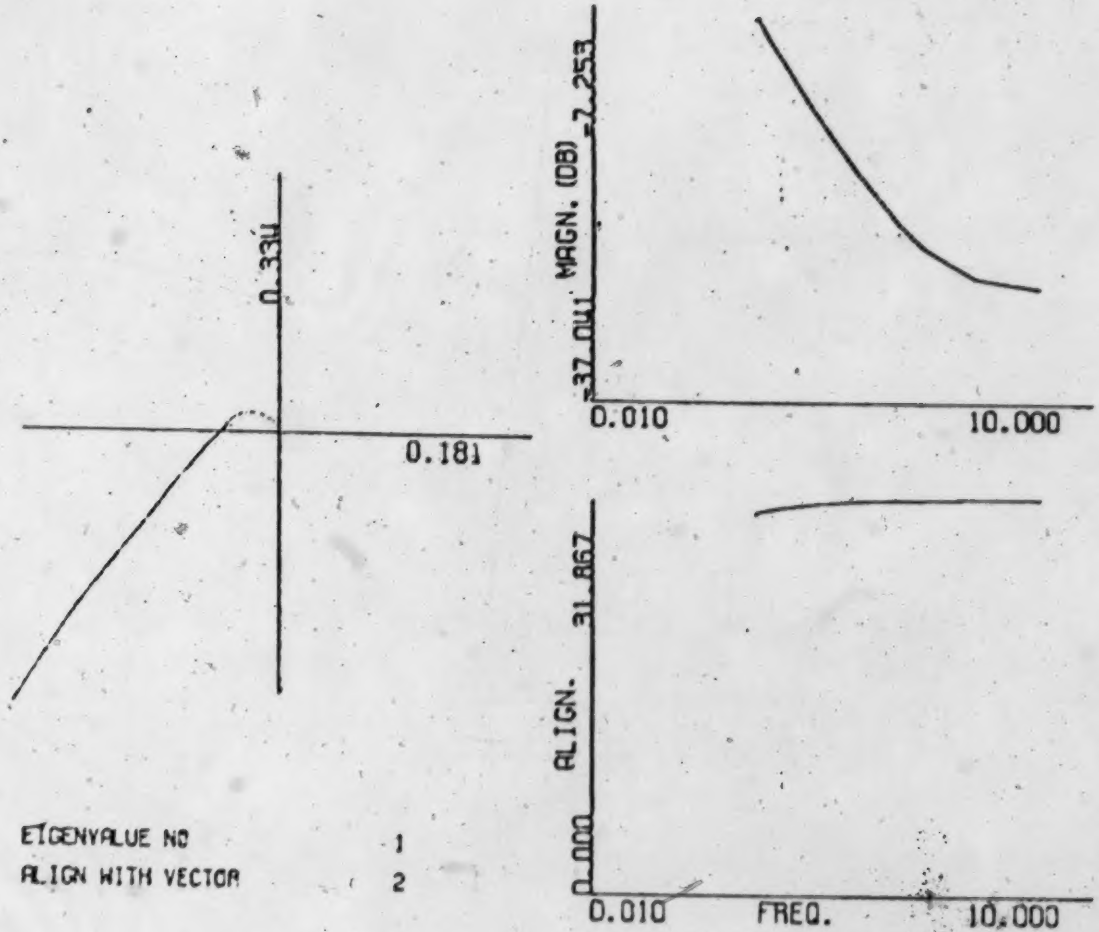

Figure 4.7 Characteristic Locus No. 1 of $Q_2(w)$
|G=3| 0.1 to 10.0 |CL| $Q_2(w)$ $|K_fK_2 = (4.25)(4.23)|$
a) Characteristic locus
b) Magnitude of the characteristic locus
c) Alignment of the corresponding eigenvector

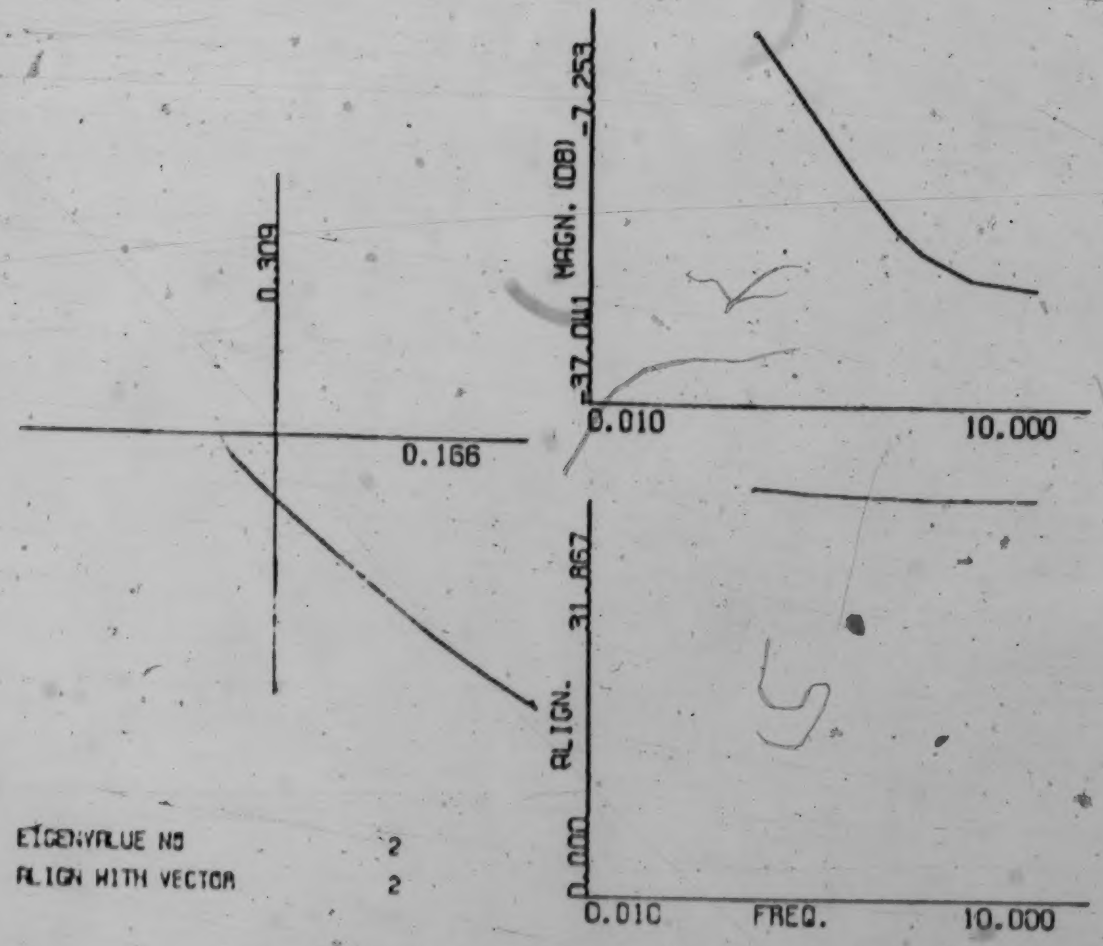

Figure 4.8. Characteristic Locus No. 2 of $Q_2(w)$
$|G=3|$ 0.1 to 10.0 - $|CL|$. $Q_2(w)$ $|K_1K_2 = (4.25)(4.23)|$
a) Characteristic locus
b) Magnitude of the characteristic locus
c) Alignment of the corresponding eigenvector

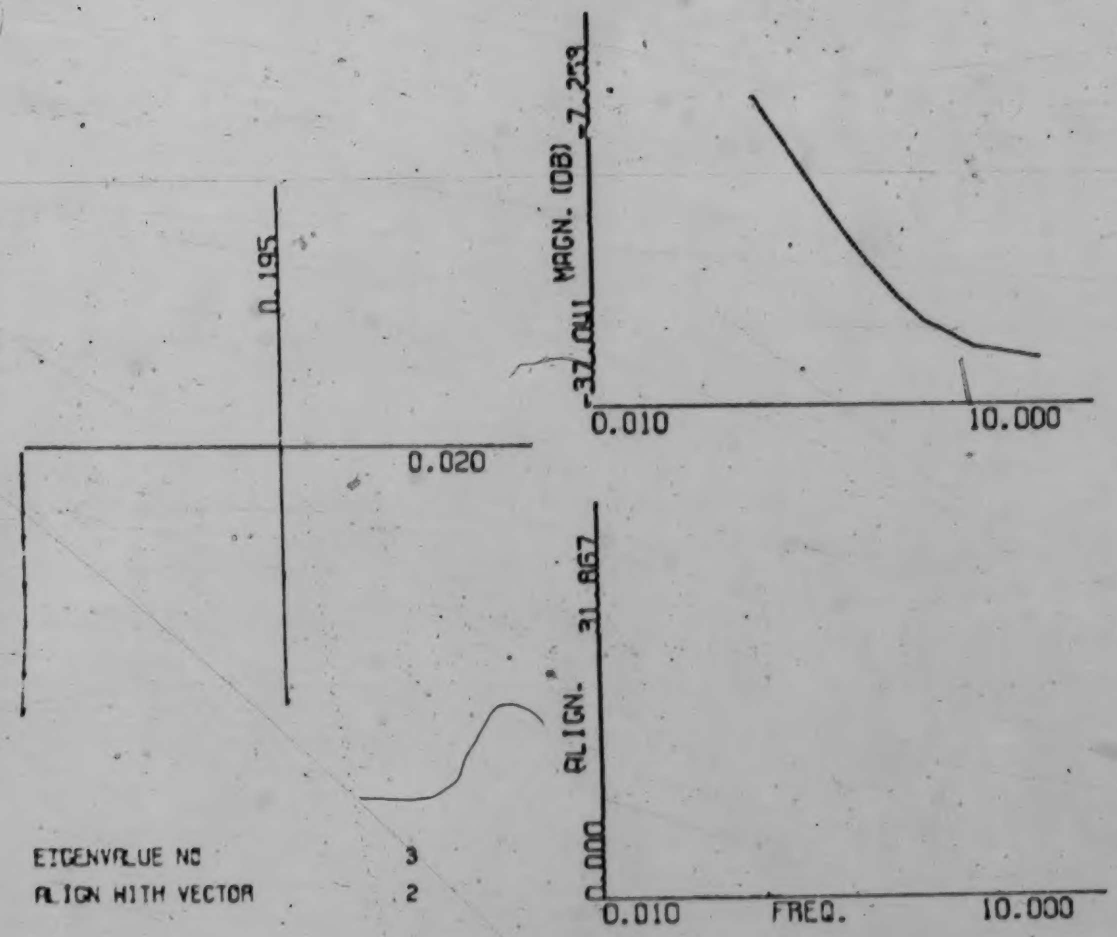

Figure 4.9 Characteristic Locus No. 3 of $Q_2(w)$
|G=3| 0.1 to 10.0 |CL| $Q_2(w)$ |K|K_2 = (4.25)(4.23)|
a) Characteristic locus
b) Magnitude of the characteristic locus
c) Alignment of the corresponding eigenvector

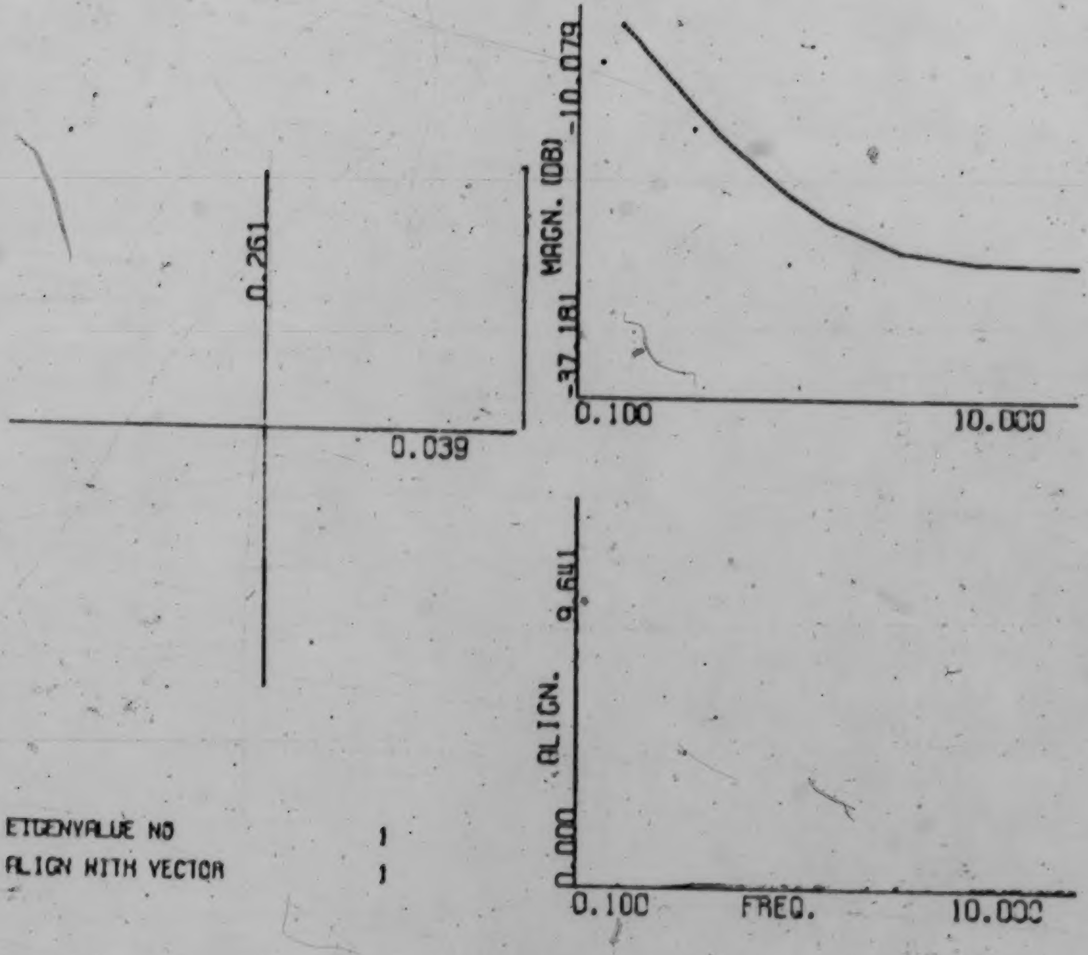

Figure 4.10 Characteristic Locus No. 1 of $Q_1^1(w)$
$|G=3|$ 0.1 to 10.0 $|CL|$ $Q_1^1(w)$ $|K_1^1 = (4.28)|$
a) Characteristic locus
b) Magnitude of the characteristic locus
c) Alignment of the corresponding eigenvector

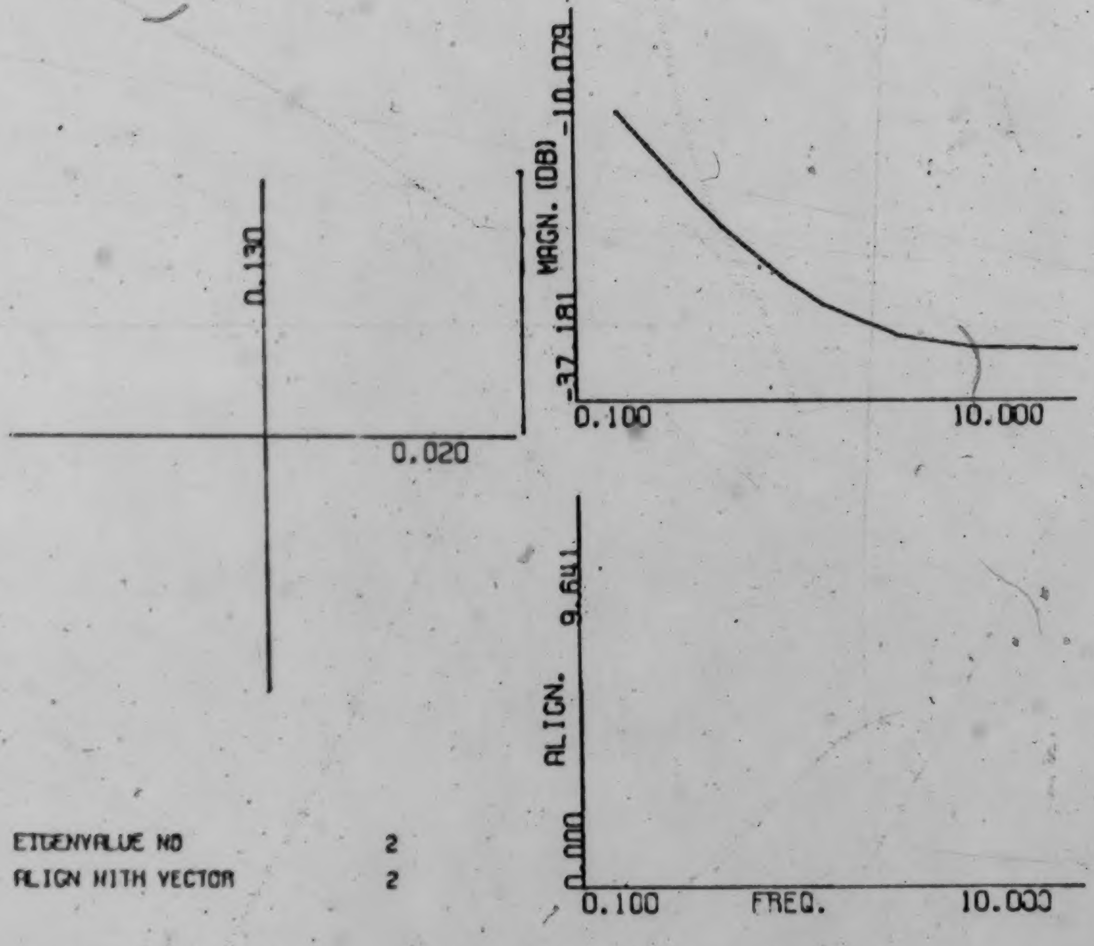

Figure 4.11 Characteristic Locus No. 2 of $Q_1^{1}(w)$
$|G=3|$ 0.1 to 10.0 $|CL|$ $Q_1^{1}(w)$ $|k_1^{1} = (4.28)|$
a) Characteristic locus
b) Magnitude of the characteristic locus
c) Alignment of the corresponding vector

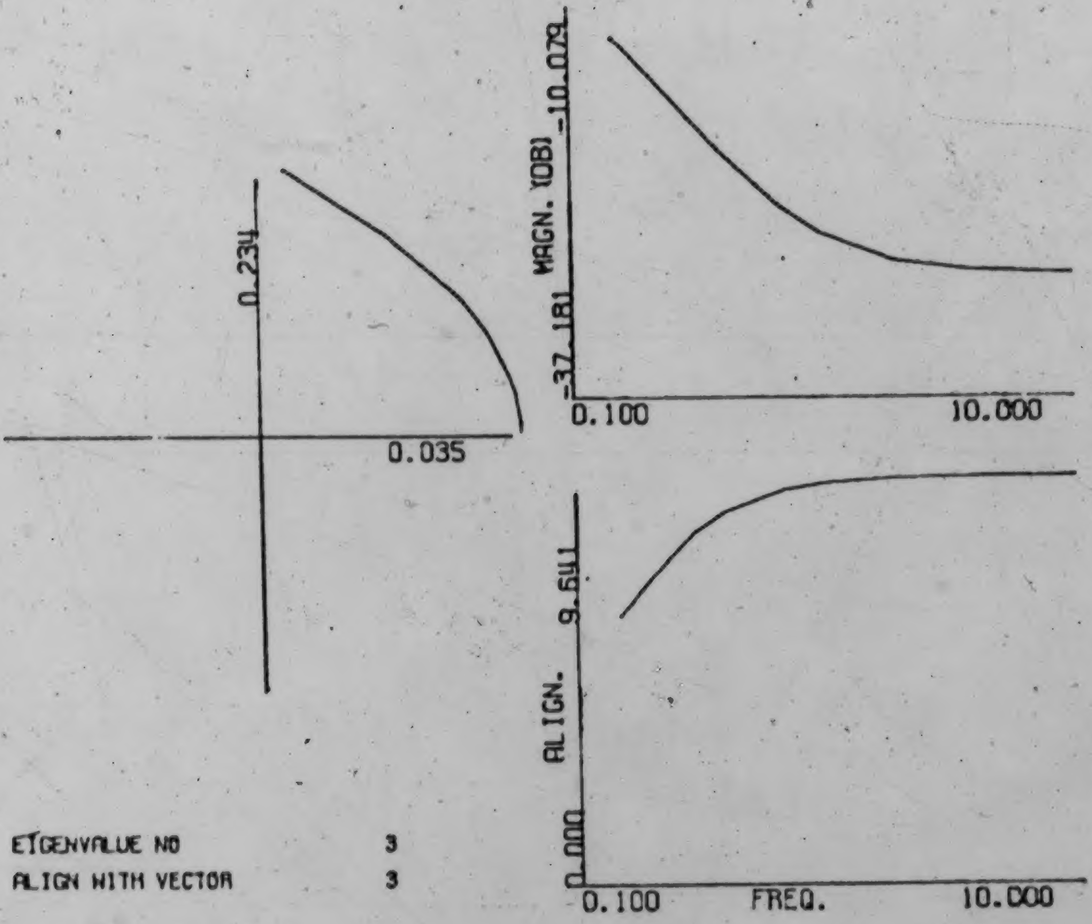

Figure 4.12 Characteristic Locus No. 3 of $Q_1^{1}(w)$
$|G=3|$ 0.1 to 10.0 $|CL|\ Q_1^{1}(w)\ |K_1^{1} = (4.28)|$
a) Characteristic locus
b) Magnitude of the characteristic locus
c) Alignment of the corresponding eigenvector

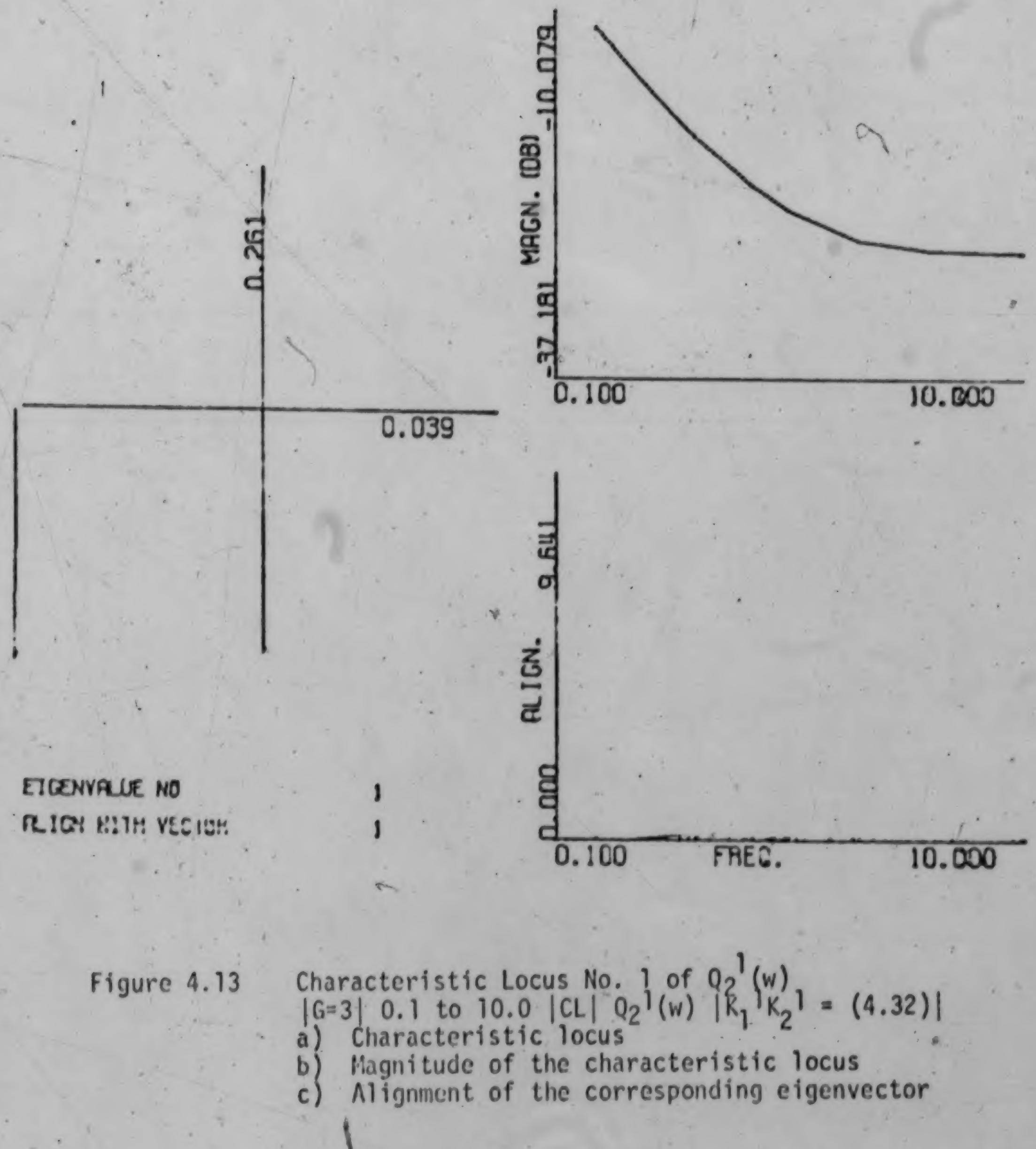

Figure 4.13 Characteristic Locus No. 1 of $Q_2^1(w)$
$|G=3|$ 0.1 to 10.0 $|CL|$ $Q_2^1(w)$ $|K_1^1 K_2^1 = (4.32)|$
a) Characteristic locus
b) Magnitude of the characteristic locus
c) Alignment of the corresponding eigenvector

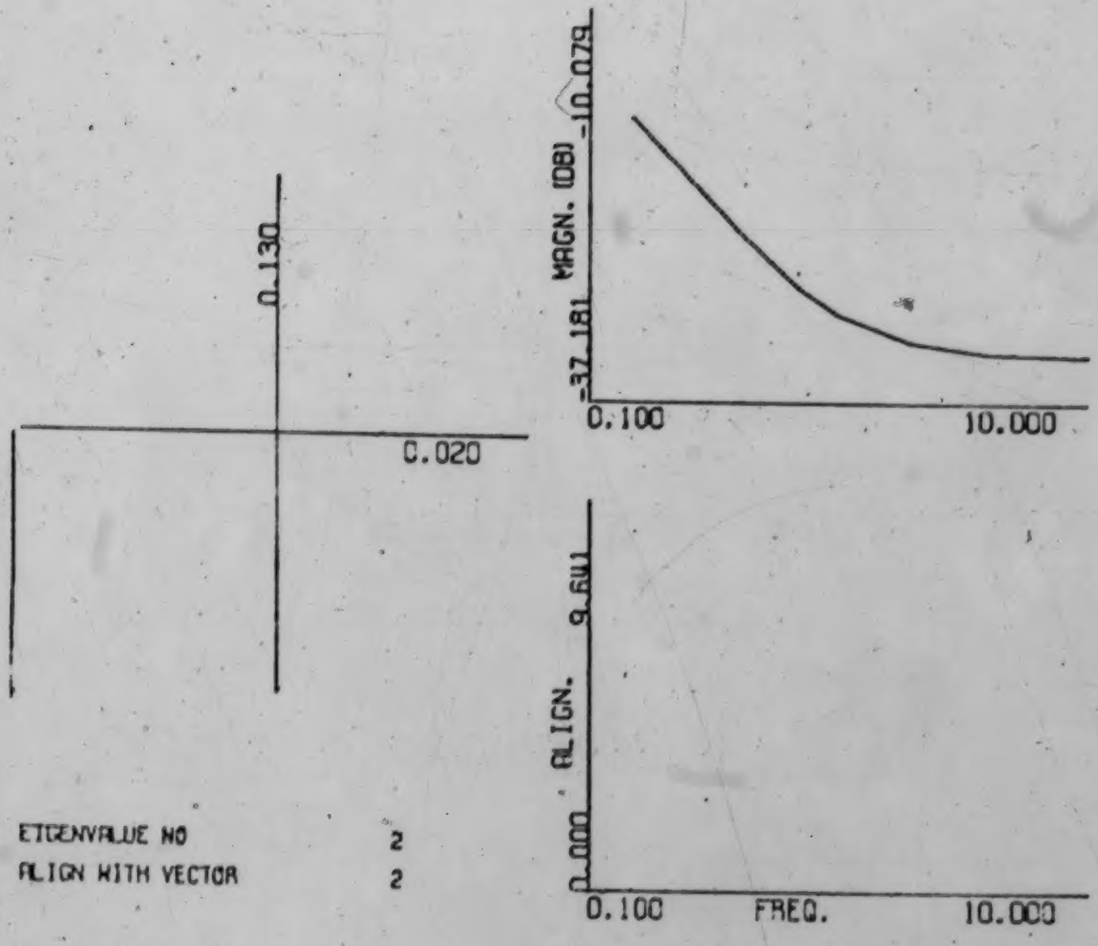

Figure 4.14 Characteristic Locus No. 2 of $Q_2^1(w)$
$|G=3|$ 0.1 to 10.0 $|CL|$ $Q_2^1(w)$ $|K_1^1 K_2^1 = (4.32)|$
a) Characteristic locus
b) Magnitude of the characteristic locus
c) Alignment of the corresponding eigenvector

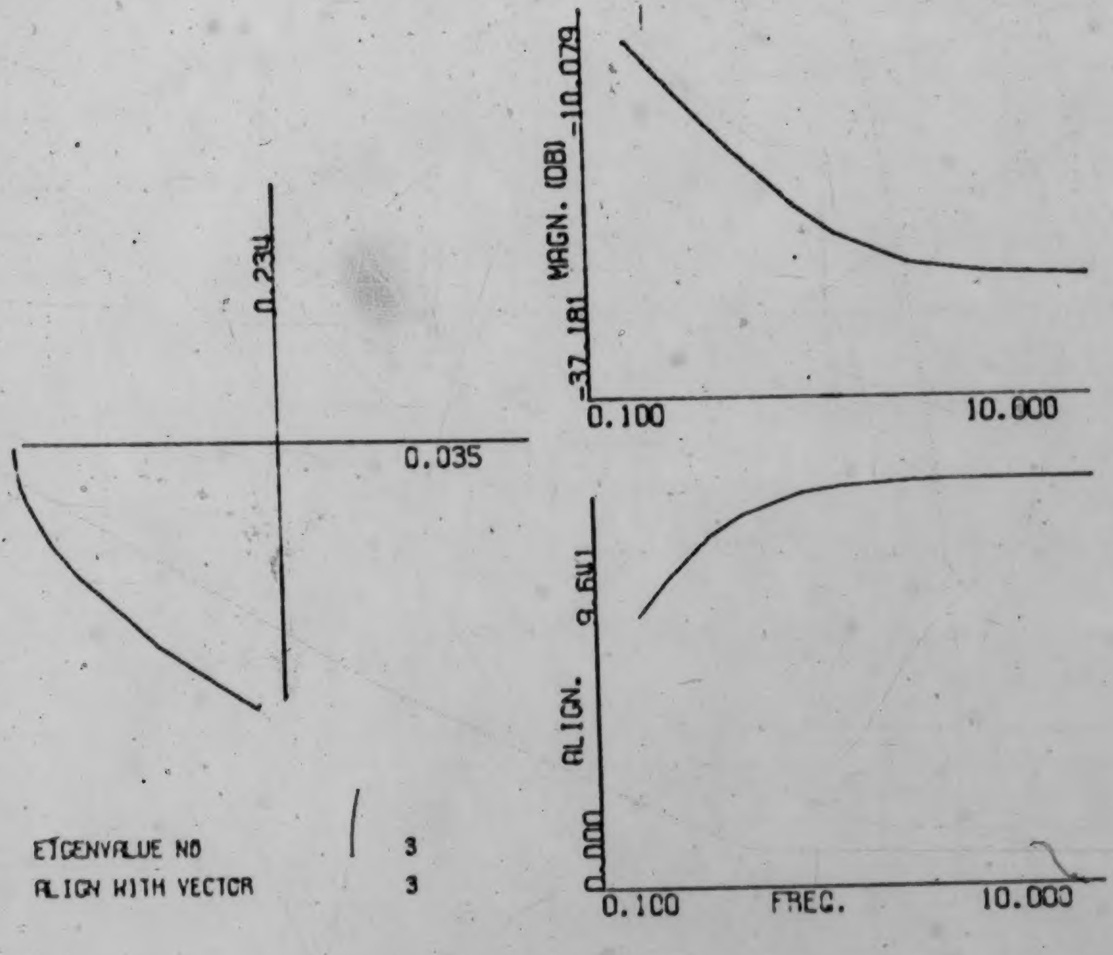

Figure 4.15 Characteristic Locus No. 3 of $Q_2^{1}(w)$
$|G=3|$ 0.1 to 10.0 $|CL|$ $Q_2^{1}(w)$ $|K_1^{1} K_2^{1} = (4.32)|$
a) Characteristic locus
b) Magnitude of the characteristic locus
c) Alignment of the corresponding eigenvector

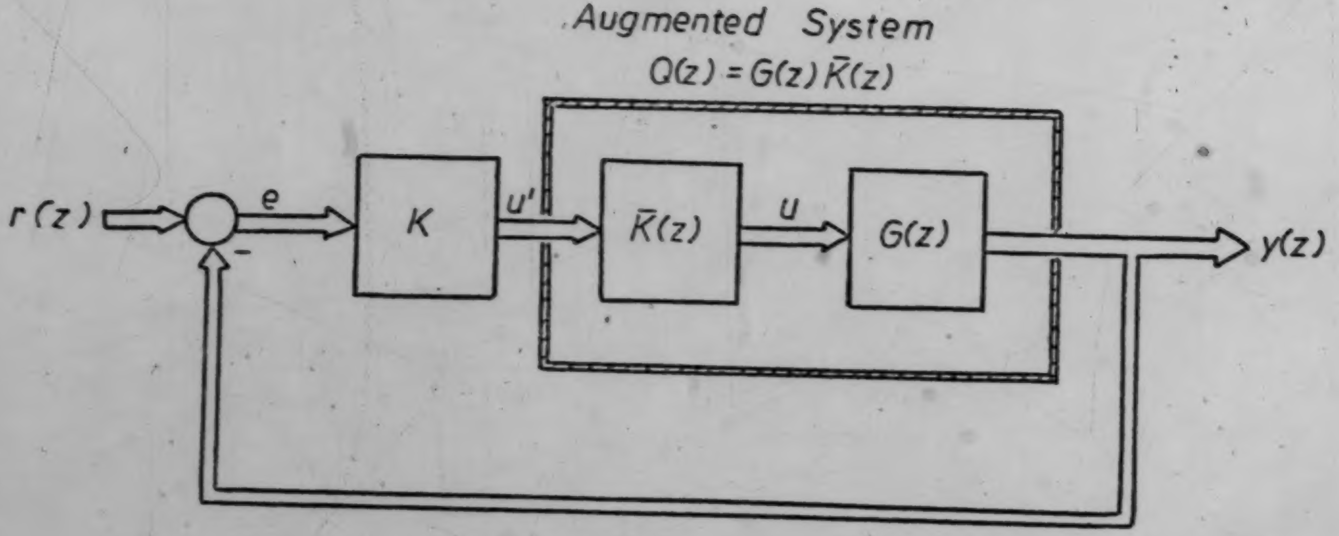
Augmented System
$Q(z) = G(z)\bar{K}(z)$
$r(z)$
e
$-$
K
u'
$\bar{K}(z)$
u
$G(z)$
$y(z)$

Figure 5.1 Multivariable Feedback Control System Expressed in Block Diagram Notation with an Open-Loop Transfer Function Matrix $Q(z) = G(z)\ K(z)$

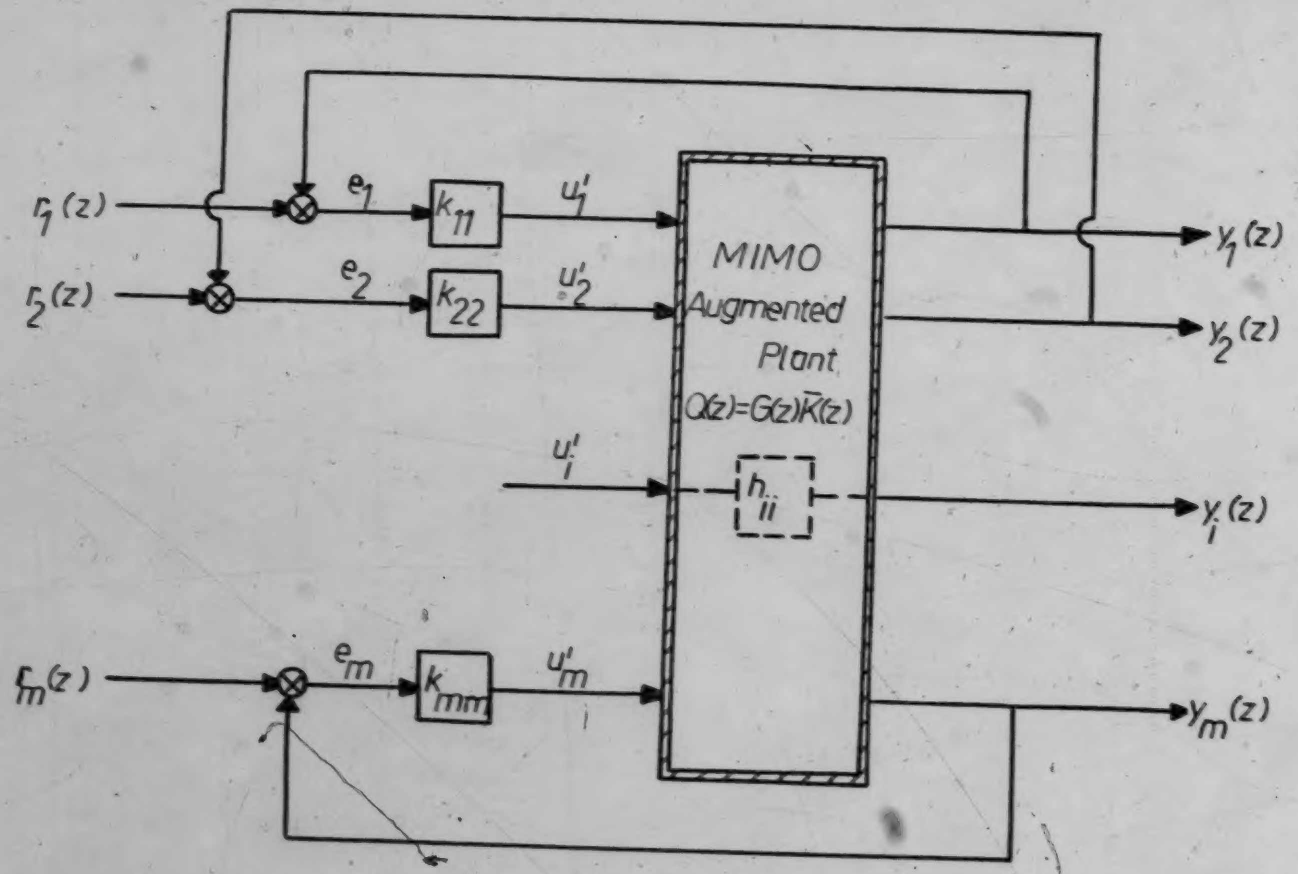
$r_1(z)$
$r_2(z)$
$r_m(z)$
e_1
e_2
e_m
k_{11}
k_{22}
k_{mm}
u_1'
u_2'
u_i'
u_m'
MIMO
Augmented
Plant
$Q(z)=G(z)\bar{K}(z)$
h_{ii}
$y_1(z)$
$y_2(z)$
$y_i(z)$
$y_m(z)$

Figure 5.2 An Expanded Representation of an Augmented Multivariable System $Q(z) = G(z)\ K(z)$. The Open-Loop Transfer Function Between u_i' and $y_i'(z)$ of the Augmented Plant when all the Other (m-1) Feedback Loops are Closed is Defined as $h_i(z)$.

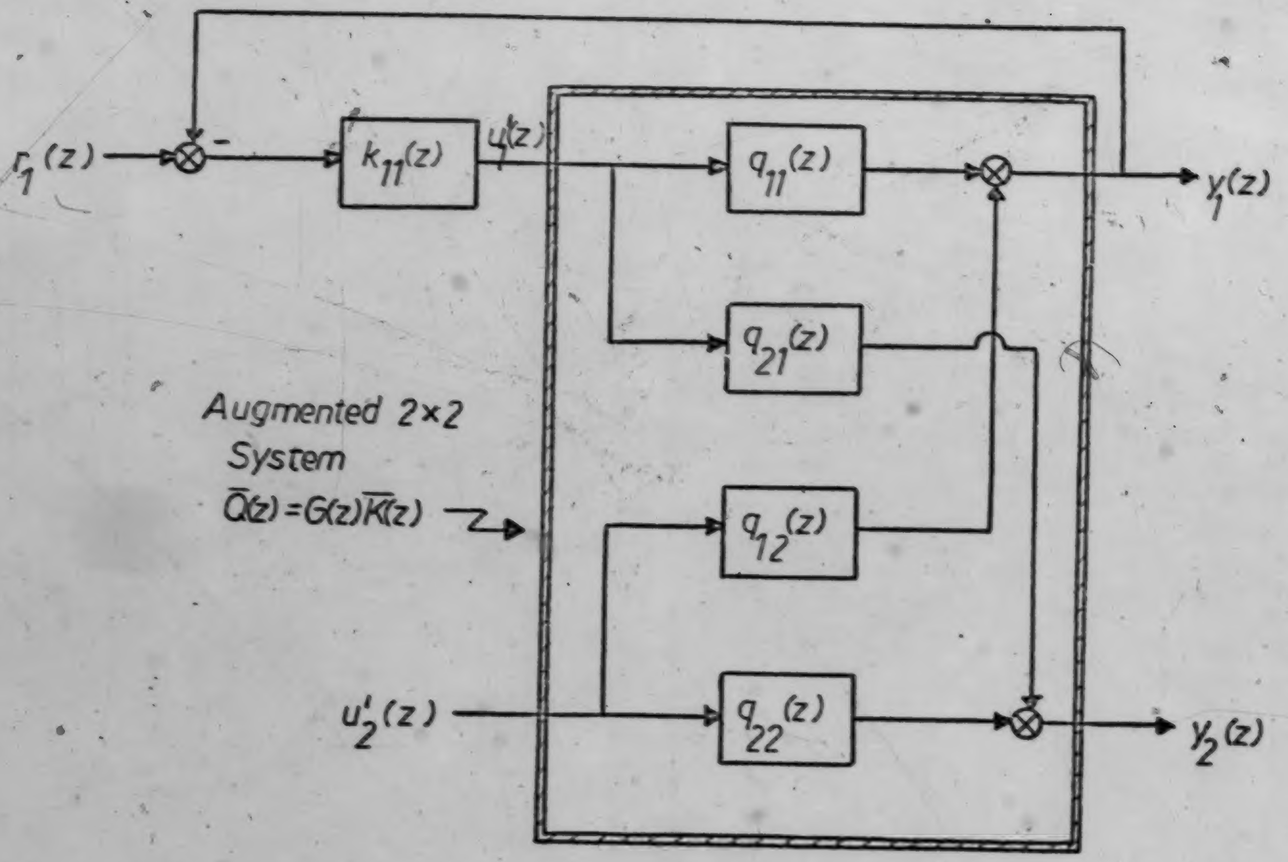
$r_1(z)$
-
$k_{11}(z)$
$u_1(z)$
$q_{11}(z)$
$y_1(z)$
$q_{21}(z)$
Augmented 2×2
System
$\bar{Q}(z) = G(z)\bar{K}(z)$
$q_{12}(z)$
$u'_2(z)$
$q_{22}(z)$
$y_2(z)$

Figure 5.3 Two-Input Two-Output System with One Loop Closed

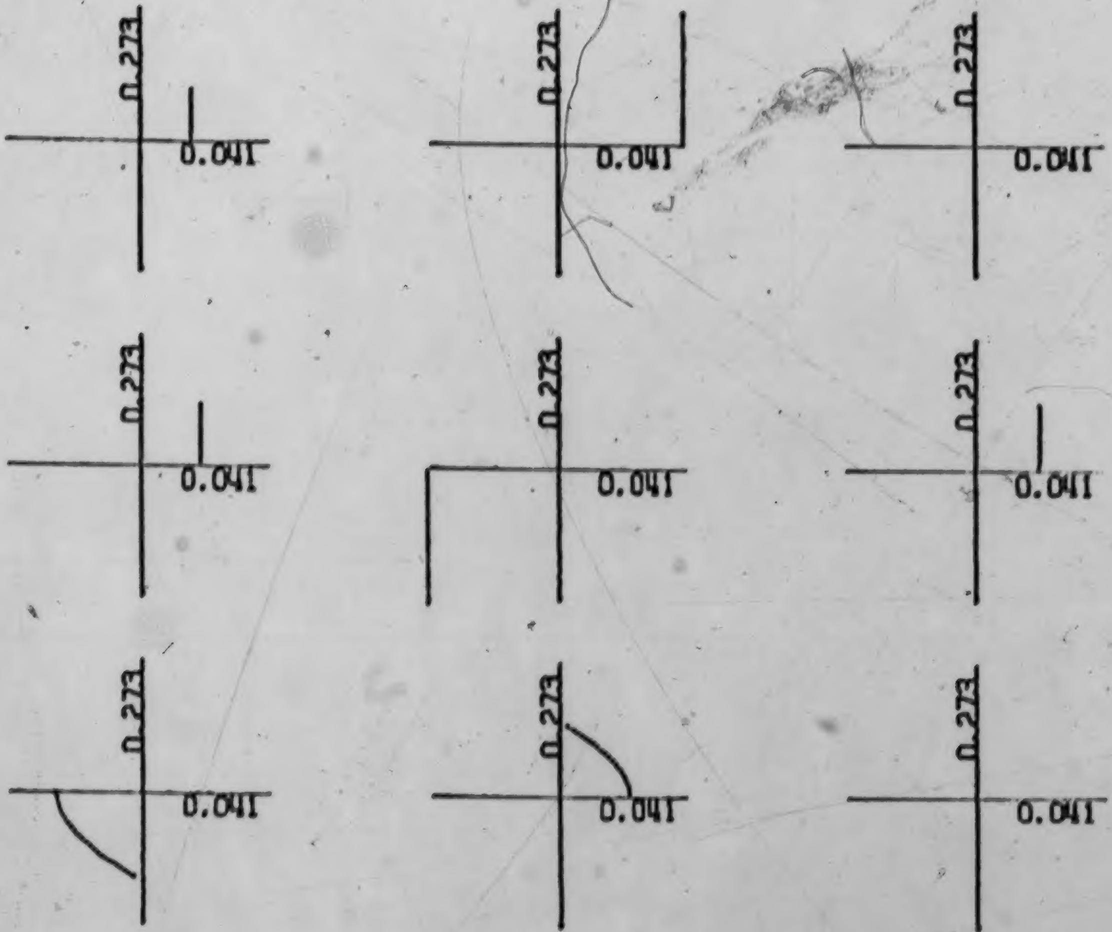

Figure 5.4 Nyquist Array of G(w)
|G=3| 0.15 to 10.0| G(w)| K = I|

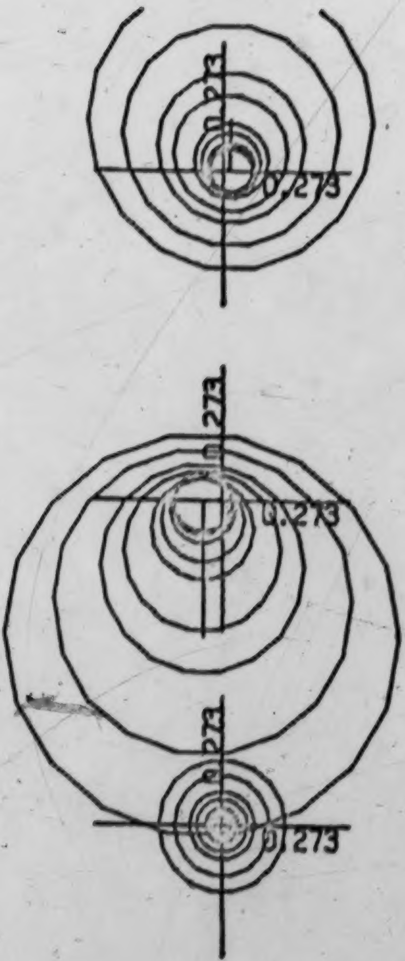

Figure 5.5 Diagonal Elements of G(w) with their Gershgorin Bands |G=3| 0.15 to 10.0| G(w)| K = I|

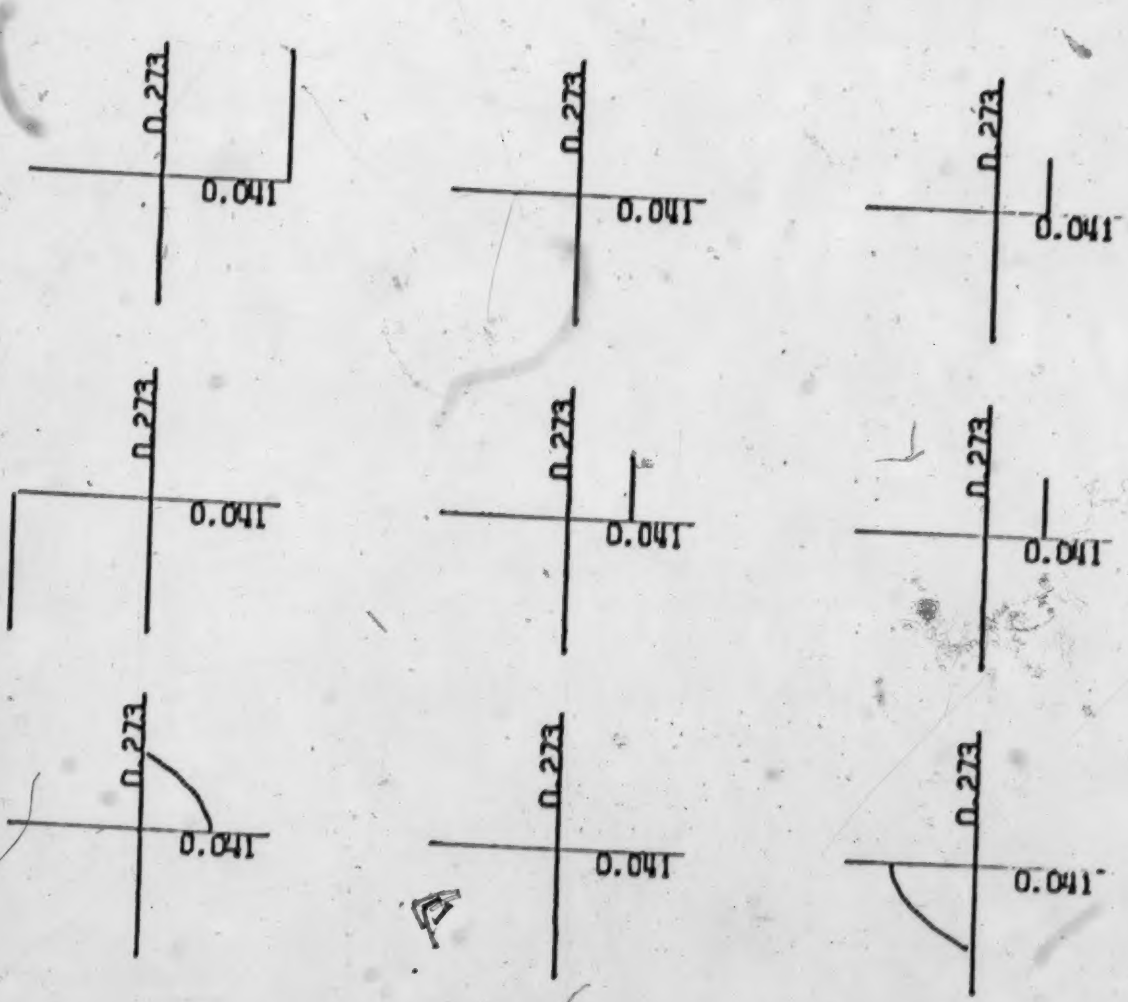

Figure 5.6 Nyquist Array of $Q_1(w)$
|G=3| 0.15 to 10.0| $Q_1(w)$| K_1 = (5.25)|

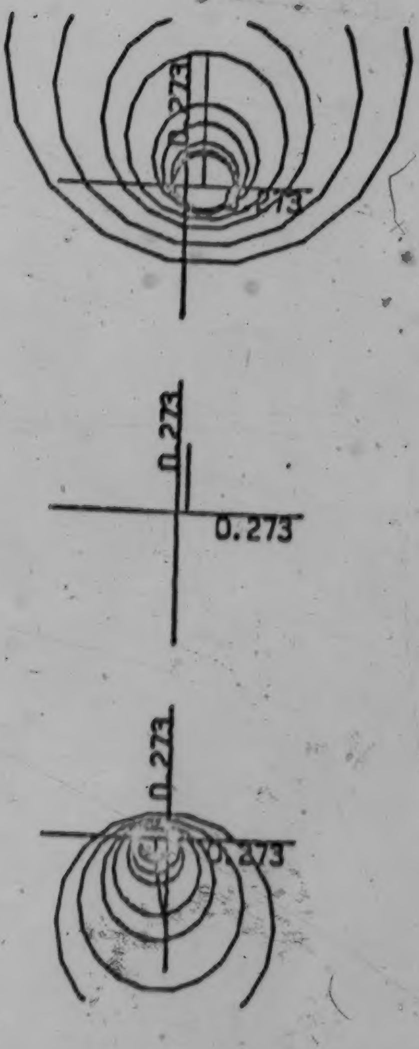

Figure 5.7 Diagonal Elements of $Q_1(w)$ with their Gershgorin Bands
|G=3| 0.15 to 10.0| $Q_1(w)$| K_1 = (5.25)|

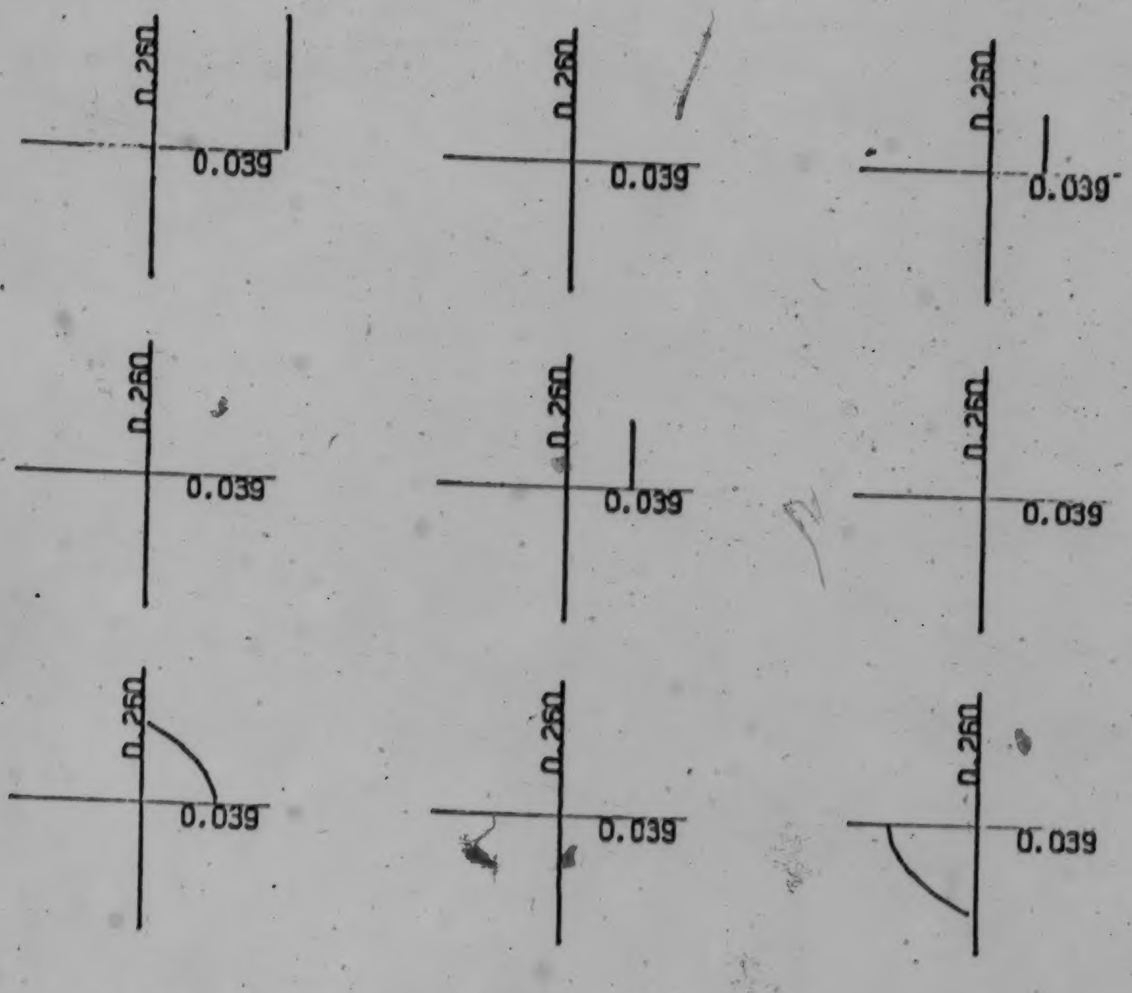

Figure 5.8 Nyquist Array of $Q_2(w)$
|G=3| 0.15 to 10.0| $Q_2(w)$| K_1K_2 = (5.25)(5.26)|

19

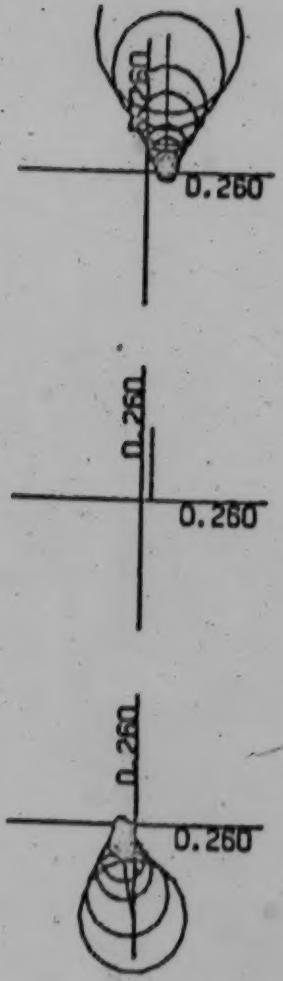

Figure 5.9 Diagonal Elements of $Q_2(w)$ with their Gershgorin Bands
|G=3| 0.15 to 10.0| $Q_2(w)$| K_1K_2 = (5.25)(5.26)(5.28)|

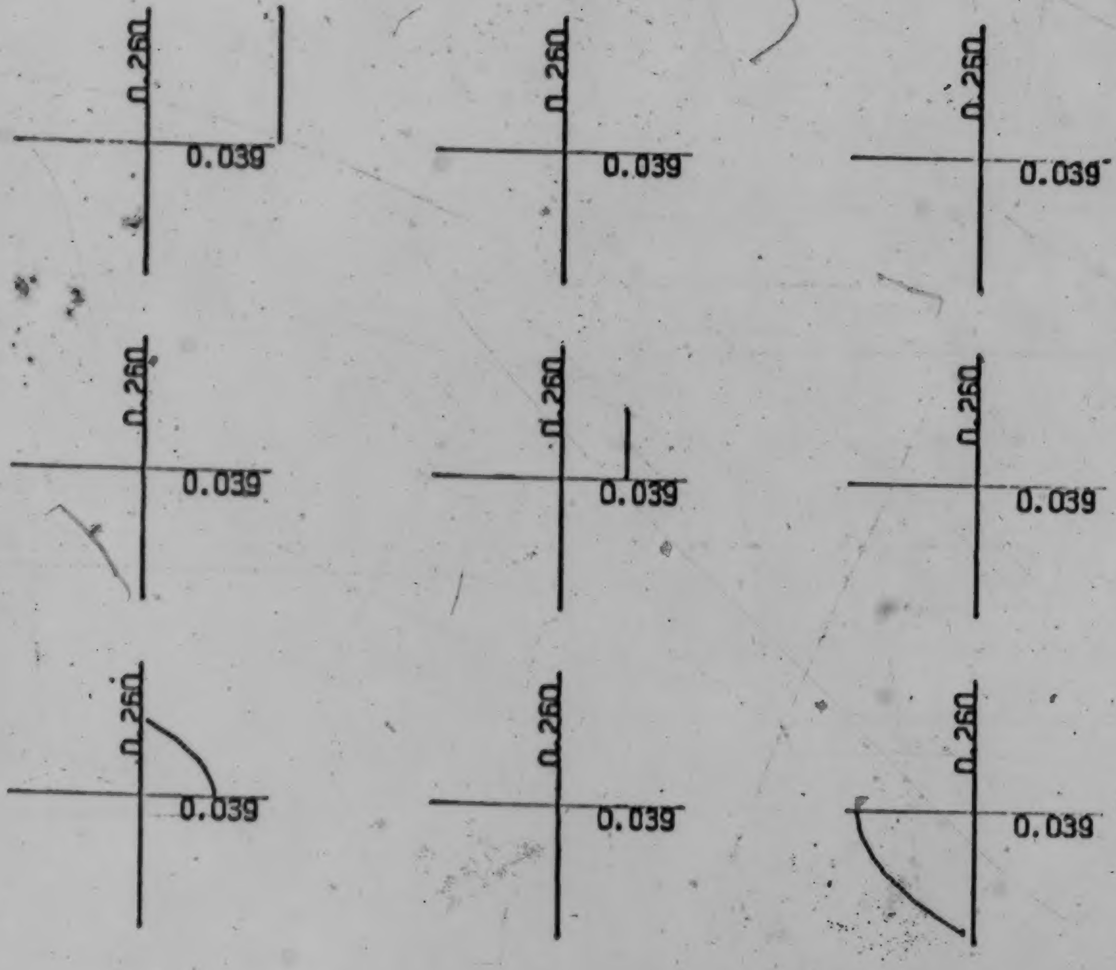

Figure 5.10   Nyquist Array of $Q_3(w)$
|G=3| 0.15 to 10.0| $Q_3(w)$| $K_1K_2K_3$ = (5.25)(5.26)(5.28)|

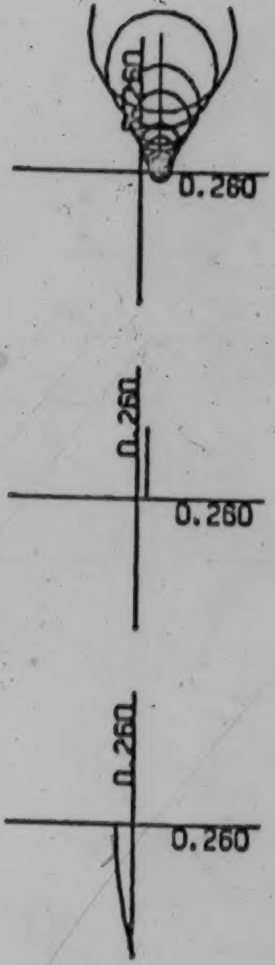

Figure 5.11 Diagonal Elements of $Q_3(w)$ with their Gershgorin Bands
|G=3| 0.15 to 10.0| $Q_3(w)$| $K_1K_2K_3$ = (5.25)(5.26)(5.28)|

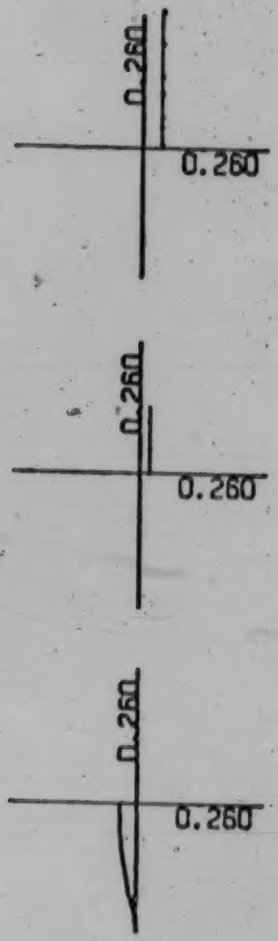

Figure 5.12 Diagonal Elements of $Q_4(w)$ with their Gershgorin Bands $|G=3|$ 0.15 to 10.0$|$ $Q_4(w)|$ $K_1K_2K_3K_4$ = (5.25)(5.26)(5.28) (5.29)$|$

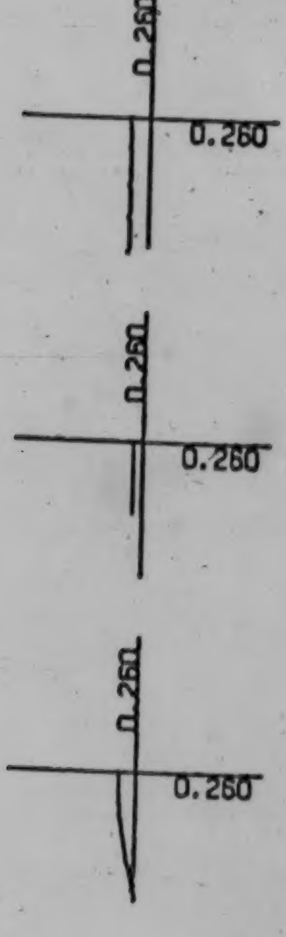

Figure 5.13 Diagonal Elements of $Q_5(w)$ with their Gershgorin Bands |G=3| 0.15 to 10.0| $Q_5(w)$| $K_1K_2K_3K_4K_5$ = (5.32)|

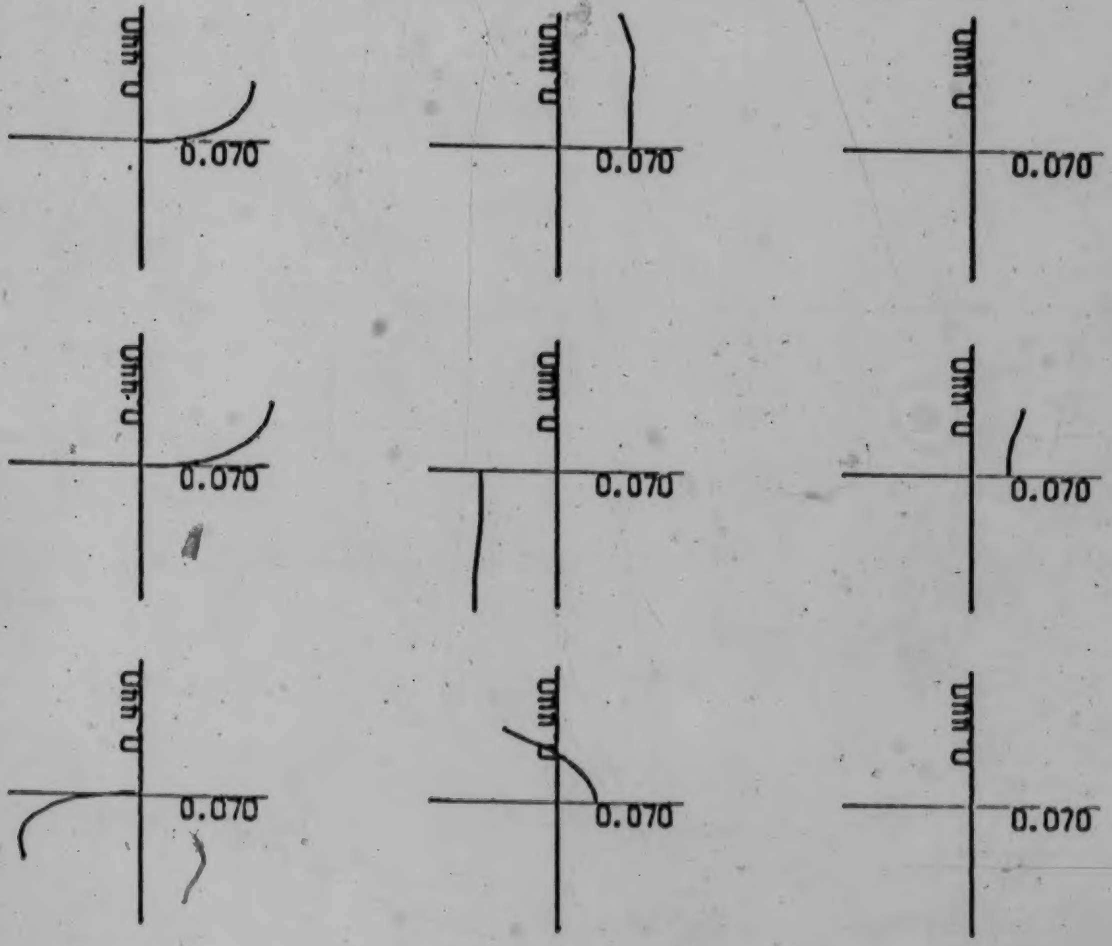

Figure 5.14 Nyquist Array of G(w)
|G=5| 0.1 to 5.0| G(w)| K = I|

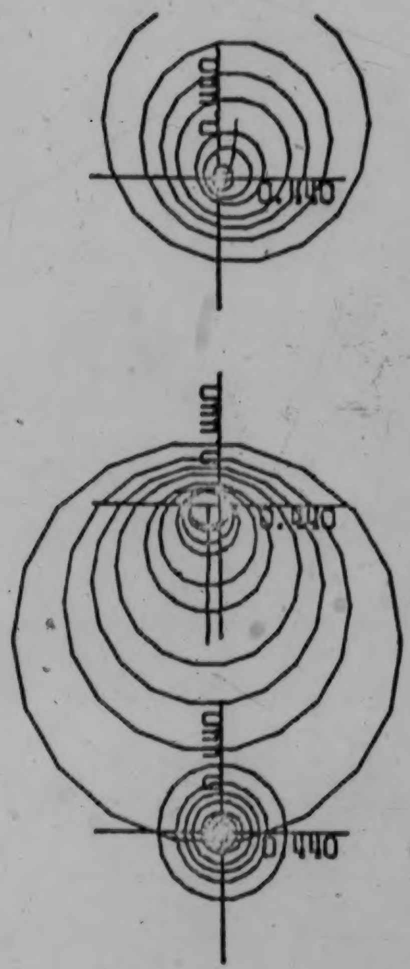

Figure 5.15 Diagonal Elements of G(w) with their Gershgorin Bands
|G=5|-0.1 to 5.0| G(w)| K = I|

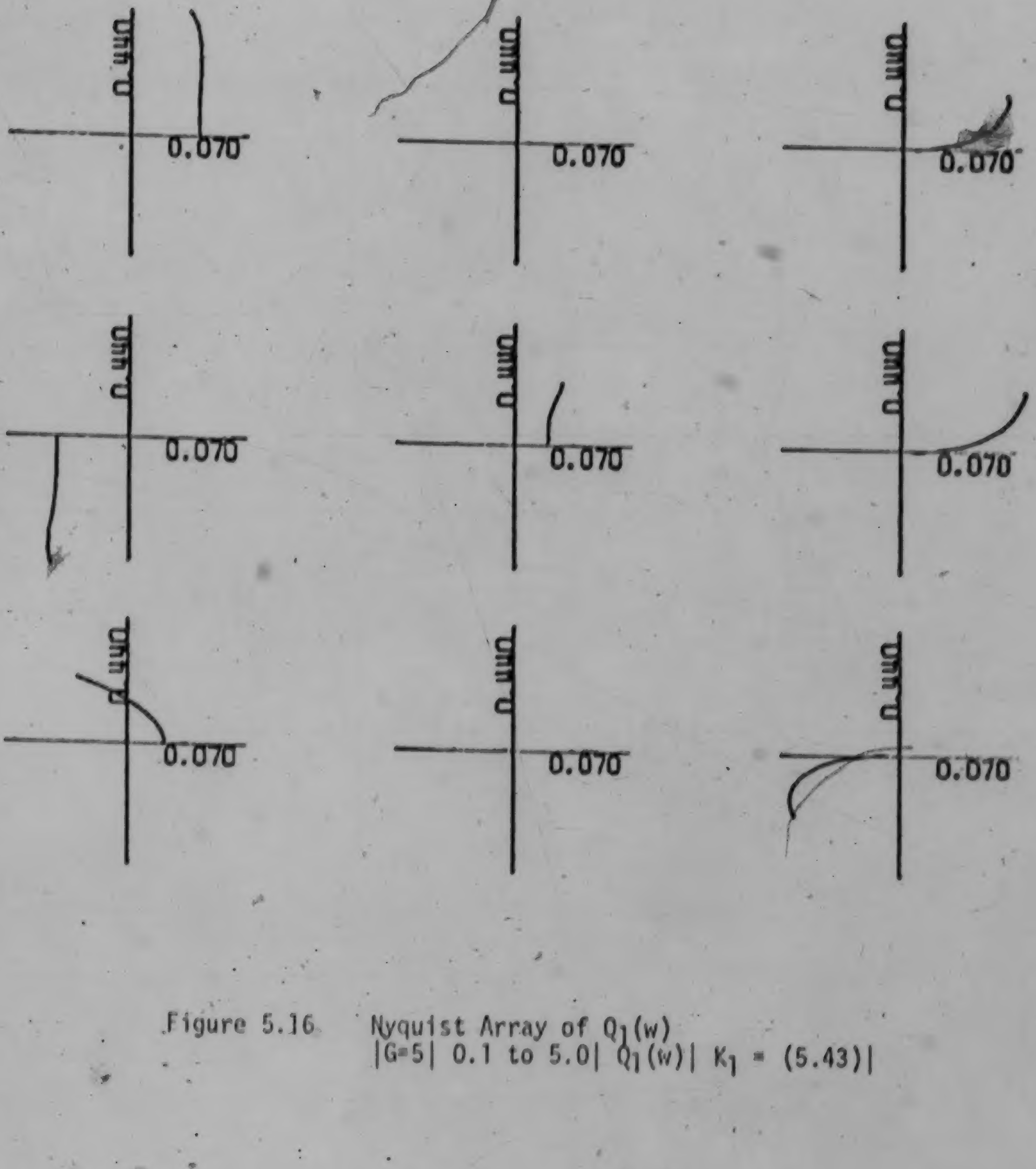

Figure 5.16 Nyquist Array of $Q_1(w)$
|G=5| 0.1 to 5.0| $Q_1(w)$| K_1 = (5.43)|

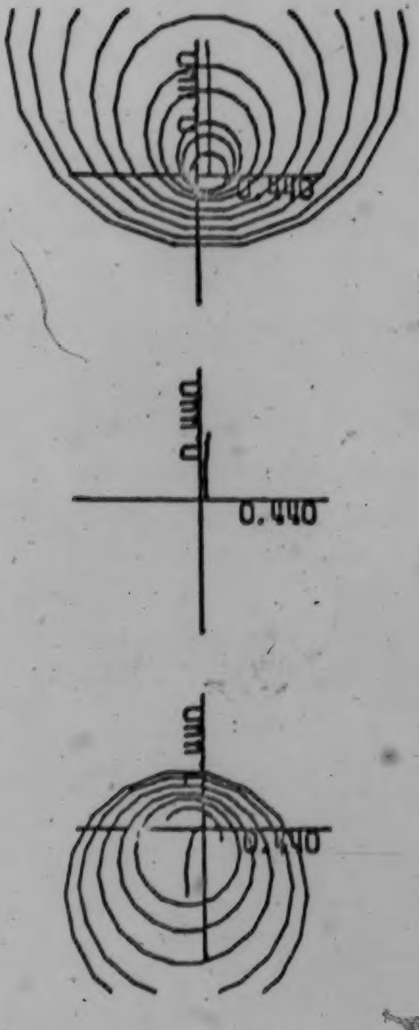

Figure 5.17 Diagonal Elements of $Q_1(w)$ with their Gershgorin Bands
|G=5| 0.1 to 5.0| $Q_1(w)$| K_1 = (5.43)|

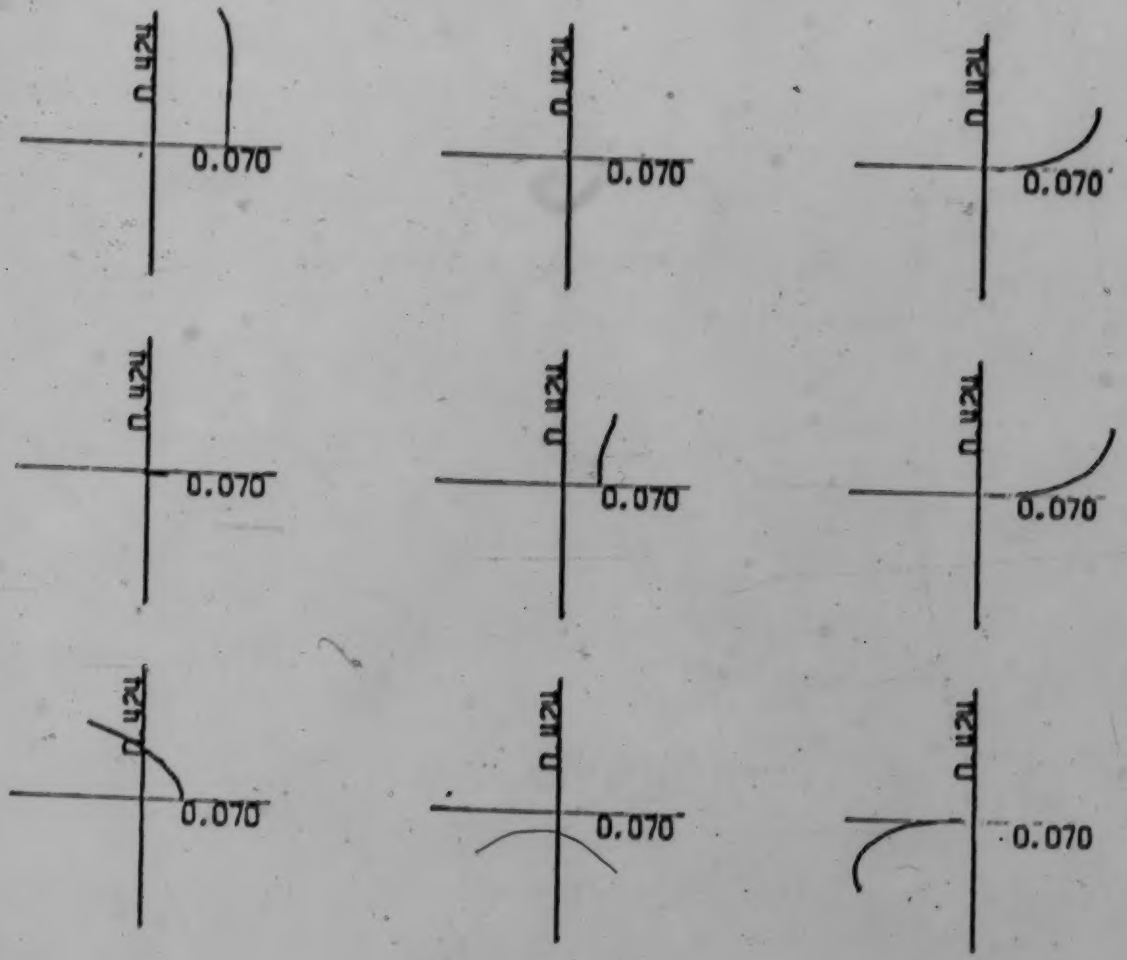

Figure 5.18 Nyquist Array of $Q_2(w)$
$|G=5|$ 0.1 to 5.0$|$ $Q_2(w)|$ K_1K_2 = (5.43)(5.44)$|$

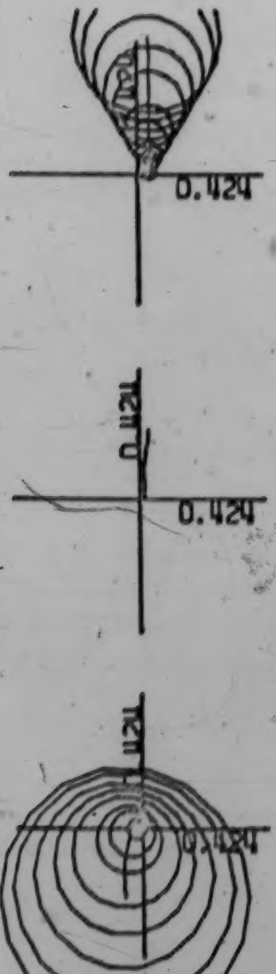

Figure 5.19 Diagonal Elements of $Q_2(w)$ with their Gershgorin Bands
|G=5| 0.1 to 5.0| $Q_2(w)$| K_1K_2 = (5.43)(5.44)|

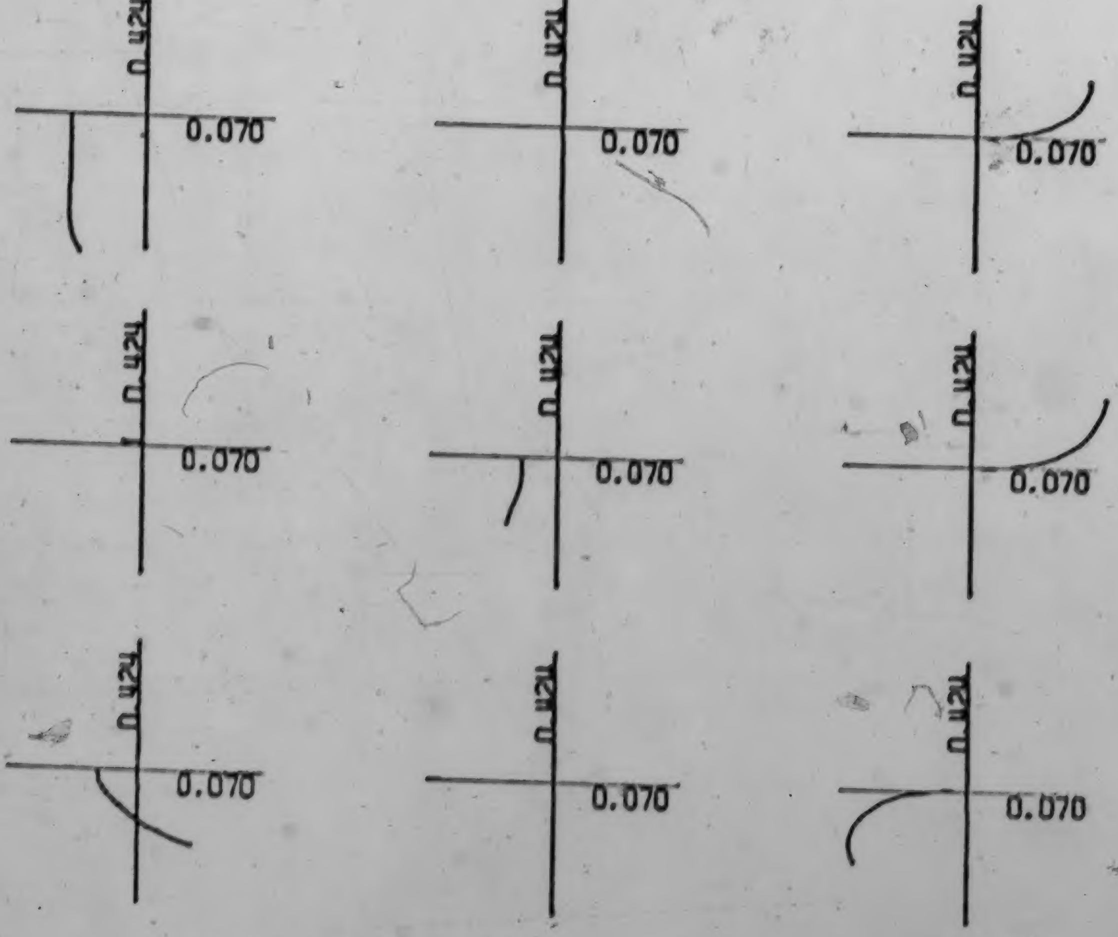

Figure 5.20 Nyquist Array of $Q_3(w)$
$|G=5|$ 0.1 to 5.0$|$ $Q_3(w)|$ $K_1K_2K_3$ = (5.43)(5.44)(5.45)$|$

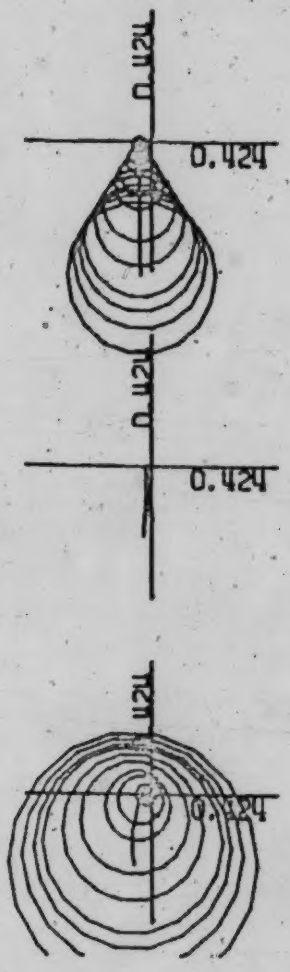

Figure 5.21 Diagonal Elements of $Q_3(w)$ with their Gershgorin Bands |G=5| 0.1 to 5.0| $Q_3(w)$| $K_1K_2K_3$ = (5.43)(5.44)(5.45)|

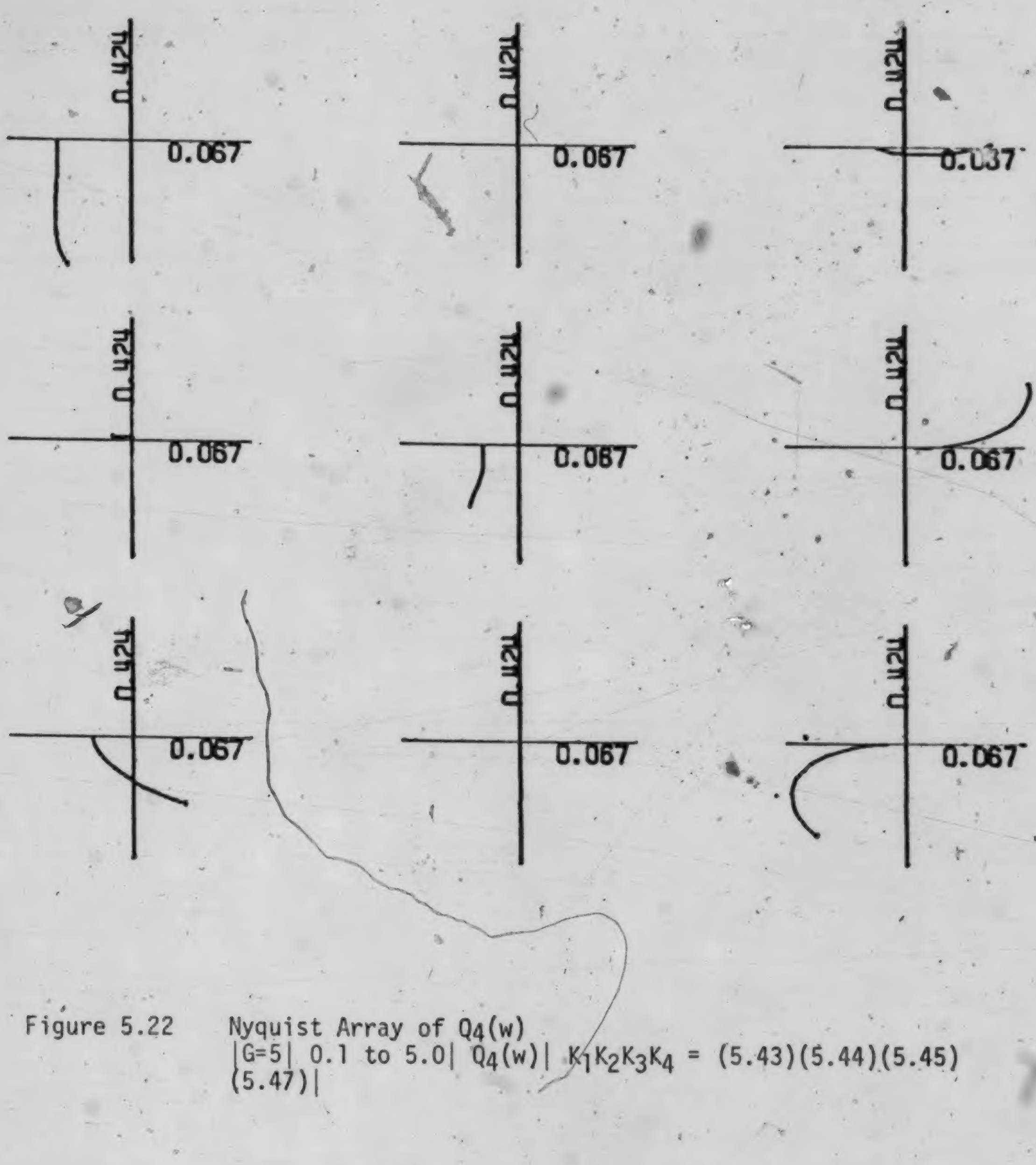

Figure 5.22 Nyquist Array of $Q_4(w)$
$|G=5|$ 0.1 to 5.0$|$ $Q_4(w)|$ $K_1K_2K_3K_4$ = (5.43)(5.44)(5.45)(5.47)$|$

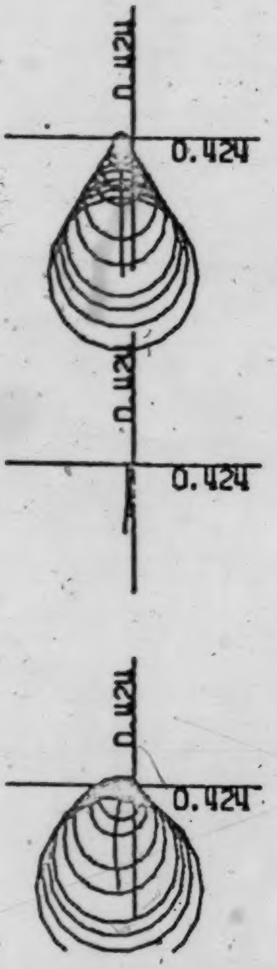

Figure 5.23 Diagonal Elements of $Q_4(w)$ with their Gershgorin Bands |G=5| 0.1 to 5.0| $Q_4(w)$| $K_1K_2K_3K_4$ = (5.43)(5.44)(5.45) (5.47)|

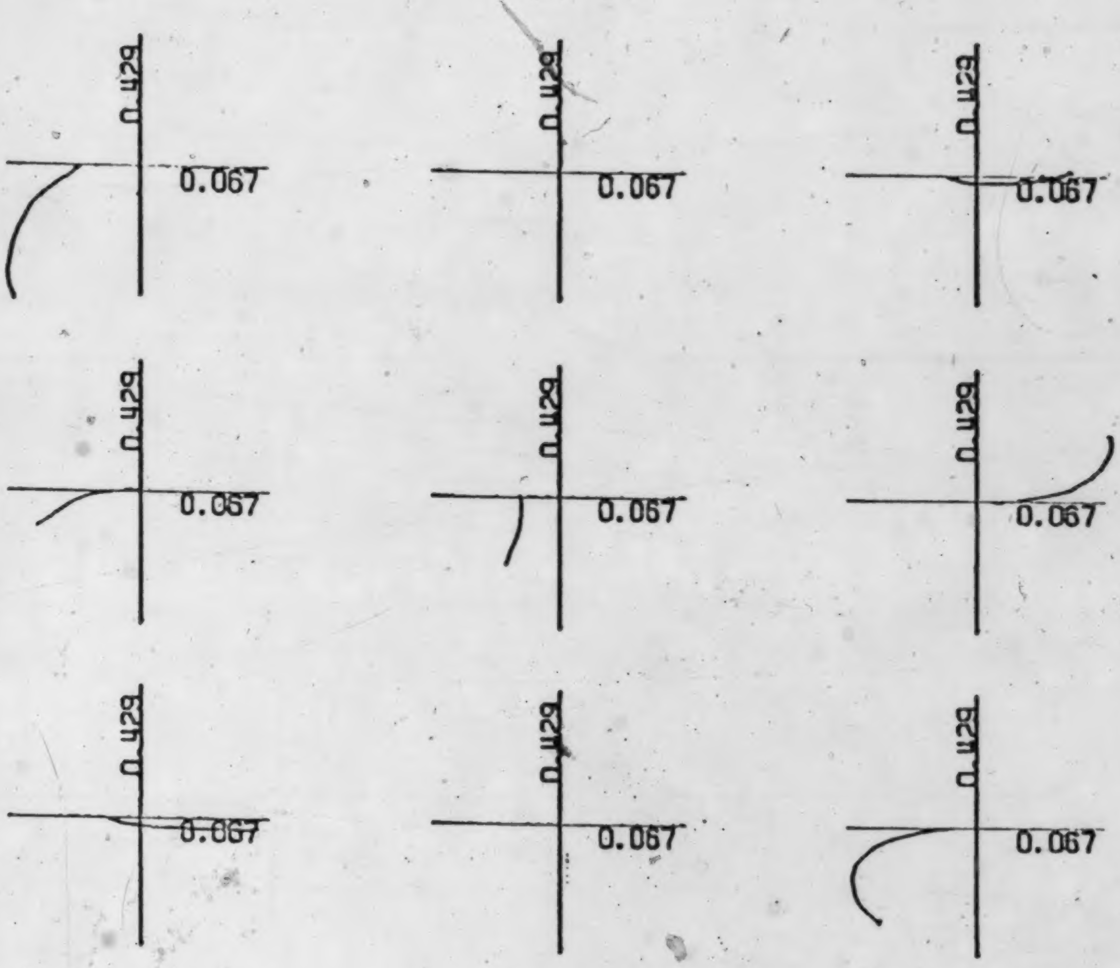

Figure 5.24 Nyquist Array of $Q_5(w)$
|G=5| 0.1 to 5.0| $Q_5(w)$| $K_1K_2K_3K_4K_5$ = (5.51)|

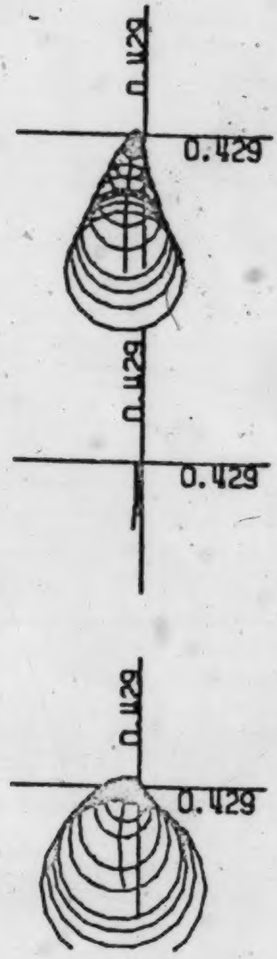

Figure 5.25 Diagonal Elements of $Q_5(w)$ with their Gershgorin Bands |G=5| 0.1 to 5.0| $Q_5(w)$| $K_1K_2K_3K_4K_5$ = (5.51)|

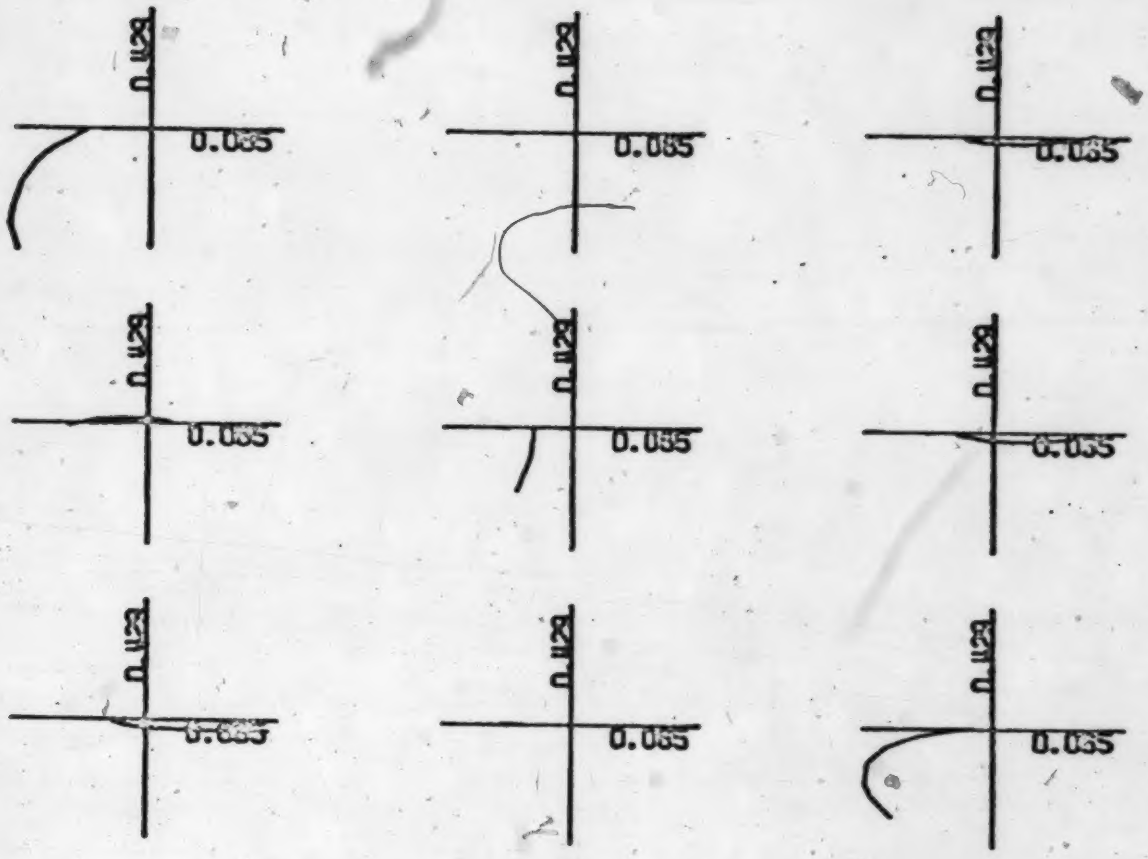

Figure 5.26 Nyquist Array of $Q_6(w)$
$|G=5|$ 0.1 to 5.0$|$ $Q_6(w)|$ $K_1K_2K_3K_4K_5K_6$ = (5.53)$|$

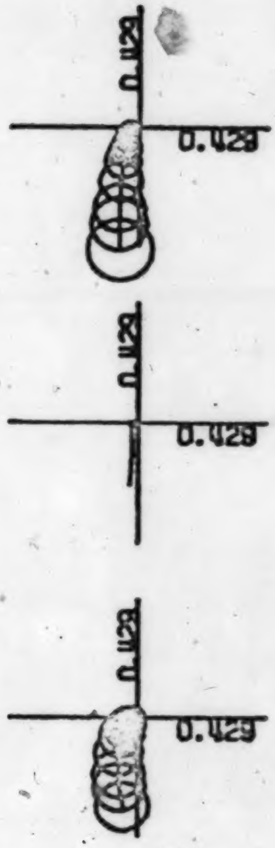

Figure 5.27 Diagonal Elements of $Q_6(w)$ with their Gershgorin Bands |G=5| 0.1 to 5.0| $Q_6(w)$| $K_1K_2K_3K_4K_5K_6$ = (5.53)|

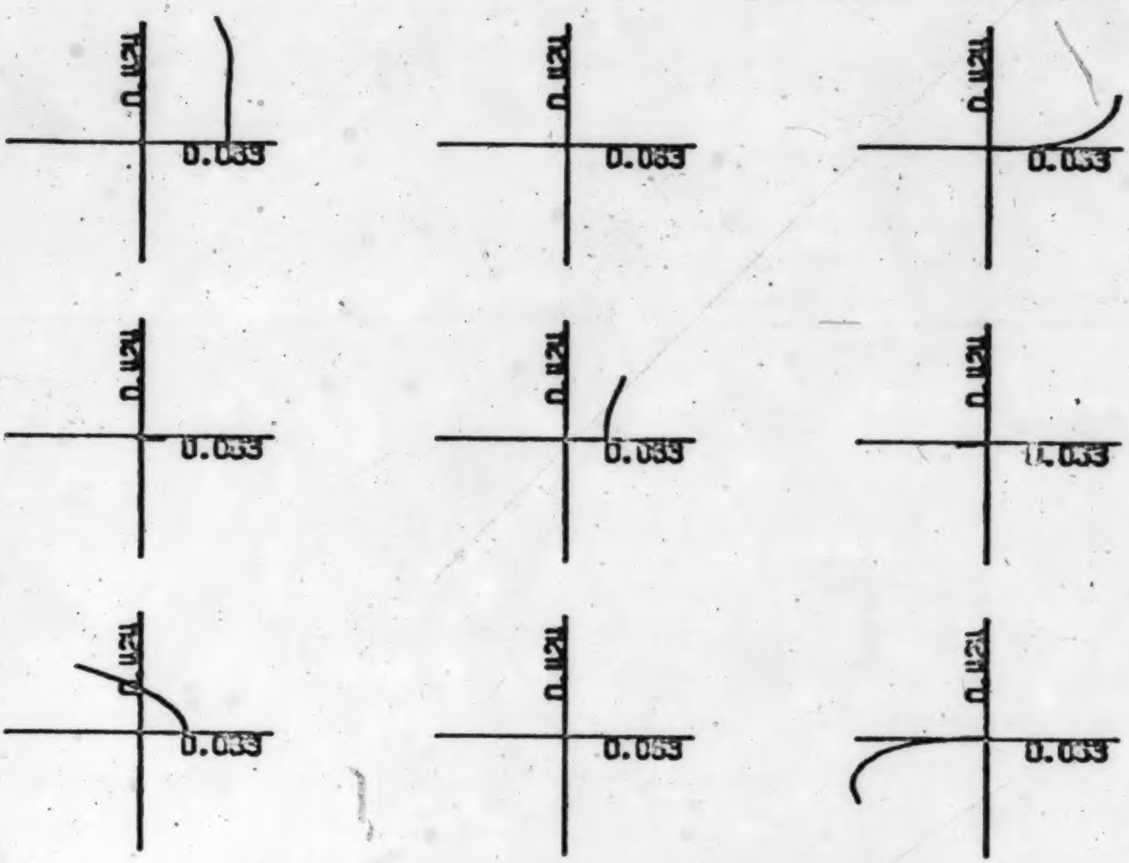

Figure 5.28 Nyquist Array of $Q_3^1(w)$
$|G=5|$ 0.1 to 5.0$|$ $Q_3^1(w)|$ $K_1K_2K_3^1 = (5.43)(5.44)(5.55)|$

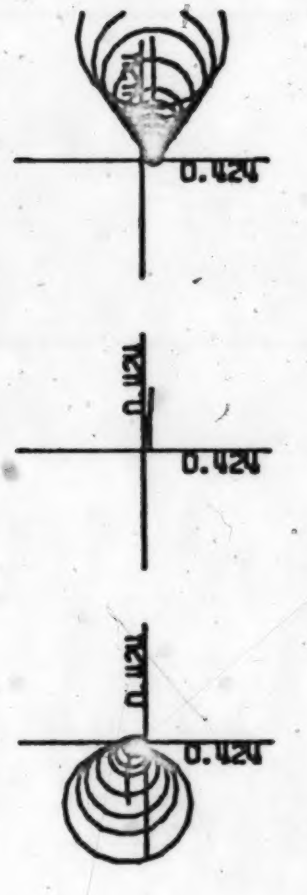

Figure 5.29 Diagonal Elements of $Q_3^1(w)$ with their Gershgorin Bands
$|G=5|$ 0.1 to 5.0$|$ $Q_3^1(w)|$ $K_1K_2K_3^1$ = (5.43)(5.44)(5.55)$|$

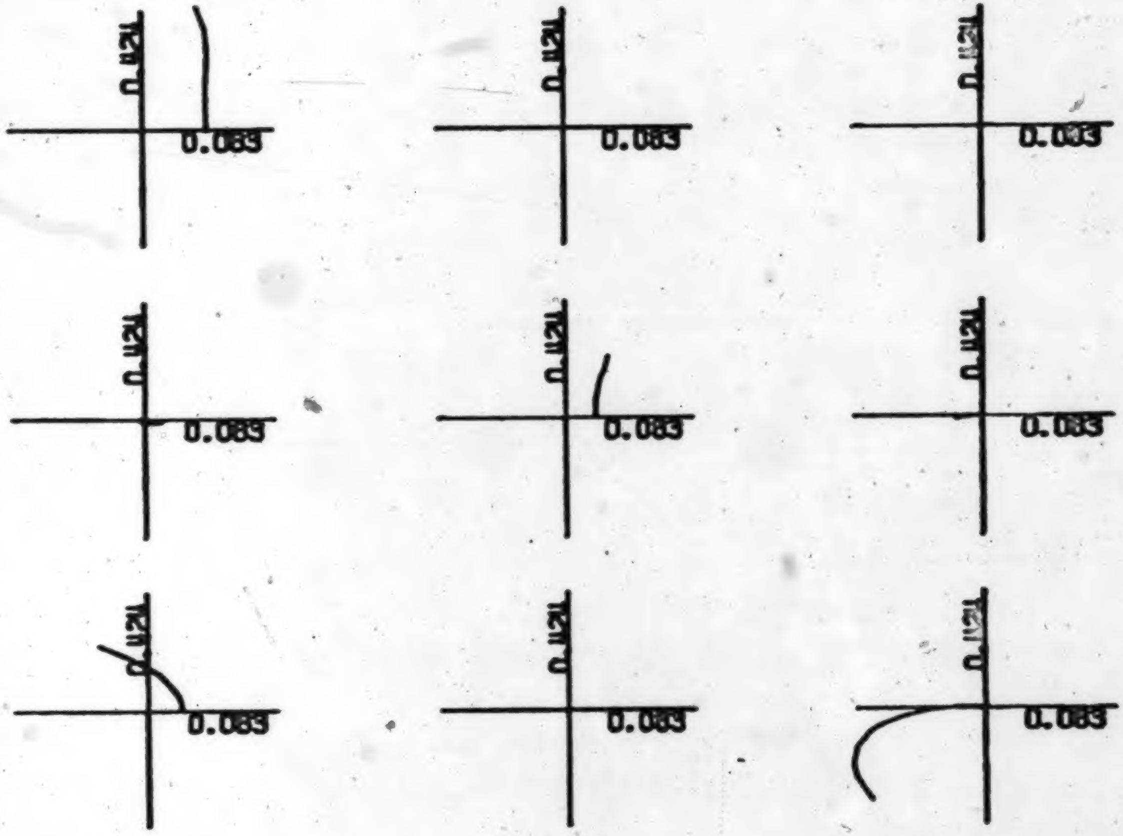

Figure 5.30 Nyquist Array of $Q_4^1(w)$
|G=5| 0.1 to 5.0| $Q_4^1(w)$| $K_1K_2K_3^1K_4^1$ = (5.43)(5.44)(5.55)
(5.58)|

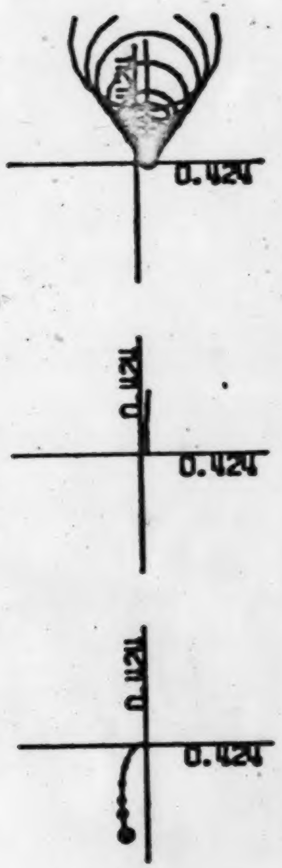

Figure 5.31 Diagonal Elements of $Q_4^1(w)$ with their Gershgorin Bands |G=5| 0.1 to 5.0| $Q_4^1(w)$| $K_1K_2K_3^1K_4^1$ = (5.43)(5.44)(5.55)(5.58)|

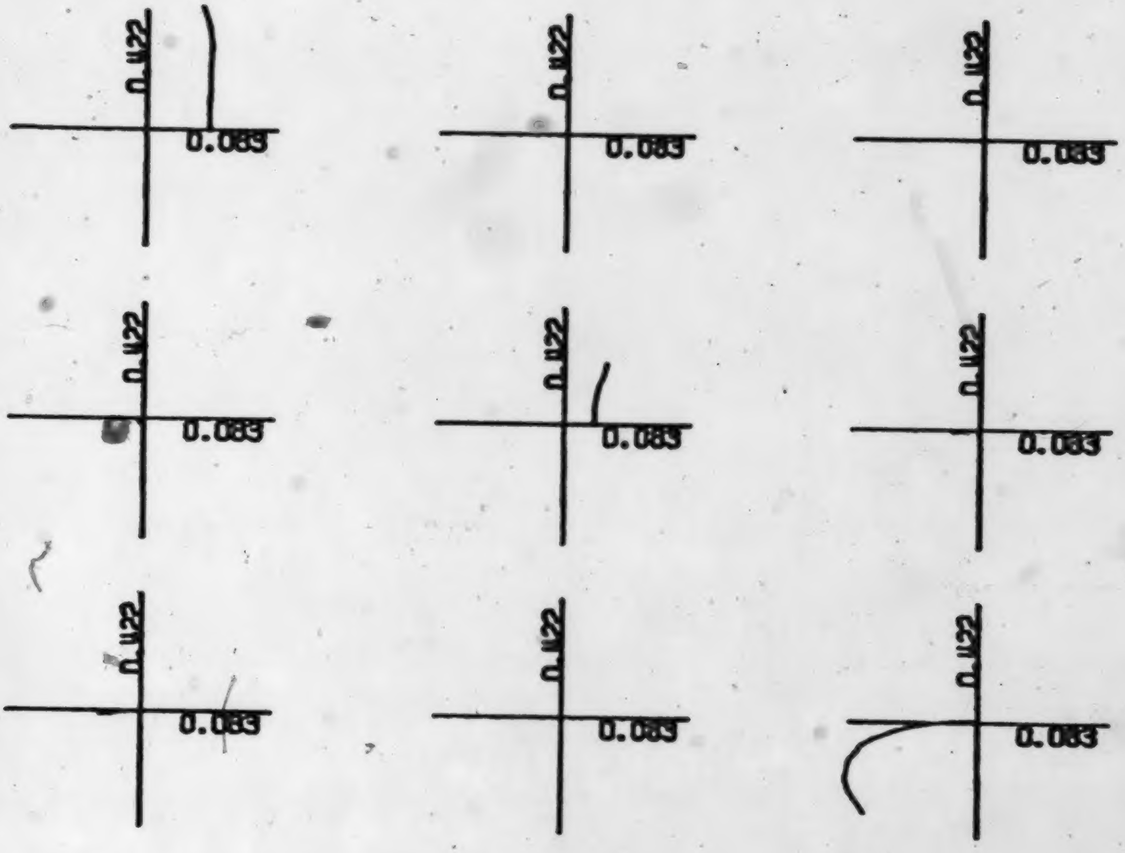

Figure 5.32 Nyquist Array of $Q_5^1(w)$
|G=5| 0.1 to 5.0| $Q_5^1(w)$| $K_1K_2K_3^1K_4^1K_5^1$ = (5.43)(5.44)(5.55) (5.58)(5.60)|

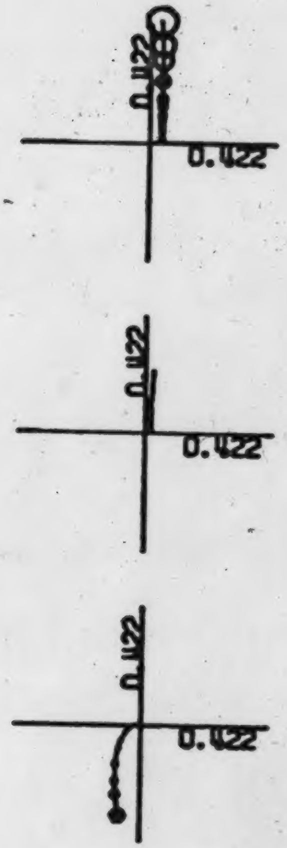

Figure 5.33 Diagonal Elements of $Q_5^1(w)$ with their Gershgorin Bands |G=5| 0.1 to 5.0| $Q_5^1(w)$| $K_1K_2K_3^1K_4^1K_5^1$ = (5.43)(5.44)(5.55)(5.58)(5.60)|

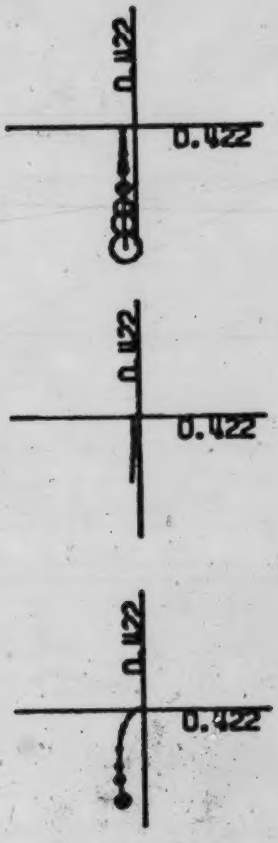

Figure 5.34 Diagonal Elements of $Q_6^1(w)$ with their Gershgorin Bands
|G=5| 0.1 to 5.0| $Q_6^1(w)$| $K_1K_2K_3^1K_4^1K_5^1K_6^1$ = (5.64)|

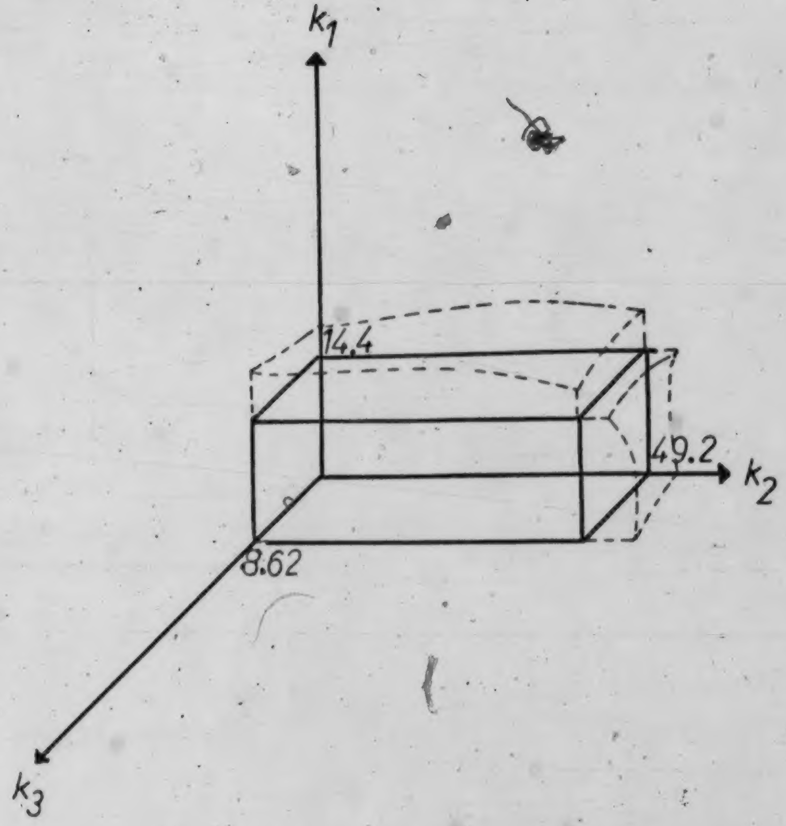
k_1
14.4
49.2
k_2
8.62
k_3

Figure 5.35 Stable Gain Space for the Fifth Order Evaporator Model when using the compensator given by Equation (5.54).

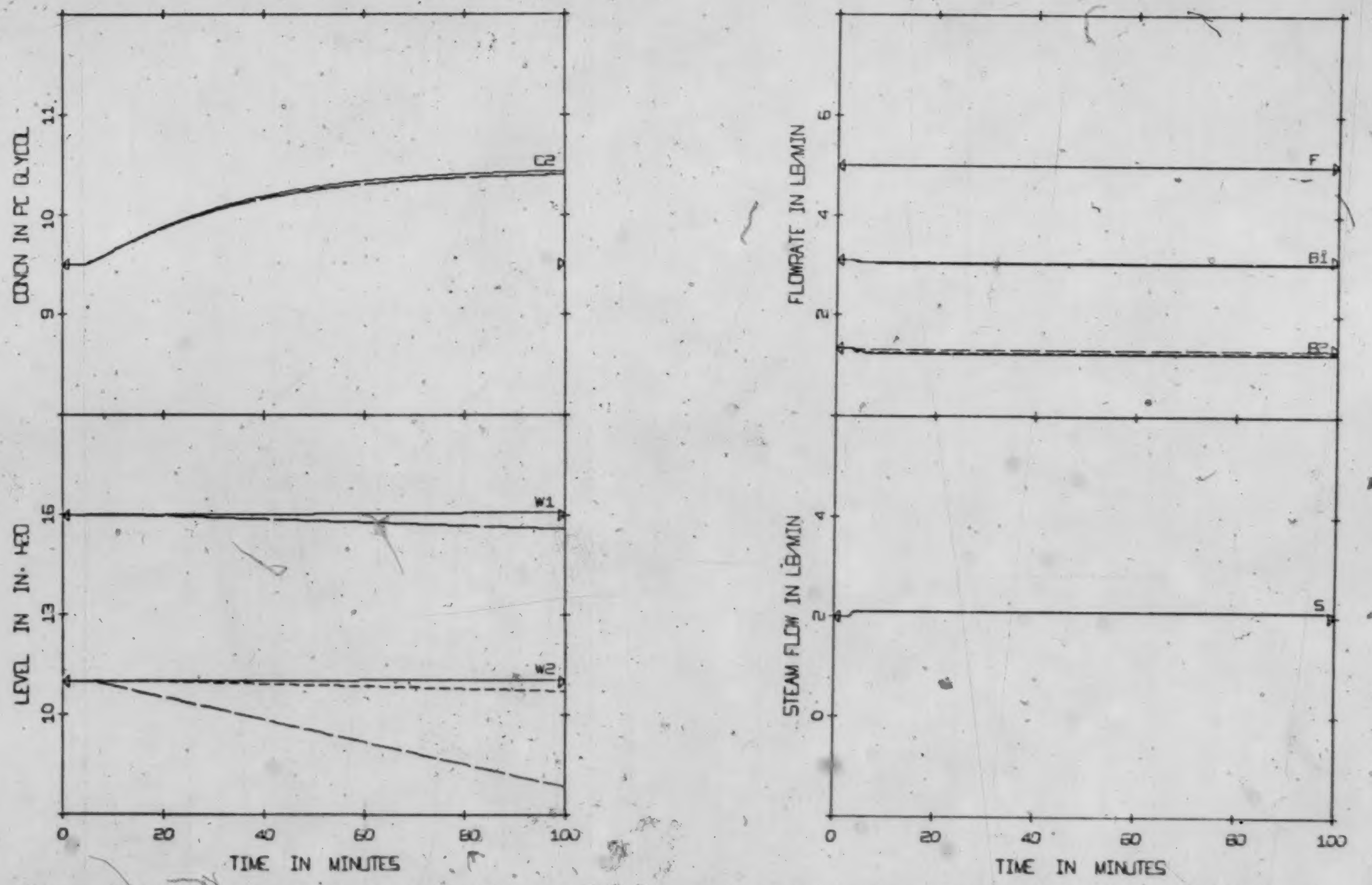

Figure 5.36 Effect of Improving Diagonal Dominance in the Open-Loop Compensated Plant. Controller K_A (Equation 5.51): — —, Controller K_B (Equation 5.53): ----, Controller $K_B^{\prime}$ (Equation 5.65): ———

|G=5| OL005| SIM 5| K = (5.51),(5.53),(5.65)| DNA| 5% C_2|

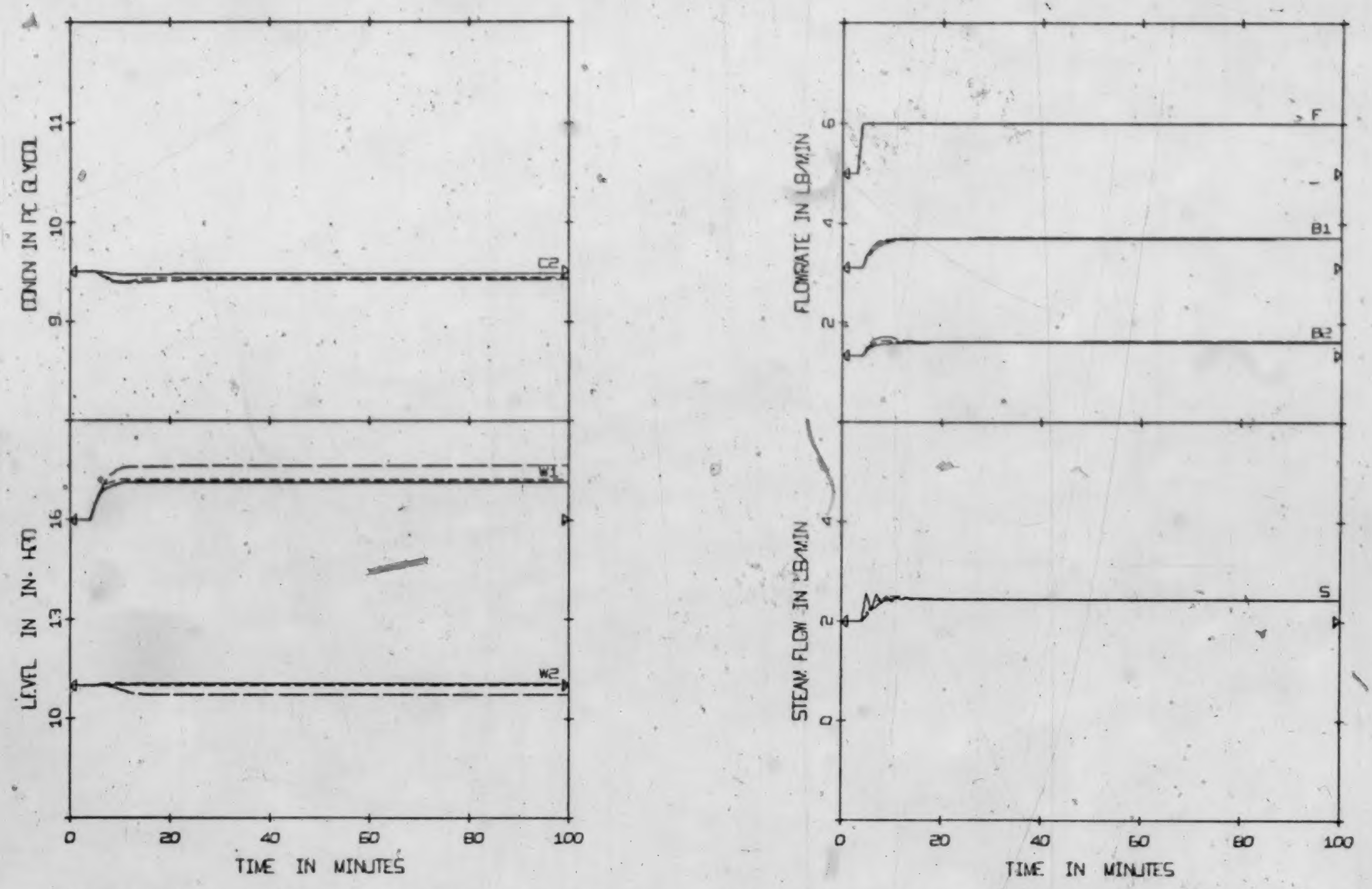

Figure 5.37 Effect of Improving Diagonal Dominance in the Closed-Loop Evaporator. DNA0520: —·—, FD0320: - - - - - -, NADY0520: ———
|G=5| DNA0520| FD0320| NADY0520| SIM 5| K = Table B.1,B.3,B.4| DNA| P| +20% F|

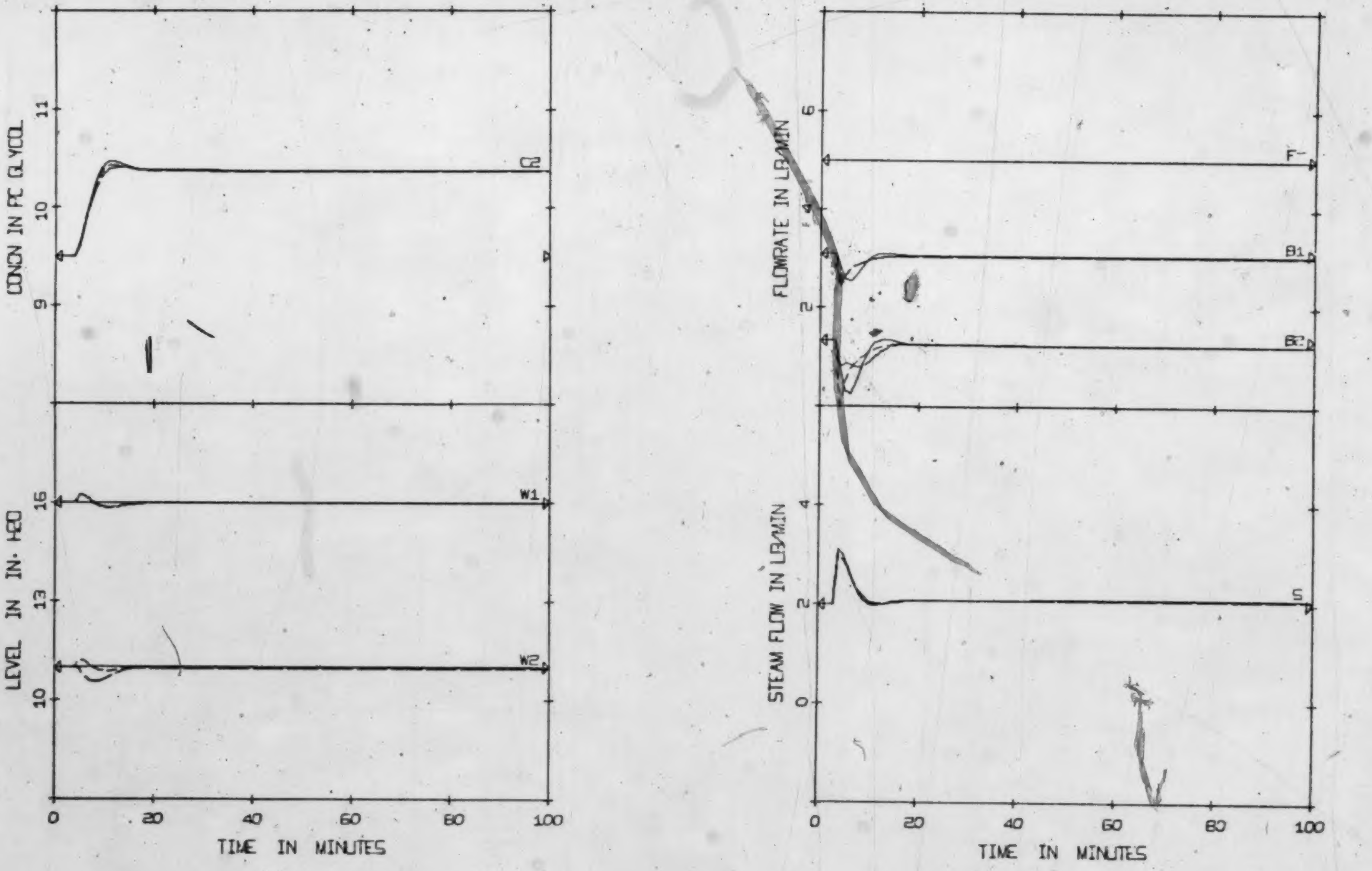

Figure 5.38 Effect of Improving Diagonal Dominance in the Closed-Loop Evaporator for a Step Change in a Setpoint. Controller K_A (Equation 5.51):—— Controller K_B (Equation 5.53): ----, Controller K_B' (Equation 5.65):____
|G=5| DNA0520| FD0320| NADY0520| SIM 5| K = Table B.1, B.3, B.4| DNA| P| +10% C_2|

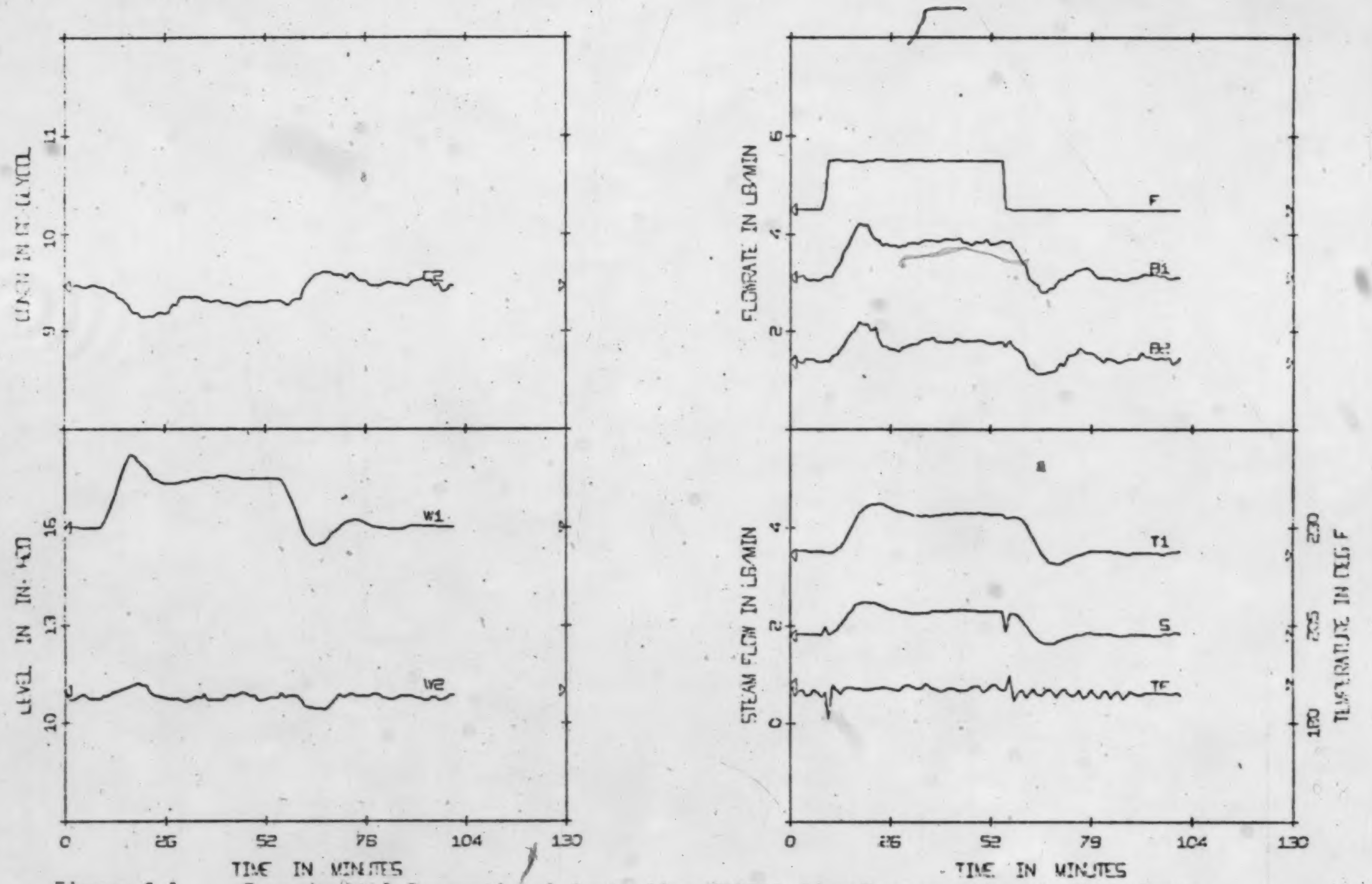

Figure 6.1 Experimental Proportional Controller FD0310 from Frequency Domain Techniques |G=3,5| FD0310| Exp| K = Table B.1| INA + DNA + CL| P| ± 20% F| 0|

Note: the explanation of the code used and a summary of the numeric values for all controllers is contained in Appendix B

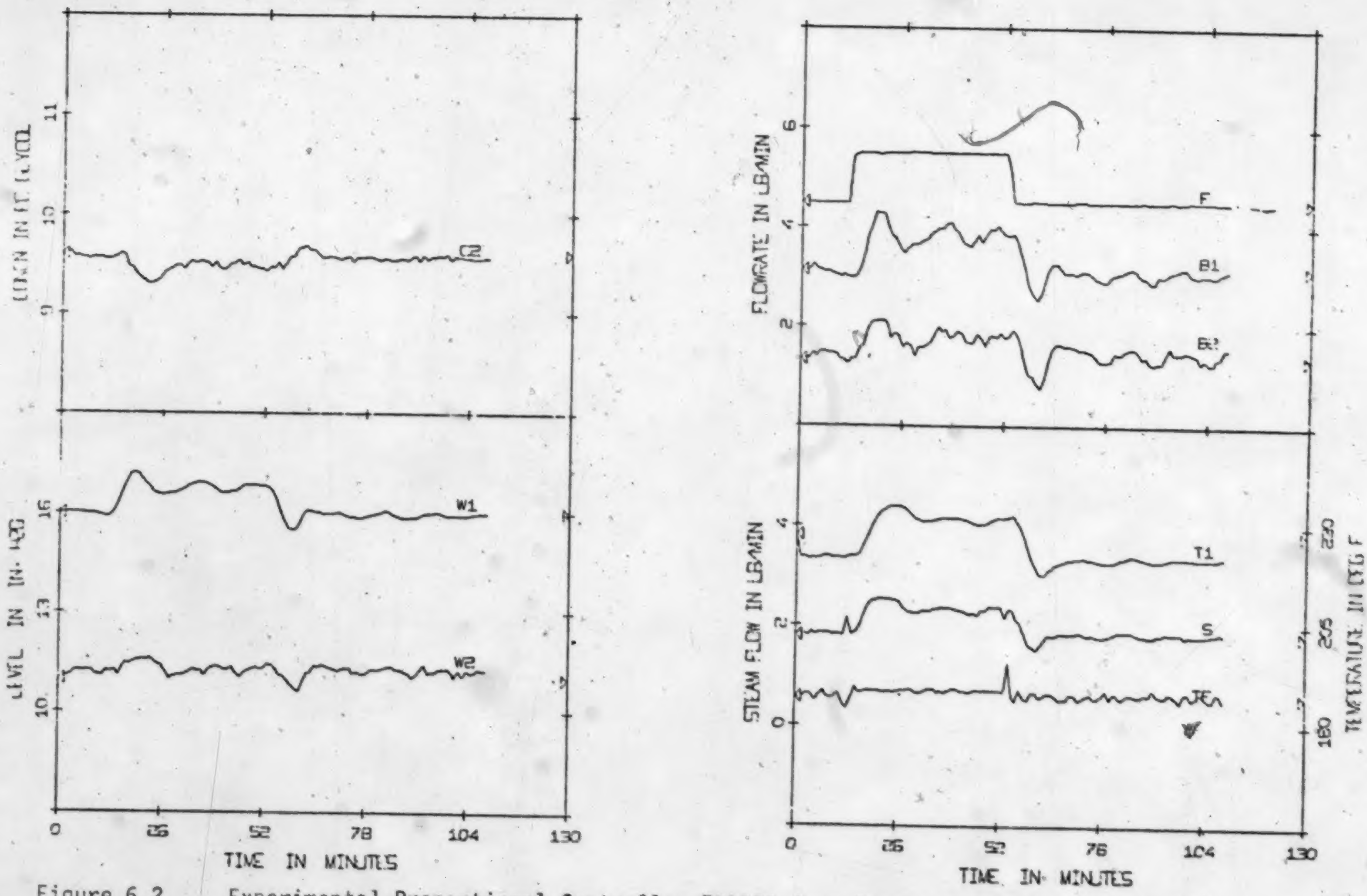

Figure 6.2 Experimental Proportional Controller FD0320 from Frequency Domain Techniques |G=3,5| FD0320| Exp| K = Table B.1| INA + DNA + CL| P| ± 20% F| 0|

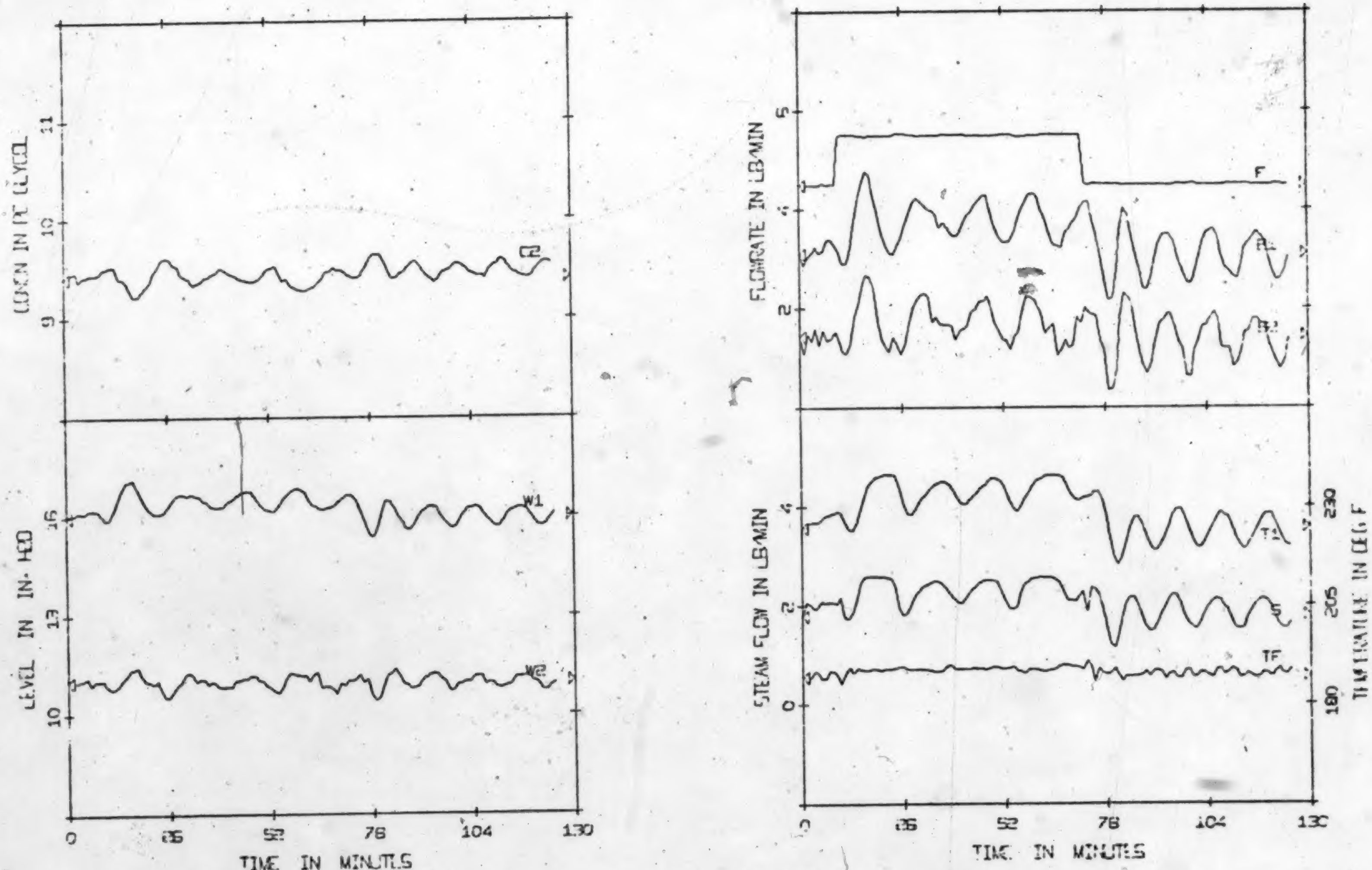

Figure 6.3 Experimental Proportional Controller FD0330 from Frequency Domain Techniques |G=3,5| FD0330| Exp| K = Table B.1| INA + DNA + CL| P| ± 20% F| 0|

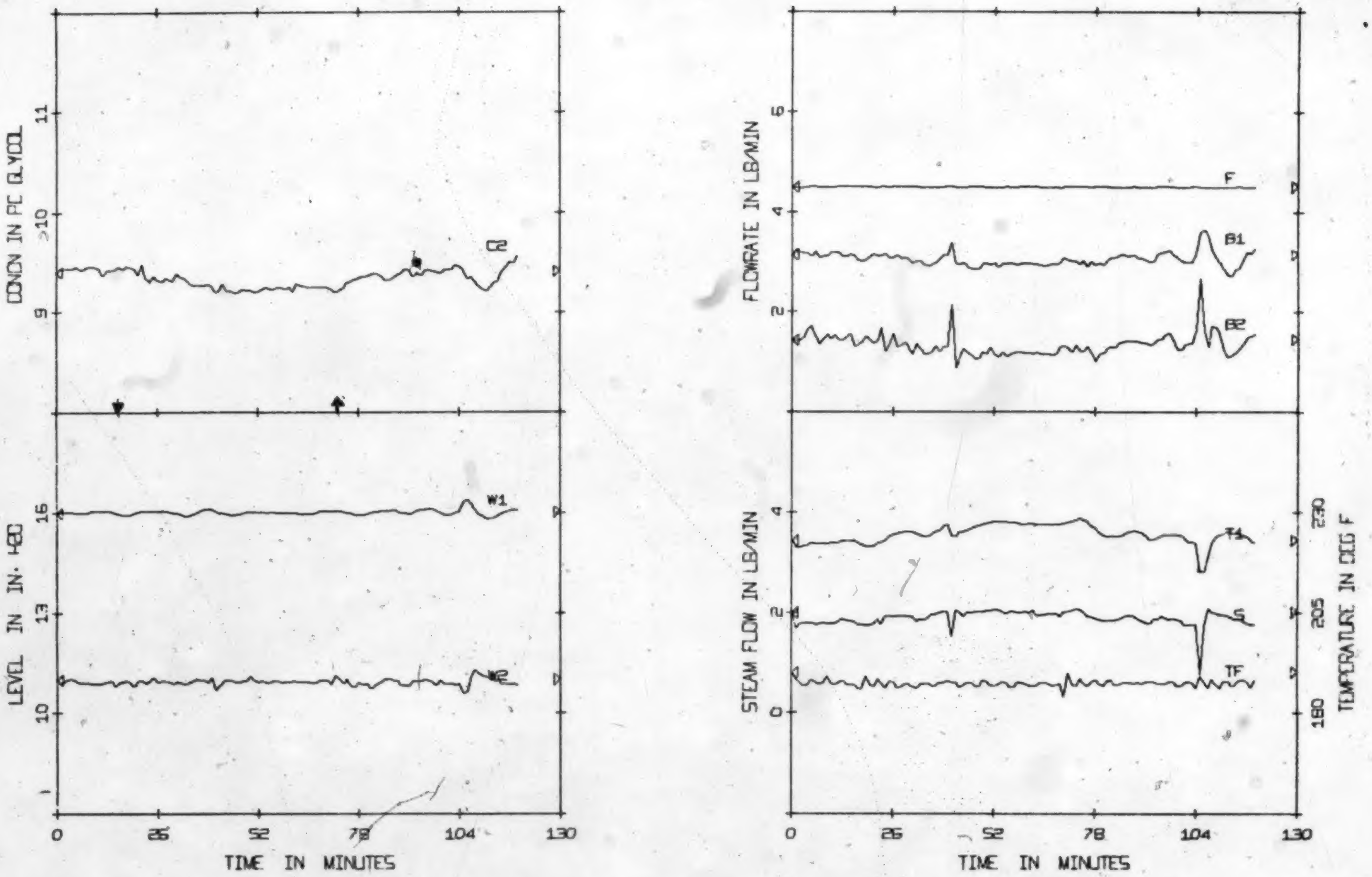

Figure 6.4 Experimental Proportional Controller FD0320 from Frequency Domain Techniques |G=3,5| FD0320| Exp| K = Table B.1| INA + DNA + CL| P| ± 20% FC| 0|

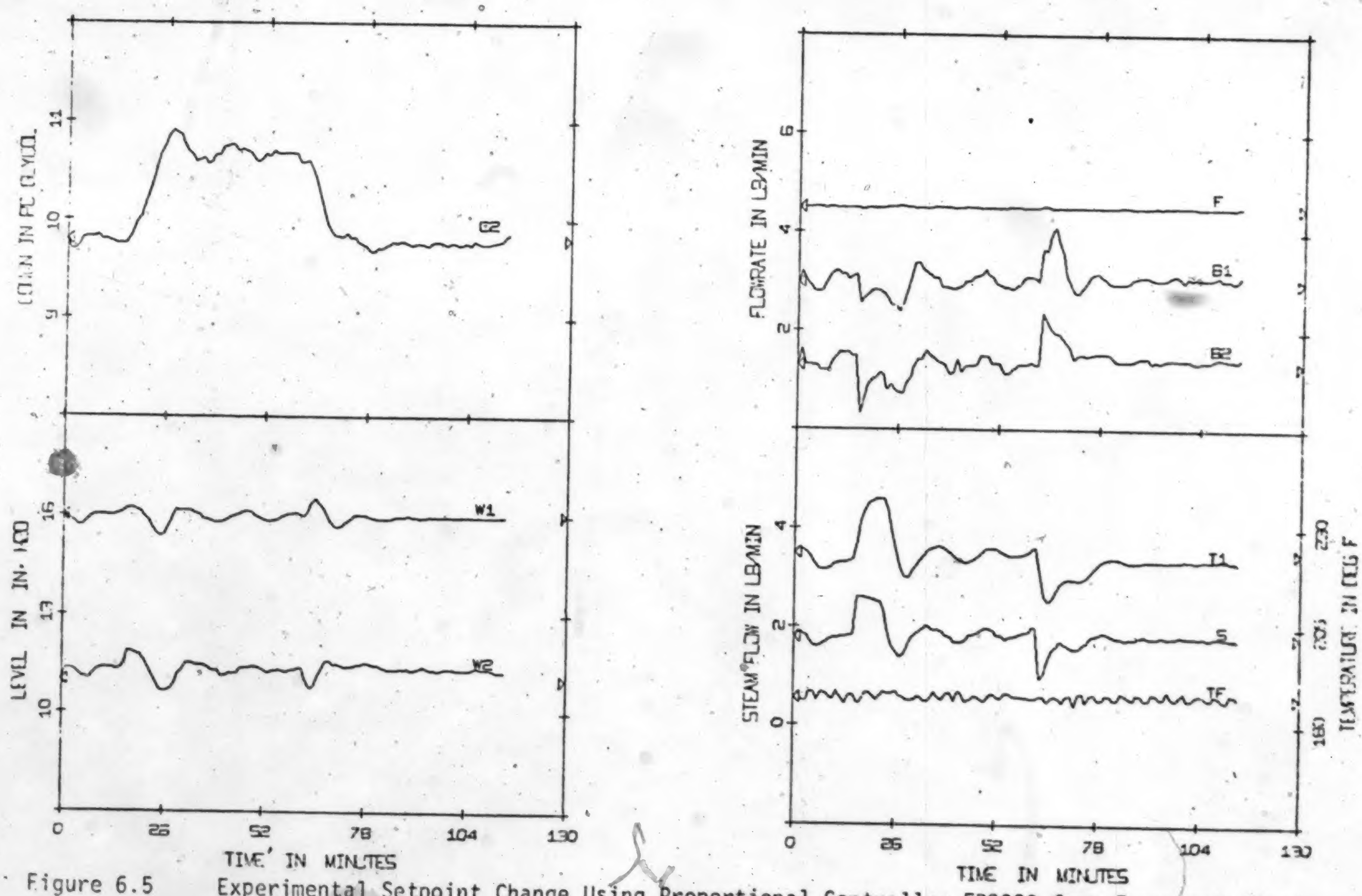

Figure 6.5 Experimental Setpoint Change Using Proportional Controller FD0320 from Frequency Domain Techniques
|G=3,5| FD0320| Exp| K = Table 3.1| INA + DNA + CL| P| ± 10% C_2| 0|

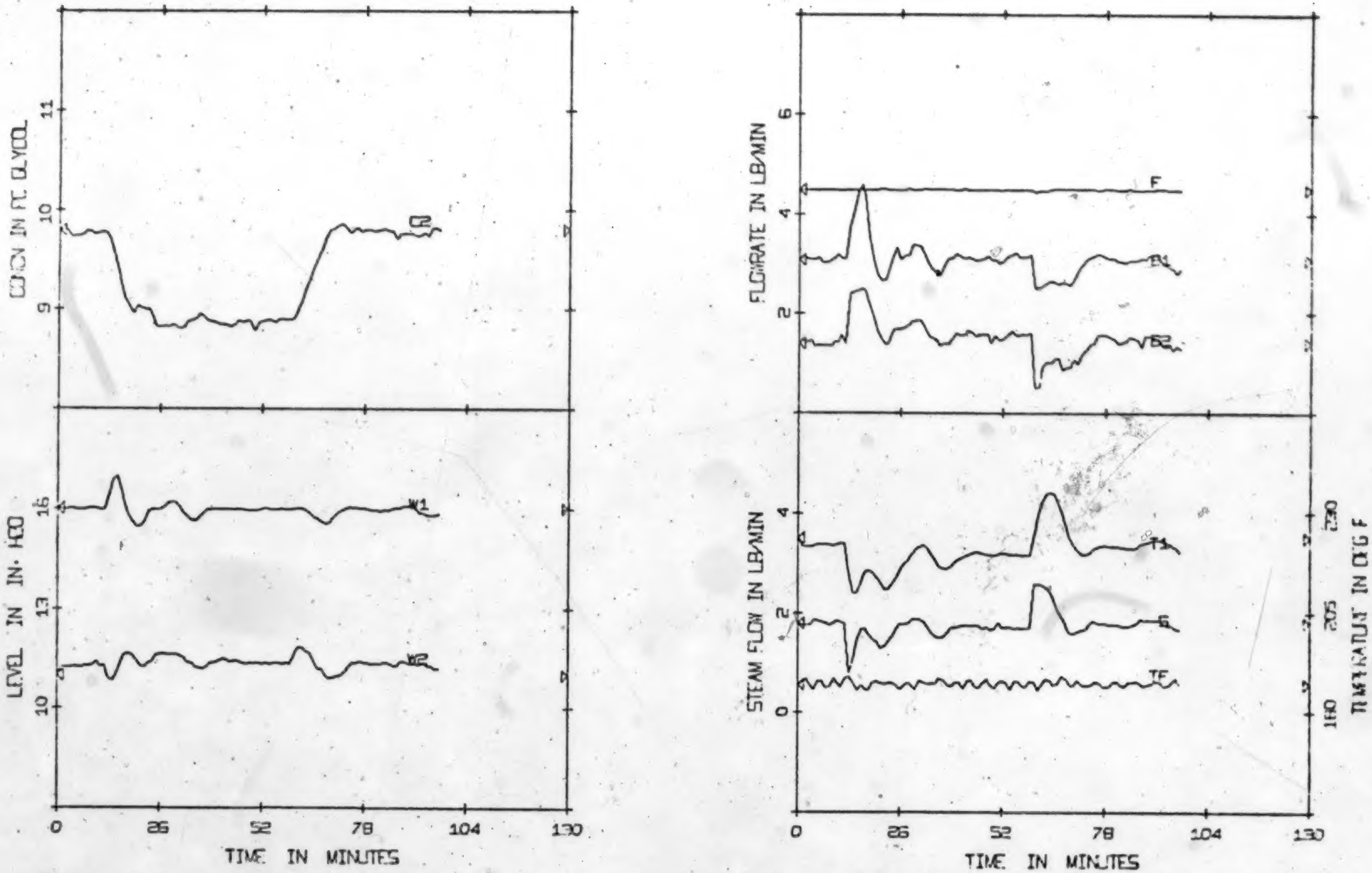

Figure 6.6 Experimental Setpoint Change Using Proportional Controller FD0320 from Frequency Domain Techniques
|G = 3,5| FD0320| Exp| K = Table 3.1| INA + DNA + CL| P| ± 10% C_2| 0|

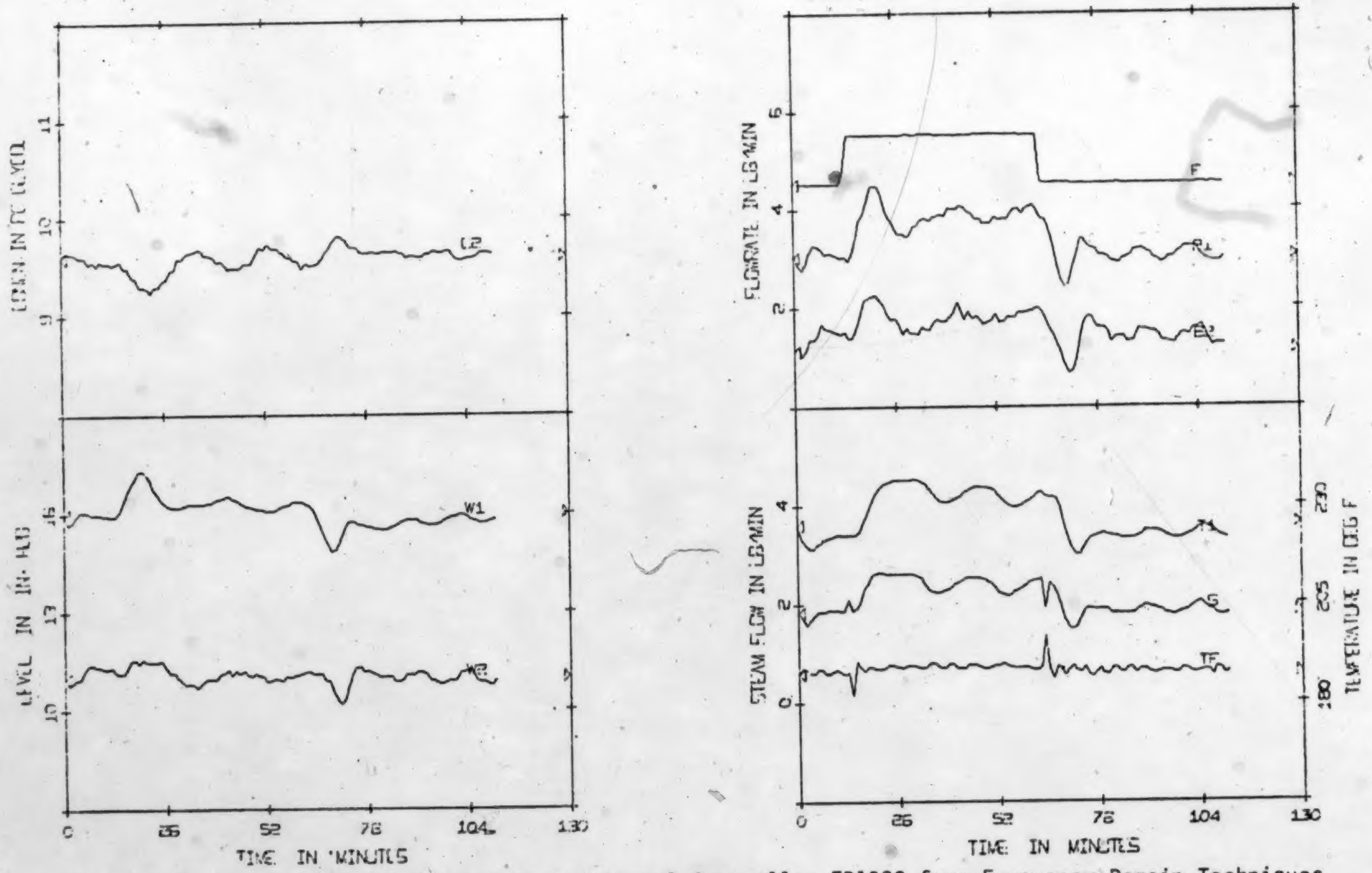

Figure 6.7 Experimental Proportional-integral Controller FD1320 from Frequency Domain Techniques |G=3,5| FD1320| Exp| K = Table B.2| INA + DNA + CL| P + I| ± 20% F| 0|

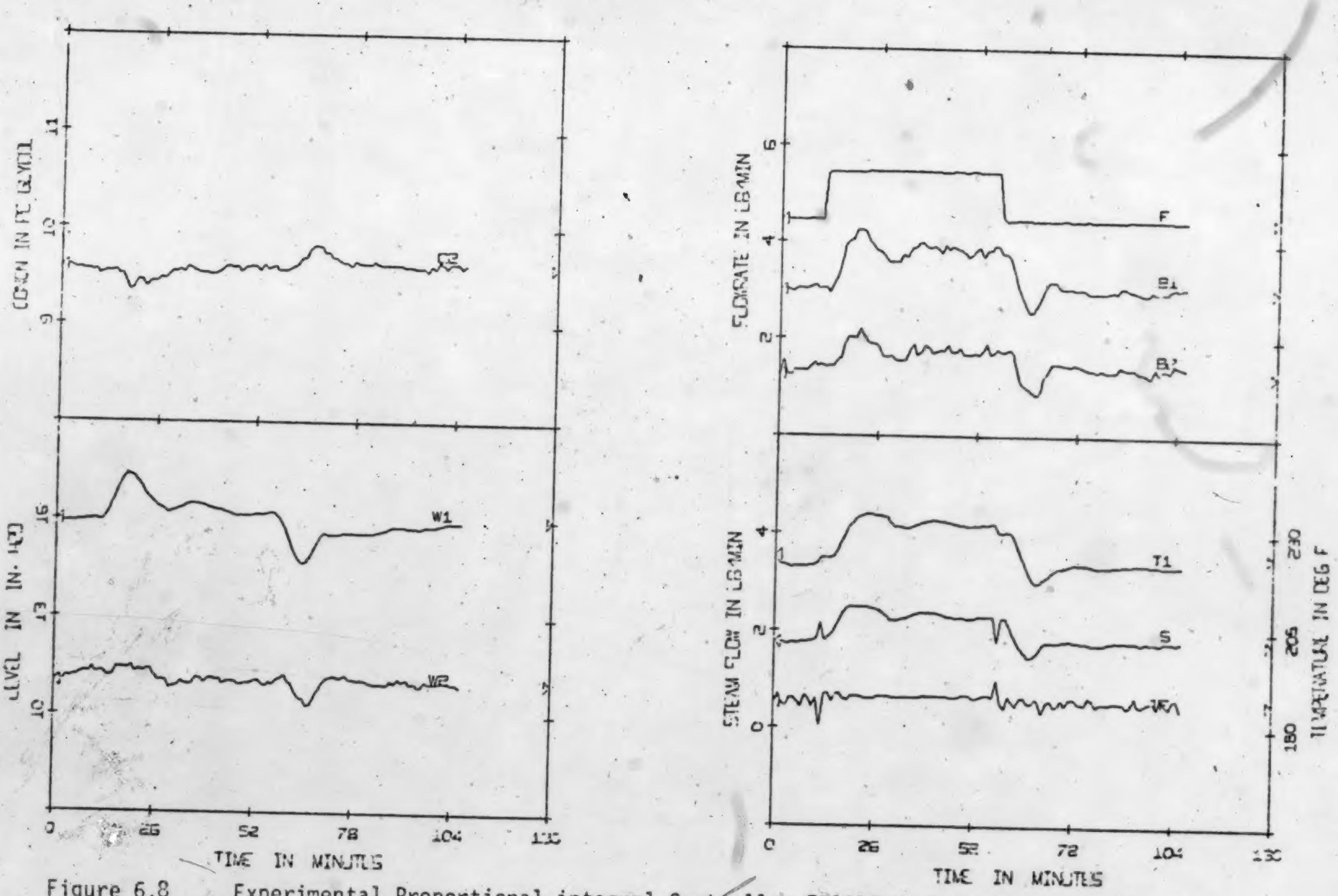

Figure 6.8 Experimental Proportional-integral Controller FD1315 from Frequency Domain Techniques |G=3,5| FD1315| Exp| K = Table B.2| INA + DNA + CL| P + I| ± 20% F| 0|

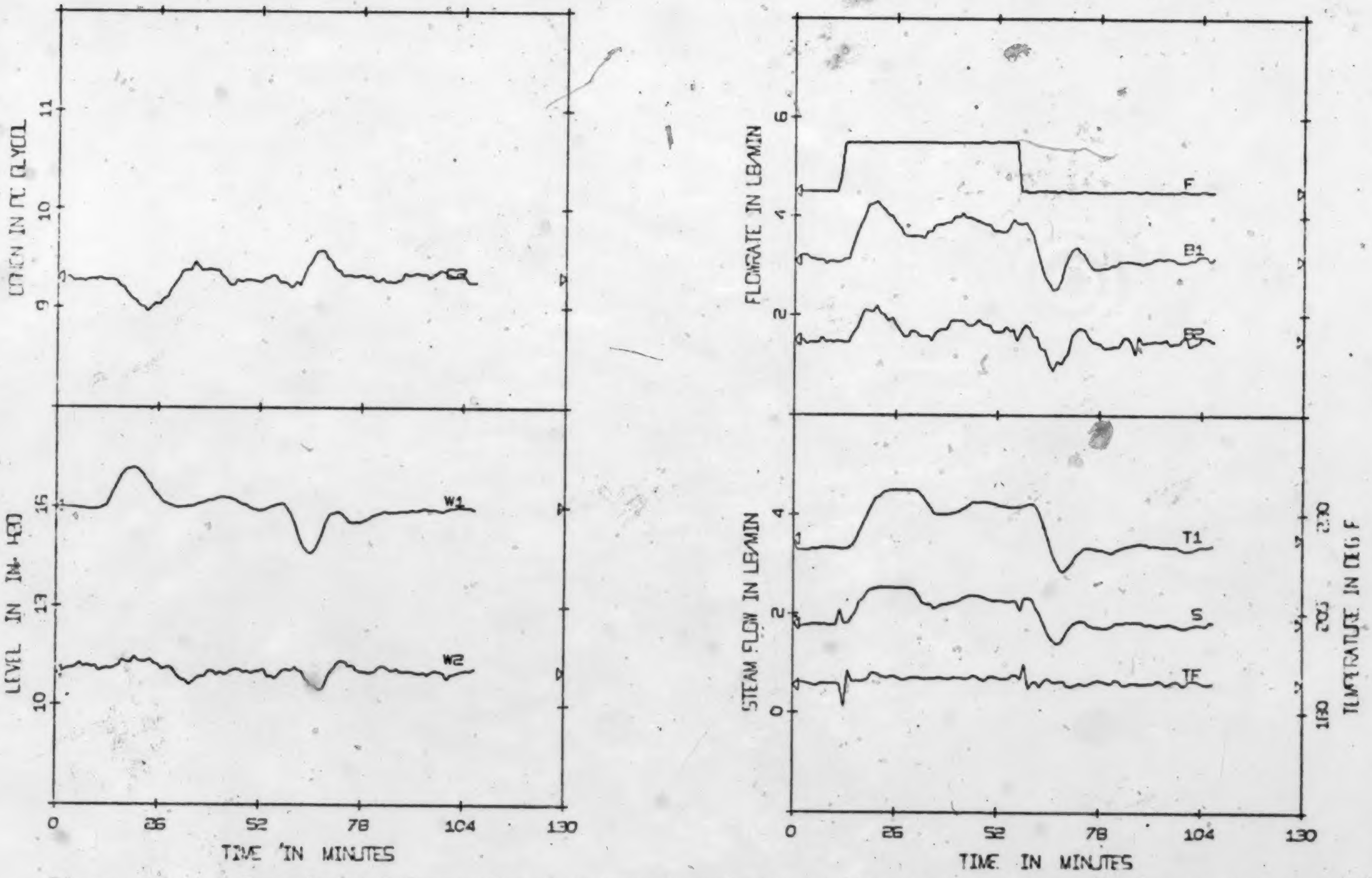

Figure 6.9 Experimental Proportional-integral Controller FD1315.1 from Frequency Domain Techniques |G=3,5| FD1315.1| Exp| K = Table B.2| INA + DNA + CL| P + I| ± 20% F| 0|

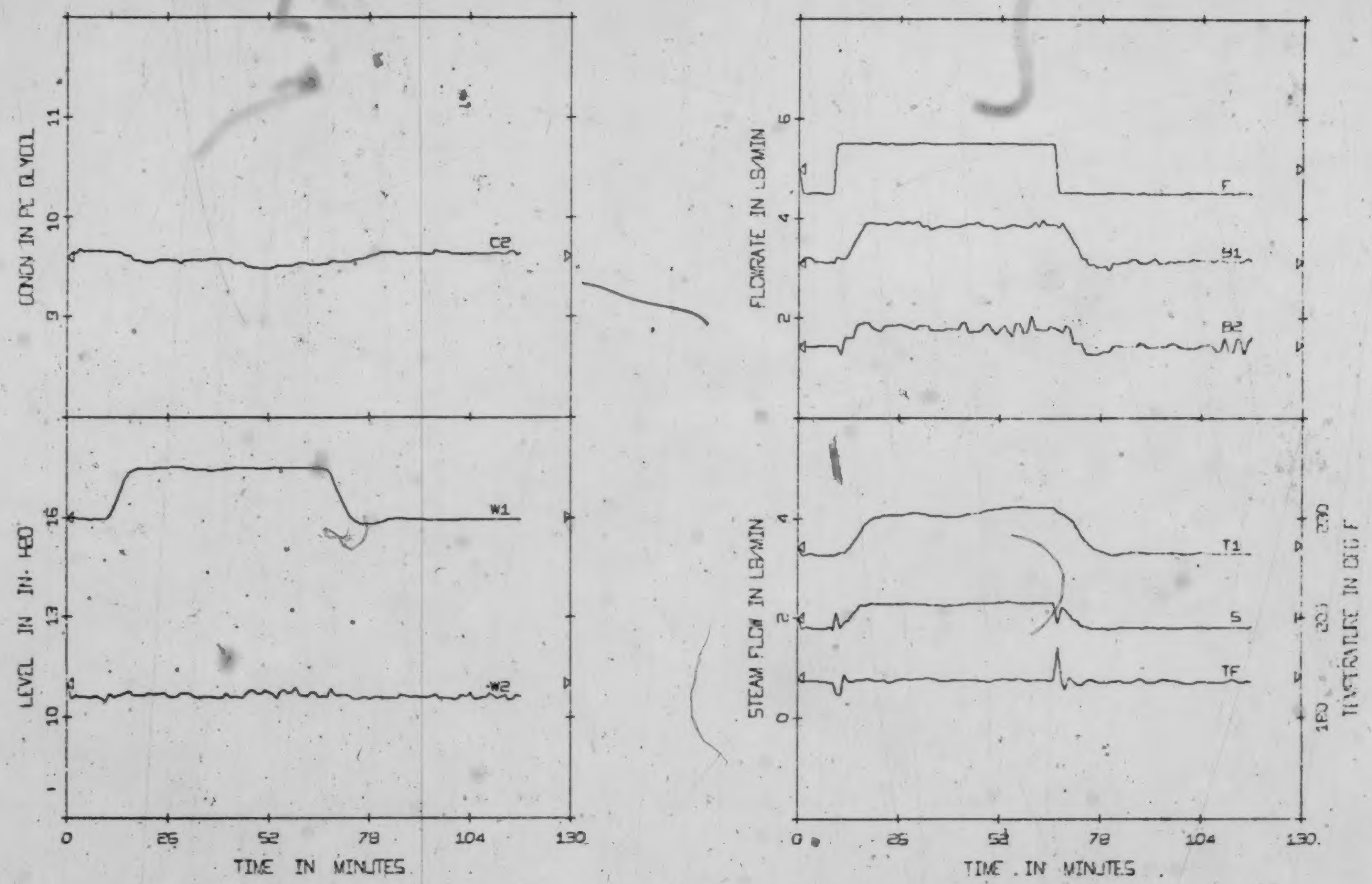

Figure 6.10 Experimental Dynamic Controller NADY0510 from Frequency Domain Techniques
|G=5| NADY0510| Exp| K = Table B.3| INA + DNA| D + P| ± 20% F| O|

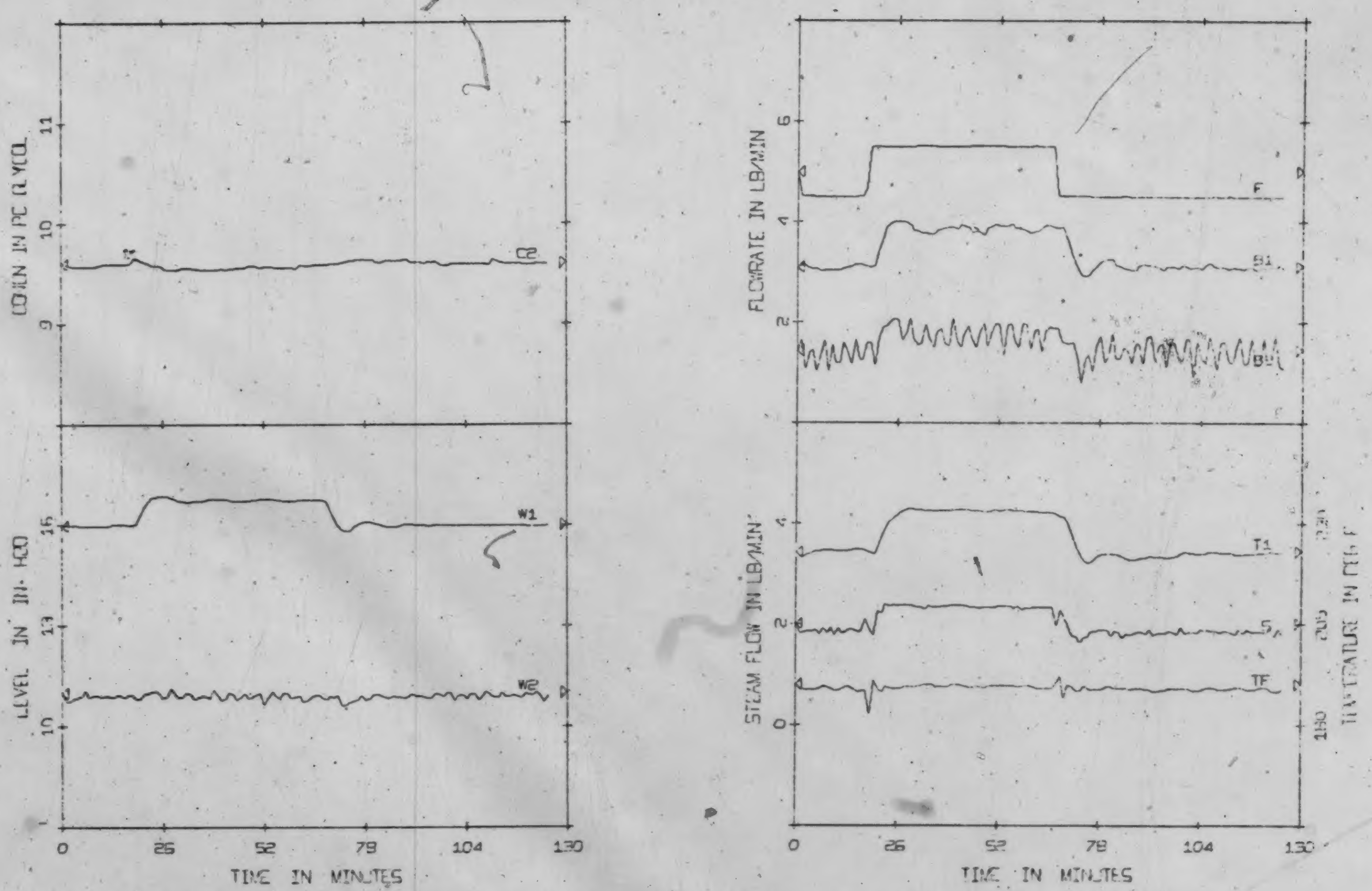

Figure 6.11 Experimental Dynamic Controller NADY0520 from Frequency Domain Techniques |G=5| NADY0520| Exp| K = Table B.3| INA + DNA| D + P| ± 20% F| N|

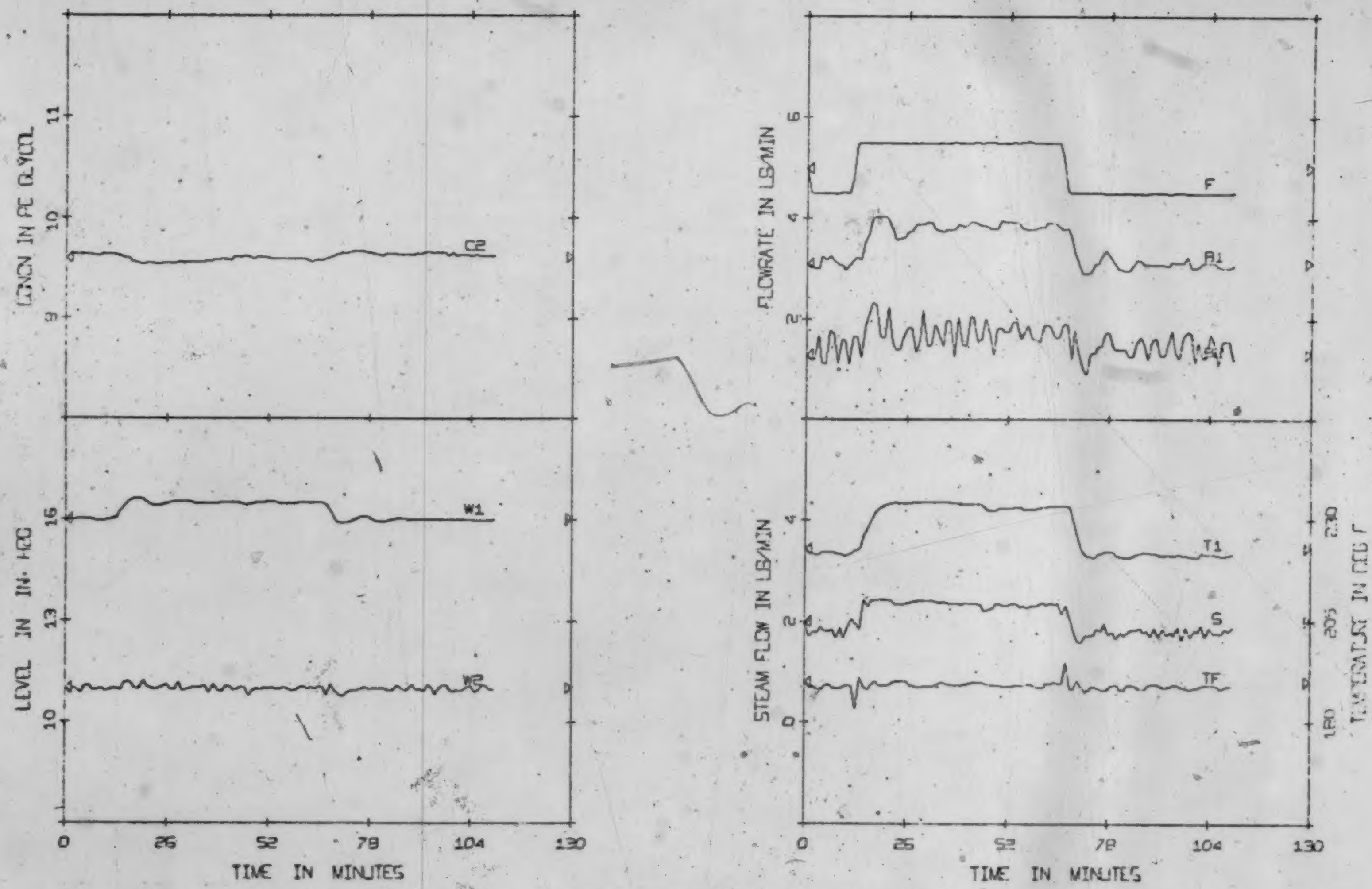

Figure 6.12 Experimental Dynamic Controller NADY0530 from Frequency Domain Techniques
|G=5| NADY0530| Exp| K = Table B.3| INA + DNA| D + P| ± 20% F| N|

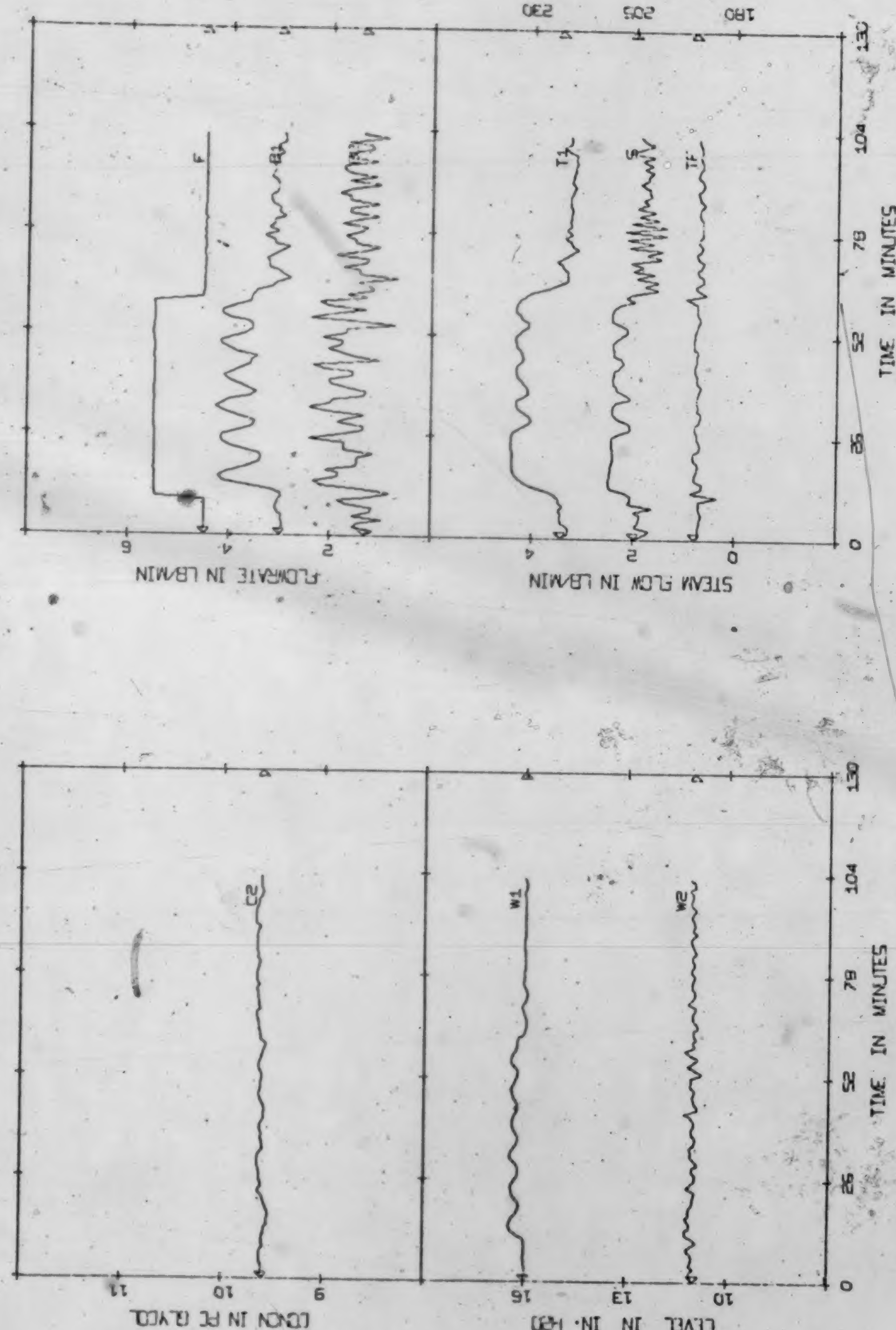

Figure 6.13 Experimental Dynamic Controller NADY0540 from Frequency Domain Techniques |G=5| NADY0540| Exp| K = Table B.3| INA + DNA| D + P| ± 20% F| N|

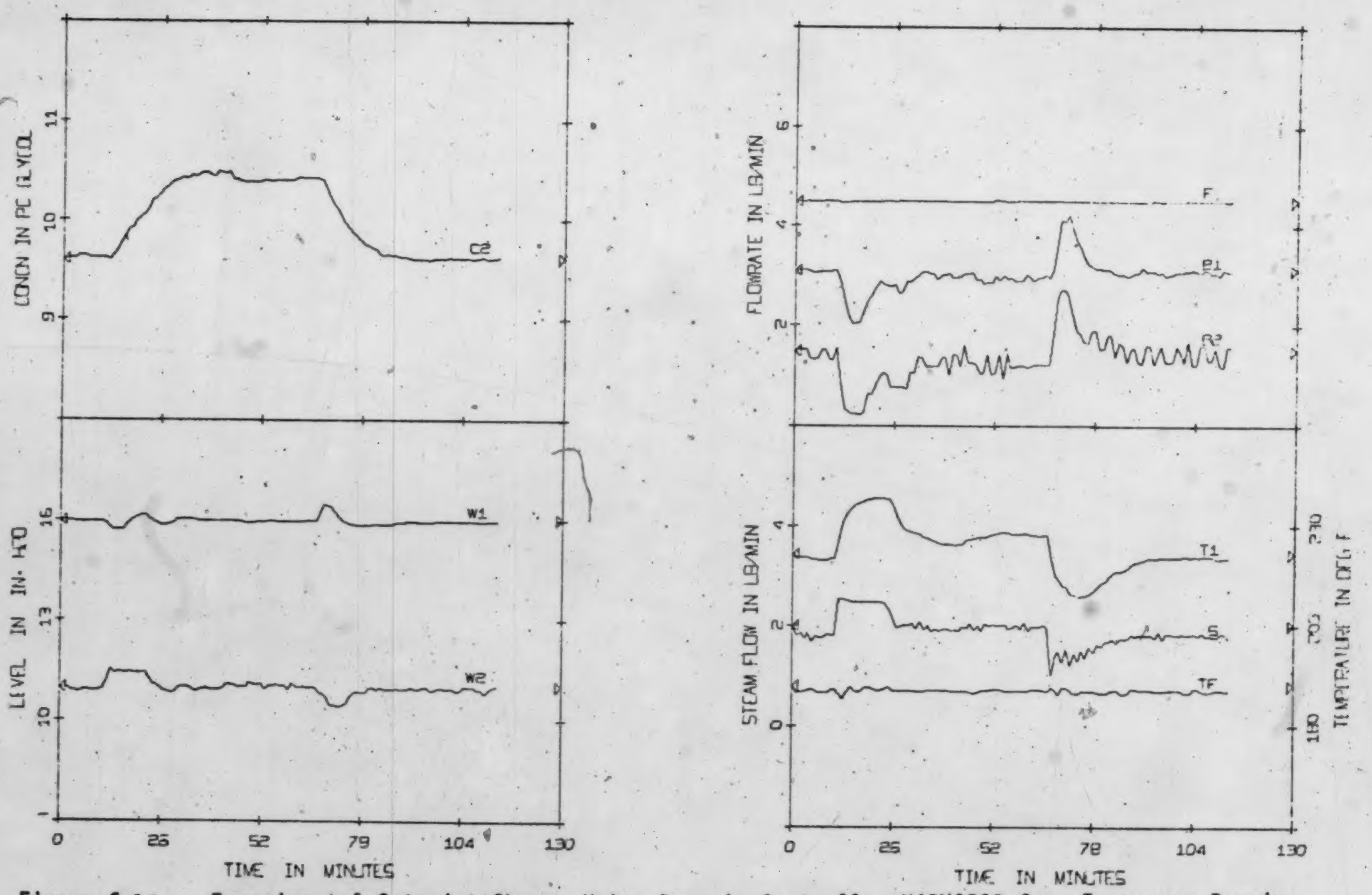

Figure 6.14 Experimental Setpoint Change Using Dynamic Controller NADY0520 from Frequency Domain Techniques
|G=5| NADY0520| Exp| K = Table B.3| INA + DNA| D + P| ± 10% C_2| N|

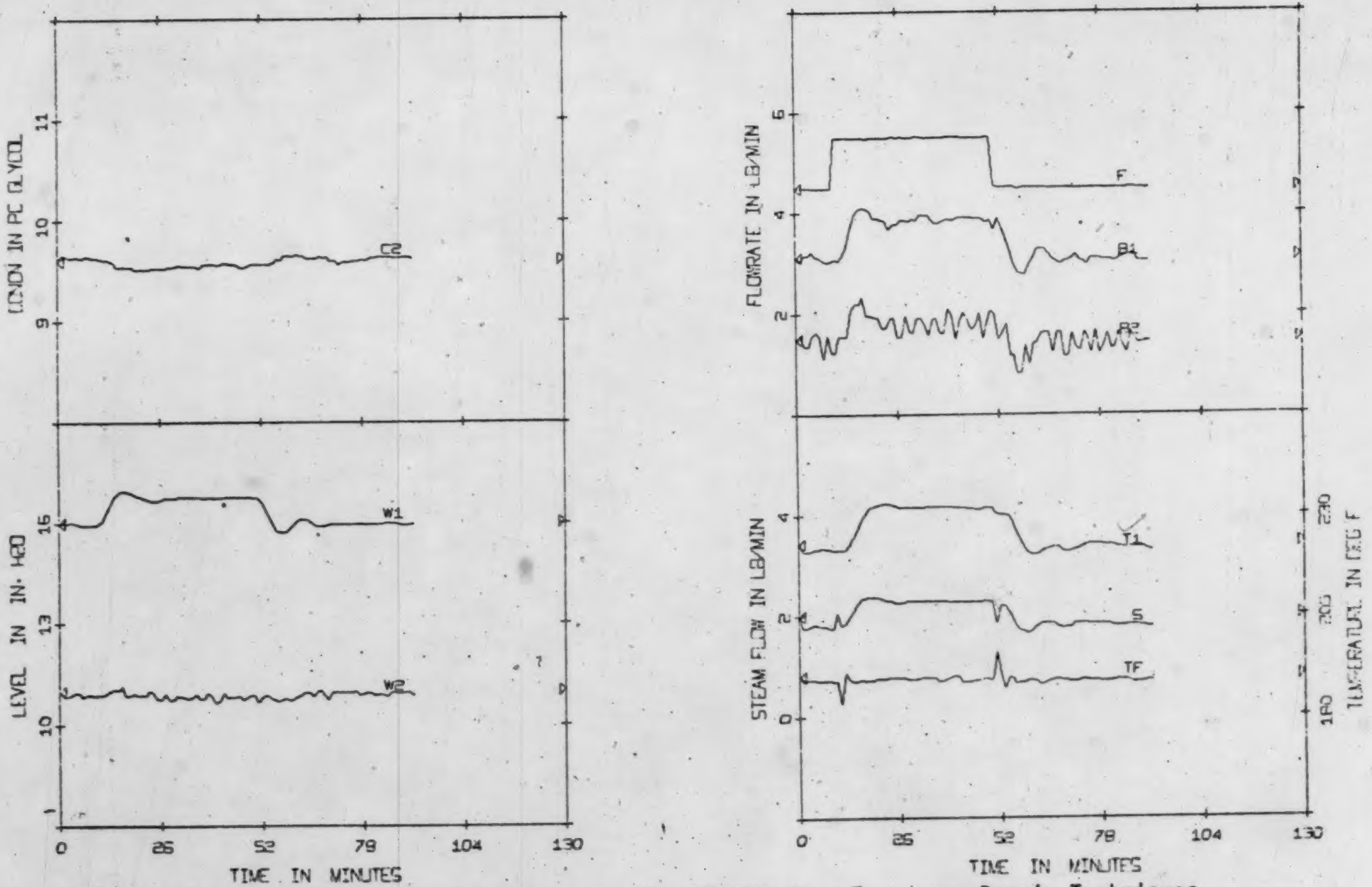

Figure 6.15 Experimental Proportional Controller FD0520 from Frequency Domain Techniques
|G=3,5| FD0520| Exp| K = Table B.1| INA + DNA + CL| P| ± 20% F| N|

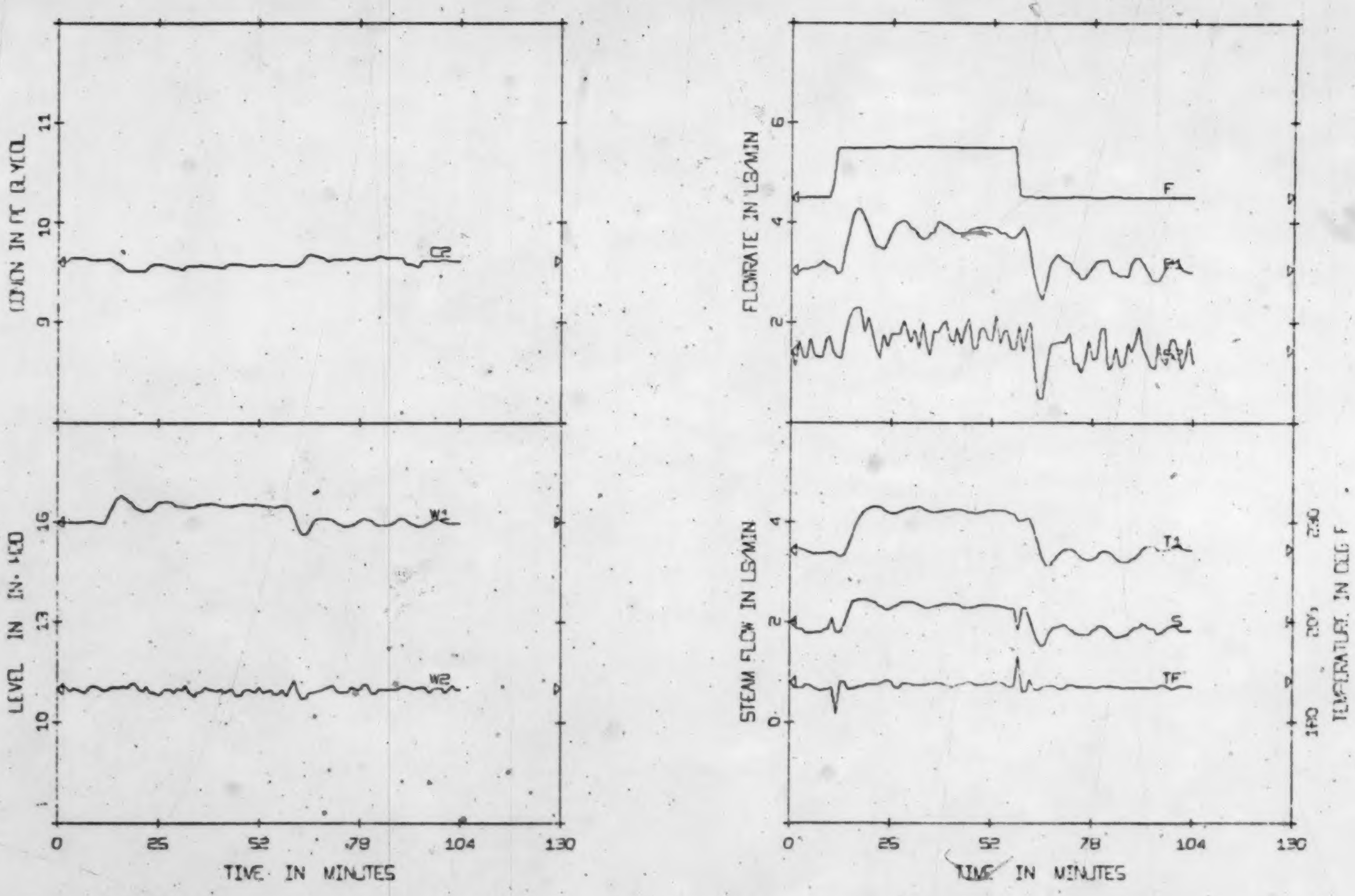

Figure 6.16 Experimental Proportional Controller FD0530 from Frequency Domain Techniques |G=3,5| FD0530| Exp| K = Table B.1| INA + DNA + CL| P| ± 20% F| N|

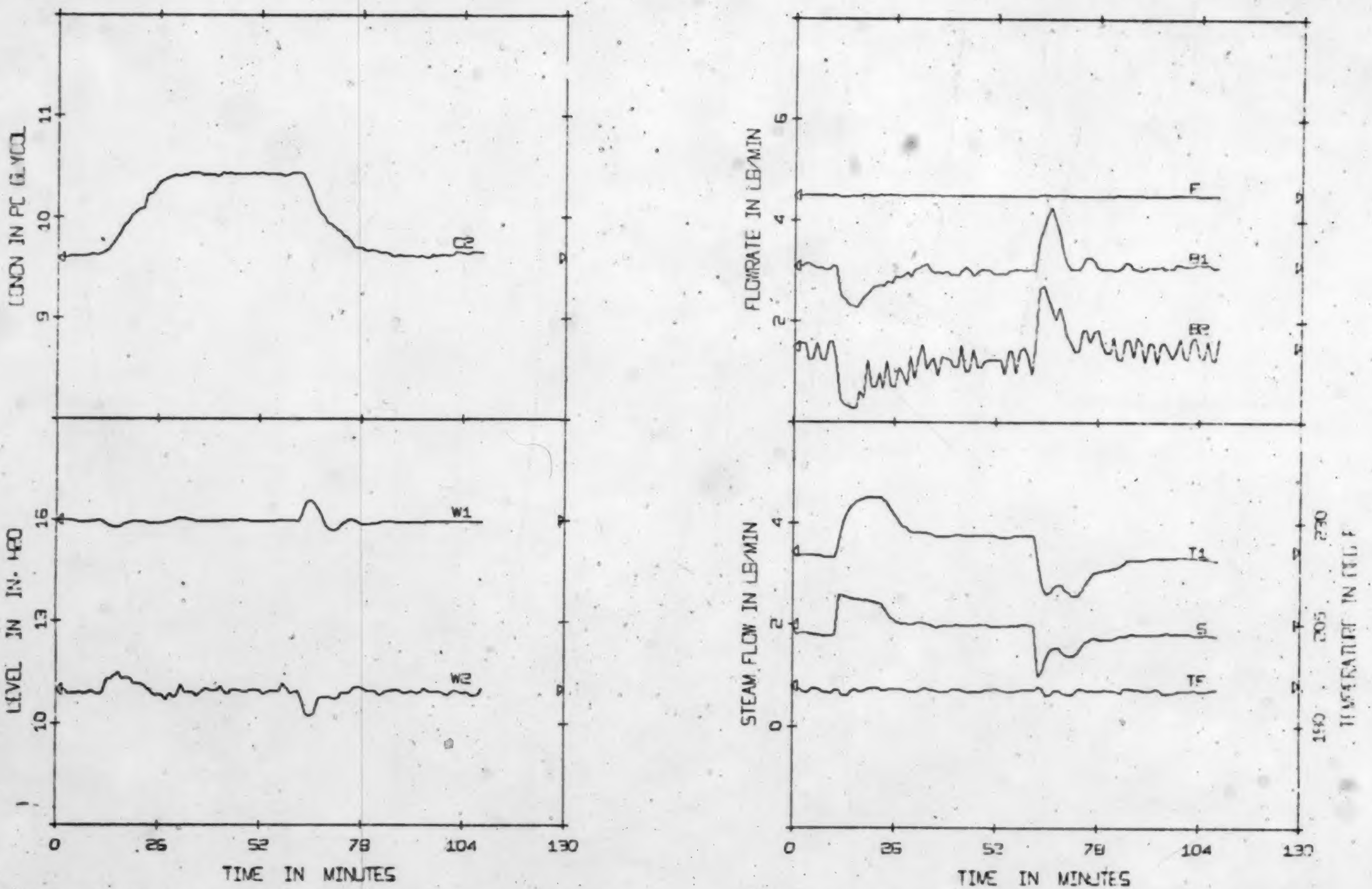

Figure 6.17 Experimental Setpoint Change Using Proportional Controller FD0520 from Frequency Domain Techniques
|G=3,5| FD0520| Exp| K = Table B.1| INA + DNA + CL| P| ± 20% F| N|

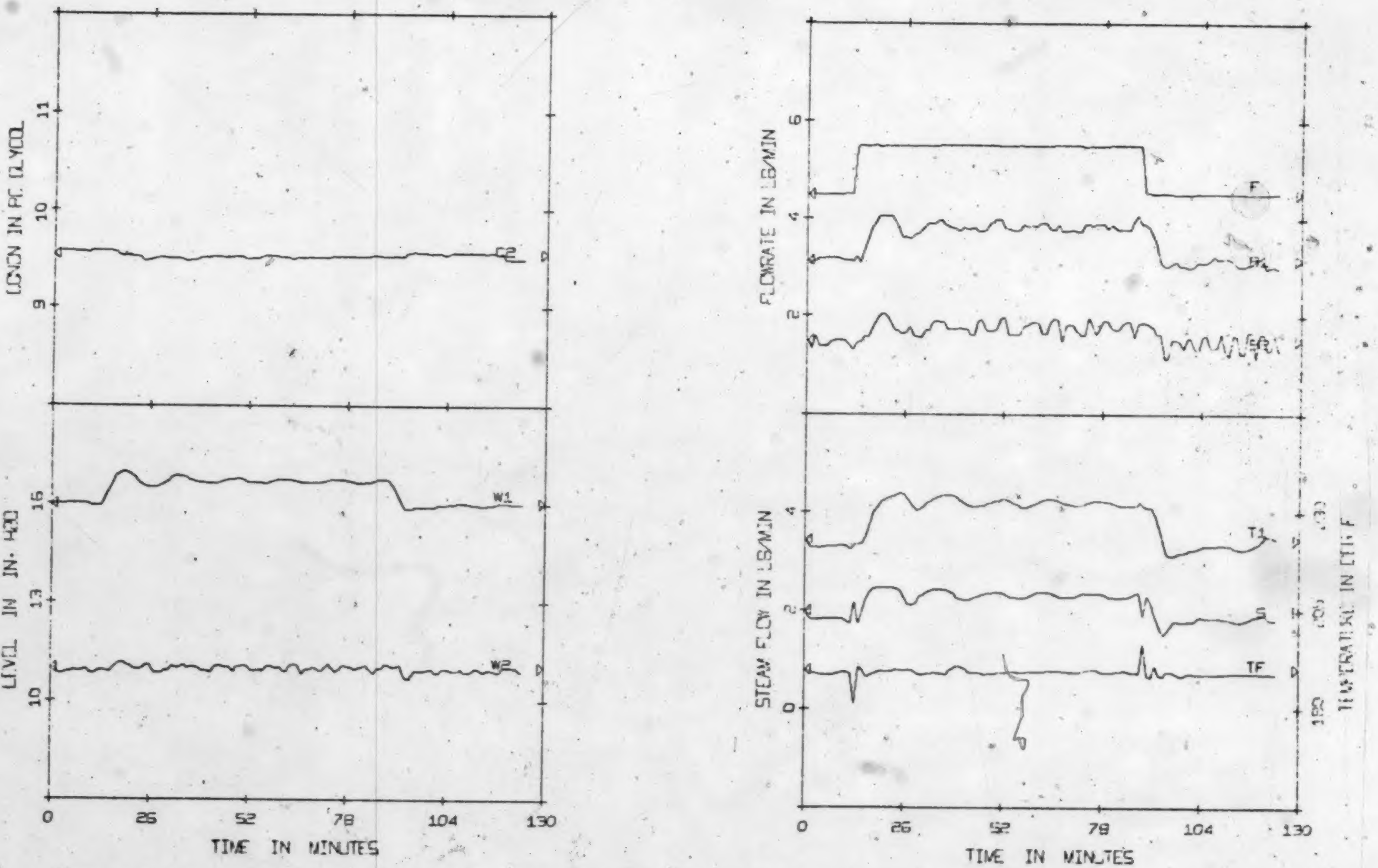

Figure 6.18 Experimental Optimal Proportional Controller OP0501
|G=5| OP0501| Exp | K = (6.19)| OPT | P | ± 20% F | N |

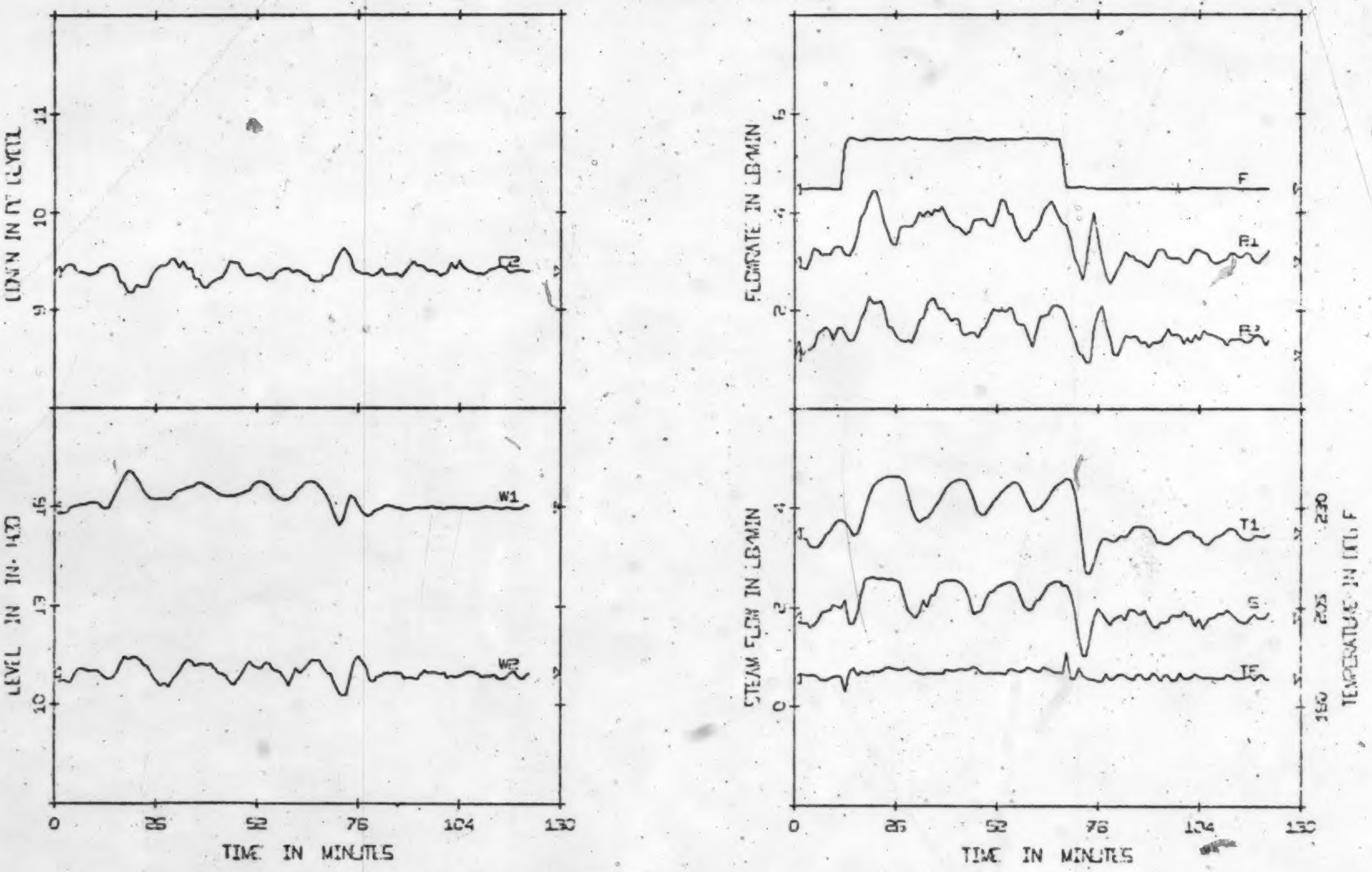

Figure 6.19 Experimental Optimal Proportional Controller OP0300
|G=3| OP0300| Exp| K = (6.13)| OPT| P| ± 20% F| 0|

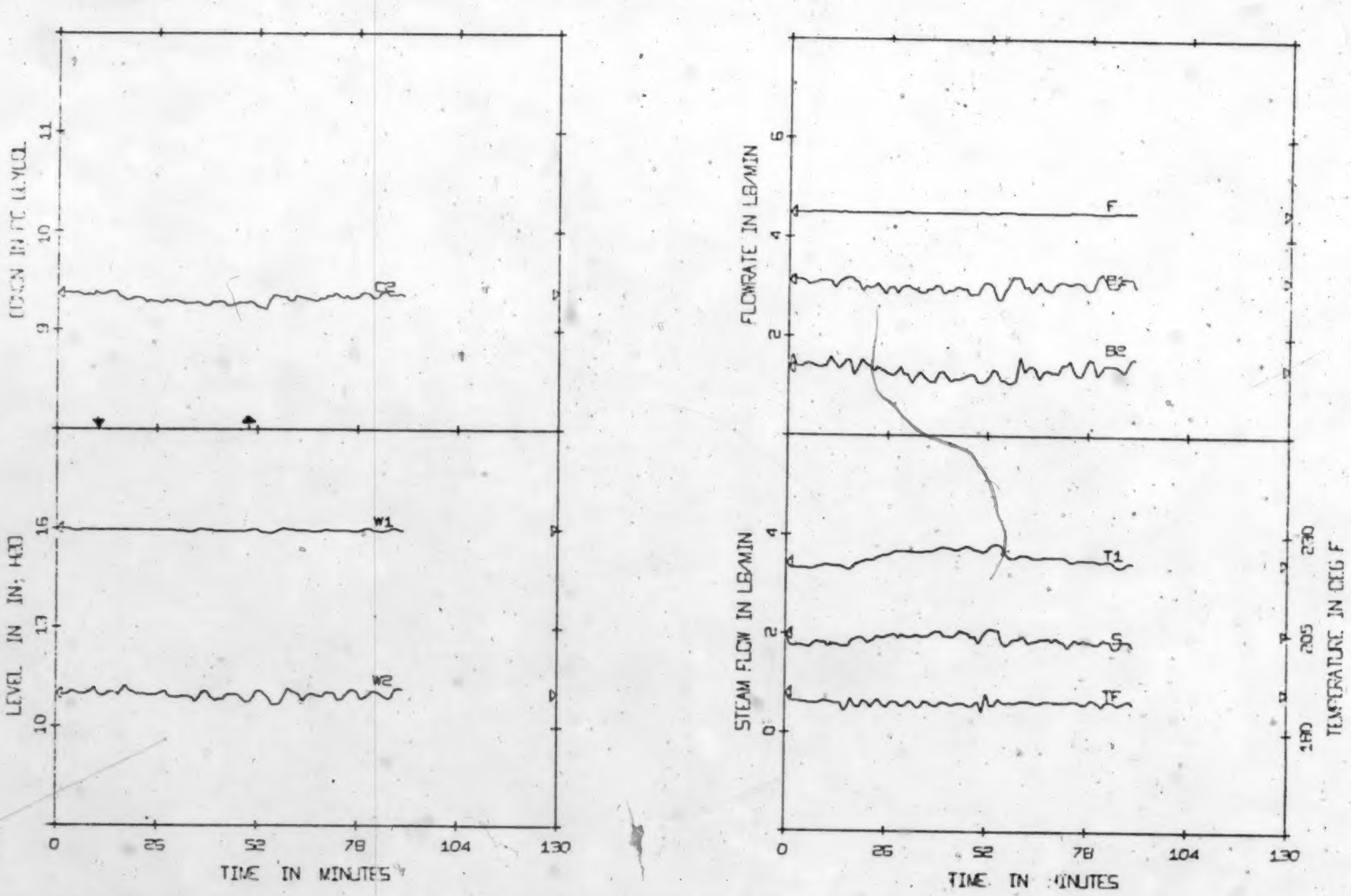

Figure 6.20 Experimental Optimal Proportional Controller OP0300
|G=3| OP0300| Exp| K = (6.13)| OPT| P| ± 20% FC| 0|

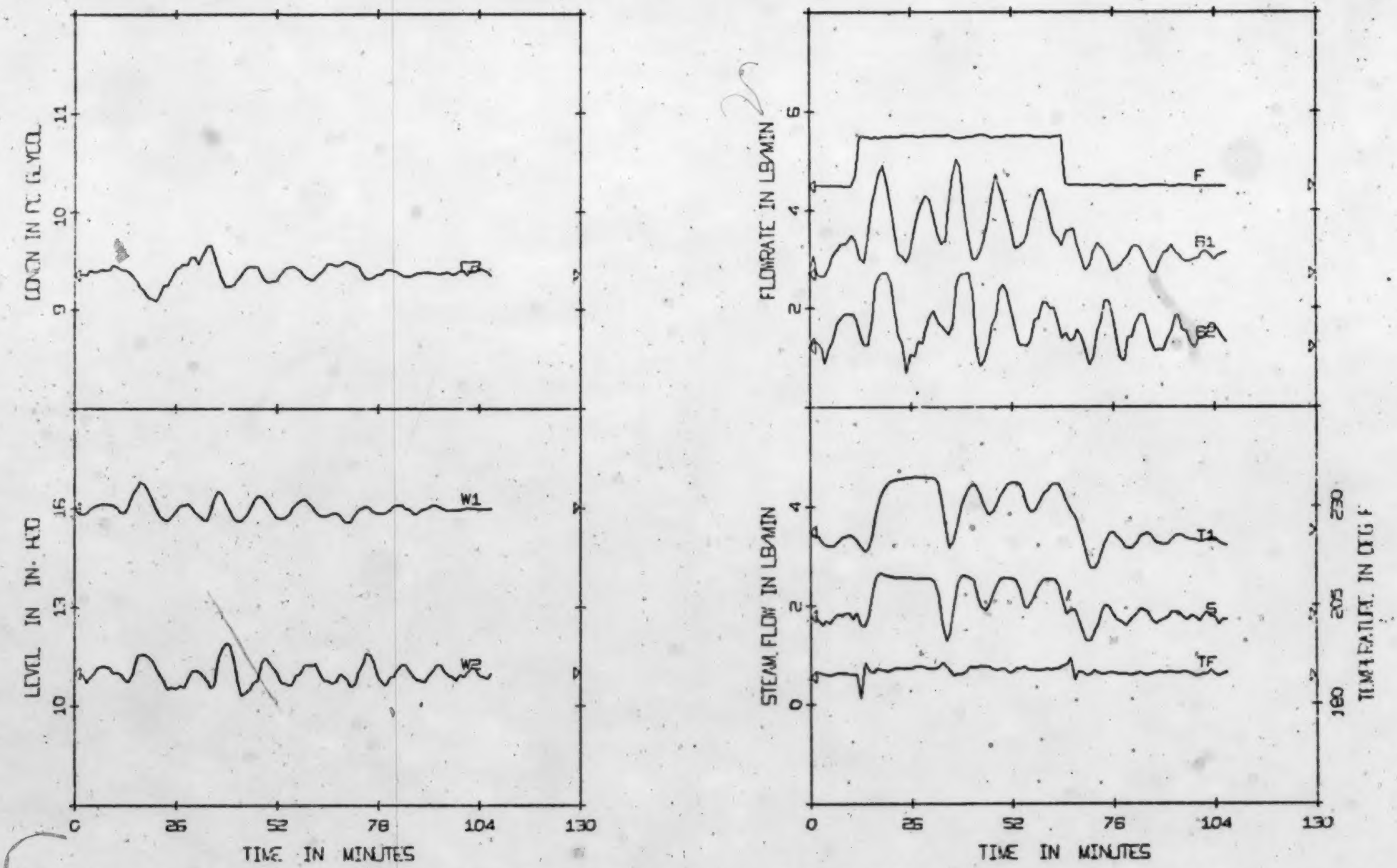

Figure 6.21 Experimental Optimal Proportional-integral Controller OPI300
|G=3| OPI300| Exp| K = (6.15)(6.16)| OPT| P + I| ± 20% F| 0|

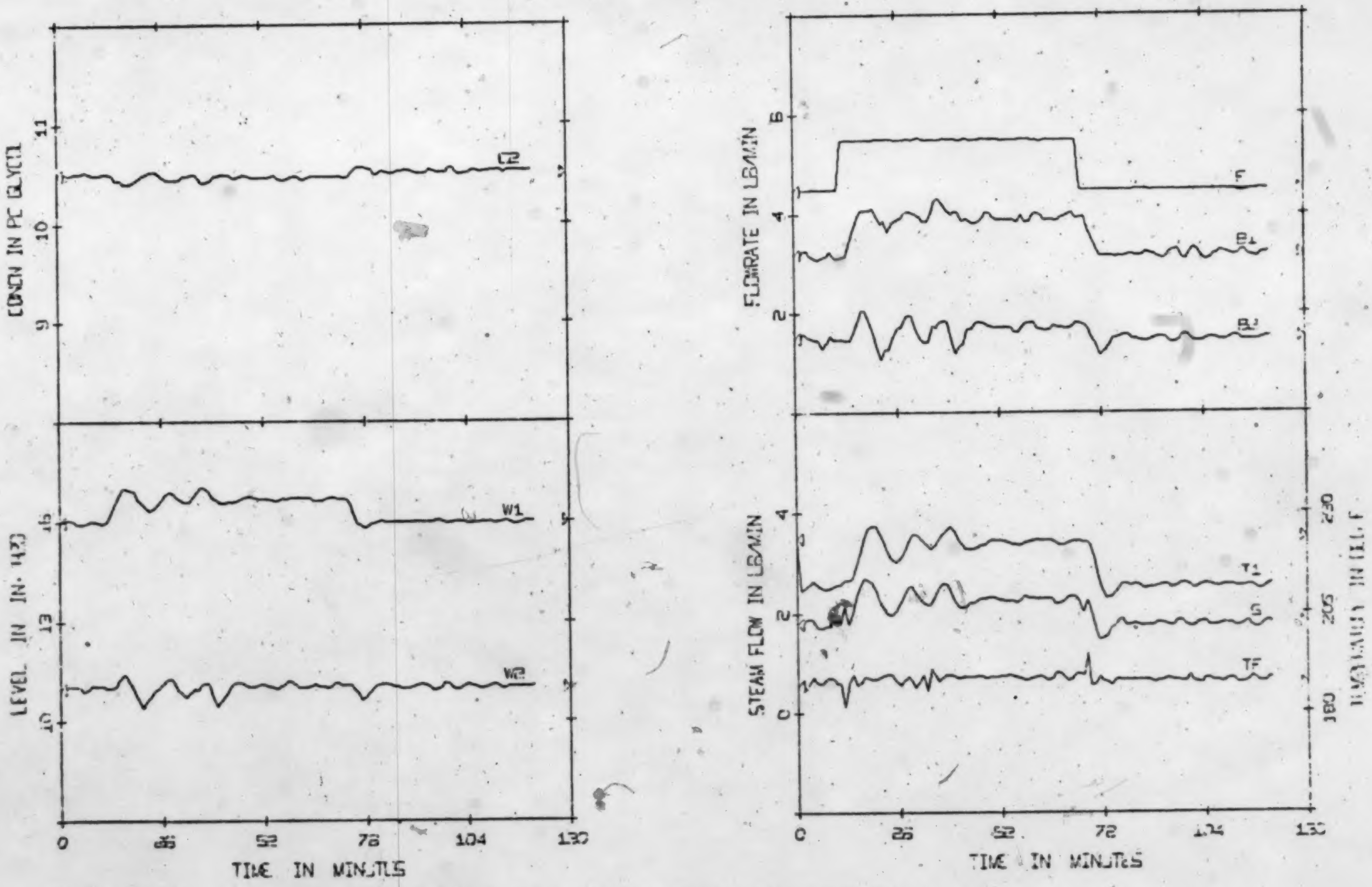

Figure 6.22 Experimental Optimal Proportional Controller OP0500
|G=5| OP0500| Exp| K = (6.19)| OPT| P| ± 20% F| N|

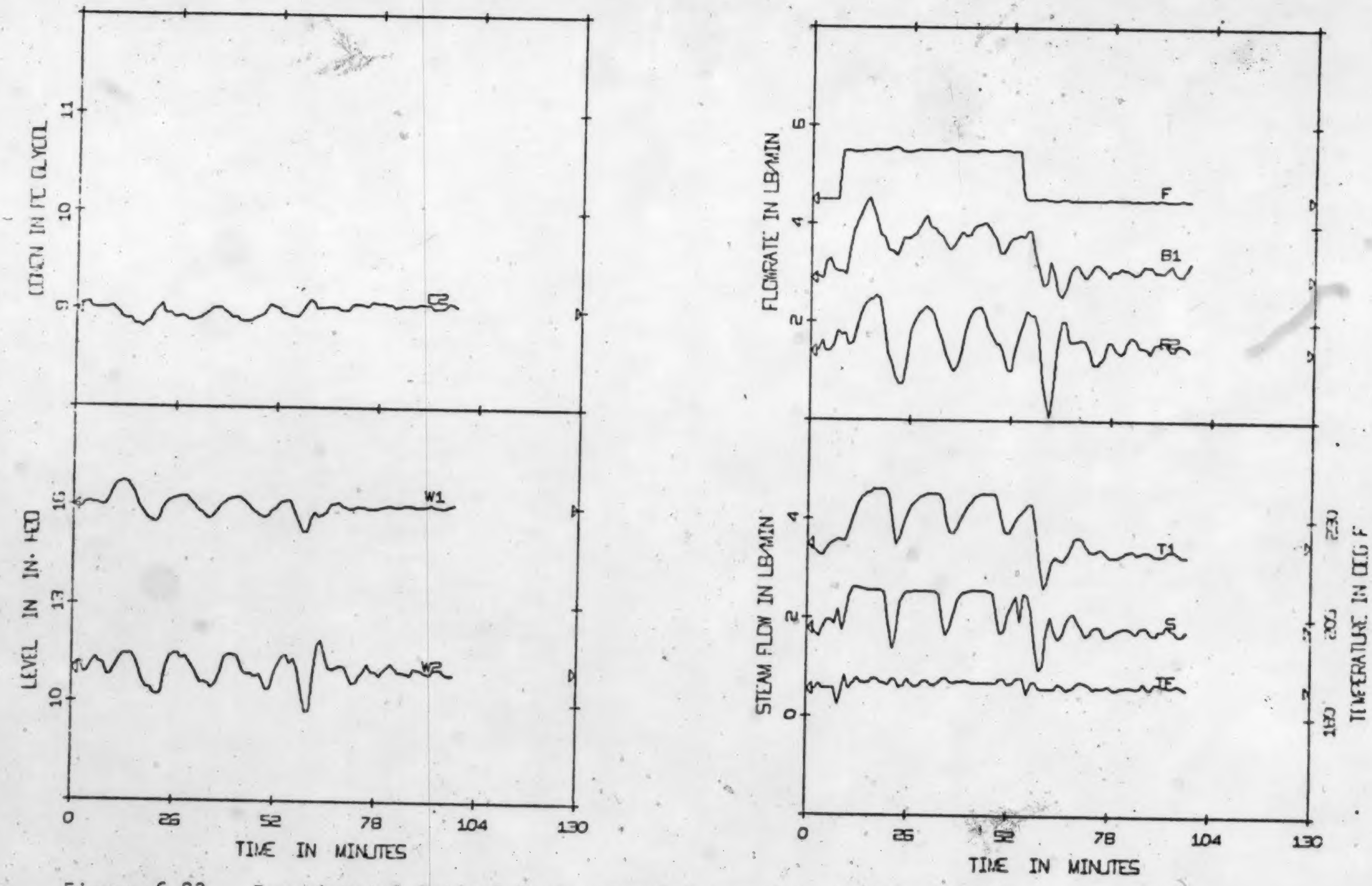

Figure 6.23 Experimental Optimal Proportional-integral Controller OPI500
|G=3| ML0200| Exp| K = Table 6.1| MUL| P| ± 20% F| 0|

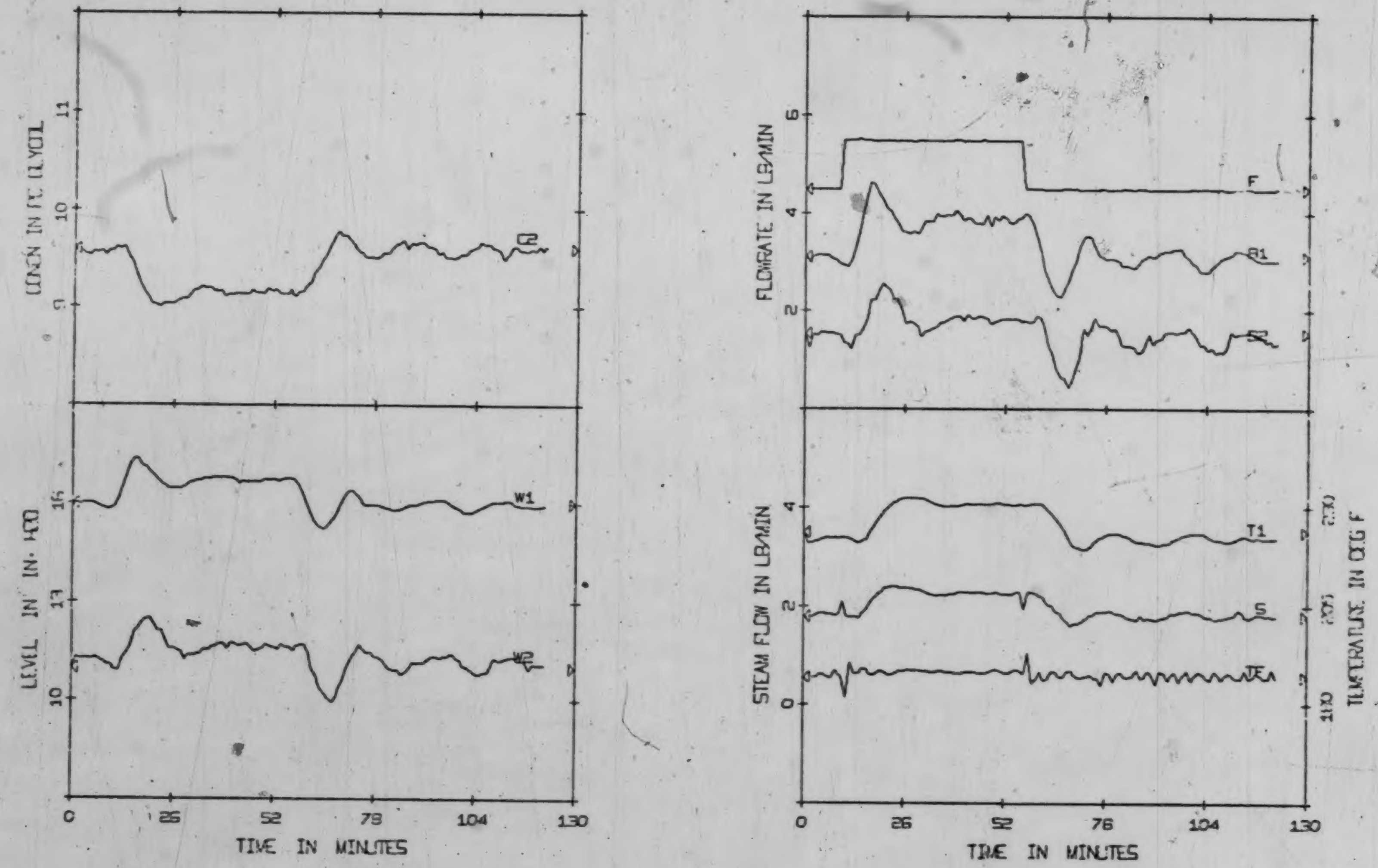

Figure 6.24 Experimental Multiloop Proportional Controller ML0200
|G=3| ML0200| Exp| K = Table 6.1| MUL| P| ± 20% F| 0|

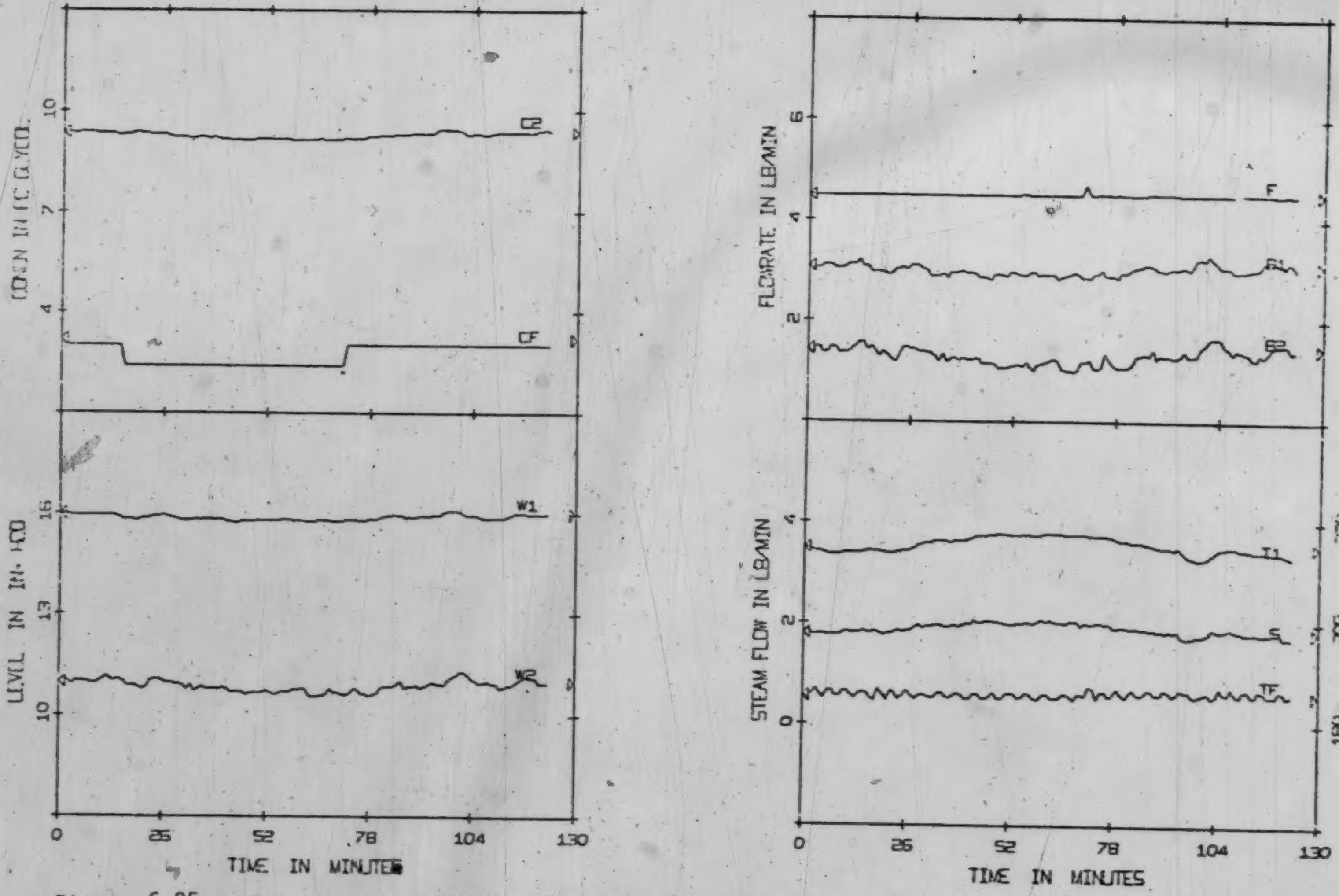

Figure 6.25 Experimental Multiloop Proportional Controller ML0200
|G=3| ML0200| Exp| K = Table 6.1| MUL| P| ± 20% FC| 0|

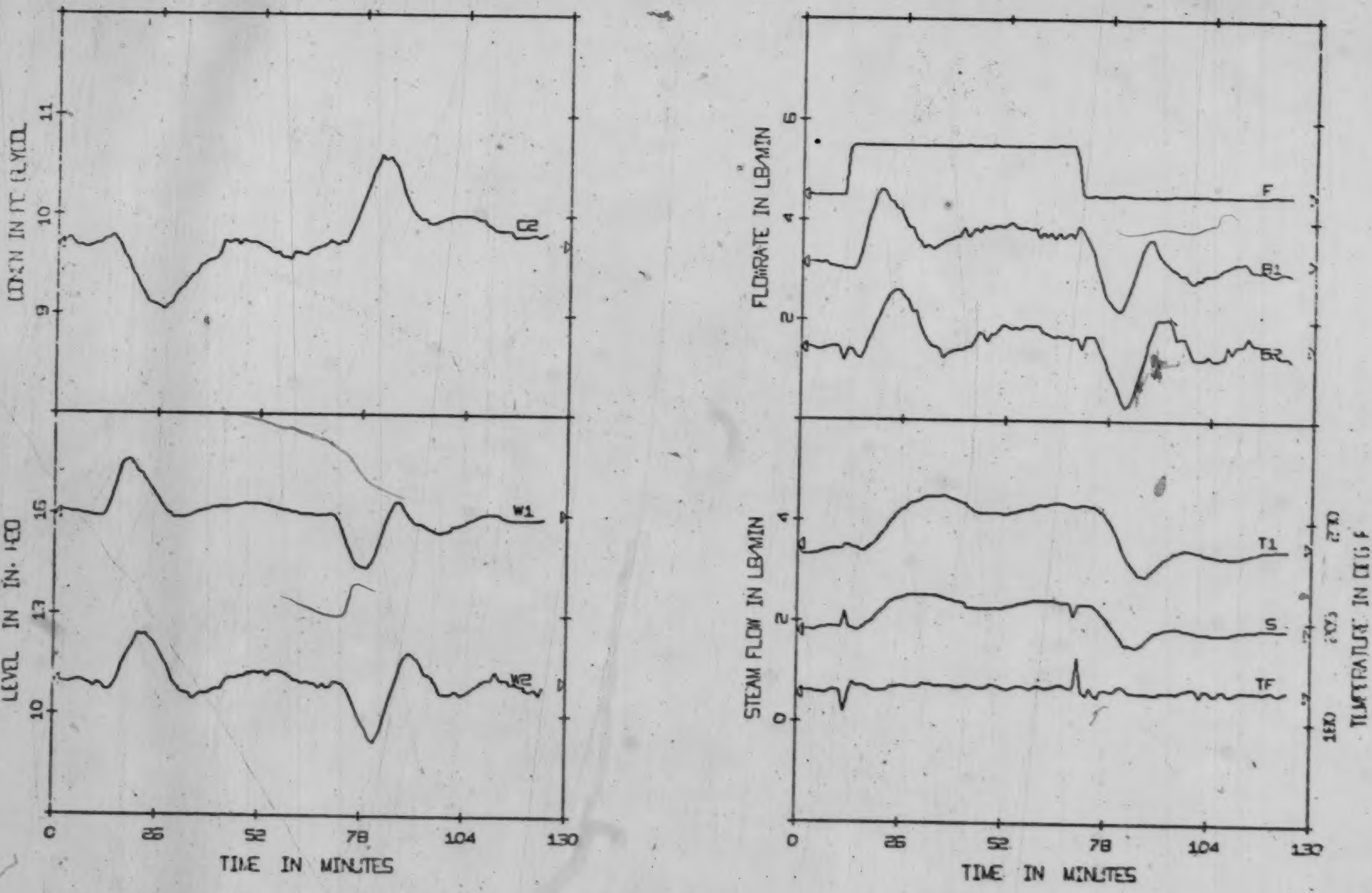

Figure 6.26 Experimental Multiloop Proportional-integral Controller MLI200
|G=3| MLI200| Exp| K = Table 6.1| MUL| P| ± 20% F| O|

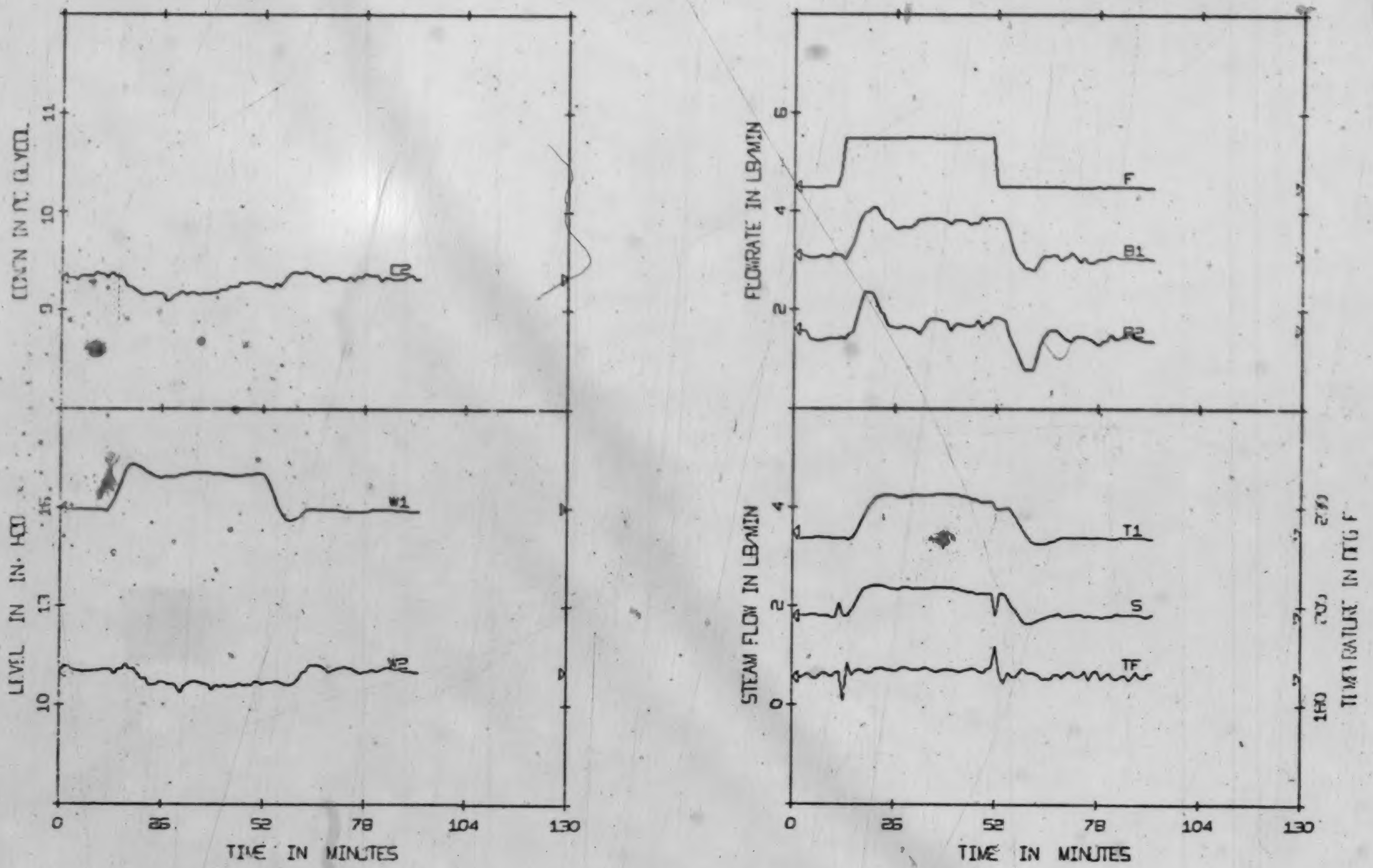

Figure 6.27 Experimental Proportional Controller DNA0520 from Nyquist Array Method
|G=5| DNA0 20| Exp| K = Table B.4| DNA| P| ± 20% F|0|

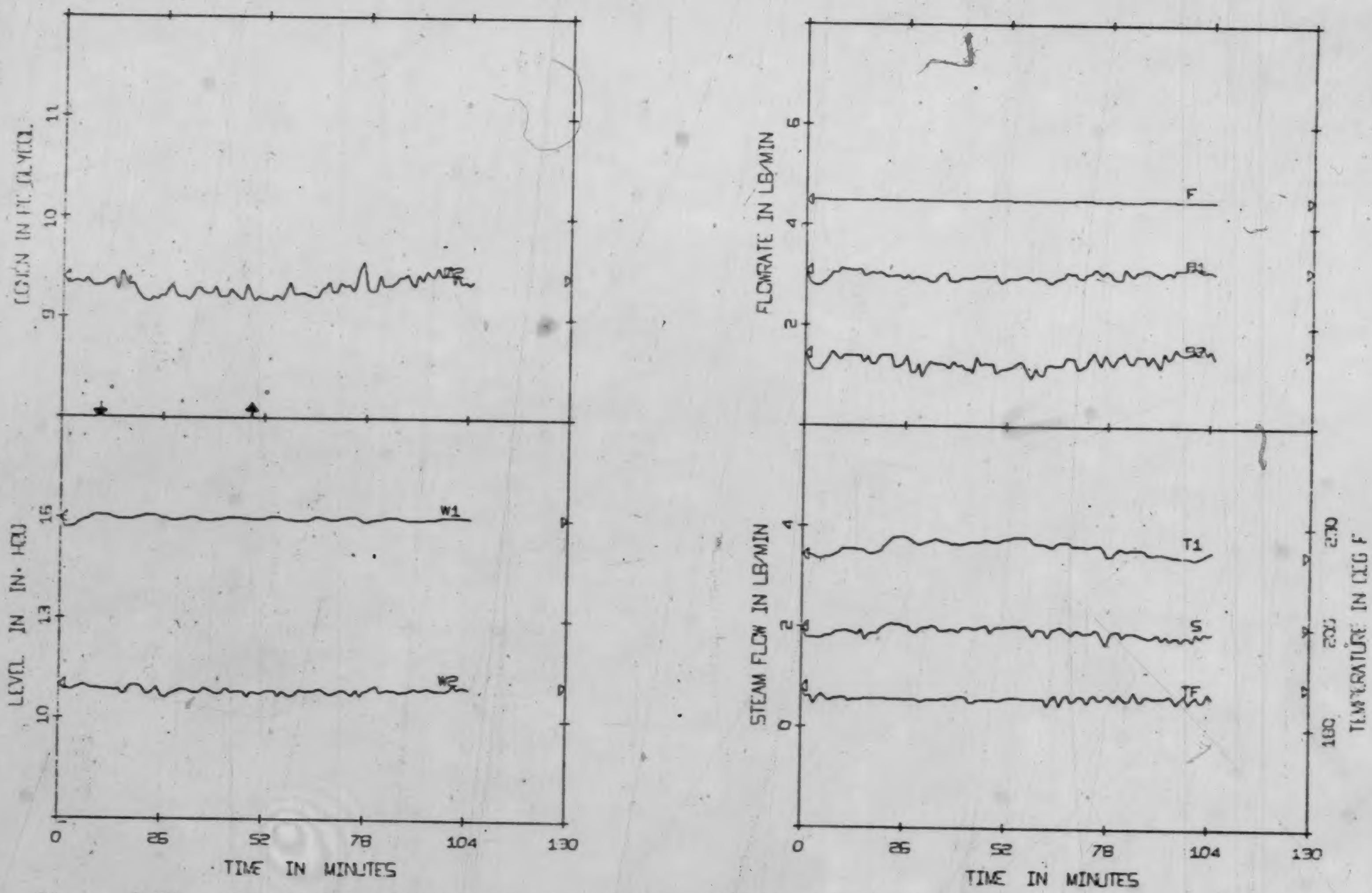

Figure 6.28 Experimental Proportional ControllerDNA0520 from Nyquist Array Method
|G=5| DNA0520| Exp| K = Table B.4| DNA| P| ± 20% FC| 0|

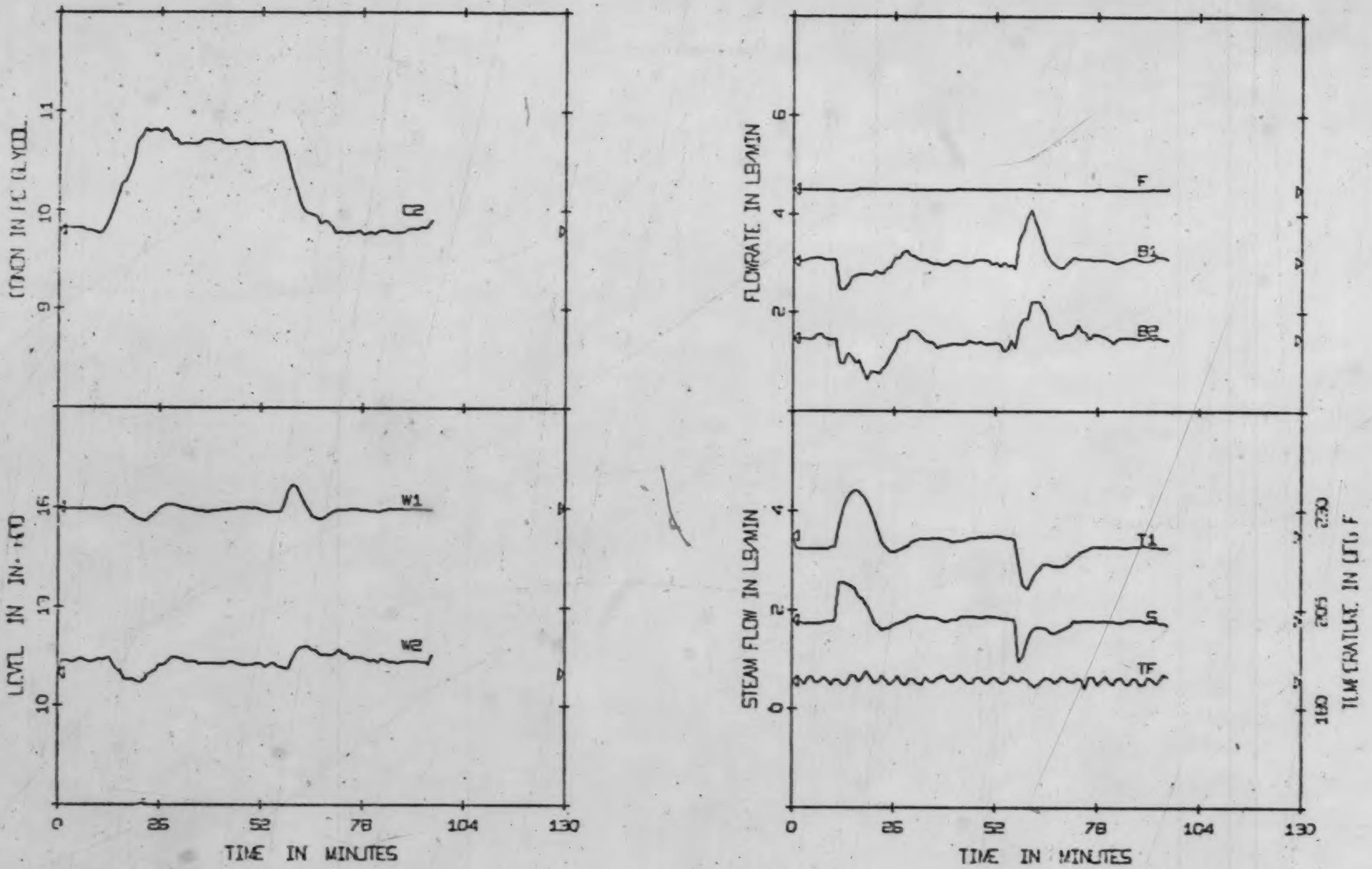

Figure 6.29 Experimental Setpoint Change Using Proportional Controller DNA0520 from Nyquist Array Method
|G=5| DNA0520| Exp| K = Table B.4| DNA| P| ± 10% C_2| 0|

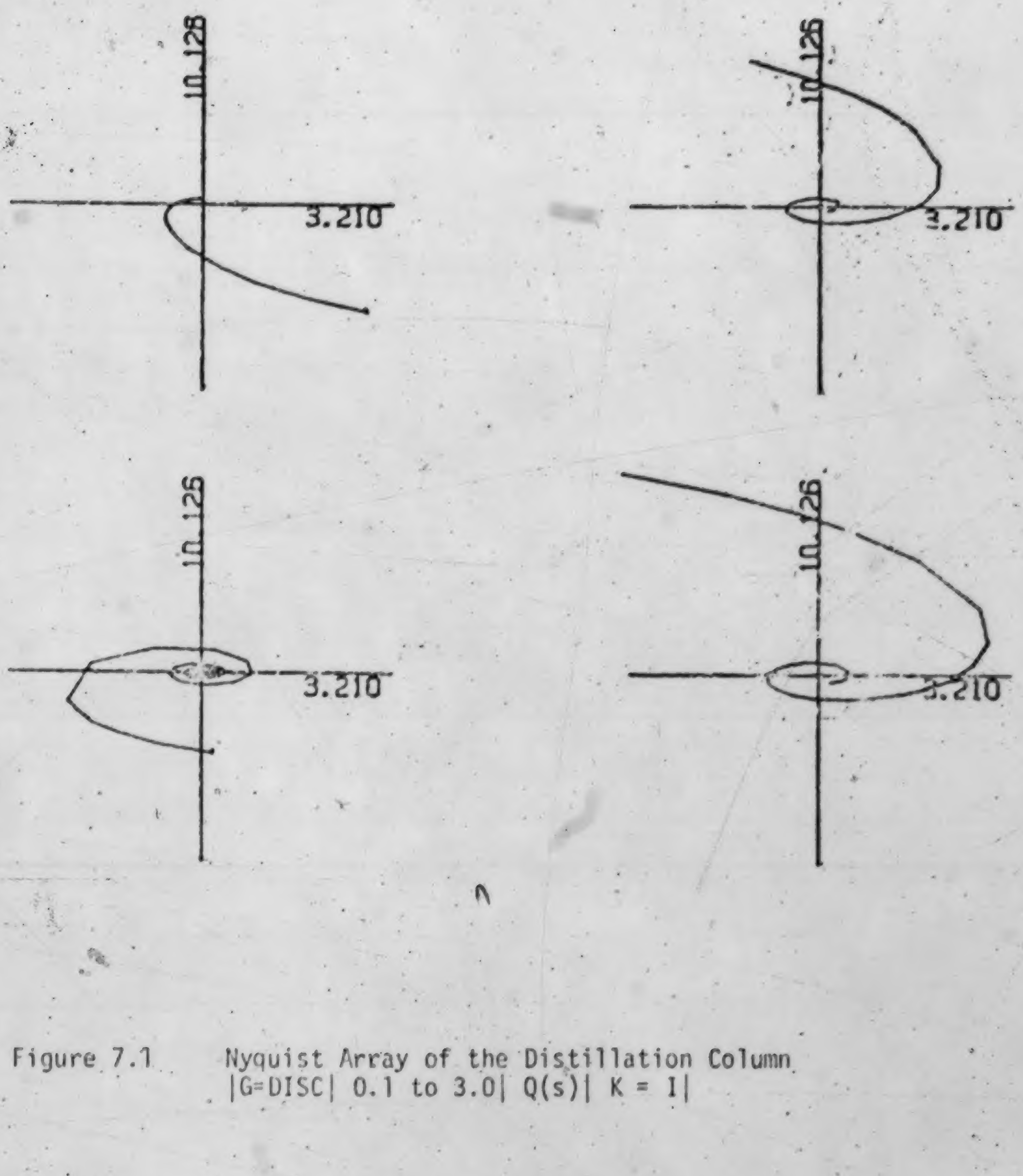

Figure 7.1 Nyquist Array of the Distillation Column
|G=DISC| 0.1 to 3.0| Q(s)| K = I|

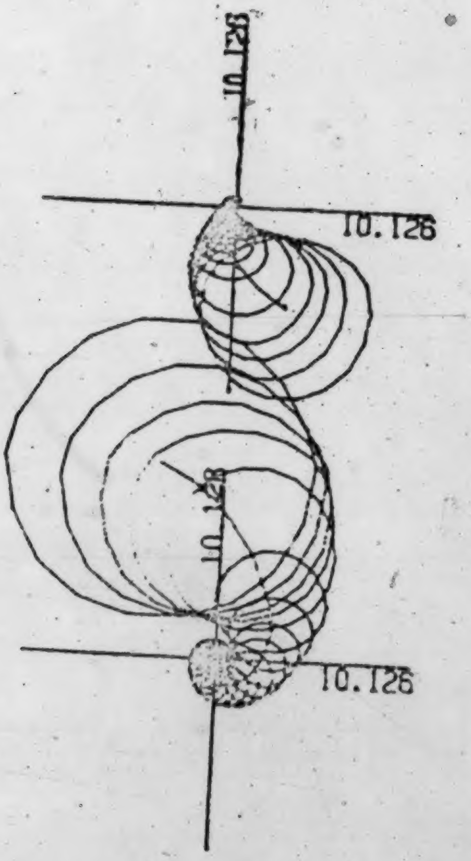

Figure 7.2 Diagonal Elements of the Distillation Column With Their Gershgorin Bands
|G=DISC| 0.1 to 3.0| Q(s)| K = I|

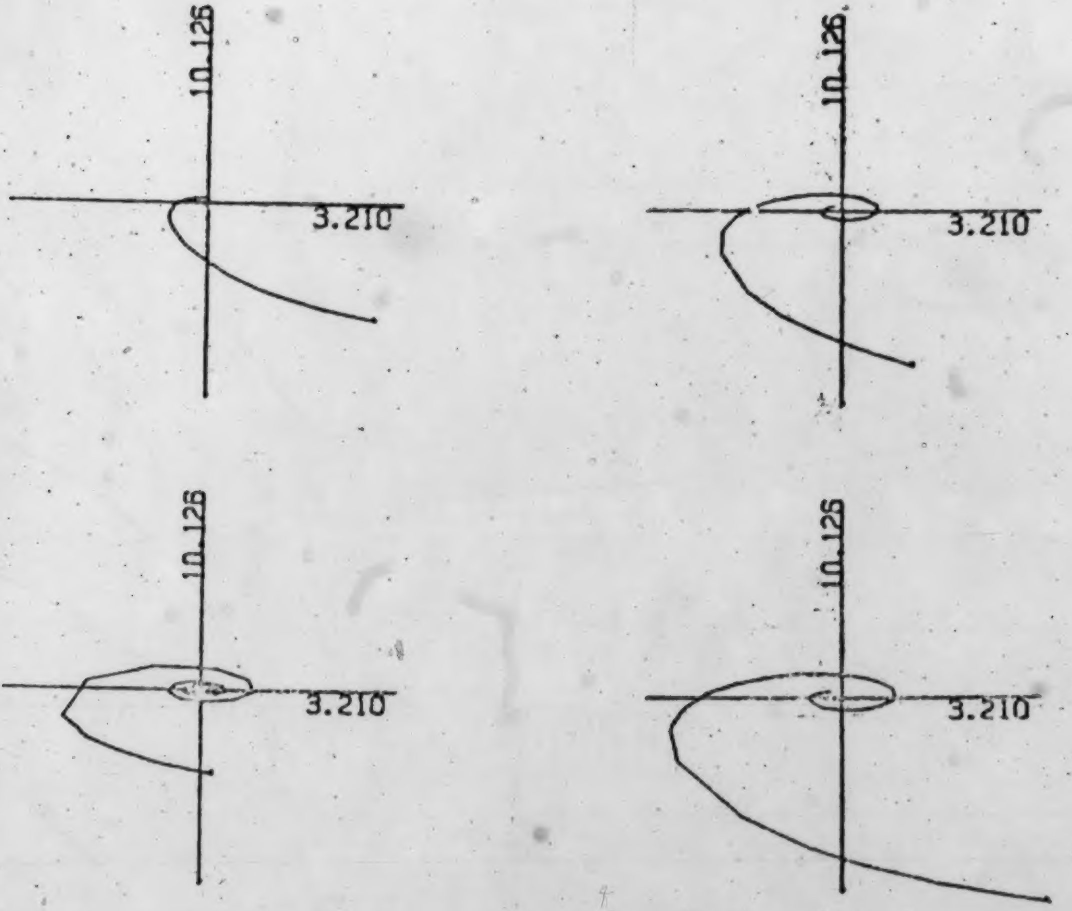

Figure 7.3 Nyquist Array of the OLTFM $Q_1(s)$
|G=DISC| 0.1 to 3.0| $Q_1(s)$| K_1 = (7.2)|

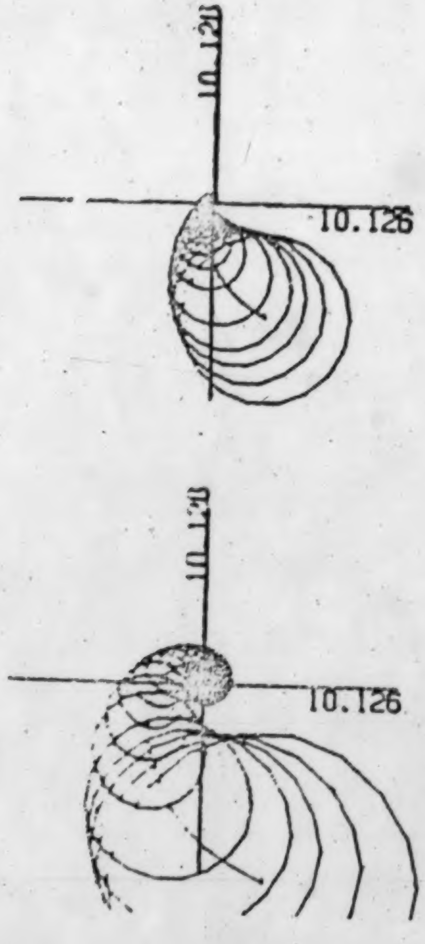

Figure 7.4 Diagonal Elements of $Q_1(s)$ With Their Gershgorin Bands
|G=DISC| 0.1 to 3.0| $Q_1(s)$| K_1 = (7.2)|

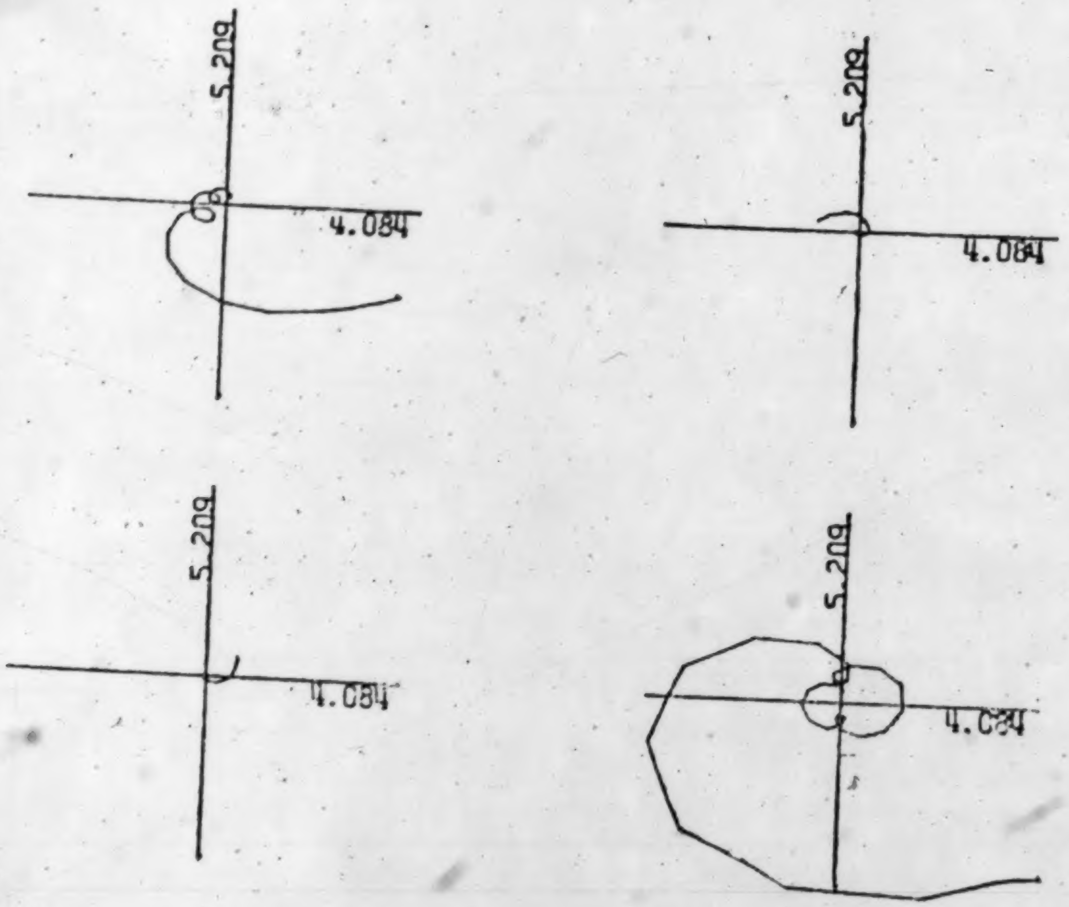

Figure 7.5 Nyquist Array of the OLTFM $Q_2(s)$
|G=DISC| 0.1 to 3.0| $Q_2(s)$| $K_1 K_2$ = (7.9)|

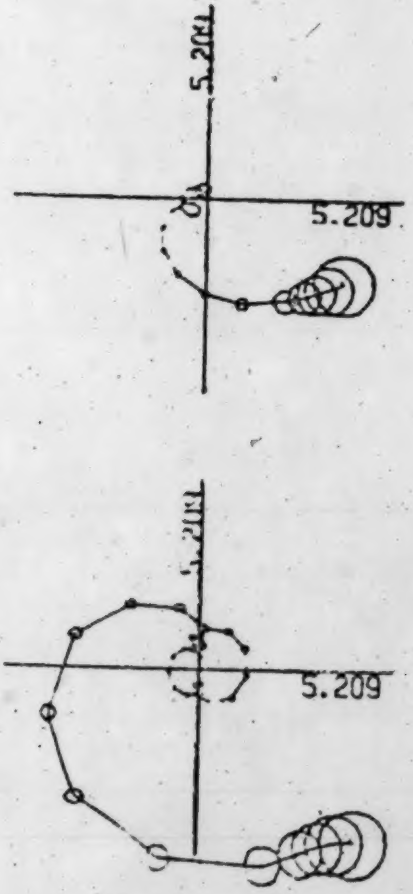

Figure 7.6 Diagonal Elements of $Q_2(s)$ with their Gershgorin Bands
|G=DISC| 0.1 to 3.0| $Q_2(s)$| K_1K_2 = (7.9)|

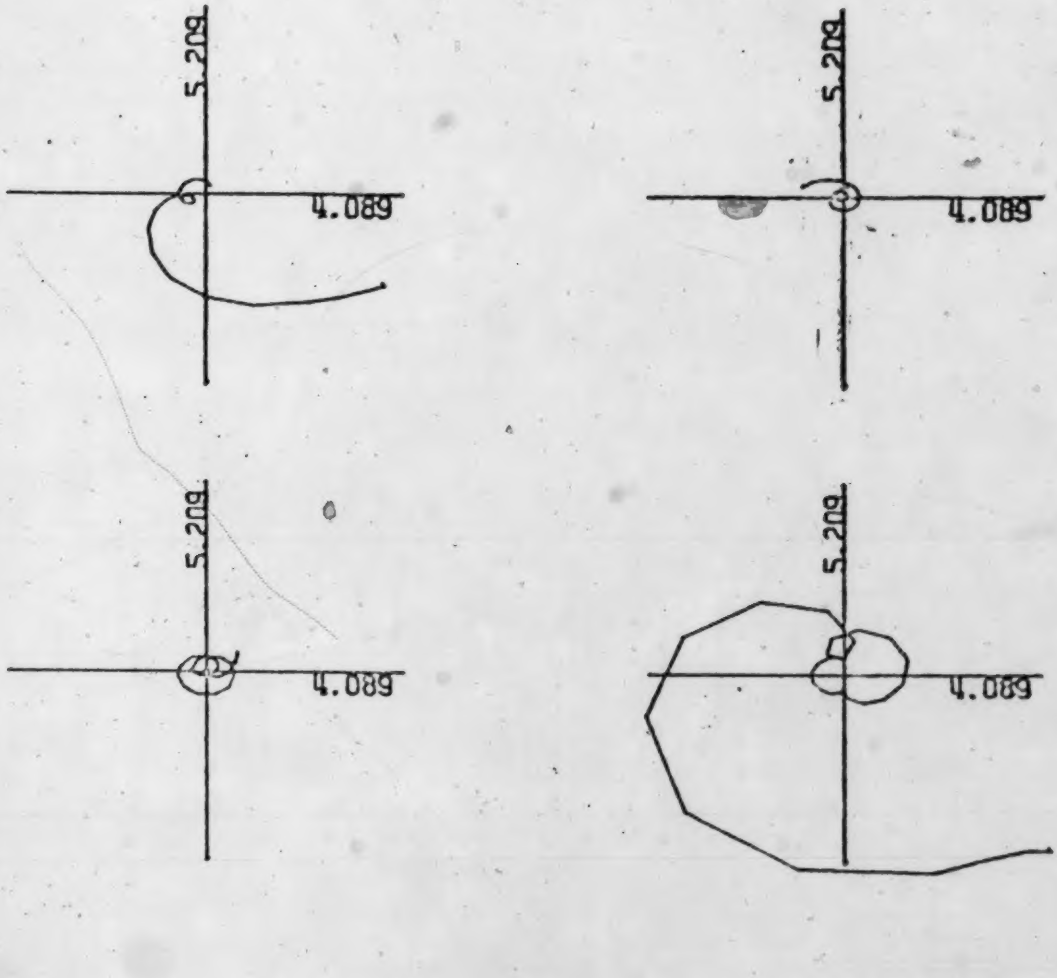

Figure 7.7 Nyquist Array of the OLTFM $Q_2(s)$ When a Second Order Pade Approximation is Used in Controller $K_2(s)$
|G=DISC| 0.1 to 3.0| $Q_2(s)$| K_1K_2 = (7.9)|

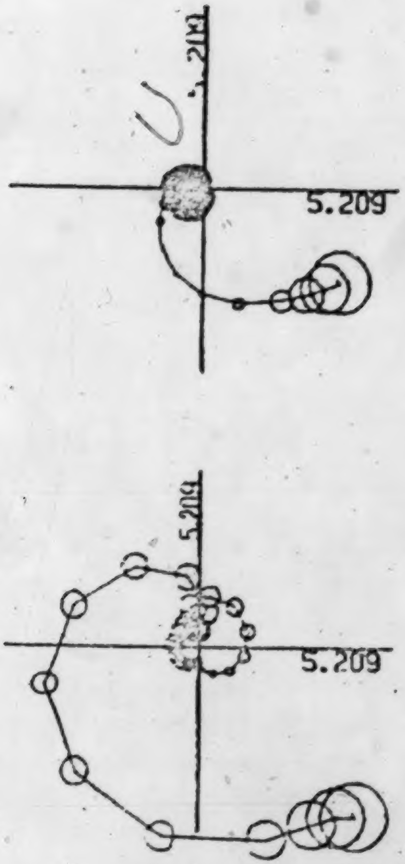

Figure 7.8 Diagonal Elements of $Q_2(s)$ when a Second Order Pade Approximation is Used in Controller $K_2(s)$
$|G=DISC| \; 0.1 \text{ to } 3.0 | \; Q_2(s) | \; K_1K_2 = (7.9)|$

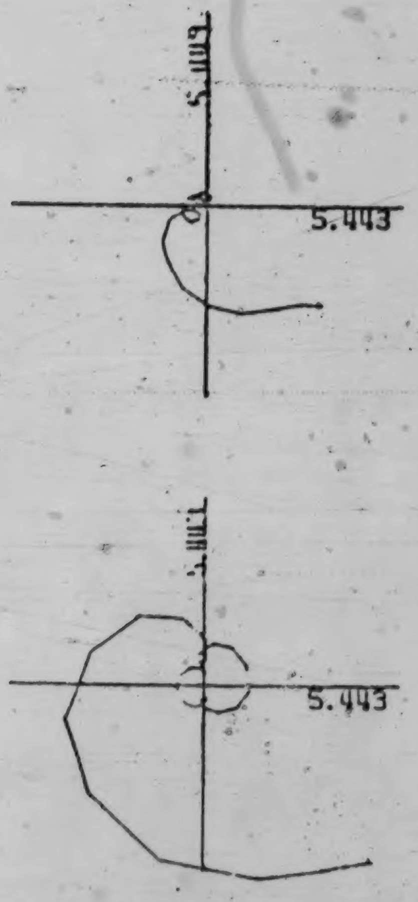

Figure 7.9 Diagonal Elements of Non-interacting OLTFM $Q_2^1(s)$
|G=DISC| 0.1 to 3.0| $Q_2^1(s)$| $K_1K_2^1$ * (7.14)|

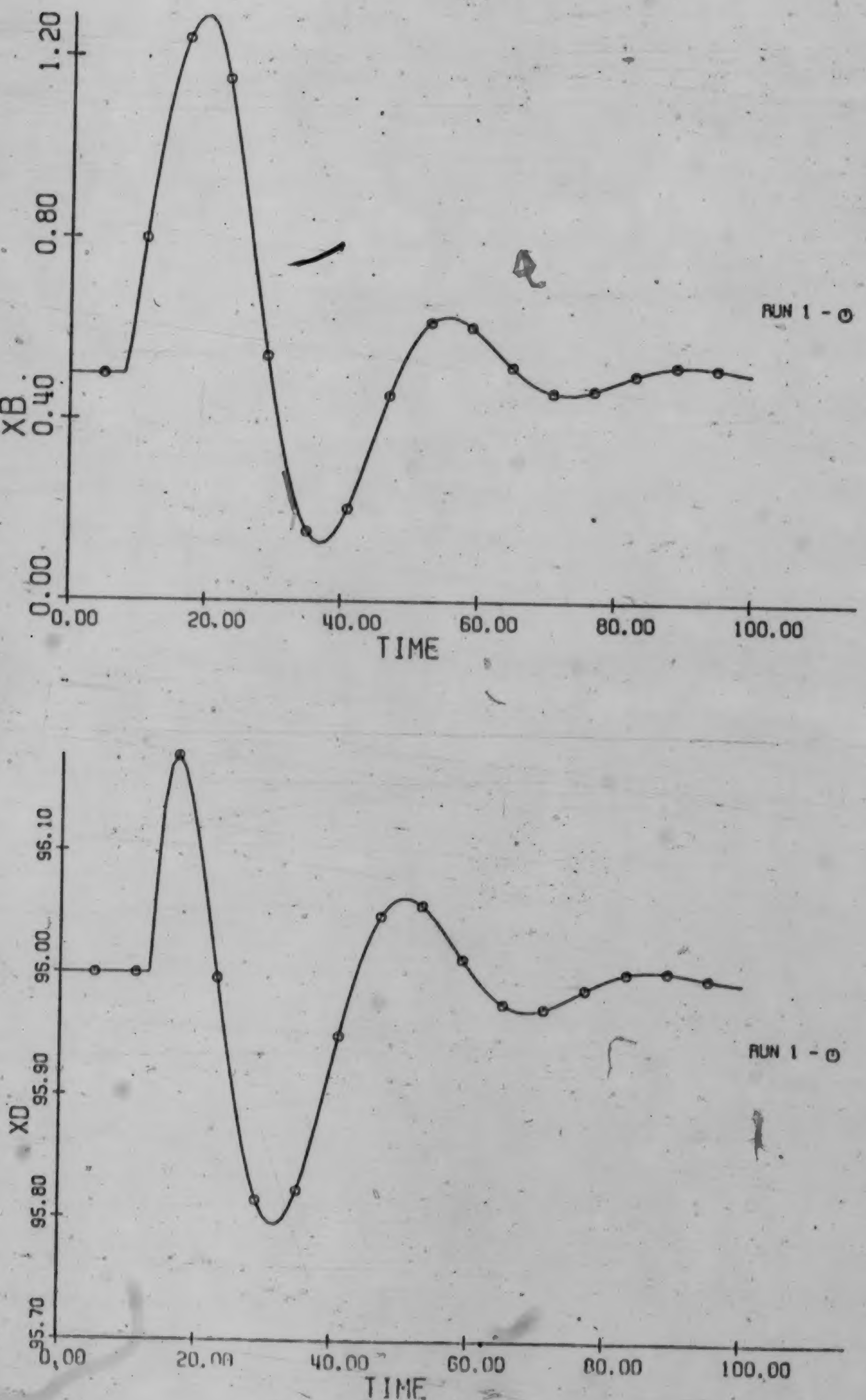

Figure 7.10 Simulated Response of the Distillation Column for a 14% Increase in Feed Flow Using a Multiloop Control

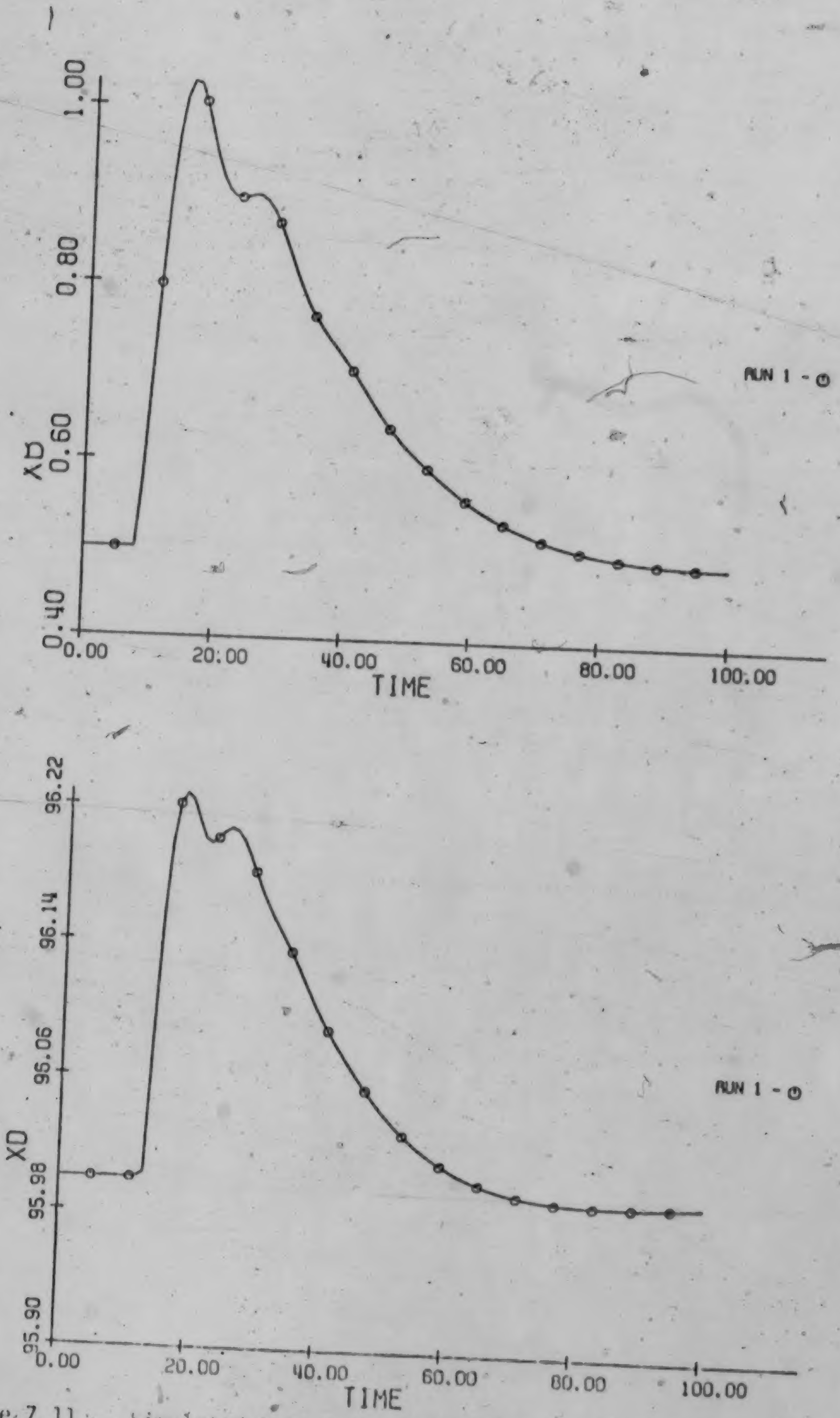

Figure 7.11 Simulated Response of the Distillation Column for a 14% Increase in Feed Flow Using a Diagonally Dominant Control System (Equation (7.9))

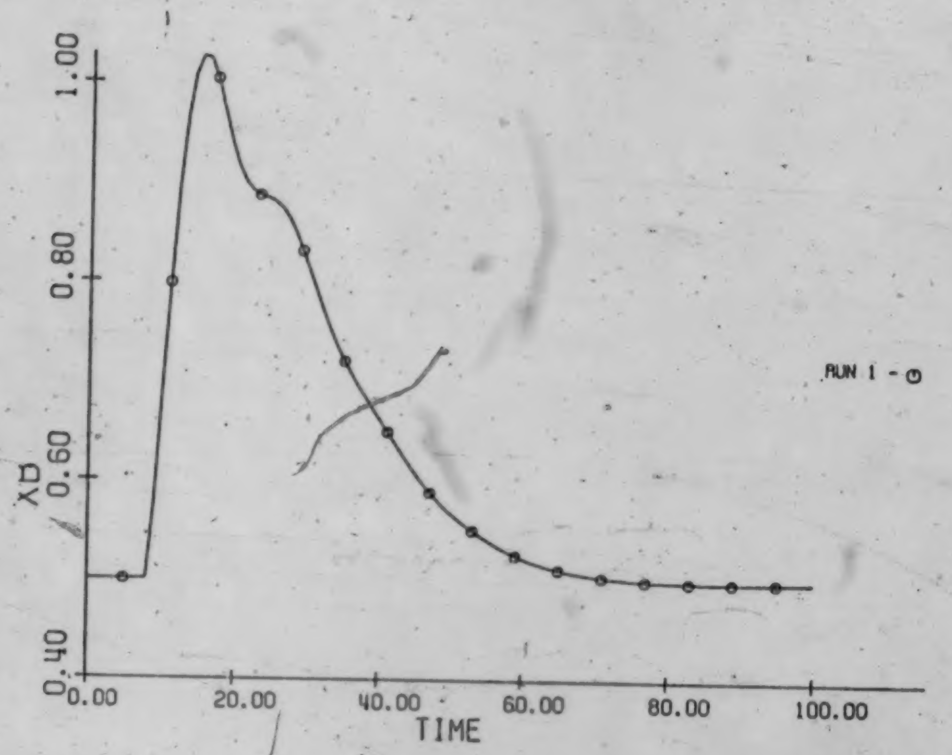

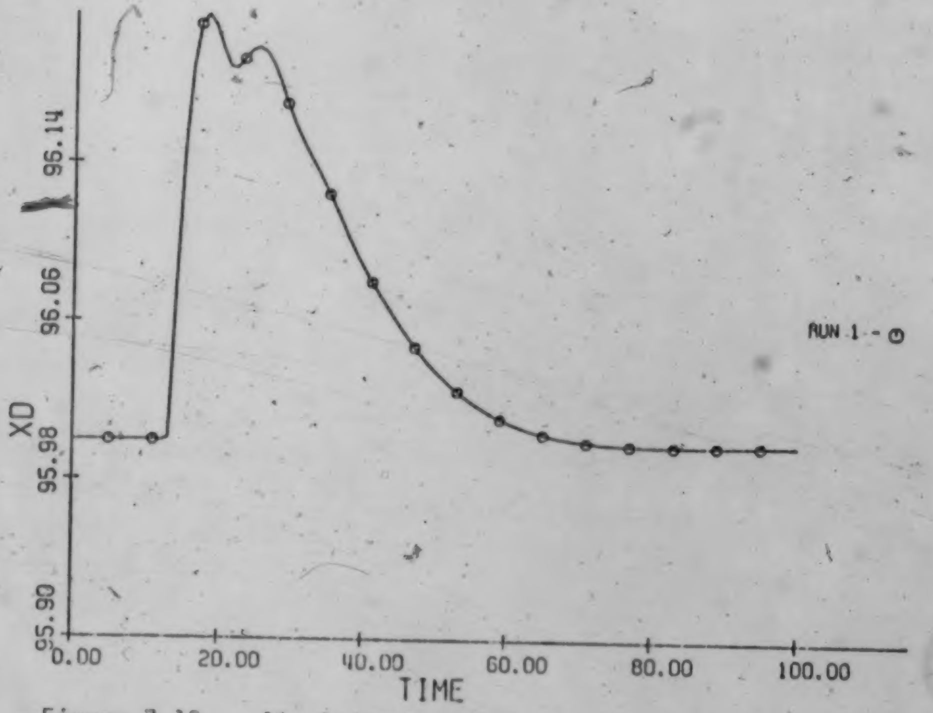

Figure 7.12 Simulated Response of the Distillation Column for a 14% Increase in Feed Flow Using a Non-interacting Control (Equation (7.14))

NOMENCLATURE

Alphabetic

A	nxn state plant matrix
B	nxℓ forcing function matrix
B_1	Double-effect evaporator first-effect bottoms flow
B_2	Double-effect evaporator second-effect bottoms flow
C	mxn output matrix
C_2	Double-effect evaporator product concentration
d	Disturbance vector
d_i	Radii of the Gershgorin circles
D	Disturbance coefficient matrix
e_i	mx1 vector whose i^{th} element is unity and the remaining elements are zero
e(z)	mx1 error vector
f	Scalar return-difference quantity
$f_i(z)$	i^{th} eigenvalue of matrix F(z)
$f_{ij}(z)$	(i,j) element of matrix F(z)
F(z)	mxm return-difference matrix
$g_i(z)$	i^{th} eigenvalue or diagonal element of matrix G(z)
$g_{.i}(z)$	i^{th} column of matrix G(z)
$g_{ij}(z)$	(i,j) element of matrix G(z)
G(z)	mxℓ or mxm plant transfer function matrix
$h_i(z)$	Transfer function between $u_i:y_i$ pair when the other loops are closed
H(z)	mxm transducer feedback matrix
I_m	mxm identity matrix
J	Linear quadratic performance index
$k_i(z)$	i^{th} diagonal element or i^{th} eigenvalue of matrix K(z)

$k_{i\cdot}(z)$	i^{th} row of matrix $K(z)$
$K(z)$	ℓxm pre-compensator matrix
ℓ	Number of input variables
$L(z)$	mxm post-compensator matrix
$L_i(z)$	Interaction term for loop i
m	Number of the plant outputs variables
n	Number of the plant state variables
n_c	Encirclements of the origin by the Nyquist locus of $\lvert R^{-1}(z)\rvert$
n_{ci}	Encirclements of the origin by the Nyquist locus of the i^{th} eigenvalue of $R^{-1}(z)$
n_{cii}	Encirclements of the origin by the Nyquist locus of the i^{th} diagonal element of $R^{-1}(z)$
p_o	Number of the right-half-plane zeros of the open-loop characteristic polynomial
$q_{ij}(z)$	(i,j) element of matrix $Q(z)$
$\hat{q}_i(z)$	i^{th} eigenvalue of matrix $Q^{-1}(z)$
$\hat{q}_{ij}(z)$	(i,j) element of matrix $Q^{-1}(z)$
Q	Quadratic performance index constant coefficient matrix
$Q(z)$	mxm open-loop transfer function matrix
$r(z)$	mx1 vector of setpoints or inputs
$r_i(z)$	i^{th} eigenvalue of matrix $R(z)$ or i^{th} element of vector $r(z)$
$r^i(z)$	Input vector at the i^{th} step
$\hat{r}_i(z)$	i^{th} eigenvalue of matrix $R^{-1}(z)$
$\hat{r}_{ij}(z)$	(i,j) element of matrix $R^{-1}(z)$
R	Distillation column reflux flow rate, or quadratic performance index constant coefficient matrix
$R(z)$	mxm closed-loop transfer function matrix
S	Double-effect evaporator steam flow to the first effect or distillation column flow rate

$t_i(z)$	i^{th} eigenvalue of matrix $T(z)$ or $Q(z)$
$T(z)$	mxm return-ratio matrix
$u(z)$	ℓx1 plant input vector
$v_j^T(z)$	Row of matrix $V(z)$
$V(z)$	Inverse of matrix $W(z)$
w	w-bilinear transform variable
$w_i(z)$	mx1 i^{th} eigenvector of matrix $Q(z)$ or $G(z)$
$W(z)$	Matrix containing the eigenvectors, $w_i(z)$, of $Q(z)$
W_1	Double-effect evaporator first-effect liquid level
W_2	Double-effect evaporator second-effect liquid level
x	nx1 state vector
X_B	Distillation column bottom product composition
X_D	Distillation column overhead product composition
$y(z)$	mx1 plant output vector
$y_i(z)$	i^{th} element of vector $y(z)$
z	z-transform operator

Greek Letters

α	Ostrowski coefficient factor
Γ	Resulting function from mapping contour D (Nyquist locus)
δ	Radii of the Gershgorin circles
$\sum$	Summation
ϕ	Interaction coefficient
ω	Frequency

Subscripts

c	Closed-loop matrix or compensator matrix
e	Error vector

f	Return-difference matrix
i	Running index, position or number of an element
ii	Diagonal element
i,j	Position of an element in a matrix
I	Integral control matrix
j	Running index, position or number of an element
o	Open-loop matrix
P	Proportional control matrix
t	Return-ratio matrix
u	Input vector

Superscripts

^	Element of the inverse of a matrix
i	Step number in the design procedure
I	Integral control matrix
P	Proportional control matrix
T	Matrix transpose
1	Second controller design for the same system and using the same design method

Abbreviations

CLCP	Closed-loop characteristic polynomial
CLTFM	Closed-loop transfer function matrix
DNA	Direct Nyquist array method
INA	Inverse Nyquist array method
MIMO	Multiple-input multiple-output system
OLCP	Open-loop characteristic polynomial
OLTFM	Open-loop transfer function matrix

SISO	Single-input single-output system
TFM	Transfer function matrix

REFERENCES

[1] Anderson, B.D.O., "Linear Multivariable Systems - A Survey", Proc. 5th IFAC Congress, Paris (1972).

[2] Athans, M., "The Role and Use of the Stochastic Linear-Quadratic-Gausian Problem in Control System Design", IEEE Trans. on Automatic Control, AC-16, 524-551 (1971).

[3] Ball, D.J. and Barney, G.C., "Application of Multivariable Control Theory to Hydraulic Models", Proc. IEE, 122, 209-212 (1975).

[4] Belletrutti, J.J. and MacFarlane, A.G.J., "Characteristic Loci Techniques in Multivariable-Control-System Design", Proc. IEE, 118, 1291-1298 (1971).

[5] Belletrutti, J.J., "Computer-aided Design and the Characteristic Locus Method", Conference on Computer-aided Design, IEE Conference Publication 96, 79-86 (1973).

[6] Berry, M.W., "Terminal Composition Control of a Binary Distillation Column", M.Sc. Thesis, Department of Chemical Engineering, The University of Alberta, Edmonton (1973).

[7] Bode, H.W., Network Analysis and Feedback Amplifier Design, Van Nostrand (1945).

[8] Bristol, E.H., "On the New Measure of Interaction for Multivariable Process Control", IEEE Trans. on Automatic Control, AC-11, 133 (1966).

[9] Bristol, E.H., "Philosophy for Single Loop Controller in a Multi-loop World", Proc. 8th ISA Conference on Instrumentation in the Chemical and Petroleum Industry, 4, 19-29 (1967).

[10] Buckley, P.S., "Techniques of Process Control", John Wiley, New York (1964).

[11] Cook, P.A., "Recent Mathematical Developments in Control", edited by D.J. Bell, Academic Press, 367 (1973).

[12] Coughanowr, D.R. and Koppel, L.B., "Process Systems Analysis and Control", McGraw-Hill, New York (1965).

[13] Desoer, C.A. and Wu, M., "Stability of Linear Time-Invariant Systems", IEEE Trans. on Circuit Theory, CT-15, 245-250 (1968).

[14] Fisher, D.G., Wilson, R.G. and Agostinis, W., "Description and Application of a Computer Program for Control System Design", Automatica, 8, 737-746 (1972).

[15] Fisher, D.G. and Kuon, J.F., "Development of the Direct Nyquist Array Method by Extension of Conventional Design Techniques", Research Report No. 750530, Department of Chemical Engineering, The University of Alberta, Edmonton (1975).

[16] Foss, A.S., "Critique of Chemical Process Control Theory", AIChE Journal, 19, 209-214 (1973).

[17] Freeman, E.A., "Stability of Linear Constant Multivariable Systems: Contraction-mapping Approach", Proc. IEE, 120, 379-384 (1973).

[18] Freedman, M.I., Falb, P.L. and Zames, G., "A Hilbert Space Stability Theory over Locally Compact Abellian Groups", SIAM J. Control, 7, 479-495 (1969).

[19] Gantmacher, F.R., Theory of Matrices, Vol. 1, Chelsea, 46 (1959).

[20] Hawkins, D.J., "Pseudodiagonalization and the Inverse Nyquist Array", Proc. IEE, 119, 337-342 (1972).

[21] Hawkins, D.J., "Graphical Technique for the Design of 2-Variable Control System", Proc. IEE, 119, 1740-1742 (1972).

[22] Hawkins, D.J. and McMorran, P.D., "Determination of Stability Regions with the Inverse Nyquist Array", Proc. IEE, 120, 1445-1448 (1973).

[23] Hodge, S.S., "Design Procedure Relating Open- and Closed-loop Diagonal Dominance", Proc. IEE, 118, 927-930 (1971).

[24] Hsu, C.H. and Chen, C.T., "A Proof of the Stability of Multivariable Feedback System", Proc. IEEE, 56, 2061-2062 (1968).

[25] Hamilton, J.C., Seborg, D.E. and Fisher, D.G., "An Experimental Evaluation of State Estimation in Multivariable Control Systems", AIChE Journal, 19, 901-909 (1973).

[26] Horowitz, I.M. and Shaked, U., "Superiority of Transfer Function over State-Variable Methods in Linear Time-Invariant Feedback System Design", IEEE Trans. on Automatic Control, AC-20, 84-97 (1975).

[27] Jacobson, B.A., "Multiloop Computer Control of an Evaporator", M.Sc. Thesis, Department of Chemical Engineering, The University of Alberta, Edmonton (1970).

[28] Kuo, B.C., "Analysis and Synthesis of Sampled-data Control Systems", Prentice-Hall, N.J. (1963).

[29] Kuon, J.F. and Fisher, D.G., "Multivariable Frequency Domain Techniques User's Manual", Research Report No. 750410, Department of Chemical Engineering, The University of Alberta, Edmonton (1975).

[30] Kuon, J.F. and Fisher, D.G., "Design Example of a Controller in the Multivariable Frequency Domain Using GEMSCOPE", Research Report No. 750320, Department of Chemical Engineering, The University of Alberta, Edmonton (1975).

[31] Kuon, J.F. and Fisher, D.G., "Console Printout from GEMSCOPE Options for Design of Controllers in the Multivariable Frequency Domain", Research Report No. 750411, Department of Chemical Engineering, The University of Alberta, Edmonton (1975).

[32] Kuon, J.F. and Fisher, D.G., "Documentation of Modifications to GEMSCOPE: Multivariable Frequency Domain Techniques", Research Report No. 741020, Department of Chemical Engineering, The University of Alberta, Edmonton (1975).

[33] Layton, J.M., "Commutative Controller: A Critical Survey", Electronics Letters, 6, 362-363 (1970).

[34] Luenberger, D.G., "Observers for Multivariable Systems", IEEE Trans. on Automatic Control, AC-11, 190-197 (1966).

[35] MacFarlane, A.G.J., "Engineering Systems Analysis", Harrap, London (1964).

[36] MacFarlane, A.G.J., "Commutative Controller. A New Technique for the Design of Multivariable Control Systems", Electronics Letters, 6, 121-123, 363-364 (1970).

[37] MacFarlane, A.G.J., "Multivariable-Control-System Design Techniques: A Guided Tour", Proc. IEE, 117, 1039-1047 (1970).

[38] MacFarlane, A.G.J., "Return-difference and Return-ratio and Their Use in the Analysis and Design of Multivariable Feedback Control System", Proc. IEE, 2037-2049 (1970).

[39] MacFarlane, A.G.J., McMorran, P.D., Dixon, B.A. and Hodge, S.S., "Applications of Multivariable Control Techniques to Aircraft Gas Turbines", 4th UKAC Conference Convention, IEE Conference Publication 78, 1-7 (1971).

[40] MacFarlane, A.G.J., "A Survey of Some Results in Linear Multivariable Feedback Theory", Automatica, 8, 455-492 (1972).

[41] MacFarlane, A.G.J., "Frequency Response Methods in Multivariable Feedback System Design", Conference on Computer-Aided Control System Design, IEE Conference Publication 96, 71-78 (1973).

[42] MacFarlane, A.G.J. and Belletrutti, J.J., "The Characteristic Locus Design Method", Automatica, 9, 575-588 (1973).

[43] Marcus, M. and Minc, H., Survey of Matrix Theory and Matrix Inequalities, Allyn and Bacon (1964).

[44] Mayne, D.Q., "The Design of Linear Multivariable Systems", Proc. 5th IFAC Congress, Paris, 29.1 (1972).

[45] Mayne, D.Q., "The Design of Linear Multivariable Systems", Automatica, 10, 405-412 (1974).

[46] Mayne, D.Q., "The Effect of Feedback on Linear Multivariable Systems", Automatica, 10, 405-412 (1974).

[47] McMorran, P.D., "Extension of the Inverse Nyquist Method", Electronics Letters, 6, 800-801 (1970).

[48] McMorran, P.D., "Design of Gas-Turbine Controller Using Inverse Nyquist Method", Proc. IEE, 117, 2050-2056 (1970).

[49] McMorran, P.D., "Application of the Inverse Nyquist Method to a Distillation Column", 4th UKAC Control Convention, IEE Conference Publication 78, 122-126 (1971).

[50] Munro, N. and Ibrahim, A., "Computer-aided Design of Multivariable Sampled-data Systems", Conference on Computer-aided Control System Design, IEE Conference Publication No. 96, 133-140 (1973).

[51] Mee, D.H. and Hannah, R.S., "Nonminimum-phase Difficulties in Multivariable Control System Design", Electronics Letters, 9, 469-470 (1973).

[52] Munro, N., "Design of Controllers for Open-loop Unstable Multivariable Systems Using Inverse Nyquist Array", Proc. IEE, 119, 1377-1382 (1972).

[53] Newell, R.B., Multivariable Computer Control of an Evaporator, Ph.D. Thesis, Department of Chemical Engineering, The University of Alberta, Edmonton (1971).

[54] Nyquist, H., "Regeneration Theory", Bell System Technical Journal, 11, 126-147 (1932).

[55] Ostrowski, A.M., "Notes on Bounds for Determinants with Dominant Principal Diagonal", Proc. Am. Math. Soc., 3, 26-30 (1952).

[56] Owens, D.H., "Dyadic Approximation Method for Multivariable Control Systems Analysis with a Nuclear Reactor Application", Proc. IEE, 20, 801-809 (1973).

[57] Owens, D.H., "Dyadic Modification to Sequential Technique for Multivariable Control Systems Design", Electronics Letters, 10, 25-26 (1974).

[58] Owens, D.H., "Sequential Design of Linear Multivariable Systems Retaining Full Output Feedback", Electronics Letters, 10, 79-80 (1974).

[59] Owens, D.H., "Dyadic Expansion for the Analysis of Linear Multivariable Systems", Proc. IEE, 121, 713-716 (1974).

[60] Owens, D.H., "Dyadic Expansion, Characteristic Loci and Multivariable Control Systems Design", Proc. IEE, 122, 315-320 (1975).

[61] Popov, V.M., "Hyperstability and Optimality of Automatic Systems with Several Control Functions", Revue Roumaine de Sciences Techniquies-Electrotechnics on Energetics, Vol. 9, Bucharest (1964).

[62] Rae, W.G., "Synthesis of Non-interacting Control Systems", Control 8, 245-247 (1964).

[63] Retallack, D.G., "Extended Root-Locus Technique for Design Multivariable Feedback Systems", Proc. IEE, 117, 618-623 (1970).

[64] Rosenbrock, H.H., "On the Design of Linear Multivariable Control Systems", Proc. 3rd Congress IFAC, London 1A1-1A16 (1966).

[65] Rosenbrock, H.H., "Design of Multivariable Control Systems Using the Inverse Nyquist Array", Proc. IEE, 116, 1929-1936 (1969).

[66] Rosenbrock, H.H., State-Space and Multivariable Theory, Nelson, G. Britain (1970).

[67] Rosenbrock, H.H., "Progress in the Design of Multivariable Control Systems", Measurement and Control, 4, 9-11 (1971).

[68] Rosenbrock, H.H., "The Stability of Multivariable Systems", IEEE Trans. on Automatic Control, 17, 105-107 (1972).

[69] Rosenbrock, H.H., "Bounds for Transfer Function in Multivariable Systems", IEEE Trans. on Automatic Control, 18, 54-56 (1973).

[70] Rosenbrock, H.H., Recent Mathematical Developments in Control, Edited by D.J. Bell, Academic Press, 345 (1973).

[71] Rosenbrock, H.H., Computer-aided Control System Design, Academic Press (1974).

[72] Rosenbrock, H.H. and Cook, P.A., "Stability and the Eigenvalues of G(s)", Int. J. Control, 21, 99-104 (1975).

[73] Sage, A.P., Optimum Systems Control, Prentice-Hall, N.J. (1968).

[74] Seborg, D.E., Fisher, D.G. and Hamilton, J.C., "An Experimental Evaluation of State Estimation in Multivariable Control Systems", Proc. IFAC Sympos., 144-155, Zurich (1974).

[75] Tsien, H.S., Engineering Cybernetics, McGraw-Hill, New York (1954).

[76] Vesty, P.,"Geometric Interpretation of Complex Vector Arising in the Frequency-Domain Analysis of Multivariable Systems", IEEE Trans. on Automatic Control, AC-20, 157-158 (1975).

[77] Wilson, R.G., "Model Reduction and Reduced Order Control Law Design", Ph.D. Thesis, Department of Chemical Engineering, The University of Alberta, Edmonton (1974).

[78] Wilson, R.G., Fisher, D.G., and Seborg, D.E., "Model Reduction for

Discrete-Time Dynamic Systems", Int. J. of Control, 16, 549-558 (1972).

[79] Wood, R.K. and Berry, M.W., "Terminal Composition Control of a Binary Distillation Column", Chem. Eng. Science, 28, 1707-1717 (1973).

ADDITIONAL REFERENCES

[501] Belletrutti, J.J, Private Comunication.

[502] Bohn, E.V., "Stabilization of Linear Multivariable Feedback Control Systems", IRE Trans. on Automatic Control, AC-5, 321-327 (1960).

[503] Bohn, E.V., "Use of Matrix Transformation and System Eigenvalues in the Design of Linear Multivariable Control Systems", Proc IEE, 110, 989-997 (1963).

[504] Desoer, C.A. and Wu, M.Y., "Stability of Multiple-Loop Feedback Linear Time-Invariant Systems", J. of Mathematical Analysis and Applications, 23, 121-129 (1968).

[505] Hawkins, D.J., "Techniques for the Design of Multivariable Control Systems", Ph. D. Thesis, Control Systems Centre, Institute of Science and Technology, The University of Manchester, Manchester (1972).

[506] MacFarlane, A.G.J., "Relationship Between Recent Developments in Linear Control Theory and Classical Design Techniques", Third IFAC Symposium on Multivariable Technology, Manchester (1974).

[507] Kontakos, T., "Algebraic and Geometry Aspects of Multivariable Control Systems", Ph. D. Thesis, Control Systems Centre, Institute of Science and Technology, The University of Manchester, Manchester (1973).

[508] Kouvaritakis, B.A., Ph. D. Thesis, Control Systems Centre, Institute of Science and Technology, The University of Manchester, Manchester (1974).

[509] Rosenbrock, H.H., "Computer-Aided Design of Multivariable Control Systems", Conference Proceedings on "How to Apply Advance Control in Industrial Automation -II- Multivariable and Non-Interacting Systems, Purdue, 1-24 (1975).

APPENDIX A

PILOT PLANT EVAPORATOR AND ITS MODELS

A.1 THE EVAPORATOR

The pilot plant evaporator used in this work is a double effect unit with the two effects operating in series. This pilot plant has been described in detail by previous workers [27,53,77]. The major pieces of process equipment are shown in the schematic diagram in Figure A.1. The control loops shown in Figure A.1 represent the multiloop control scheme applied to the evaporator in previous studies [27,53,77].

The first effect has natural circulation through its 18 inch long, 3/4 inch O.D. tubes. It is heated by process steam. The second effect is a long tube vertical unit which is run in its forced circulation mode. It has three, six foot long, one inch O.D. tubes. It is operated at a lower pressure than the first effect and is heated by the vapour produced in the first effect.

The evaporator is fully instrumented and can be controlled by either Foxboro electronic controllers or under Direct Digital Control (DDC) from an IBM 1800 Data Acquisition and Control Computer operating under MPX. Multiloop DDC can be applied directly using the computer control package; and advanced control schemes by user written programs which utilize a set of system programs to interface between the user and system control programs.

A.2 THE EVAPORATOR MODEL

The complete development of the double-effect evaporator

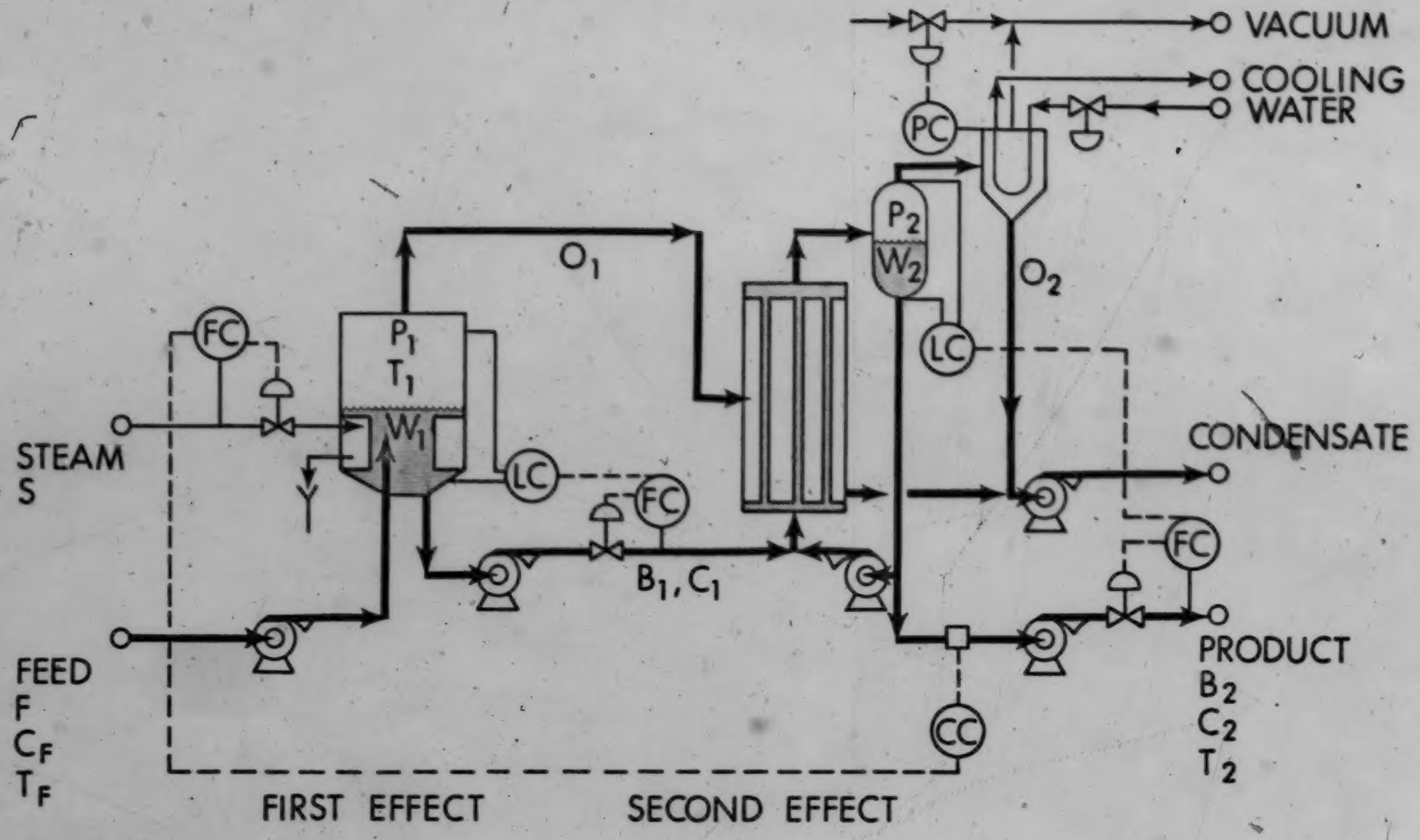
VACUUM
COOLING WATER
PC
P_2
W_2
O_2
LC
O_1
FC
P_1
T_1
W_1
STEAM
S
LC
FC
CONDENSATE
FC
B_1, C_1
PRODUCT
B_2
C_2
T_2
FEED
F
C_F
T_F
CC
FIRST EFFECT
SECOND EFFECT

FIGURE A1: Schematic Diagram of the Double Effect Pilot Plant Evaporator used for this work.

model has been presented by Newell [53] who derived fifth and tenth order non-linear models. Based on these models Wilson [77] calculated discrete five-state and three state, linear, time-invariant models using a linearization procedure and Marshall's model reduction method [78].

The linearized models in the discrete form can be represented by:

$$\underline{x}(n+1) = \underline{\underline{\Phi}}\underline{x}(n) + \underline{\underline{\Delta}}u(n) + \underline{\underline{\Theta}}\underline{d}(n) \qquad \text{(A-1)}$$

and

$$y(n) = \underline{\underline{C}}\ \underline{x}(n) \qquad \text{(A-2)}$$

The elements of the vectors $\underline{x}$, $\underline{u}$, $\underline{d}$, $\underline{y}$ are defined as normalized perturbation variables:

$$x_1 = \frac{W_1 - W_{1ss}}{W_{1ss}} \qquad \text{(A-3)}$$

where W_{1ss} is the normal steady state value of W_1.

The vectors $\underline{x}$, $\underline{u}$, $\underline{d}$ and $\underline{y}$ for the fifth order discrete model are defined in Table A-1. The coefficient matrices of this discrete time model, with a 64 second sampling interval, are shown in Table A-2.

For the third order discrete model the state vector $\underline{x}$ is given by:

$$\underline{x} = (W_1, W_2, C_2)^T \qquad \text{(A-4)}$$

The elements of the state vector are defined in Table A-1. The vectors $\underline{u}$, $\underline{d}$ and $\underline{y}$ are equal to the ones defined in Table A-1. The coefficient matrices for this model, with a 64 second sampling interval, are shown in Table A-3.

TABLE A-1

DESCRIPTION OF THE EVAPORATOR VARIABLES

State Vector, $\underline{x}$		Normal Steady State Value
$\underline{x}^T = [W1, C1, H1, W2, C2]$		
W1	First effect holdup	45.5 lb.
C1	First effect concentration	4.59% glycol
H1	First effect enthalpy	189.2 BTU/lb.
W2	Second effect holdup	41.5 lb.
C2	Second effect concentration	10.11% glycol
Control Vector, $\underline{u}$		
$\underline{u}^T = [S, B1, B2]$		
S	Steam flow	2.0 lb./min.
B1	First effect bottoms flow	3.485 lb./min.
B2	Second effect bottoms flow	1.581 lb./min.
Disturbance Vector, $\underline{d}$		
$\underline{d}^T = [F, CF, HF]$		
F	Feed flow	5.0 lb./min.
CF	Feed concentration	3.2% glycol
HF	Feed enthalpy	156.9 BTU/lb.
Output Vector, $\underline{y}$		
$\underline{y}^T = [W1, W2, C2]$		

TABLE A-2

FIFTH ORDER DISCRETE EVAPORATOR MODEL (T = 64 sec.)

$$\underline{\underline{\phi}} = \begin{bmatrix} 1.0 & -0.0008 & -0.0912 & 0 & 0 \\ 0 & 0.9223 & 0.0871 & 0 & 0 \\ 0 & -0.0042 & 0.4376 & 0 & 0 \\ 0 & -0.0009 & -0.1052 & 1.0 & 0.0001 \\ 0 & 0.0391 & 0.1048 & 0 & 0.9603 \end{bmatrix}$$

$$\underline{\underline{\Delta}} = \begin{bmatrix} -0.0119 & -0.0817 & 0 \\ 0.0116 & 0 & 0 \\ 0.0116 & 0 & 0 \\ -0.0138 & 0.0848 & -0.0406 \\ 0.0137 & -0.0432 & 0 \end{bmatrix} \qquad \underline{\underline{\theta}} = \begin{bmatrix} 0.1182 & 0 & -0.0050 \\ -0.0351 & 0.0785 & 0.0049 \\ -0.0136 & -0.0002 & 0.0662 \\ 0.0012 & 0 & -0.0058 \\ 0.0019 & 0.0016 & 0.0058 \end{bmatrix}$$

$$\underline{\underline{C}} = \begin{bmatrix} 1.0 & 0 & 0 & 0 & 0 \\ 0 & 0 & 0 & 1.0 & 0 \\ 0 & 0 & 0 & 0 & 1.0 \end{bmatrix}$$

TABLE A-3

THIRD ORDER DISCRETE EVAPORATOR MODEL

(T = 64 sec)

$$\underline{\underline{\phi}} = \begin{bmatrix} 1.0 & 0 & 0 \\ 0 & 1.0 & 0 \\ 0 & 0 & 0.9602 \end{bmatrix} \qquad \underline{\underline{\Delta}} = \begin{bmatrix} -0.0326 & -0.0811 & 0 \\ 0.0378 & 0.0854 & -0.0406 \\ 0.0529 & -0.0442 & 0 \end{bmatrix}$$

$$\underline{\underline{\theta}} = \begin{bmatrix} 0.1200 & 0 & -0.0135 \\ 0.0033 & 0 & -0.0157 \\ -0.0219 & -0.0400 & 0.0219 \end{bmatrix} \qquad \underline{\underline{C}} = \begin{bmatrix} 1.0 & 0 & 0 \\ 0 & 1.0 & 0 \\ 0 & 0 & 1.0 \end{bmatrix}$$

APPENDIX B

CONTROLLER MATRICES

This appendix contains an explanation of the code used for the figures presented in this thesis. It also includes the numerical values of the control matrices that were implemented on the double-effect evaporator pilot plant. These matrices were designed based on the third or fifth order evaporator model and using the following frequency domain techniques: inverse Nyquist array, characteristic locus and direct Nyquist array method.

TABLE B-1

PROPORTIONAL CONTROL MATRICES DESIGNED FOR THE THIRD AND FIFTH ORDER EVAPORATOR MODEL USING THE INVERSE NYQUIST ARRAY, THE CHARACTERISTIC LOCUS AND THE DIRECT NYQUIST ARRAY METHODS

Controller Designation	Relationship to the Ultimate Gain, k_u	k_1	k_2	k_3	Proportional Controller K
FD0310	0.1 k_u	2.46	4.92	2.78	$\begin{bmatrix} -1.55 & 0.0 & 2.78 \\ -1.84 & 0.0 & -1.11 \\ -2.42 & -4.92 & -4.92 \end{bmatrix}$
FD0320	0.2 k_u	4.92	9.84	5.56	$\begin{bmatrix} -3.10 & 0.0 & 5.56 \\ -3.68 & 0.0 & -2.22 \\ -4.85 & -9.84 & -9.84 \end{bmatrix}$
FD0330	0.3 k_u	7.38	14.76	8.34	$\begin{bmatrix} -4.65 & 0.0 & 8.34 \\ -5.52 & 0.0 & -3.33 \\ -7.27 & -14.76 & -14.76 \end{bmatrix}$
FD0520*	0.2 k_u	4.92	9.84	4.45	$\begin{bmatrix} -3.10 & 0.0 & 4.45 \\ -3.68 & 0.0 & -1.78 \\ -4.85 & -9.84 & -7.89 \end{bmatrix}$
FD0530**	0.3 k_u	7.38	14.76	6.67	$\begin{bmatrix} -4.65 & 0.0 & 6.67 \\ -5.52 & 0.0 & -2.66 \\ -7.27 & -14.76 & -11.81 \end{bmatrix}$

* The effective gain used in the C_2 measurement transducer was 0.16 k_u.

** The effective gain used in the C_2 measurement transducer was 0.24 k_u.

....continued

TABLE B-1 (Continued)

Controller Designation	Relationship to the Ultimate Gain	k_1	k_2	k_3	Proportional Controller
FD0350	$0.5\ k_u$	12.3	24.6	13.9	$\begin{bmatrix} -7.75 & 0 & 13.9 \\ -9.20 & 0 & -5.56 \\ -12.12 & -24.6 & -24.6 \end{bmatrix}$

TABLE B-2

PROPORTIONAL+INTEGRAL MATRICES DESIGNED FOR THE THIRD AND FIFTH ORDER EVAPORATOR MODEL USING THE INVERSE NYQUIST ARRAY, THE CHARACTERISTIC LOCUS AND THE DIRECT NYQUIST ARRAY METHOD

Controller Designation	Proportional Gains				Integral Gains			Proportional Matrix K_P			Integral Matrix K_I		
	Gain	k_{P1}	k_{P2}	k_{P3}	k_{I1}	k_{I2}	k_{I3}						
FD1320	$0.2k_u$	4.92	9.84	5.56	0.153	0.205	0.173	-3.10	0.0	5.56	-0.096	0.0	0.173
								-3.68	0.0	-2.22	-0.115	0.0	-0.069
								-4.85	-9.84	-9.84	-0.151	-0.205	-0.307
FD1315	$0.15k_u$	3.69	7.38	4.17	0.153	0.205	0.173	-2.32	0.0	4.17	-0.096	0.0	0.173
								-2.76	0.0	-1.67	-0.115	0.0	-0.069
								-3.63	-7.38	-7.38	-0.151	-0.205	-0.307
FD1315.1	$0.15k_u$	3.69	7.38	4.17	0.230	0.307	0.259	-2.32	0.0	4.17	-0.144	0.0	0.259
								-2.76	0.0	-1.67	-0.172	0.0	0.104
								-3.63	-7.38	7.38	-0.226	-0.307	-0.460

TABLE B-3

DYNAMIC CONTROLLERS DESIGNED FOR THE FIFTH ORDER MODEL USING THE INVERSE AND DIRECT NYQUIST ARRAY METHODS

Controller Designation	Gain	k_1	k_2	k_3	Dynamic Controller
NADY0510*	0.1 k_u	1.79	4.92	4.07	$\begin{bmatrix} -5.62a & 0 & 2.72 \\ -1.79 & 0 & -0.41b \\ -1.79 & -4.92 & -1.78b \end{bmatrix}$
NADY0520*	0.2 k_u	3.58	9.84	8.14	$\begin{bmatrix} -11.14a & 0 & 5.44 \\ -3.58 & 0 & -0.82b \\ -3.58 & -9.84 & -3.56b \end{bmatrix}$
NADY0530*	0.3 k_u	5.37	14.76	12.21	$\begin{bmatrix} -16.59 & 0 & 8.16 \\ -5.37 & 0 & -1.23b \\ -5.37 & -14.76 & -5.34b \end{bmatrix}$

. . . continued

Table B-3 (continued)

Controller Designation	Gain	k_1	k_2	k_3	Dynamic Controller
NADY0550*	$0.5\ k_u$	8.95	24.60	20.35	$\begin{bmatrix} -28.10a & 0 & 13.60 \\ -8.95 & 0 & -2.05b \\ -8.95 & -24.60 & -8.90b \end{bmatrix}$

* The effective gain used in the C_2 measurement transducer is 80% of the indicated value

$$a = \frac{z - 0.4383}{z + 0.7619} \qquad b = \frac{z + 0.7619}{z - 0.4383}$$

TABLE B-4

PROPORTIONAL CONTROL MATRICES DESIGNED FOR THE FIFTH ORDER EVAPORATOR MODEL USING THE DIRECT NYQUIST ARRAY METHOD

Controller Designation	Final Prop. Gain	k_1	k_2	k_3	Proportional Controller
DNA0500		1.0	1.0	1.0	$\begin{bmatrix} -0.600 & 0 & 1.0 \\ -0.760 & 0 & -0.4 \\ -1.520 & -1.0 & -0.8 \end{bmatrix}$
DNA0520	0.2 k_u	3.6	9.52	5.0	$\begin{bmatrix} -2.16 & 0 & 5.0 \\ -2.73 & 0 & -2.0 \\ -5.47 & -9.52 & -4.0 \end{bmatrix}$

TABLE B-5

EXPLANATION OF THE CODE USED FOR FIGURES(1)

Code	Explanation
G=3	Third order evaporator model has been used to produce the Nyquist array, characteristic locus or the control matrix.
G=5	Fifth order evaporator model has been used.
G=DISC	Distillation column model has been used.
0.1 to 10.0	Frequency range used to produce the Nyquist diagrams (rad/sec. or rad/min.)
$Q_2(w)$	The Nyquist array, or diagonal elements, of the open-loop matrix $Q_2(w)$ is displayed.
$Q_2^{-1}(w)$	The Nyquist array, or diagonal elements, of matrix $Q_2^{-1}(w)$ is displayed.
K_1K_2=(5.43)(5.44)	Control matrices K_1 and K_2 has been used. They are given by Equations (5.43) and (5.44) respectively.
FD0320	Control matrix designation (see Tables in this Appendix).
FD	Frequency Domain Techniques (Inverse Nyquist Array, Characteristic Locus, and Direct Nyquist Array Method) were used to design controller.
NADY	Dynamic compensator obtained using the Nyquist array methods.
DNA	Direct Nyquist array method.
INA + CL + DNA	Inverse Nyquist array or characteristic locus or direct Nyquist array method has been used to produce the control matrix under consideration, i.e. all produce the same controller.

---

(1) Note: vertical bars are used to delimit each element of the code.

Table B-5 (continued)

Code	Explanation
SIM 5	Fifth order evaporator model has been used to simulate the results.
Exp	Experimental results.
K=Table B-1	The numerical value of the control matrix is contained in Table B-1.
P	Proportional control only.
P + I	Proportional plus integral control.
MUL	Multi-loop control.
OPT	Optimal control.
+20%F	A 20% step change in the feed flow was used in the run under consideration.
±10% C_2	A 10% step change (up and down) in the set point of the product concentration was introduced in the run under consideration.
±20% FC	A 20% step change in feed concentration was used as the disturbance variable in the run under consideration.
O	Part of first set of experimental runs.
N	Part of second set of experimental runs.

APPENDIX C

LIMITING VALUES FOR THE $\phi_{ji}(z)$ FACTORS

This appendix derives the basic relationships that lead to the Gershgorin and Ostrowski bands and shows that they can be regarded as limiting values, or bounds, on the location of the Nyquist locus of the "exact" transfer function, h(z).

When the return-difference matrix, F(z), is diagonally dominant, the limiting value of the $\phi_{ji}(z)$ factors in Equation (5.18) is given by

$$|\phi_{ji}(z)| < 1 \tag{C.1}$$

A specific case of a third order system has been chosen to show the validity of Equation (C.1). The second order case is trivial and the same approach can be used to prove Equation (C.1) for higher order systems.

Equation (5.17) which gives the open-loop relationship between the input of the augmented plant u_2' and output y_2 for a third order system when the other loops are closed can be written in the following general way:

$$h_2(z) = q_{22}(z) + \phi_{12}(z)\, q_{12}(z) + \phi_{32}(z)\, q_{32}(z) \tag{C.2}$$

where:

$$\phi_{12}(z) = \frac{\left(\frac{k_{11}q_{31}(z)}{1+k_{11}q_{11}(z)}\right)\left(\frac{k_{33}q_{23}(z)}{1+k_{33}q_{33}(z)}\right) - \left(\frac{k_{11}q_{21}(z)}{1+k_{11}q_{11}(z)}\right)}{\left[1 - \left(\frac{k_{11}q_{31}(z)}{1+k_{11}q_{11}(z)}\right)\left(\frac{k_{33}q_{13}(z)}{1+k_{33}q_{33}(z)}\right)\right]} \tag{C.3}$$

and

$$\phi_{32}(z) = \frac{\left[\left(\frac{k_{11}q_{21}(z)}{1+k_{11}q_{11}(z)}\right)\left(\frac{k_{33}q_{13}(z)}{1+k_{33}q_{33}(z)}\right) - \left(\frac{k_{33}q_{23}(z)}{1+k_{33}q_{33}(z)}\right)\right]}{\left[1 - \left(\frac{k_{11}q_{31}(z)}{1+k_{11}q_{11}(z)}\right)\left(\frac{k_{33}q_{13}(z)}{1+k_{33}q_{33}(z)}\right)\right]} \qquad (C.4)$$

Given these Equations the problem can be stated in the following way:

Show that

$$|\phi_{12}(z)| < 1 \qquad (C.5)$$

and

$$|\phi_{32}(z)| < 1 \qquad (C.6)$$

When the return-difference matrix is diagonally dominant, then

$$\alpha_1 = \frac{|k_{11}|\{|q_{21}(z)| + |q_{31}(z)|\}}{|1 + k_{11}q_{11}(z)|} < 1 \qquad (C.7)$$

$$\alpha_2 = \frac{|k_{33}|\{|q_{13}(z)| + |q_{23}(z)|\}}{|1 + k_{33}q_{33}(z)|} < 1 \qquad (C.8)$$

Equation (C.3) can be written in the following ways

$$\phi_{12} = \frac{\beta}{\left[1 - \left(\frac{k_{11}q_{31}}{1+k_{11}q_{11}}\right)\left(\frac{k_{33}q_{13}}{1+k_{33}q_{33}}\right)\right]} \qquad (C.9)$$

where the z's have been dropped for convenience and β is defined by

$$\beta = \left(\frac{k_{11}q_{31}}{1+k_{11}q_{11}}\right)\left(\frac{k_{33}q_{23}}{1+k_{33}q_{33}}\right) - \left(\frac{k_{11}q_{21}}{1+k_{11}q_{11}}\right) \qquad (C.10)$$

Taking absolute values Equation (C.9) gives:

$$|\phi_{12}| = \frac{|\beta|}{|1 - \left(\frac{k_{11}q_{31}}{1+k_{11}q_{11}}\right)\left(\frac{k_{33}q_{13}}{1+k_{33}q_{33}}\right)|} \qquad (C.11)$$

or

$$|\phi_{12}| \leq \frac{|\beta|}{|1| - |\frac{k_{11}q_{31}}{1+k_{11}q_{11}}|\ |\frac{k_{33}q_{13}}{1+k_{33}q_{33}}|} \qquad (C.12)$$

$|1|$ can be expressed in the following way

$$|1| = 1 = \alpha_1\alpha_2\Theta \qquad (C.13)$$

where α_1, α_2 are given by Equations (C.7) and (C.8) respectively and Θ is a factor greater than one defined by this equation. It should also be noted that following inequalities are valid:

$$\Theta\alpha_1 > 1 \qquad (C.14)$$

and

$$\Theta\alpha_2 > 1 \qquad (C.15)$$

Replacing Equation (C.13) into Equation (C.12) we obtain

$$|\phi_{12}| \leq \frac{|\beta|}{\Theta\alpha_1\alpha_2 - |\frac{k_{11}q_{31}}{1+k_{11}q_{11}}|\ |\frac{k_{33}q_{13}}{1+k_{33}q_{33}}|} \qquad (C.16)$$

or

$$|\phi_{12}| < \frac{|\beta|}{\Theta\alpha_1\alpha_2 - \Theta|\frac{k_{11}q_{31}}{1+k_{11}q_{11}}|\ |\frac{k_{33}q_{13}}{1+k_{33}q_{33}}|} \qquad (C.17)$$

since $\Theta > 1$

Equation (C.17) can be simplified by multiplying α_1 by α_2 and eliminating the common factors, then

$$|\phi_{12}| < \frac{|\beta|}{\Theta \left|\frac{k_{11}q_{31}}{1+k_{11}q_{11}}\right| \left|\frac{k_{33}q_{23}}{1+k_{33}q_{33}}\right| + \Theta\alpha_2 \left|\frac{k_{11}q_{21}}{1+k_{11}q_{11}}\right|} \tag{C.18}$$

or

$$|\phi_{12}| < \frac{\left|\frac{k_{11}q_{31}}{1+k_{11}q_{11}}\right| \left|\frac{k_{33}q_{23}}{1+k_{33}q_{33}}\right| + \left|\frac{k_{11}q_{21}}{1+k_{11}q_{11}}\right|}{\Theta \left|\frac{k_{11}q_{31}}{1+k_{11}q_{11}}\right| \left|\frac{k_{33}q_{23}}{1+k_{33}q_{33}}\right| + \Theta\alpha_2 \left|\frac{k_{11}q_{21}}{1+k_{11}q_{11}}\right|} \tag{C.19}$$

But $\Theta\alpha_2 < \Theta$, therefore

$$|\phi_{12}| < \frac{\left|\frac{k_{11}q_{31}}{1+k_{11}q_{11}}\right| \left|\frac{k_{33}q_{23}}{1+k_{33}q_{33}}\right| + \left|\frac{k_{11}q_{21}}{1+k_{11}q_{11}}\right|}{\Theta\alpha_2 \left|\frac{k_{11}q_{31}}{1+k_{11}q_{11}}\right| \left|\frac{k_{33}q_{23}}{1+k_{33}q_{33}}\right| + \Theta\alpha_2 \left|\frac{k_{11}q_{21}}{1+k_{11}q_{11}}\right|} \tag{C.20}$$

or

$$|\phi_{12}| < \frac{1}{\Theta\alpha_2} = \alpha_1 < 1 \tag{C.21}$$

which shows the validity of Equation (C.5). Following the same approach it can be proved that

$$|\phi_{32}| < \alpha_2 < 1 \tag{C.22}$$

It should be noticed that the Ostrowski factor to determine the radius of the Ostrowski circles is given by:

$$\text{Ostrowski factor} = \max(\alpha_1, \alpha_2) \tag{C.23}$$

Equations (C.21) and (C.22) indicate that the region of uncertainty about where $h_2(z)$ is located, can be narrowed slightly by using the appropriate factor α_1 and α_2 instead of the maximum of these values.

APPENDIX D

STABILITY THEOREM

D.1 BASIC EQUATION

Let $\{h_i(z), i=1,..m\}$ be the transfer function between input i and output i when loop i is open and all the others are closed as defined by Equation (5.18) and as illustrated in Figure 5.2. Also let $F^{ji}(z)$ be the cofactor of element (j,i) of the return-difference matrix, $F(z)$.

Equation (5.18) was derived independently but follows directly from the results obtained by Rosenbrock [68]. Using the notation defined above $h_i(z)$ can be written:

$$h_i(z) = q_{ii}(z) + \frac{\sum_{\substack{j=1 \\ j\neq i}}^{m} q_{ji}(z)\, F^{ji}(z)}{F^{ii}(z)} \qquad \text{(D.1)}$$

If loop i in Figure 5.2 is closed using the controller k_i the closed-loop characteristic polynomial for loop i will be given by:

$$1 + k_i h_i(z) = 1 + k_i q_{ii}(z) + \frac{\sum_{\substack{j=1 \\ j\neq i}}^{m} q_{ji}(z) F^{ji}(z) k_i}{F^{ii}(z)} \qquad \text{(D.2)}$$

or, bringing to a common denominator

$$1 + k_i h_i(z) = \frac{(1 + k_i q_{ii}(z))F^{ii}(z) \quad \sum_{\substack{j=1 \\ j\neq i}}^{m} k_i q_{ji}(z) F^{ji}(z)}{F^{ii}(z)} \qquad \text{(D.3)}$$

Equation (D.3) then will be equal to

$$1 + k_i h_i(z) = \frac{|F(z)|}{F^{ii}(z)} \qquad \text{(D.4)}$$

where $|F(z)|$ is the determinant of matrix $F(z)$.

When all the loops $\{i=1,\dots m\}$ are considered Equation (D.4) becomes

$$\prod_{i=1}^{m} (1 + k_i h_i(z)) = \left[\frac{|F(z)|^{m-1}}{\prod_{i=1}^{m} F^{ii}(z)}\right] |F(z)| \tag{D.5}$$

Belletrutti and MacFarlane [4] have shown that, for the systems of interest in this work, the stability of the closed-loop system can be determined by the encirclements of the origin by the mapping of the contour D by $|F(z)|$.(See Chapter Four). In the following discussion it will be shown that, when $F(z)$ is diagonally dominant the net encirclements of the origin contributed by the term in square brackets is zero and hence that the closed-loop system stability can be determined from the Nyquist plots of $\{h_i(z),\ i=1,..m\}$.

D.2 STABILITY THEOREM

1) Let the return-difference matrix, $F(z)$, be diagonally dominant and assume that the plant $G(z)$ has p_0 unstable poles.
2) Let D be the contour shown in Figure 3.1 and described in Section 3.2.
3) Let $|F(z)|$ map D into Γ_f encircling the origin n_f times clockwise.
4) Let the diagonal elements, $\{f_{ii}(z),\ i=1,..m\}$, of $F(z)$ map D into Γ_{ii} encircling the origin n_{ii} times clockwise.
5) Let $k_i h_i(z)$ map D into Γ_{hi} encircling the critical point (-1,0) n_{hi} times clockwise.
6) Let $F^{jj}(z)$ map D into Γ_{mj} encircling the origin m_{fj} times clockwise.

Then if F(z) is diagonally dominant it has been shown [68] that

$$n_f = \sum_{i=1}^{m} n_{ii} \qquad (D.6)$$

Consequently since the minors $F^{jj}(z)$ are also diagonally dominant

$$m_{fi} = \sum_{\substack{i=1 \\ j \neq i}}^{m} n_{ii} \qquad (D.7)$$

Thus the number of encirclements of the origin by the mapping of D by $|F(z)|^{m-1}$ will be equal to n_T, where

$$n_T = (m - 1) \sum_{i=1}^{m} n_{ii} \qquad (D.8)$$

The number of encirclements of the origin by the mapping of D by $\prod_{i=1}^{m} F^{ii}(z)$ will also be equal to n_T. Consequently from the principle of the argument it follows that the number of encirclements of the origin by $|F(z)|^{m-1}$ will be cancelled by the number of encirclements of the origin by $\prod_{i=1}^{m} F^{ii}(z)$ and hence the stability of the closed-loop will be determined only by the number of encirclements of the critical point (-1,0) by the mapping of D by $\{k_i h_i(z),\ i=1,..m\}$ which is equal to the number of encirclements of the origin by the mapping of D by $|F(z)|$. Thus the closed-loop system will be stable if and only if

$$\sum_{i=1}^{m} n_{hi} = -p_0 \qquad (D.9)$$

where p_0 is the number of zeros of the OLCP outside the unit circle.

If the plant is asymptotically stable $p_0 = 0$ and then the system will be stable if and only if none of the Nyquist diagrams of

$k_i h_i(z)$ encircles the critical point (-1,0).

APPENDIX E

DIAGONALIZATION OF THE DOUBLE-EFFECT PILOT PLANT EVAPORATOR (NON-INTERACTING CONTROL)

E.1 DIAGONALIZATION OF AN OPEN-LOOP TRANSFER FUNCTION MATRIX.

Rosenbrock [65] has shown that when the plant transfer function matrix, G(z), is non-singular and the poles of G(z) and the zeros of det G(z) lie inside the unit circle a stable control matrix, K(z), can be found, by performing elementary column operations on G(z), that will make the OLTFM, Q(z) = G(z)K(z), diagonal. Furthermore the OLTFM will have all its poles and zeros inside the unit circle in the complex plane.

Although the third and fifth order evaporator models each have two poles at the (-1,0) point these models can be considered to be stable and by drawing a small semicircle at z = 1 the poles can be considered to be located inside the unit circle. The determinants of the transfer function matrices also have their zeros located inside the unit circle. Thus it is possible in both cases to find a stable controller matrix that will produce a stable open-loop transfer function matrix.

For the third and fifth order evaporator model a non-interacting controller has been designed that will mathematically cancel the off-diagonal elements. The controller and the OLTFM obtained for both cases are presented in the next sections.

E.2 DIAGONALIZATION OF THE THIRD ORDER MODEL IN TABLE 3.1

The non-interacting controller, K(z), designed for the third order model is given by:

$$K(z) = \begin{bmatrix} -0.62658 & 0 & 1.0 \\ -0.74844 & 0 & -0.40148 \\ -0.99229 & 1.0 & -1.77564 \end{bmatrix} \qquad (E.1)$$

and the resulting open-loop transfer function matrix, Q(z)=G(z)K(z) is equal to:

$$Q(z) = \begin{bmatrix} \frac{0.0811}{z - 1} & 0 & 0 \\ 0 & \frac{0.04062}{z - 1} & 0 \\ 0 & 0 & \frac{0.07045}{z - 1} \end{bmatrix} \qquad (E.2)$$

The controller obtained using the direct Nyquist array method (Equation 5.32) was approximately the same as Equation (E.1).

E.3 DIAGONALIZATION OF THE FIFTH ORDER EVAPORATOR MODEL IN TABLE 3.5

For the fifth order evaporator model the designed controller, K(z), which makes the OLTFM diagonal is given by:

$$K(z) = \begin{bmatrix} -3.1357\ \frac{b}{a} & 0 & 1.0 \\ -1.0 & 0 & -0.14577\ a \\ -1.0258\ c & 1.0 & -0.64340\ a \end{bmatrix} \qquad (E.3)$$

where:

$$a = \frac{z + 0.7628}{z - 0.4384} \qquad b = \frac{z - 0.9216}{z - 0.8898} \qquad c = \frac{z - 0.8561}{z - 0.8898}$$

and the resulting open-loop transfer function matrix is equal to:

$$Q(z) = \begin{bmatrix} 0.1190\ e & 0 & 0 \\ 0 & 0.4058\ f & 0 \\ 0 & 0 & 0.02202\ g \end{bmatrix} \qquad (E.4)$$

where:

$$e = \frac{(z \text{ [illegible] } 0.899)}{(z - \text{[illegible]})\ (z - 0.8898)}$$

$$f = \frac{0.4058}{z - 1}$$

$$g = \frac{(z+0.7628)\ (z - 0.8998)}{(z - 0.9603)\ (z - 0.9216)\ (z - 0.4384)}$$

The non-interacting controller is slightly more complicated than the dynamic compensator obtained using the direct Nyquist array method (cf. Equation (5.65)).